

PROJECT REPORT
ON
THERMODYNAMIC STUDY OF BARDEEN
BLACKHOLE AND TAUB NUT CHARGED
BLACKHOLE

SUBMITTED BY
NELOFAR T.A
REGISTER NO. : AM20PHY011

in partial fulfillment of
the requirements for award of the postgraduate degree in physics



DEPARTMENT OF PHYSICS AND CENTRE FOR RESEARCH
ST.TERESA'S COLLEGE (AUTONOMOUS) ERNAKULAM

2020-2022

ST TERESA'S COLLEGE (AUTONOMOUS) ERNAKULAM



M.Sc. PHYSICS PROJECT REPORT

Name : NELOFAR T.A

Register Number : AM20PHY011

Year of Work : 2020'22

This is to certify that the project "**THERMODYNAMIC STUDY OF BARDEEN BLACKHOLE AND TAUB NUT CHARGED BLACKHOLE**" is the work done by **Nelofar T.A**

Priya
Dr. Priya Parvathi Ameena Jose

Head of the Department

Susan
Dr. Susan Mathew

Guide in Charge

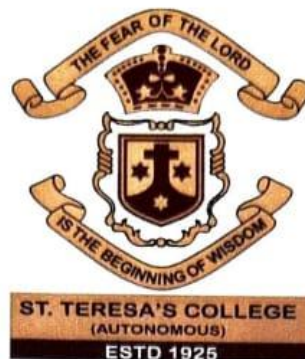


Submitted for the University Examination held in St Teresa's College, Ernakulam

Date :14.06.2022.....

Examiners 1) Dr. Issai Paul
2) Dr. Krishnamoorthy Mathew

DEPARTMENT OF PHYSICS
ST TERESAS COLLEGE (AUTONOMOUS), ERNAKULAM



CERTIFICATE

This is to certify that the project report entitled "**THERMODYNAMIC STUDY OF BARDEEN BLACKHOLE AND TAUB NUT CHARGED BLACKHOLE**" is the bonafide work done by **Ms. Nelofar T.A** (Reg. No: AM20PHY011) under the guidance of **Dr.THARANATH .R**, Assistant Professor, Department of Physics, Aquinas College, Edacochin and **Dr. SUSAN MATHEW**, Assistant Professor, Department of Physics and Centre for Research, St. Teresa's College, Ernakulam in partial fulfilment of the award of the Degree of Master of Science in Physics, St. Teresa's College, Ernakulam affiliated to Mahatma Gandhi University, Kottayam

Priya
Dr .Priya Parvathi Ameena Jose

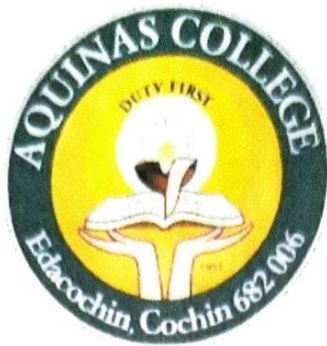
Head of the Department

Susan
Dr.Susan Mathew

Guide in Charge



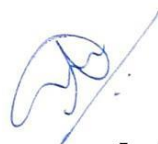
DEPARTMENT OF PHYSICS
AQUINAS COLLEGE, EDACOCHIN



CERTIFICATE

This is to certify that the project work "**THERMODYNAMIC STUDY OF BARDEEN BLACK HOLE AND TAUB NUT CHARGED BLACK HOLE**" is an authentic record of work carried out by **Ms. Nelofar T.A** under my guidance for the partial fulfilment of the award of the Degree of Master of Science in Physics in St.Teresa's college (Autonomous), Ernakulam.

LACE:Edacochin



Dr.Tharanath. R

DATE:

Assistant Professor,
Department of Physics
Aquinas college, Edacochin

DECLARATION

I, hereby declare that the project work entitled "**THERMODYNAMIC STUDY OF BARDEEN BLACK HOLE AND TAUB NUT CHARGED BLACK HOLE**" is a record of an original work done by me under the guidance of **Dr.THARANATH R**, Assistant Professor, Department of Physics ,Aquinias College Edacochin, and **Dr .SUSAN MATHEW**, Assistant Professor, Department of Physics and centre for Research, St Teresa's College, Ernakulam in the partial fulfilment of the requirements for the award of the Degree of Master of Physics. I further declare that the data included in the project is collected from various sources and are true to the best of my knowledge.

Nelofar T.A

ACKNOWLEDGEMENTS

The success and final outcome of this project required a lot of guidance and assistance from many people and we are extremely grateful to have got this all along the completion of my project work. Primarily, we thank God almighty for being with us throughout all the days and helping us complete the project successfully.

It is with great pleasure I express my sincere gratitude to Dr .Tharanath. R, Assistant Professor, Department of Physics, Aquinas College, Edacochin, my supervising guide, for his able guidance and encouragement throughout the course of this work.

I am thankful to Dr.Susan Mathew, Department of Physics, St. Teresa's College, Ernakulam for her valuable support and suggestions. I am deeply indebted for the personal support you had given me during moments of uncertainty.

I would like to thank Dr. Priya Parvathi Ameena Jose, Head of the Department of Physics, St. Teresas College, Ernakulam for her support and guidance.

I also express my sincere thanks to Ms.Henna Mary Jose for her whole hearted cooperation and help. A special thanks to my family for being a strong pillar in times of stress and struggle.

ABSTRACT

Black holes are the robust predictions of Einstein's General Relativity. The study of the thermodynamics properties of black hole is a major research theme of contemporary theoretical physics. In this project work we have studied the thermodynamics of Reissner–Nordström , Bardeen black hole and Taub NUT blackhole. We have derived the thermodynamic quantities such as Mass, Temperature, Entropy, Heat Capacity and Free Energy and plotted their variations with respect to entropy. Bardeen black hole shows a smooth variation of temperature with respect to entropy, which excludes the chance of first order phase transition. Furthermore, the discontinuity in heat capacity for a particular value of entropy in Bardeen black hole shows the presence of a second order phase transition. For Taub-NUT, heat capacity is negative and it indicates that the black hole is unstable and the free energy falls to negative above a certain value.

CONTENTS

1	Introduction	2
1.1	General Theory of Relativity	
1.2	The space-time metric	
1.3	Einstein's field equations	
1.4	Basic Thermodynamics	
1.5	Blackhole	
2.	Blackhole Thermodynamics	21
2.1	Introduction	
2.2	Laws of Blackhole Thermodynamics	
3.	Anti de Sitter space.....	25
4.	Taub-NUT space.....	28
5.	Thermodynamics of Reissner Nordstrom	
	Anti De Sitter Black hole.....	31
6.	Thermodynamics of Bardeen Black hole.....	36
7.	Thermodynamics of Taub-NUT Charged	
	Black hole.....	40
8.	Conclusion.....	46
9.	Bibliography.....	47

CHAPTER-1

INTRODUCTION

For more than two hundred years, Newton's theory of gravitation was accepted as the valid theory to describe the gravitational force. The framework, provided by Newton was considered as extremely successful to describe the motion of celestial objects. However, there were several incongruities in this theory such as: it could not explain the perihelion precession of Mercury; also, it could not explain how the gravitational force comes into play between two objects which are very far from each other and not connected via any medium.

In spite of these limitations, the theory, proposed by Newton, was widely regarded as the appropriate theory for gravity as it was highly successful in describing the motion of the objects under the influence of gravity. Thus, in 1915, when Einstein came up with General Relativity (GR), describing gravity in terms of the geometry of the spacetime itself, it took a while for people to accept it as the better theory for describing gravity. However, the famous experimental test during the solar eclipse of 1919, carried out by Arthur Eddington and Frank Dyson, made the theory famous overnight. A few years ago, in 2015, we have completed hundred years since Einstein proposed the theory of general relativity (GR), which is now considered as one of the most wonderful theories of physics ever proposed in the human history. Not only the theory can explain several observational phenomena, like the bending of light, perihelion precession of Mercury, gravitational lensing, gravitational redshift etc., but also the theory is sublime in its mathematical foundation. The recent discovery of gravitational

waves in 2016, which was also the prediction of Einstein's GR, has added another feather to the crown of this theory. Time and again, this theory has proved to be the most viable theory for gravity.

A few months after Einstein's new formulation of GR, in 1916, Karl Schwarzschild found the solution of Einstein's equation for a point mass. About the same time, Johannes Droste independently arrived to the same solution. The solution had a strange behaviour which, nowadays, known as the Schwarzschild radius where the Einstein's equation becomes infinite. In 1958, David Finkelstein identified the surface area of the Schwarzschild radius as the event horizon as it acts as a one way membrane and any causal curve can cross it only in one direction. This result paved the idea of black hole (BH) and the research on black holes became one of the most active areas in theoretical physics till the date.

Later in 1963, Roy Kerr discovered the solution of the rotating black holes—known as the Kerr black hole. Meanwhile, the no-hair theorem emerged, which states that the stationary black holes can be completely described by only three parameters: mass, charge and the angular momentum. For a long time, some people doubted the existence of black holes. However, the recent discovery of gravitational waves abolished the doubt regarding the real existence of black hole. A year ago, in 2019, the first ever image of black hole and its surroundings was published, which was observed earlier by Event Horizon Telescope in 2017. Now, in the very last month of May, 2022 astronomers have unveiled the first image of the supermassive black hole at the centre of our own Milky Way galaxy observed by Event Horizon Telescope.

In the decade of 1970's, several remarkable works came up which added new perception to the study of black hole theory. These new results have shown the connection of gravity with the thermodynamics. In one of his famous works, Hawking had shown some important results for black holes in general relativity. Most importantly, the paper provided the area increase theorem of black hole

horizon, which states that the horizon area of a black hole horizon always increases when the specific energy condition is satisfied. Bekenstein realized that the black holes must have entropy and he ascribed the entropy of the black hole to be proportional to its horizon surface area. Thereafter, the four laws of blackhole mechanics were shown by Bardeen, Carter and Hawking, which had an astonishing similarity with the four laws of thermodynamics. However, the authors in this paper refrain themselves from claiming it as the thermodynamic laws of black holes. Instead, they claimed it as an analogy with the conventional thermodynamics.

In fact, this analogy became a robust correspondence with the thermodynamics when Hawking revealed that the black holes can radiate when quantum effects are taken into the consideration. This radiation was later famously known as the Hawking radiation. Although Hawking initially tried to disapprove Bekenstein's idea about black hole entropy, this work by Hawking justifies the earlier claim by Bekenstein and also fix the proportionality constant of black hole entropy with the horizon area as $1/4$ in natural unit.

In the meantime, Fulling Davies and Unruh had shown that the accelerating observer observes thermal radiation in the Minkowski vacuum whereas the inertial observer does not. The temperature of the Unruh particles have the same form as of the Hawking temperature, except the surface gravity of black hole horizon is replaced by the acceleration of the observer. This radiation was later known as the Unruh radiation. The Unruh radiation and the Hawking radiation are equivalent on the basis of Einstein's equivalence principle. These were the stepping stone which laid the foundation of black hole thermodynamics. Since then, there have been numerous works in the direction of black hole thermodynamics and it became one of the most high-yielding domains for the theoretical physicists over the years.

Later several thermodynamic features were found in black hole thermodynamics and the earlier analogies (the area of the black hole horizon as the entropy, surface gravity of the horizon as the temperature etc.) were firmly identified as the physical thermodynamic parameters of black holes.

Phase transition is another important aspect of thermodynamics, which is also found in black hole thermodynamics as well and it has been studied for several decades. There are several types of phase transitions which are present in black hole thermodynamics. It was first introduced by Davies who argued that black holes undergo a second order phase transition when it passes through a point, which known as the Davies' point, where the heat capacity diverges. However, later Kaburaki et. approved that the Davies's point is not the critical point. Instead, it is a turning point, where the stability changes.

Another type of black hole phase transition was found in the work of Hawking. It was found that a black hole in AdS space makes transition to a no-black-hole state (or radiation) at a critical temperature. In addition, the transition of black holes from a non-extremal to an extremal one is also been found out as a phase transition of black holes, which is known as the extremal phase transition.

1.1 GENERAL THEORY OF RELATIVITY

General theory of relativity (GTR), published by Albert Einstein in 1915, is the current description of gravitation in modern physics. The general theory of relativity is proposed after special theory of relativity (STR). GTR comes to the main frame that STR must be modified to include the presence of gravity. This is because the STR is similar to dealing Newton's equations of motion without considering friction. When it comes to the realistic situation gravity is inevitable so a generalized concept of relativity is needed.

The Einstein way of describing gravity is to avoid the notion that it is a force and it is to find suitable non-Euclidean space time geometry and matter under no force moving in straight line trajectories with uniform speed as measured in terms of the rules of the new geometry. General relativity pictures gravity as a warping of space time due to the presence of a body of matter. An object nearby experiences an attractive force as a result of this distortion, much as a marble roll towards the bottom of depression in a rubber sheet. According to J. A. Wheeler, spacetime tells mass how to move, and mass tells space time how to curve.

The principle of equivalence is central to general relativity. An observer in a closed laboratory cannot distinguish between the effect produced by a gravitational field and those produced by an acceleration of the laboratory. To understand this, consider two observers. Let one of them be in a room which is at rest in a uniform gravitational field at the surface of earth and the second observer be in a room inside a rocket accelerating at g . Now if the former drops a pebble, it will accelerate towards the floor with acceleration g . This would be the same situation happening to the second observer. i.e. in both cases the observers are unable to distinguish the two situations by local experiments. This cancellation of gravitational fields by inertial forces is applicable to all freely falling systems. So that no local experiments can be distinguished between uniform inertial and gravitational accelerations.

1.2 THE SPACE TIME METRIC

We use a coordinate system to map the space around us. Consider the collection of all possible events that occur in the universe- that can be happened in the past, events happening now or the one that will happen in the future. The collection of these events is called spacetime. Let us assume that we use a linear coordinate

system, so that we can use linear algebra to describe it. Physical objects can then be described in terms of the basis-vectors belonging to the coordinate system.

Let (x, y, z) denote a Cartesian coordinate system and that would give the spatial location of the event and t , the time measured by an observer O at rest in an inertial frame , that is an observer who is acted on by no force. Let two neighbouring events in space and time be labelled by the coordinates (x, y, z, t) and $(x + dx, y + dy, z + dz, t + dt)$. The square of the ‘distance’ between the two events is given by

$$ds^2 = c^2 dt^2 - dx^2 - dy^2 - dz^2$$

The distance ds is invariant under Lorentz transformation, in the sense that if another inertial observer O' using a different coordinate system (x', y', z', t') to measure this distance will find the same answer. The above equation is the one commonly used in special theory, when we transform from special theory to general theory, the presence of gravitation requires a more complicated form. This can be conveniently written as,

$$ds^2 = \sum_{i,k=0}^3 g_{ik} dx^i dx^k$$

with $i = 1, 2, 3$ representing the three space coordinates and $i = 0$ the time coordinate. Here g_{ik} are the components of a second rank tensor. The matrix elements representing the tensors are the coefficient functions that multiply the differentials in the metric. The expressions for ds^2 is referred to as the metric. Now for convenience we can drop the summation symbol Σ by using Einstein’s summation convention (For example, $\sum_{i=0}^3 A_i B^i$ can be written as $A_i B^i$) the rule being that, whenever an index appears once as a subscript and once as a superscript in the same expression, it is automatically summed over all the values (here it is from 0 to 3) . Thus, we can write

$$ds^2 = g_{ik} dx^i dx^k .$$

1.3 EINSTEIN'S FIELD EQUATIONS

The ground breaking discovery of General theory of relativity was that it describes gravity as the effect of curvature in the fabric of spacetime geometry, a 4-dimensional picture that unifies space and time into a single framework. Coming to the field equations,

$$R_{ab} - \frac{1}{2}g_{ab}R = \frac{8\pi G}{c^4} T_{ab},$$

where R_{ab} is the Ricci curvature tensor, T_{ab} is the stress-energy tensor, g_{ab} is the metric tensor, R is the Scalar curvature, G is the Newtonian constant of gravitation and c is the speed of light in vacuum. It consists of a coupled system of ten partial differential equations. The right hand side of the equation describes the distribution of the mass and energy, whereas the left-hand side describes the geometry of space time.

In other words, Einstein's field equations give how mass and energy curve spacetime give rise to gravity. The right-hand side of the equation would be zero if there are no matter fields. Those are known as vacuum Einstein field equation. Einstein, using his field equations, predicted the perihelion motion of planet mercury; explained the bending of light in the vicinity of sun and the gravitational red shift.

1.4 BASIC THERMODYNAMICS

Thermodynamics is a branch of physics that deals with heat, work, and temperature, and their relation to energy, radiation, and physical properties of matter. It describes how thermal energy is converted to and from other forms of energy and how it affects matter. Thermal energy is the energy a substance or system has due to its temperature .The study of thermodynamics deals with

systems having large number of particles enclosed in a surrounding. It can be a liquid in vacuum flask or a canister of gas and the walls of the system prevents the exchange of energy. An ideal insulating wall is purely a theoretical notion. So when coming to the real experiments, the wall would not be perfect insulators. The observations of these experiments are now formulated to be the laws of thermodynamics. The study of thermodynamics can follow two paths, classical thermodynamics and statistical thermodynamics. The former approach concentrates on the gross behaviour of matter, evaluate measurable properties

1.4.1 Thermodynamic equilibrium

When the energy flow stops between the systems and all measurable properties are independent of time, the combined system is said to be in equilibrium. Consider an example to describe the state equilibrium. Consider two closed canisters, each having a piston attached to it. Let the piston be pinned so as to make the system rigid. Let the pistons be attached by a rod in common so that moving one piston moves the second. If we let the pin that place the piston in place to move, the two pistons move. Both the pistons may not have the same pressure and does not move alike, but after sometime the pistons would stop moving, making the pressure on the two pistons equal. This can be described as a state of equilibrium. There are three different aspects of equilibrium between systems. When there is no unbalanced force in the interior of a system and also none between a system and surroundings the system is said to be in a state of mechanical equilibrium.

When a system in mechanical equilibrium does not tend to undergoes a spontaneous change of internal structure such as chemical reaction or a transfer of matter from one part of the system to another such as diffusion or solution, however slow then it is said to be in a state of chemical equilibrium. Thermal

equilibrium exists when there is no spontaneous change in the coordinates of a system in mechanical and chemical equilibrium when it is separated from its surroundings by a diathermic wall. All parts of system are at the same temperature and this temperature is the same as that of surroundings

When these conditions are not satisfied a change of state will take place until thermal equilibrium is reached. When the conditions for all three types of equilibrium are satisfied the system is said to be in a state of thermodynamic equilibrium.

1.4.2 Laws of thermodynamics

Fowler discovered the phenomenon of thermal equilibrium in 1935. All the three laws of thermodynamics were discovered before 1935 thus newly discovered law was named the Zeroth law of thermodynamics.

Zeroth law states that if systems A and B are separately in thermal equilibrium with C, then systems A and B are in thermal equilibrium with each other. The law indicates that when system A and B are placed in contact with each other, no property of either system A or B changes with time which indicates that no energy flows between them if the system are in same temperature.

First Law of Thermodynamics states that a small amount o heat given to a system is partly used in doing external work and partly to increase the internal energy. Consider a quantity called the internal energy of the system, denoted by the symbol U. We choose U to ensure that the total energy of the system is constant. To preserve the law of conservation of energy we write the change in internal energy from its initial value U_i to its final value U_f as

$$\Delta U = U_f - U_i$$

$$\Delta U = W + Q$$

where Q is defined as the heat which is added to the system, W is the work done on the system. The change in the internal energy is the sum of the work done on the system and the heat added. The first law of thermodynamics says that energy is conserved if heat is taken into account.

The limitation of the first law is that it doesn't tell us about the direction in which the process occurs. This limitation was solved by the discovery of the second law. Second Law of thermodynamics states that Energy prefers to flow from a body with higher temperature to one with a lower temperature. Heat will not flow spontaneously from a cold object to a hot object.

Statement of the second law due to Clausius: It is impossible to construct a machine which operating in a cycle produces no other effect than to transfer heat from a colder to a hotter body. It is not possible for heat to flow from a colder body to a warmer body without any work having been done to accomplish this flow. Another statement of the second law is due to Kevin and Planck: It is impossible for an engine, operating in a cycle to take heat from a single reservoir, produce an equal amount of work and to have no other effect. It is impossible to extract an amount of heat Q_H from a hot reservoir and use it all to do work W . Some amount of heat Q_C must be exhausted to a cold reservoir. This precludes a perfect heat engine.

Now, before going through the statement of third law, we have to know about Entropy which is measure of a system's thermal energy per unit temperature that is unavailable for doing useful work. Entropy is a thermal inertia of the system. Only changes in entropy of a system can be calculated. It is a point function and is an extensive property of the system. Entropy is constant in a reversible adiabatic process. It is defined as

$$ds = \frac{\delta Q}{T} J/K$$

Nernst suggested that Entropy change of a transformation between phases approaches zero when Temperature approaches zero. And this led to the Third Law of Thermodynamics. If entropy of every element in its stable state is taken to be zero, then every substance has a positive entropy which at T=0 may become zero. Entropy become zero for all perfectly ordered states of condensed matter. Third law excludes disordered materials.

To simplify the analysis of the system, the laws are reformulated to change the variables. The method Legendre differential transformations is used to change the variable and that would yield functions that are fundamentally important in thermodynamics.

If a function of two variables $f(x, y)$ describes the state of a system, which satisfies the equation

$$df = u dx + v dy$$

and to change the description to one involving a new function $g(u, y)$, satisfying similar equation in terms of du and dy , then the necessary Legendre transform

$$g(u, y) \text{ is } g = f - ux.$$

The g satisfies the equation

$$dg = -x du + v dy.$$

Now, consider a characteristic function H , called enthalpy defined as

$$H = U + PV$$

Since internal energy, U ; pressure, P ; volume, V are all state functions; H is also a state function.

In differential form,

$$dH = V dP + TdS,$$

where H is a function characterized by P and S .

The first law can be written as,

$$dU = TdS - PdV$$

The requirement for a characteristic function other than enthalpy was met by defining the Helmholtz free energy and is given by

$$A = U - TS$$

In differential form,

$$dA = - SdT - PdV$$

where A is a function of T and V .

Gibbs function G , is generated by a Legendre transformation of

$$dH = TdS + VdP$$

$$\text{i.e., } G = H - TS$$

which is also a state function.

In differential form

$$dG = VdP - SdT$$

where G is a function characterized by P and T

Characteristic functions $U(V, S)$, $H(P, S)$, $A(V, T)$ and $G(P, T)$ are known as thermodynamic potential functions. When the characteristic function is minimum the system will be in stable equilibrium. The thermodynamic potential is defined as the function which is minimized subject to all the constraints that are imposed on the system.

The relations among the above functions can be represented with the help of mathematical aids. If a relation exists among three variables x, y and z, then if we express z as a function of x and y; then

$$dz = \left(\frac{\partial z}{\partial x}\right)_y dx + \left(\frac{\partial z}{\partial y}\right)_x dy.$$

Let $M = \left(\frac{\partial z}{\partial x}\right)$ and $N = \left(\frac{\partial z}{\partial y}\right)_x$

Then $dz = Mdx + Ndy$,

where z, M and N are all functions of x and y.

Partially differentiating M with respect to y and N with respect to x,

we get $\left(\frac{\partial M}{\partial y}\right)_x = \frac{\partial^2 z}{\partial x \partial y}$

and $\left(\frac{\partial N}{\partial x}\right)_y = \frac{\partial^2 z}{\partial y \partial x}$

Since the second derivatives of right hand terms are equal it follows that

$$\left(\frac{\partial M}{\partial y}\right)_x = \left(\frac{\partial N}{\partial x}\right)_y$$

This is known as the condition for exact differentials and it applies to all for thermodynamic potentials.

Applying the above result to the our exact differentials; dU, dH ,dA,dG

We obtain;

$$dU = TdS - PdV ; \quad \text{hence } \left(\frac{\partial T}{\partial V}\right)_S = -\left(\frac{\partial P}{\partial S}\right)_V$$

$$dH = V dP + TdS ; \quad \text{hence } \left(\frac{\partial T}{\partial P}\right)_S = \left(\frac{\partial V}{\partial S}\right)_P$$

$$dA = - SdT - PdV ; \quad \text{hence } \left(\frac{\partial S}{\partial V}\right)_T = \left(\frac{\partial P}{\partial T}\right)_V$$

$$dG = VdP - SdT ; \quad \text{hence } \left(\frac{\partial S}{\partial P}\right)_T = -\left(\frac{\partial V}{\partial T}\right)_P$$

The four equations on the right are known as Maxwell's relations. These equations express relations which hold at any equilibrium state of a hydrostatic system. These equations can be used to find equivalent terms related to entropy and can provide relationships between measurable quantities and those which either cannot be measured or difficult to measure.

1.4.3 Phase Transitions

The phase is defined as a state of matter that is uniform throughout, not only in chemical composition but also in physical state. A phase transition is a change in state from one phase to another. It occurs when there is an abrupt change in one or more properties of the system. The electrical resistivity of a material goes from zero to a finite value in a superconducting to normal phase transition. In a ferromagnetic phase transition the magnetic properties of a system change abruptly from those of a paramagnet to those of a ferromagnet. An abrupt change in properties is one sign of a phase transition. Another sign of a phase transition is the appearance of two phases coexisting side by side.

The phases having higher thermodynamic potential will be unstable and will eventually decay into the stable one. In order to simplify the notation, we describe all thermodynamic potentials as a simple mathematical function, $\Phi(\phi)$, where ϕ is the quantity which can vary. Thus, $\Phi(\phi)$, could be the generalized Gibbs free energy as a function of volume, so that $\phi = V$; or $\Phi(\phi)$ could represent the magnetic free energy, F with ϕ the magnetization.

The thermodynamic potential is analogous to the potential energy, $V(x)$, of a particle in a one-dimensional well. Just like the particle lowers its energy by sitting at the bottom of the potential well; the thermodynamic system lowers its free energy by sitting at the bottom of the thermodynamic potential. If $\Phi(\phi)$, has two minima the more stable state is the one with the lower energy. The other

minimum is unstable and will eventually decay into the lower minimum. We say that the system is metastable.

One minimum could correspond to the liquid phase of matter, the other minimum to the gas phase. Suppose the two minima evolve as the temperature (or pressure) increases so that one minimum is lower over one range of temperatures, the other is stable over another range. When the system evolves from one stable minimum to the other the phase changes, say from liquid to gas

Phase transitions are of two types: First order Phase Transitions are discontinuous. They involve a latent heat. Discontinuous phase transitions are characterized by a discontinuous change in entropy at a fixed temperature. Examples are solid-liquid and liquid-gas transitions at temperatures below the critical temperature. Second order phase transitions are continuous transitions which involve a continuous change in entropy which means there is no latent heat. n. If all the first derivatives of the thermodynamic potential are continuous at the transition, we call it a continuous transition.

The entropy is continuous at a continuous transition. Examples are liquid-gas transitions at temperature above the critical temperature. Bose condensation and paramagnetic to ferromagnetic phase transitions are also examples of a second order phase transition

Common examples of phase transitions are the ice melting and the water boiling, or the transformation of graphite into diamond at high pressures. The first order phase transitions are accompanied by abrupt changes in the specific volume and entropy. A first-order phase transition is determined by the relations:

$$T_1 = T_2 \text{ and } P_1 = P_2$$

$$G_1(P, T) = G_2(P, T)$$

where T , P , G are the temperature, pressure, and the Gibbs thermodynamic potential, respectively. Using the above relation, we can derive the Clausius–Clapeyron equation, which defines the slope of the phase equilibrium curves:

$$\frac{dP}{dT} = \frac{\Delta S}{\Delta V}$$

where ΔS and ΔV are the volume and entropy changes at the phase transition. The second-order phase transitions include transitions associated with an emergence of magnetism, superconductivity, superfluidity, orientational order, etc. Ehrenfest proposed equations relating the slope of the phase transition curve to discontinuities in the heat capacity, compressibility, and thermal expansion coefficient.

1.5 BLACK HOLE

A black hole is a region of spacetime where gravity is so strong that no particles or even electromagnetic radiation such as light can escape from it. The story of the black hole begins with Schwarzschild's discovery of the Schwarzschild solution in 1916, soon after Einstein's foundation of the general theory of relativity.

The Schwarzschild radius is the boundary of the black hole which is determined by Karl Schwarzschild and it completely depends on the mass of Black hole. If escape velocity is greater than velocity c the light cannot escape and we have a black hole .Any object with a physical radius smaller than Schwarzschild radius will be a Black hole. Anything that crosses the event horizon needs to be travelling at speed greater than velocity of light c .We see a black sphere reflecting nothing. So it is the event horizon which is the Black part.'Hole' part in black hole comes from the Singularity.

When a massive star has exhausted the internal thermonuclear fuels in its core at the end of its life, the core becomes unstable and gravitationally collapses inward upon itself, and the star's outer layers are blown away. The crushing weight of constituent matter falling in from all sides compresses the dying star to a point of zero volume and infinite density called the singularity. This singularity is covered by Event Horizon. Radius of the sphere representing the event horizon is called the Schwarzschild radius, $R_s = \frac{2GM}{c^2}$

1.5.1 No hair theorem

According to no-hair theorem only three parameters are required to define the most general black hole. They are mass M, charge Q and angular momentum J. Black holes have no hair whereas Star has many hairs (or parameters)

1.5.2 Classes of Black hole

Based on no-hair theorem the black holes can be characterized into three,

- a. Static black holes with no charge, described by Schwarzschild solution.
- b. Black holes with electrical charge described by Reissner Nordström solutions
- c. Rotating black holes described by Kerr solutions

a. Schwarzschild black hole

Karl Schwarzschild in 1916 gives the First solution of Einstein's equations of General Relativity. He describes gravitational field in empty space around a nonrotating mass space-time interval in Schwarzschild's solution Schwarzschild

metric is a spherically symmetric black hole. It is the simplest kind parametrized by a single parameter mass, M. Its line element is defined as

$$ds^2 = - \left(1 - \frac{2M}{r}\right) dt^2 + \left(1 - \frac{2M}{r}\right)^{-1} dr^2 + r^2 (d\theta^2 + \sin^2\theta d\phi^2)$$

It exhibits a singularity at the Schwarzschild radius $r= 2M$. This is the surface below which one can no longer escape from the black hole.

b. Reissner-Nordstrom black hole

The Reissner-Nordström geometry describes the geometry of empty space surrounding a charged black hole. The German aeronautical engineer Reissner and the Finnish physicist Nordström independently solved the Einstein- Maxwell field equations for charged spherically symmetric systems, in 1916 and 1918, respectively since most stars, and thus most black holes formed from the collapse of stars, have angular momentum, it is desirable to generalize the spherical, non-rotating Schwarzschild solution to that of rotating source. So, the difference from Schwarzschild metric is that this has an additional Coulomb field. The line element for Reissner- Nordström black holes is given by

$$ds^2 = - \left(1 - \frac{2M}{r} + \frac{Q^2}{r^2}\right) dt^2 + \left(1 - \frac{2M}{r} + \frac{Q^2}{r^2}\right)^{-1} dr^2 + r^2 (d\theta^2 + \sin^2\theta d\phi^2)$$

As the charged black holes in a realistic environment will quickly attract opposite charges from the surroundings and get neutralized, this solution is not of astrophysical interest.

c. Kerr black hole

Both the Schwarzschild and Reissner- Nordström black holes are spinless. The solution for a rotating black hole was put forward by Kerr in 1963 with an

additional 37 parameter, the angular momentum, J . The line element for black hole having mass and angular momentum is given by,

$$ds^2 = \frac{\Delta}{\rho^2} (dT - h \sin^2\theta d\phi)^2 - \frac{\rho^2}{\Delta} dR^2 - \rho^2 d\theta^2 - \frac{\sin^2\theta}{\rho^2} [(R^2 + h^2) d\phi - h dT]^2$$

where $h \equiv \frac{J}{M}$ = angular momentum per unit mass,

$$\Delta = R^2 - 2GMR + h^2$$

$$\rho^2 = R^2 + h^2 \cos^2\theta.$$

As charged black holes are not considered physically, astrophysical black holes are mainly Kerr.

d. Kerr Newman black hole

The Kerr–Newman metric is an asymptotically flat, stationary solution of the Einstein–Maxwell equations in general relativity. It describes the spacetime geometry in the region surrounding an electrically charged, rotating mass. It generalizes the Kerr metric by taking into account the field energy of an electromagnetic field, in addition to describing rotation

Such solutions do not include any electric charges other than that associated with the gravitational field, and are thus termed as vacuum solutions[1]. Newman combined the RN solution with Kerr solution and generated the spacetime geometry for a charged spinning mass. The metric equation for charged rotating black holes is as same as equation but with Δ defined as

$$\Delta = R^2 - 2GMR + h^2 + GQ^2$$

Chapter 2

BLACKHOLE THERMODYNAMICS

2.1 INTRODUCTION

Bekenstein and Hawking showed that the black holes have an entropy which is proportional to the area of the black hole. This was analogous to the second law of thermodynamics.

The entropy of black hole is given by,

$$S = \frac{kC^3 A}{4G\hbar} \quad \text{Bekenstein–Hawking formula}$$

Where A is the area of the event horizon, L_P is the Planck length, G is the Newton's gravity constant, \hbar is the reduced Planck's constant.

This laid a milestone in the study of black holes. In later years the four complete laws of black hole thermodynamics were introduced. These laws have a strong resemblance with the laws of thermodynamics. Thus, it became clear that the black holes do indeed behave as thermodynamic system. The crucial step in this realization was Hawking's remarkable discovery of 1974 that quantum processes allow a black hole to emit thermal flux particles.

2.2 LAWS OF BLACKHOLE THERMODYNAMICS

a) Zeroth law

By the zeroth law of black hole mechanics, the surface gravity of a stationary black hole must be constant over the event horizon of the black hole. This is analogous to the zeroth law of thermodynamics which states that the temperature is uniform throughout a system in thermal equilibrium. Here the surface gravity κ playing the role of temperature. The black holes have a well-defined temperature, which is as a matter of fact proportional to the surface gravity:

$$T = \frac{\hbar}{2\pi} \kappa$$

b) First Law

First law for a stationary black hole gives relation between change in mass M , angular momentum J and area A ,

$$dM = \frac{k dA}{8\pi G} + \Omega dJ$$

where Ω is the angular velocity of the event horizon.

For a rotating charged black hole, the First law takes the form,

$$dM = \frac{k dA}{8\pi G} + \Omega dJ$$

This is analogous to the first law of ordinary thermodynamics.

According to first law of thermodynamics all the thermodynamic processes are subjected to the principle of conservation of energy. The first law states that the change in internal energy is equal to the difference of change in heat transfer and work done by the system

$$\delta E = T \delta S + \text{work done.}$$

We see that the analogous quantities are, $E \leftrightarrow M$, $T \leftrightarrow \alpha\kappa$, and $S \leftrightarrow A/8\pi\alpha$, where α is a constant.

c) Second Law

The Area theorem of general relativity states that the area of a black hole can never decrease in any process i.e.,

$$\Delta A \geq 0.$$

Bekenstein observed that this is analogous to the second law of thermodynamics. By second law the total entropy of a closed system can never decrease through any process. This law requires black hole to have entropy. If it carried no entropy, falling of mass into a black hole would violate the second law. But this law is not informative in its original form. For example, if an ordinary system falls into a black hole, the ordinary entropy becomes invisible to an exterior observer, so from the observer's point of view, the concept of saying increase in ordinary entropy doesn't provide any insight. Thus, the ordinary second law is transcended.

Including the black hole entropy, gives a more useful law, the generalized second law of thermodynamics the sum of ordinary entropy outside black holes and the total black hole entropy never decreases and typically increases as a consequence of generic transformations of the black hole. When matter entropy flows into a black hole, the law requires an increase in black hole entropy more than compensate of ordinary entropy from sight. During the process of Hawking radiation, the black hole's area decreases, in violation of the area theorem. The generalized second law predicts that the emergent Hawking radiation entropy shall more than compensate for the drop in black hole entropy.

d) Third Law

We have already seen the statement of third law in ordinary thermodynamics. They are:

- The entropy of a system at absolute zero temperature either vanishes or becomes independent of the intensive thermodynamic parameters.
- To bring a system to absolute zero temperature involves an infinite number of processes or steps.

The third law of black hole mechanics states that it is not possible to form a black hole with vanishing surface gravity. That is, $\kappa = 0$ cannot be achieved. A black hole with $T=0$ has, $\kappa = 0$. This corresponds to an extreme Kerr black hole with $J = M^2$

Chapter 3

ANTI DE SITTER SPACE

The most ideal black holes are those which extend to asymptotically flat empty space. But they are of little relevance. The asymptotically flat black holes cannot reach thermodynamic stability, due to the inevitable so-called Hawking radiation. In order to obtain a better understanding of the thermodynamic properties and phase transition of black holes, we must ensure that the black hole can achieve stability in the sense of thermodynamics . During the formulations of General Theory, the universe was assumed to be static. The cosmological constant was introduced by Einstein in 1917 to allow for the possibility of a static universe but was dismissed as a mistake after the expansion of the universe was discovered . Einstein considered it to be his “greatest mistake,” but it has turned out to be a required ingredient of modern cosmology since 1998 . The physical effect this constant is to impose, on a large scale, a small repulsive force . This force, if adjusted in just the right way, can be made to compensate precisely for the average gravitational attraction between the galaxies . Weinberg showed as in order to permit our existence as observers the value of cosmological constant must be very small and positive.

The black holes with zero cosmological constant describe homogenous and isotropic universe and are called flat-Minkowski space. We can also have solutions to Einstein equations with non-zero cosmological constants. If $\Lambda > 0$

the solutions tend asymptotically to de Sitter space and if $\Lambda < 0$ the solution would tend to Anti-de Sitter space. The Einstein equation with cosmological constant can be written in the form

$$R_{ab} - \Lambda g_{ab} = \frac{8\pi G}{c^4} (T_{ab} - \frac{1}{2}g_{ab}R)$$

Just like the black holes in a flat space, the one in de Sitter and Anti de Sitter do exhibits properties including temperature, entropy and free energy. It was found that a black hole in de Sitter space would emit particles with temperature determined by the surface gravity of the black hole horizon

Anti-de Sitter space has been regarded as of little physical interest. The major reason for it is because of the negative value of Λ . It when interpreted as a negative energy density, there would be a negative energy density corresponding to it.. AdS space has no natural temperature associated with it just like the flat space. The main interest for these spaces has come from string theory and M- Theory, but also cosmological models with extra dimensions use properties of the anti-de Sitter spacetimes . A black hole in anti-de Sitter space has a minimum temperature which occurs when its size is of the order of the characteristic radius of the anti-de Sitter space .

If we take the asymptotically flat black hole as a thermodynamic system, it does not meet the requirements to achieve thermodynamic stability due to its negative heat capacity. Comparing with the asymptotically flat black holes, AdS black holes can be in thermodynamic equilibrium and stable state, because the heat capacity of the system is positive when the system parameters take certain values. Recently, increasing attention has been paid to the possibility that the cosmological constant Λ could be an independent thermodynamic parameter (pressure), and the first law of thermodynamics of AdS black hole may also be established with $P-V$ terms In anti-de Sitter space the gravitational potential relative to any origin increases at large spatial distances from the origin. This

means that the locally measured temperature of a thermal state decreases and that the total energy of the thermal radiation is finite [3].

The metric of anti-de Sitter space in static form is given by

$$ds^2 = -(r) dt^2 + f(r)^{-1} dr^2 + r^2 (d\theta^2 + \sin^2 \theta d\phi^2)$$

$$\text{where } f(r) = 1 + \frac{r^2}{L^2}$$

where L is the AdS length scale and is related to the cosmological constant as

$$L^2 = \frac{-3}{\Lambda}$$

Chapter:4

TAUB-NUT SPACE

4.1 INTRODUCTION

The Taub–NUT metric is an exact solution to Einstein's equations. It may be considered a first attempt in finding the metric of a spinning black hole. Taub–NUT solution was first discovered by Taub (1951), but expressed in a coordinate system which only covers the time-dependent part of what is now considered as the complete space-time.

It was initially constructed on the assumption of the existence of a four-dimensional group of isometries so that it could be interpreted as a possible vacuum homogeneous cosmological model. This solution was subsequently rediscovered by Newman, Tamburino and Unti (1963) whose initials constitute the “NUT” of the TN spacetimes.

They rediscovered it as a simple generalisation of the Schwarzschild space-time. Although they presented it with an emphasis on the exterior stationary region, they expressed it in terms of coordinates which cover both stationary and time-dependent regions.

In addition to a Schwarzschild-like parameter m which is interpreted as the mass of the source, it contained two additional parameters – a continuous parameter l which is now known as the NUT parameter, and the discrete 2-space curvature

parameter which is denoted here by ϵ . In 1963, when Roy Kerr introduced the Kerr metric for rotating BHs, he came up with a 4-parameter solution, one of which was the mass of the central body and the other was its angular momentum.

The NUT-parameter or the so-called NUT charge was one of the two remaining parameters, which was eliminated from his solution because Kerr believed that it was nonphysical since it made the metric non-asymptotically flat. However, 3 other researchers interpret it either as a gravomagnetic monopole parameter of the central mass or a twisting property of the surrounding spacetime.

It is only the case in which $\epsilon = +1$, which includes the Schwarzschild solution, that was obtained by Taub. The cases with other values of ϵ are generalisations of the other A-metrics. We will follow the usual convention of referring to the case in which $\epsilon = +1$ as the Taub–NUT solution.

Two different interpretations: Both of these have unsatisfactory aspects in terms of their global physical properties. In one interpretation, the space-time contains a semi-infinite line singularity, part of which is surrounded by a region that contains closed timelike curves. The other interpretation, which is due to Misner (1963), contains no singularities. These are removed only at the expense of introducing a periodic time coordinate throughout the stationary region. However, this also has other undesirable features, such that Misner was led to conclude that the complete space-time has no reasonable physical interpretation

4.2 NUT Parameter

In recent years, it has become common to refer to the NUT parameter ϵ as the magnetic mass or the gravitomagnetic monopole moment. This interpretation is

based on an analogue of one aspect of a property of one of the possible interpretations, but is not relevant in the context of the alternative global interpretation of the space-time.

In Misner's interpretation, the Taub–NUT solution has a number of properties that are usually considered to be undesirable in any reasonable representation of a spacetime. This is so much the case that Misner (1967) has presented it as “a counter-example to almost anything”

Chapter 5

Thermodynamics of Reissner Nordstrom Anti De Sitter Black hole

The RN-AdS black hole gives a spherically symmetric, stationary black hole.

Its line element is determined by two parameters: charge Q and mass M .

It also contains a negative cosmological constant.

The metric equation for RN-anti de Sitter black hole is given by

$$ds^2 = g_{ik}dx^i dx^k \quad \text{----- 1.1}$$

$$= -(r)dt^2 + \frac{1}{f(r)}dr^2 + r^2 d\Omega^2 \quad \text{-----} 1.2$$

$$\text{where, } f(r) = 1 - \frac{2M}{r} + \frac{r^2}{L^2} + \frac{Q^2}{r^2} \quad \dots \dots \dots \quad 1.3$$

$d\Omega^2$ represents the line element of unit-2 sphere, or

$$d\Omega^2 = d\theta^2 + \sin^2\theta d\phi^2 \quad \dots \dots \dots \quad 1.4$$

and L is the AdS length scale and is related to the cosmological constant as

$$\Lambda = -\frac{3}{L^2} \quad \dots \dots \dots \quad 1.5$$

This black hole solution has two event horizons and one cosmological horizon .

The vacuum pressure of the AdS spacetime depends on the cosmological constant and is given by

$$P = -\frac{\Lambda}{8\pi} = \frac{3}{8\pi L^2} \quad \dots \dots \dots \quad 1.6$$

$f(r)$ satisfies the relation $f(r) = 0$, with r , the event horizon

Solving for M,

$$M = \frac{r}{2} + \frac{Q^2}{2r} + \frac{r^3}{L^2} \quad \dots \dots \dots \quad 1.7$$

We have the relation between r and S

$$S = \pi r^2 \quad \dots \dots \dots \quad 1.8$$

Replacing r in terms of S gives

$$M = \frac{1}{2} \sqrt{\frac{S}{\pi}} + \frac{Q^2}{2} \sqrt{\frac{\pi}{S}} + \left(\frac{S}{\pi}\right)^{3/2} \frac{1}{2L^2} \quad \dots \dots \dots \quad 1.9$$

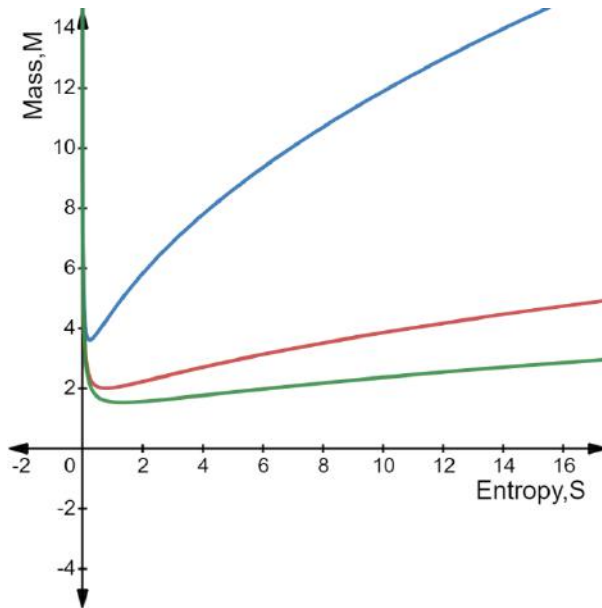


FIGURE1.1 The graph shows the variation of mass with entropy with charge Q unity and length scale $L = 0.5, L = 1.0, L = 1.5$

Thermodynamic Potential of a charge black hole is given by,

$$\begin{aligned}\emptyset &= \frac{\partial M}{\partial Q} \\ &= \sqrt{\frac{\pi}{S}} Q \quad \text{----- 1.10}\end{aligned}$$

The temperature of the black hole is given by,

$$\begin{aligned}T &= \frac{\partial M}{\partial S} \\ &= \frac{\partial}{\partial S} \left(\frac{1}{2} \sqrt{\frac{S}{\pi}} + \frac{Q^2}{2} \sqrt{\frac{\pi}{S}} + \left(\frac{S}{\pi}\right)^{3/2} \frac{1}{2L^2} \right) \\ T &= \frac{1}{4\sqrt{\pi S}} - \frac{Q^2\sqrt{\pi}}{4^3\sqrt{S}} + \frac{3\sqrt{S}}{4L^2 3\sqrt{\pi}} \quad \text{----- 1.11}\end{aligned}$$

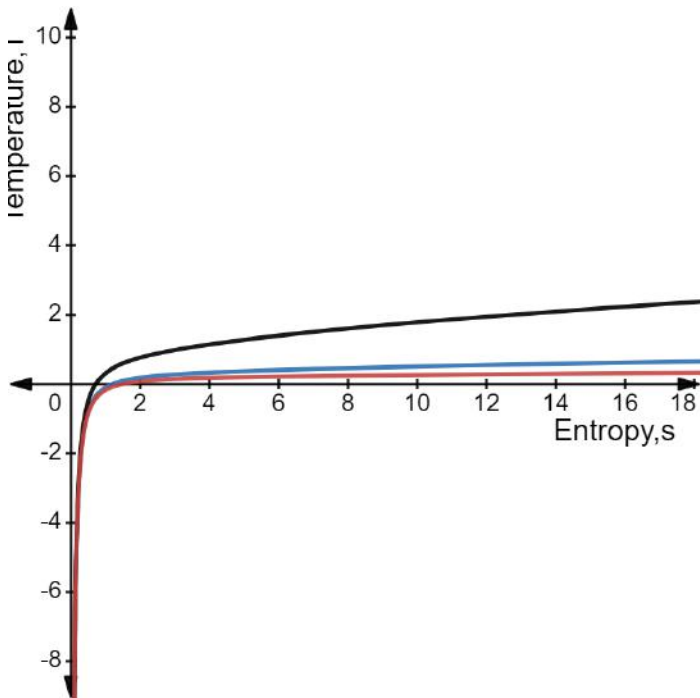


Figure 1.2 The variation of temperature with S , with $L=0.5$, $L=1$, $L=1.5$ and $Q=1$ is shown in the graph above.

The Heat capacity is given by

$$C = T \frac{\partial S}{\partial T}$$

$$= T \left(\frac{\partial T}{\partial S} \right)^{-1}$$

$$\frac{\partial T}{\partial S} = - \frac{1}{4\sqrt{\pi} 2S^{3/2}} + \frac{Q^2 \sqrt{\pi}}{4} \frac{3}{2} S^{-5/2} + \frac{3}{4 2\sqrt{S} \pi^{3/2} L^2}$$

$$= \frac{1}{8L^2 \pi^{3/2} S^{5/2}} (-L^2 \pi S + L^2 Q^2 3\pi^{5/2} + 3S^2)$$

$$C = \left(\frac{1}{4\sqrt{\pi} S} - \frac{Q^2 \sqrt{\pi}}{4^3 \sqrt{S}} + \frac{3}{4L^2 3\sqrt{\pi}} \sqrt{S} \right) \left(\frac{8L^2 \pi^{3/2} S^{5/2}}{-L^2 \pi S + L^2 Q^2 3\pi^{5/2} + 3S^2} \right)$$

$$C = \frac{6S^3 - 2SQ^2L^2\pi^2 + 2L^2\pi S^2}{3S^2 - L^2\pi S + 3L^2Q^2\pi^{5/2}} \quad ----- 1.12$$

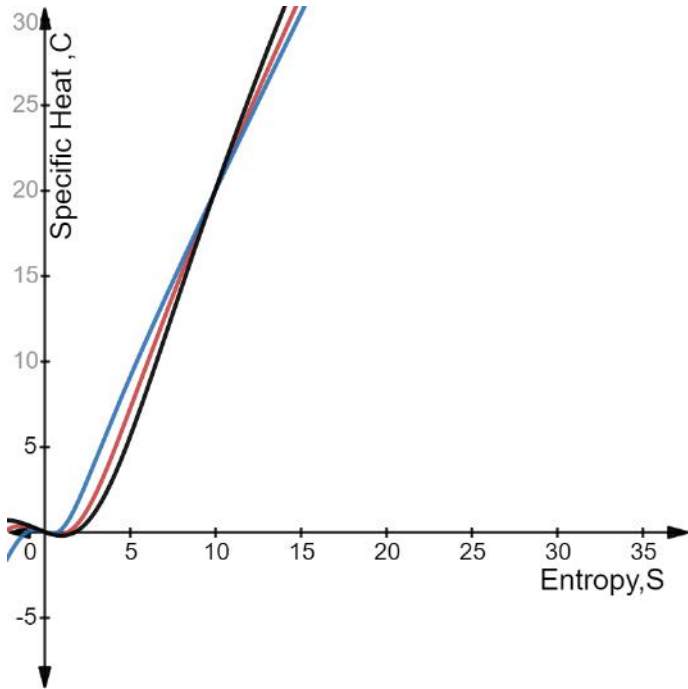


Figure 1.3 The figure shows the variation of heat capacity with entropy. The charge of the black hole is assumed to be unity and the length scale is varied as $L= 0.5$, $L= 1.0$ and $L= 1.5$

The free energy of the black hole given by,

$$F = M - TS$$

$$= \left(\frac{1}{2} \sqrt{\frac{S}{\pi}} + \frac{Q^2}{2} \sqrt{\frac{\pi}{S}} + \left(\frac{S}{\pi} \right)^{3/2} \frac{1}{2L^2} \right) - S \left(\frac{1}{4\sqrt{\pi}S} - \frac{Q^2\sqrt{\pi}}{4} \frac{3}{3\sqrt{S}} + \frac{3\sqrt{S}}{4L^2 3\sqrt{\pi}} \right)$$

$$= \frac{1}{2} \sqrt{\frac{S}{\pi}} + \frac{Q^2}{2} \sqrt{\frac{\pi}{S}} + \left(\frac{S}{\pi} \right)^{3/2} \frac{1}{2L^2} - \frac{1}{4} \sqrt{\frac{S}{\pi}} + \frac{Q^2}{4} \sqrt{\frac{\pi}{S}} - \frac{3}{4L^2} \frac{3\sqrt{S}}{\pi}$$

$$F = \frac{1}{4} \sqrt{\frac{S}{\pi}} - \frac{1}{4L^2} \left(\frac{S}{\pi} \right)^{3/2} + \frac{3Q^2}{4} \sqrt{\frac{\pi}{S}} \quad ----- 1.13$$

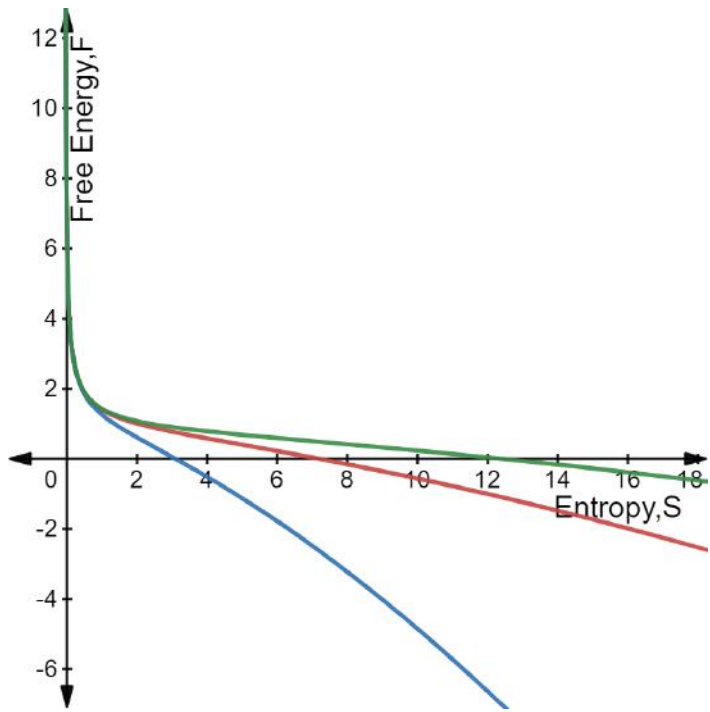


Figure 1.4 The graph showing variation of free energy for three different values of L . Q is chosen to be unity.

Chapter 6

THERMODYNAMICS OF BARDEEN BLACKHOLE

Bardeen's solution of Einstein's equation in the presence of nonlinear electromagnetic field is parametrized by mass M and charge q. The static and spherically symmetric line element is given by

$$ds^2 = f(r)dt^2 - \frac{dr^2}{f(r)} - r^2(d\theta^2 + \sin^2\theta d\varphi^2) \quad (2.1)$$

where,

$$f(r) = 1 - \frac{\frac{2Mr^2}{(r^2+q^2)^{\frac{3}{2}}}}{(r^2+q^2)^{\frac{3}{2}}} \quad (2.2)$$

Using the area law, ($S = 4\pi r^2$), we can write the mass in terms of the entropy S and the q as:

$$M = \frac{(S+\pi q^2)^{\frac{3}{2}}}{2\sqrt{\pi}S} \quad (2.3)$$

Temperature of the black hole is given by the relation, $T = \frac{\partial M}{\partial S}$ as,

$$\begin{aligned} T &= \frac{\partial}{\partial S} \left[\frac{(S+\pi q^2)^{\frac{3}{2}}}{2\sqrt{\pi}S} \right] \\ &= \frac{3(S+\pi q^2)^{\frac{1}{2}}}{4\sqrt{\pi}S} - \frac{(S+\pi q^2)^{\frac{3}{2}}}{2\sqrt{\pi}S} \\ &= \frac{(S+\pi q^2)^{\frac{1}{2}}}{4\sqrt{\pi}S^2} (3S - 2(S + \pi q^2)) \\ T &= \frac{(S-2\pi q^2) \sqrt{S+\pi q^2}}{4\sqrt{\pi}S^2} \end{aligned} \quad (2.4)$$

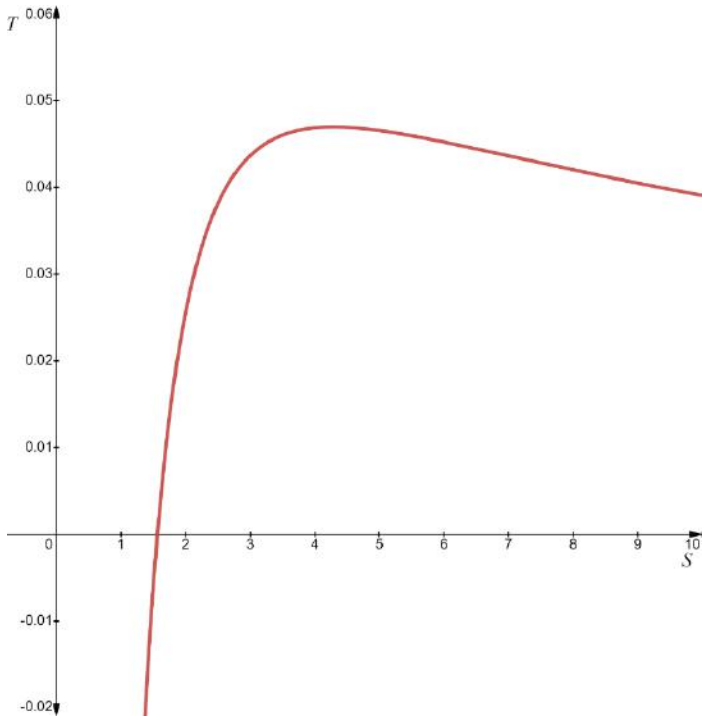


Figure 1. Variation of temperature with respect to entropy S of Bardeen black hole.

We will now calculate the heat capacity, $C = T \frac{\partial S}{\partial T}$, of the black hole and is given by

$$\begin{aligned}
 C &= T \left[\frac{\partial T}{\partial S} \right]^{-1} = T \frac{\partial}{\partial S} \left[\frac{(S-2\pi q^2) \sqrt{S+\pi q^2}}{4\sqrt{\pi} s^2} \right]^{-1} \\
 &= T \frac{8\sqrt{\pi} S^3}{[S(S+\pi q^2)^{-\frac{1}{2}}(S-2\pi q^2)-\sqrt{S+\pi q^2}(2S-8\pi q^2)]} \\
 &= \frac{2S(S-2\pi q^2) \sqrt{S+\pi q^2}}{[S(S+\pi q^2)^{-\frac{1}{2}}(S-2\pi q^2)-\sqrt{S+\pi q^2}(2S-8\pi q^2)]}
 \end{aligned}$$

Dividing numerator and denominator with $\sqrt{(S + \pi q^2)}$

$$C = \frac{-2S(2\pi q^2 - S)(S + \pi q^2)}{8\pi^2 q^4 + 4\pi q^2 S - S^2} \quad (2.5)$$

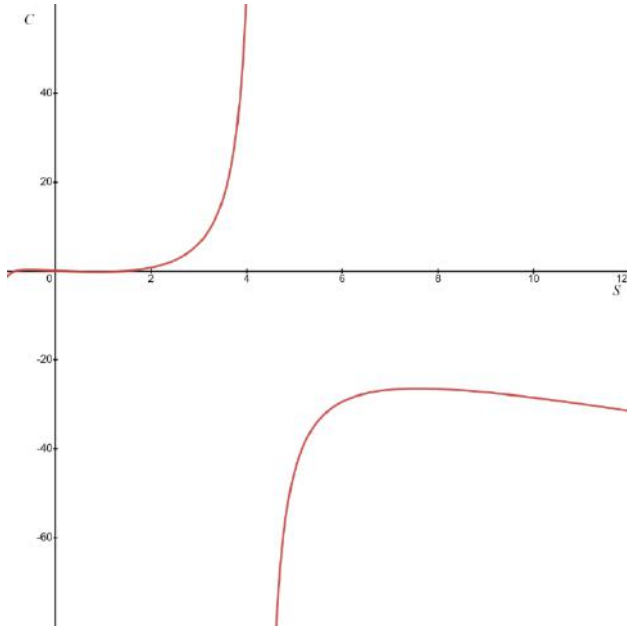


Figure 3. Variation of heat capacity with respect to entropy S of Bardeen black hole.

Then the Gibb's free energy, $F = M - TS$, is given by

$$F = \frac{(S + \pi q^2)^{\frac{3}{2}}}{2\sqrt{\pi}S} - \frac{(S - 2\pi q^2)\sqrt{S + \pi q^2}}{4\sqrt{\pi}S} \quad (2.6)$$

Now we study whether this black hole will undergo a second order phase transition or not. This can be done in two ways.

The first method is by studying the variation of the heat capacity with entropy and we can see a discontinuity in heat capacity (Fig3) for a particular value of entropy ($S = 4.1, q = 0.5$). And we also note that heat capacity possesses a positive

phase below this value of S and a negative phase above this value of S . The second method is by studying the variation of free energy(F) with temperature(T).

A second order phase transition is obvious for two reasons. First, of course the heat capacity shows an infinite discontinuity (at $S = 4.1$, where $q = 0.5$) and possesses both positive and negative phases. The positive phase exists for small values of S and the black hole is stable only in this region. The same result can also be seen from the parametric plot between the free energy and the temperature (Fig4) which shows a cusp type double point (at $T = 0.046$, where $S = 4.1$ and $q = 0.5$). The $F-T$ variation shows that there are two branches of the curve, for one of the branches, the free energy decreases with the increase of Hawking temperature to the minimum limit, while for the other branch F increases rapidly with T . This behavior also signals a second order phase transition. (The numerical values are obtained from the corresponding graphs.)

Chapter 7

Thermodynamics of Taub-NUT Charged Blackhole

Introduction

Taub-NUT black hole solution depends on three parameters: Mass M, NUT parameter l,

$$ds^2 = -f(r)(dt - 2l\cos\theta d\varphi)^2 + \frac{dr^2}{f(r)} + (r^2 + l^2)(d\theta^2 + \sin^2\theta d\varphi^2)$$

where $f(r) = \frac{r^2 - 2mr - l^2}{r^2 + l^2}$

When $l = 0$ and $m \neq 0$, the metric reduces to the *Schwarzschild solution* in which m is the familiar parameter representing the mass of the source.

Newman, Tamburino and Unti (1963) have shown that, when l is small, the inclusion of this parameter induces a small additional advance in the perihelion of approximately elliptic orbits in the stationary region of the space-time. However, when $l \neq 0$, the space-time has very different global properties to that of Schwarzschild.

TAUB NUT CHARGED BLACK HOLE

Charged TNBH solution depends on three parameters: Mass M, NUT parameter l, and charge q and the metric of CTNBH describes the vacuum spacetime around a source

$$ds^2 = f(r)(dt - 2l\cos\theta d\varphi)^2 - \frac{dr^2}{f(r)} - (r^2 + l^2)(d\theta^2 + \sin^2\theta d\varphi^2)$$

$$\text{where } f(r) = 1 - \frac{2(Mr + l^2) + q^2}{r^2 + l^2}$$

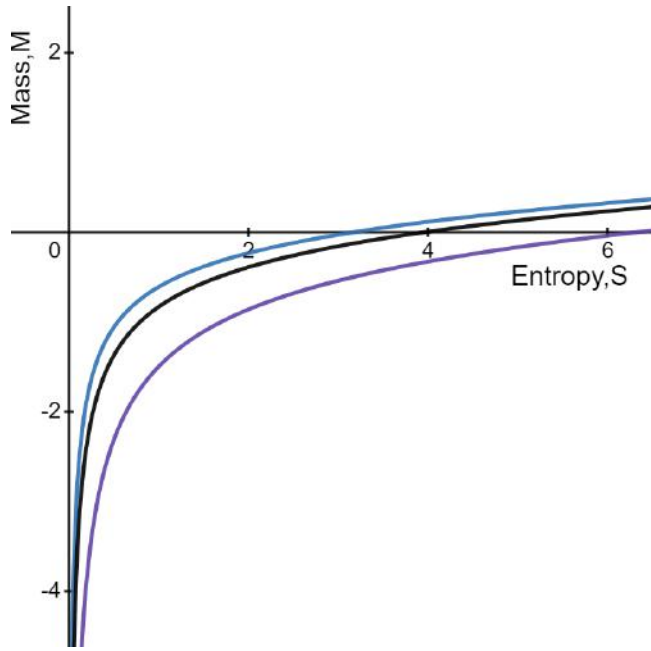
$f(r)$ satisfies the relation $f(r) = 0$,

Solving for M; using the relation between r and S as $S = \pi r^2$

And replacing r in terms of entropy S gives,

$$M = \frac{1}{2} \sqrt{\frac{s}{\pi}} - \frac{q^2}{2} \sqrt{\frac{\pi}{s}} - \frac{l^2}{2} \sqrt{\frac{\pi}{s}}$$

Variation of mass with respect to entropy for length L=0,L=0.5,L=1 with charge Q=1.



The temperature of the blackhole is given by

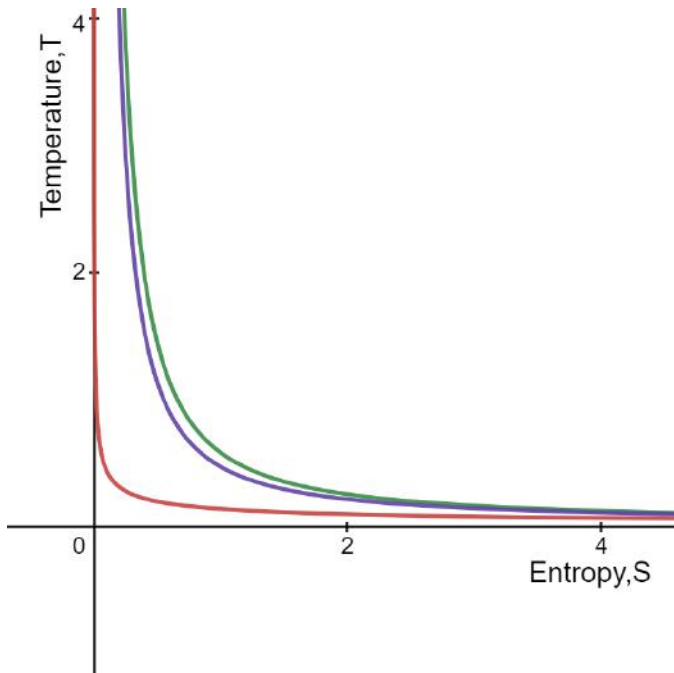
$$T = \frac{\partial M}{\partial S} = \frac{\partial}{\partial S} \left(\frac{1}{2} \sqrt{\frac{s}{\pi}} - \frac{q^2}{2} \sqrt{\frac{\pi}{s}} - \frac{l^2}{2} \sqrt{\frac{\pi}{s}} \right)$$

$$T = \frac{1}{4\sqrt{\pi s}} + \frac{q^2 \sqrt{\pi}}{4s^{\frac{3}{2}}} + \frac{\sqrt{\pi} l^2}{4s^{\frac{3}{2}}}$$

$$T = \frac{\pi l^2 + s + \pi q^2}{4\sqrt{\pi} s^{\frac{3}{2}}}$$

$$T = \frac{1}{4\sqrt{\pi s}} + \frac{q^2 \sqrt{\pi} + \sqrt{\pi} l^2}{4s^{\frac{3}{2}}}$$

Variation of temperature with respect to entropy for length L=0,L=0.5,L=1 with charge Q=1



Heat capacity is given by,

$$C = T \frac{\partial S}{\partial T}$$

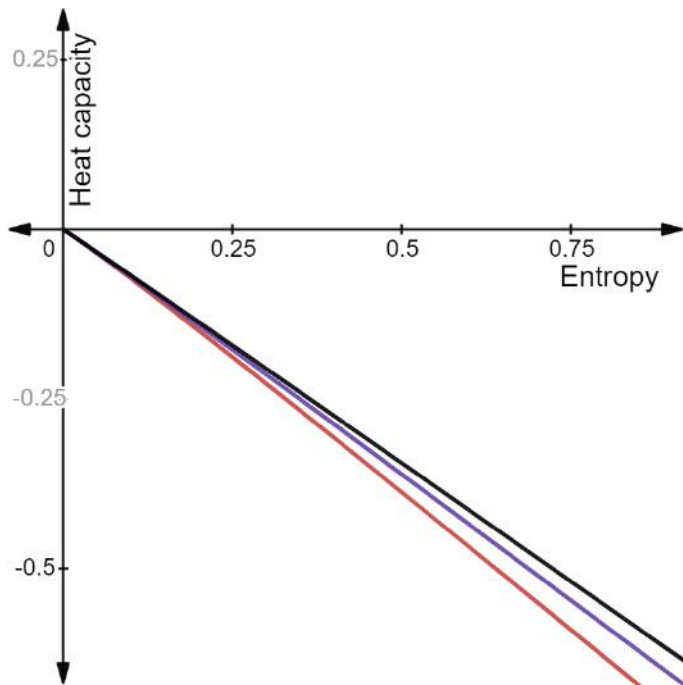
$$C = T \left[\frac{\partial T}{\partial S} \right]^{-1}$$

$$\frac{\partial T}{\partial S} = \frac{-3q^2\pi - 3l^2\pi - s}{8\sqrt{\pi}s^{\frac{5}{2}}}$$

$$C = \left(\frac{1}{4\sqrt{\pi}s} + \frac{q^2\sqrt{\pi}}{4s^{\frac{3}{2}}} + \frac{\sqrt{\pi l^2}}{4s^{\frac{3}{2}}} \right) \left(\frac{8\sqrt{\pi}s^{\frac{5}{2}}}{-3q^2\pi - 3l^2\pi - s} \right)$$

$$C = \left(\frac{s(q^2\pi + l^2\pi + \sqrt{s})}{-3q^2\pi - 3l^2\pi - s} \right)$$

Variation of heat capacity with respect to entropy for length L=0,L=1,L=2 with charge Q=1



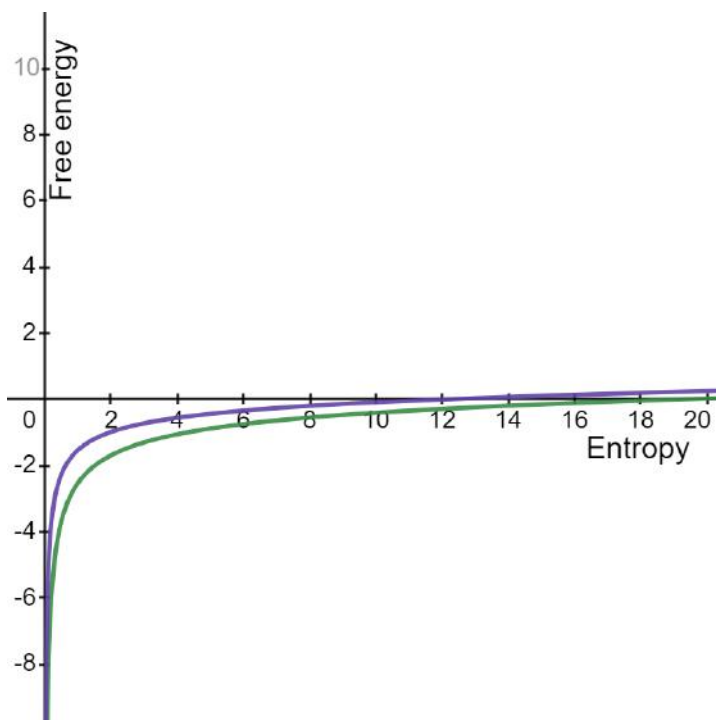
Free energy of a blackhole is given by

$$F = M - TS$$

$$F = \left(\frac{1}{2} \sqrt{\frac{s}{\pi}} - \frac{q^2}{2} \sqrt{\frac{\pi}{s}} - \frac{l^2}{2} \sqrt{\frac{\pi}{s}} \right) - S \left(\frac{1}{4\sqrt{\pi s}} + \frac{q^2 \sqrt{\pi}}{4s^2} + \frac{\sqrt{\pi} l^2}{4s^2} \right)$$

$$F = \left(\frac{1}{4} \sqrt{\frac{s}{\pi}} - \frac{q^2}{4} \sqrt{\frac{\pi}{s}} - \frac{l^2}{4} \sqrt{\frac{\pi}{s}} \right)$$

The graph shows the variation of free energy with entropy with length scale L=1 and L=0.5 with charge Q=1



Chapter -8

CONCLUSION

In this project we studied RN-AdS black hole, Bardeen black hole and Taub NUT black hole. We have derived the thermodynamic quantities, and plotted their variations with respect to entropy.

In Bardeen black hole, from the temperature entropy diagram we have eliminated the possibility of a first order phase transition. A second order phase transition is obvious, since the heat capacity shows an infinite discontinuity and possesses both positive and negative phases. The positive phase exists for small values of S and the black hole is stable only in this region.

In RN-AdS black hole, below a certain value of entropy the mass increases with decrease in entropy and the mass and gives an infinite discontinuity at zero entropy. At very low values of entropy the temperature of the black hole shows an abnormal behaviour. For RN-AdS black hole the heat capacity is negative lower values of entropy and reaches zero at a certain value. The free energy of the black holes falls to negative above a certain value.

For Taub-NUT black hole, there is a smooth variation of mass with entropy. The black hole shows finite temperature for all values of entropy. For Taub-NUT, heat capacity is negative and it indicates that the black hole is unstable and the free energy falls to negative above a certain value.

CHAPTER-9

BIBLIOGRAPHY

1. Weinberg, Steven. *Gravitation and Cosmology: Principles and applications of general theory of relativity*, Wiley India Pvt. Limited, 2008
2. Narlikar, Jayant V. *An introduction to relativity*. Cambridge University Press, 2010
3. Hall, Michael J W. *General Relativity: An Introduction to Black Holes, Gravitational Waves, and Cosmology*. N.p., Morgan & Claypool Publishers, 2018.
4. Guidry, Mike. *Modern General Relativity: Black Holes, Gravitational Waves, and Cosmology*. United Kingdom, Cambridge University Press, 2019.
5. Ong, Yen Chin. *Evolution of Black Holes in Anti-de Sitter Spacetime and the Firewall Controversy*. Germany, Springer Berlin Heidelberg, 2015.
6. Britannica, The Editors of Encyclopaedia. "Black hole". Encyclopedia Britannica, 13 Oct. 2020, <https://www.britannica.com/science/black-hole>. Accessed 25 March 2021.
7. Puri, S. P.. *General Theory of Relativity*. India, Pearson Education India, 2013.
8. Bowley, Roger, and Sánchez, Mariana. *Introductory Statistical Mechanics*. United Kingdom, Clarendon Press, 1999
9. Kumar, Prasanna. *Thermodynamics*. India, Pearson Education India, 2013.

10. Poisson, Eric. *A Relativist's Toolkit: The Mathematics of Black-Hole Mechanics*. Cambridge University Press, 2004.
11. Hawking, S. W. "Black holes and thermodynamics." *Phys. Rev. D.* 13,2, Jan 1976, 191-197
12. Jacob d, Bekenstein (2008) *Bekenstein-hawking Entropy*, Scholarpedia, 3(10): 7375. http://www.scholarpedia.org/article/Bekenstein-Hawking_entropy Accessed on (11-04-2021)
13. Grøn, Øyvind, Sigbjørn Hervik. *Einstein's General Theory of Relativity*. Springer-Verlag New York, 2007
14. Zemansky, Mark W, and Richard Dittman. *Heat and Thermodynamics: An Intermediate Textbook*. New York: McGraw-Hill, 1997.
15. https://en.wikipedia.org/wiki/Kerr%E2%80%93Newman_metric
16. Stenflo, J. (2019). *Origin of the cosmological constant*. *Astrophysics and Space Science*. 364.
17. Einstein, Albert, and Robert W. Lawson. *Relativity: The Special and General Theory*. New York: Holt, 1921. Print. 4
18. S. W. Hawking and Don N. Page. *Thermodynamics of black holes in antide sitter space*. *Communications in Mathematical Physics*, 87(4):577–588, Dec 1983
19. Al-Badawi, Kanzi, and Sakalli, "Fermionic and Bosonic Greybody Factors as Well as Quasinormal Modes for Charged Taub NUT Black Holes."
20. Jerry.B.Griffith, Podolsky, "Exact space-times in general relativity".

DIGITAL THERMOMETER USING ARDUINO AND LM35
TEMPERATURE SENSOR

PROJECT REPORT

Submitted by

NIVEDITHA RAMESH

Reg.No: AB19PHY021

Under the guidance of

Dr. Sunsu Kurian, Assistant Professor

**Department of Physics, St.Teresa's College(Autonomous), Ernakulam
Kochi, 682011**

Submitted to,

Mahatma Gandhi University, Kottayam

In partial fulfilment of the requirement for the Award of
BACHELOR'S DEGREE OF SCIENCE IN PHYSICS



ST.TERESA'S COLLEGE (AUTONOMOUS)
ERNAKULAM



CERTIFICATE

This is to certify that the project report entitled "**DIGITAL THERMOMETER USING ARDUINO AND LM35 TEMPERATURE SENSOR**" is a bonafide work by Niveditha Ramesh, St.Teresa's College Ernakulam, under my supervision at the Department of Physics, St.Teresa's College, Ernakulam for the partial fulfilment of the award of Degree Of Bachelor of Science in Physics during the academic year 2020-'21 .The work presented in this dissertation has not been submitted for any other degree in this or any other university.

Supervising Guide

Sunni
Dr. Sunni Kurian
Assistant Professor

Place:Ernakulam

Date: 09/05/2022

Head of the Department

Priya
Dr.Priya Parvati Ameena Jose,
Associate Professor

ST. TERESA'S COLLEGE(AUTONOMOUS)

ERNAKULAM



BSc PHYSICS

PROJECT REPORT

Name : NIVEDITHA RAMESH

Register Number : AB19PHY021

Year of work : 2021 - 2022

This is to certify that this project work entitled '**DIGITAL THERMOMETER USING ARDUINO AND LM35 TEMPERATURE SENSOR**' is an authentic work done by Niveditha Ramesh(AB19PHY021).

Staff member in-charge

Dr. SUNSU KURIAN



Sunsu
Kurian

Head of the Department

Dr. PRIYA PARVATI AMEENA JOSE

Submitted for the University examination held at St. Teresa's College, Ernakulam.

DATE: 09-05-2022

EXAMINERS:

Niveditha
Suson

ST. TERESA'S COLLEGE(AUTONOMOUS)

ERNAKULAM



BSc PHYSICS

PROJECT REPORT

Name : NIVEDITHA RAMESH

Register Number : AB19PHY021

Year of work : 2021 - 2022

This is to certify that this project work entitled '**DIGITAL THERMOMETER USING ARDUINO AND LM35 TEMPERATURE SENSOR**' is an authentic work done by Niveditha Ramesh(AB19PHY021).

Staff member in-charge

Dr. SUNSU KURIAN

Head of the Department

Dr. PRIYA PARVATI AMEENA JOSE

Submitted for the University examination held at St. Teresa's College, Ernakulam.

DATE: 09-05-2022

EXAMINERS:

ACKNOWLEDGMENT

I am bringing out this project report with immense pleasure and sense of satisfaction.I feel obliged to acknowledge the support and guidance that came from various quarters during the course of competition of this project.I would like to express our sincere gratitude to Dr. Sunsu Kurian, the project in charge , for guiding me throughout the entire duration of the project work. This work would not have succeeded without her support and motivation.

I would also like to extend our sincere thanks to all the faculty members of the Physics Department for their valuable suggestions and corrections.I would also like to thank all our friends for being with us whenever we were in need. Above all,I owe my heartfelt gratitude to the Almighty for showers abundant blessings upon me to get through this project.

ABSTRACT

The main objective of the project is to develop a digital thermometer and measure its accuracy. The project is designed by using an Arduino UNO Board, LM35 temperature sensor, LED display, potentiometer, connecting wires and breadboard. The sensor LM35 is a temperature sensor that outputs an analog signal which is proportional to the instantaneous temperature. The output voltage can easily be interpreted to obtain a temperature reading in Celsius. Due to its small size the temperature sensor can be used in a wide variety of applications.

CONTENTS

Chapter No.	Chapter Name	Page No.
1	Introduction 1.1 Literature Review	8 9
2	Existing System of Thermometers 2.1 Thermometers 2.11 Conventional Thermometers 2.12 Digital Thermometers 2.12.1 Digital Thermometer Components 2.12.2 Modern available Digital Thermometers 2.2 Advantages of Digital Thermometers 2.3 Applications of Digital Thermometers	10 11 12 13
3	Proposed System 3.1 Advantages of the System 3.2 Advantages and Economical Importance of Digital Thermometer	14 15
4	Overview of Components 4.1 Hardware Components 4.11 Arduino UNO R3 4.12 LM35 Temperature Sensor 4.13 LCD Display 4.14 10K Potentiometer 4.15 Breadboard 4.2 Software Specifications	16 17 18 20 21 22
5	Methodology 5.1 Construction 5.2 Digital Thermometer using Arduino UNO,LM35 and LCD Circuit 5.3 LM35 Voltage Conversion to Temperature Formula/Equation Derivation for Arduino 5.4 Coding 5.5 Working 5.6 Observation 5.7 Experimental Results 5.8 Future Scope of Proposed System	24 25 26 28 29 31 32
	Conclusion References	33 34

CHAPTER 1

INTRODUCTION

Temperature measurement in today's industrial environment encompasses a wide variety of needs and applications. Temperature is a very critical and widely measured variable for most mechanical engineers. To a medical practitioner's temperature is a fundamental quantity that must be measured in order to attain a healthy life in the world of medicine but in the world of engineering temperature is either conserved for the purpose of effective work or release not to damage the job. The need to measure and quantify the temperature of something started around 150 AD when Galen determined the 'complexion of someone based on four observable quantities. The actual science of 'thermometry' did not evolve until the growth of the sciences in the 1500's the first actual thermometer was an air-thermoscope described in Natural Magic (1558, 1589), which all led to the development of thermometer. The first calibrated thermometer was the liquid in glass thermometer which was later divided into mercury in glass thermometer and alcohol in glass thermometer. During the invention of this thermometer some facts were not in place which led to their disadvantages and with the aid of technological advancement digital thermometer came into existence. Microcontroller based temperature measurement in today's environment encompasses a wide variety of needs and applications. To meet this wide array of needs the process controls industry has developed a large number of sensors and devices to handle this demand. In this project we will be using LM35 temperature sensors thus , will be able to understand the concepts and use of the LM35 sensor all together . In advancement in technology, digital thermometers can be added to home automation utilises, IOT service for medical records, industrial jobs and many more.

1.1 LITERATURE REVIEW

Literature review is an assignment of previous tasks done by some authors and collection of information or data from research papers published in journals to progress our task. It is a way through which we can find new ideas, concept. There is a lot of literature published before on the same task; some papers are taken into consideration from which idea of the project is taken. [1].

Microcontroller can be regarded as a single-chip special-purpose computer dedicated to executing a specific application. As in general purpose computers,a microcontroller consists of memory (RAM, ROM, and Flash), I/O peripherals, and processor core. However, in a microcontroller, the processor core is not as fast as in a general purpose-computer, the memory size is also smaller. Microcontroller has been widely used in embedded systems such as, home appliances, vehicles, and toys. There are several microcontroller products available in the market, for example, Intel's MCS-51 (8051 family), Microchip PIC, and Atmel's Advanced RISC Architecture (AVR). We mention Atmel ATmega8535 and LM35 temperature sensor in this project.

CHAPTER 2

EXISTING SYSTEM OF THERMOMETERS

2.1 Thermometers

A thermometer is a device used to measure the temperature of any particular device or living body and displays the reading. A thermometer scale can be in Fahrenheit or Celsius.

2.11 Conventional thermometers used earlier are

1.Bulb or Mercury Thermometers

These thermometers consist of a sealed glass tube with a bulb-like glass container at the end. It works on the principle that liquids expand on getting heated. However, a disadvantage of these thermometers is that they can measure temperature only up to a certain extent.



Fig: 1 :Mercury Thermometer

2.Bimetallic Thermometers:

These thermometers consist of two metals joined together and as these metals get heated, they get expanded at different rates causing the bending of either of the metals. This bimetallic strip is attached to a dial with a calibrated temperature scale to indicate the

readings. However, these systems are also easily prone to breakage. The calibration is not accurate and can change easily.

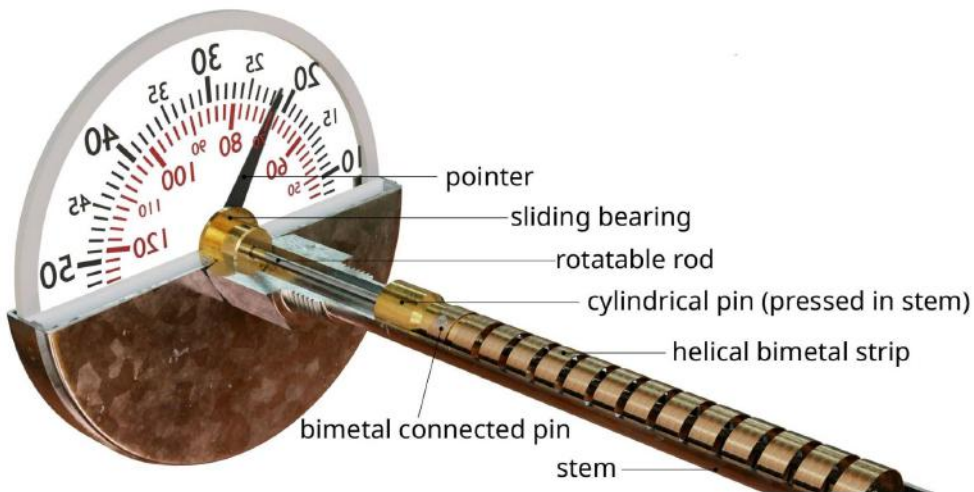


Fig 2:Bimetallic Thermometers

2.12 Digital Thermometer

It consists of a thermistor to sense the temperature and an electronic display of the temperature. Digital thermometers are used orally, rectally, or under the arm. It can read the temperature from 94°F to 105°F .



Fig 3 : Digital Thermometer

Principle of Working:

The digital thermometer basically consists of a sensor that measures the change in resistance due to heat and converts this change in resistance to temperature. It relies on the principle that

the electrical resistance of metal changes with temperature. All the sensors work by producing a resistance, current or voltage in reaction to a change in temperature. These changes are referred to as analogue output signal.

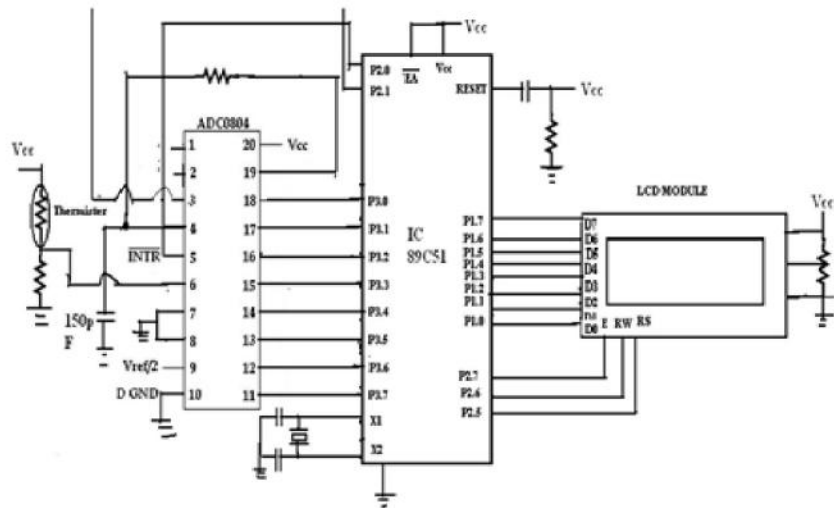


Fig 4:Digital Thermometer Circuit

2.12.1 Digital Thermometer components:

- 1.Battery: It is a button cell LR41 battery made up of metal and provides around 1.5V supply to the thermometer.
- 2.Body: The body of the thermometer is made up of hard plastic and is 100.5mm long and its width varies from bottom to top, with the bottom being thinner.
- 3.Thermistor: It is a semiconductor material made up of ceramic and is used to sense the temperature. It is placed at the tip of the thermometer by binding with epoxy and is enclosed inside a cap made up of stainless steel.
- 4.LCD: It is the display of the thermometer and measures around 15.5mm long and 6.5mm wide. It displays the reading for 3 seconds and then starts flashing indicating the next temperature to be measured.
- 5.Circuit: It consists of an ADC and a microcontroller along with some passive components.

2.12.2 Modern Available Digital Thermometers:

- 1.Digital Thermometer ref ECT-1: It measures temperature from 32°C to 42°C with an accuracy of 0.1°C. It is used mainly in medical applications.
- 2.Digital Thermometer Model Number: EFT-3: It measures temperature from 50°C to 125°C. It is used to measure the temperature of solid and liquid food
- 3.Thermolab digital thermometer IP65: It measures temperature range from 50 to 200 °C with an accuracy of +/-1°C.

2.2 Advantages of Digital Thermometers:

- Accuracy: The temperature reading doesn't depend on scale reading and instead shown directly on the display. Hence temperature can be read exactly and accurately.
- Speed: Digital thermometers can reach a final temperature in 5 to 10 seconds compared to conventional thermometers.
- Safety: Digital thermometers don't use mercury, hence the hazards of mercury are eliminated in case the thermometer breaks.
- Strong: The thermometer doesn't need to be shaken for the proper mercury level, hence the risk of the tube getting broken is eliminated.

2.3 Applications of Digital Thermometer:

- Medical Applications: The digital thermometers are used to measure human body temperature around 37°C. These thermometers are mostly probe type or ear type. It measures oral, rectal, and armpit body temperature.
- Marine Applications: Digital thermometers with a high-temperature exhaust gas sensor as the temperature sensor can be used in marine applications for measuring the local temperature.
- Industrial Applications: Digital thermometers are also used in power plants, nuclear power plants, blast furnaces, shipbuilding industries, etc. They can measure temperature from -220°C to +850°C

CHAPTER 3

PROPOSED SYSTEM

The proposed system is to design a Digital Thermometer using Arduino and LM35 Temperature Sensor that is more accurate, precise, cost effective and efficient compared to the existing system. In the proposed system, digital temperature sensor with Arduino Uno is used to control the whole process. Temperature measurement in today's industrial environment encompasses a wide variety of needs and applications. Industry has developed a large number of sensors and devices to handle this demand. An LM35 temperature sensor is used for sensing environment temperature which gives 1 degree temperature on every 10mV change at its output pin. The measured temperature will be directly displayed on a 16*2 LCD. Here LM35 is capable of reading the temperature in Centigrade scale. The output voltage of the sensor is directly proportional to temperature in Centigrade scale. Also there is no need of physical contact to measure temperature. The work is accomplished by proper mounting of the circuit and execution.

3.1 Advantages of the system

The LM35 series are precision integrated-circuit temperature devices that have an advantage over linear temperature sensors calibrated in Kelvin, as the user is not required to subtract a large constant voltage from the output to obtain convenient Centigrade scaling. The LM35 sensor has low-output impedance and precise inherent calibration which makes interfacing to readout or control circuitry especially easy. The device is used with single power supplies, or with plus and minus supplies and most suitable for remote applications. It is easily applied in the same way as other integrated-circuit temperature sensors. Glue or cement the device to a surface and the temperature should be within about 0.01°C of the surface temperature. Typically operates from 4 to 30 volts and draws only $60 \mu\text{A}$ from the supply, and has a very low self-heating of less than 0.1°C in still air. We can monitor temperature or can make a power cut off when heat exceeds above limits using this digital thermometer and can be used in multiple ways. The small size of the sensor makes it useful for a wide range of application. The LM35 is a very popular sensor hence its very easy to use and has varied applications. It does not need any additional circuit to be used. It is powered directly from a 5V source and delivers an analog output between 0V to 1.5V. This analog voltage can be read

by the ADC from a microcontroller like PIC or Arduino, Can be used to measure skin temperature and also to measure liquids temperature but covering the pins with water proof materials, can be used in transportation vehicles to determine the icing conditions of the road. Based on the readings of the thermometer, the air conditioning systems, heating and cooling systems can be controlled either manually or automatically. Sensor is small so it can be used in a wide variety of applications *viz* thermometers, thermostats, monitoring systems, home automation utilises, IOT service for medical records, industrial jobs also in restaurants and schools.^[2]

3.2 ADVANTAGES AND ECONOMIC IMPORTANCE OF DIGITAL THERMOMETER:

- Digital thermometer can accurately take, decide and measure temperature with the aid of a temperature sensor and digital display.
- Digital thermometer is easier to read compare to glass thermometer
- Digital thermometers are fast, accurate and convenient for use.
- In digital thermometers using Arduino UNO and LM35 the temperature is calculated by converting it from volt to Celcius , making it more accurate.
- Digital thermometer has a wide range of applications, it is usually applied to measure gas, liquid and solid temperature. In numerous fields, it can be applied in several areas such as the Hospital, restaurant and schools.

CHAPTER 4

OVERVIEW OF COMPONENTS

The following table shows the hardware and software components required to design the room model of the proposed system of digital thermometer.

Hardware components	Software components
<ul style="list-style-type: none">● Arduino UNO R3 Development Board● LM35 Analog Temperature Sensor● LCD Display● 10k Potentiometer● 2 Breadboards● Connecting wires● Personal computer or laptop	<ul style="list-style-type: none">● Arduino IDE(Integrated Development Environment)for arduino board programming version-1.8.14.0

Table 1.0 : Hardware and software components

4.1 Hardware specifications

These are the hardware components used to implement the proposed system of Digital thermometer :-

4.11 ARDUINO UNO R3

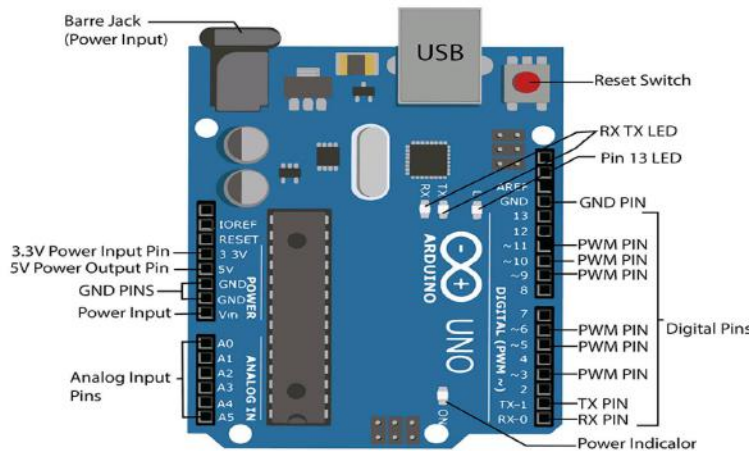


Fig 4.1 Arduino Board

Arduino UNO is a largely and most widely used microcontroller based on ATMEGA328P, which was developed by Arduino.cc. The board has both the set of digital and analog input/output pins. The board contains 14 digital pins and 6 analog pins. It is programmable with Arduino IDE(Integrated development environment)based on the programming languages,C and C++. It can be powered by the USB cable or by an external battery. The main advantage of using arduino UNO is that you can directly load the programs into the device without the need of a hardware programmer to burn the program.^[3]

Features Of Arduino Uno Board Microcontroller ATmega328.

- Operating Voltage 5V
- Input Voltage (recommended) 7-12V Input Voltage (limits) 6-20V
- Digital I/O Pins 14 (of which 6 provide PW output)
- Analog Input Pins 6 DC Current per I/O Pin 40 mA
- DC Current for 3.3V Pin 50 mA

- Flash Memory 32 KB (ATmega328) of which 05
- KB used by bootloader SRAM 2 KB (ATmega328)
- EEPROM 1 KB (ATmega328) Clock Speed 16 MHz

4.12 LM35 TEMPERATURE SENSOR

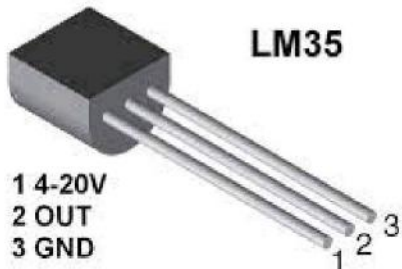


Fig 4.2 LM35 TEMPERATURE SENSOR

LM35 sensor is a temperature measuring device having an analog output voltage proportional to the temperature. It provides output voltage in Centigrade (Celsius). It does not require any external calibration circuitry. The sensitivity of LM35 is 10 mV/degree Celsius.^[5] As temperature increases, output voltage also increases. It is a 3-terminal sensor used to measure surrounding temperature ranging from -55 °C to 150 °C. LM35 gives temperature output which is more precise than thermistor output.

FEATURES:

- | | |
|---|---|
| • Calibrated Directly in Celsius (Centigrade) | • Low Self-Heating, 0.08°C in Still Air |
| • Linear + 10-mV/°C Scale Factor | • Non-linearity Only $\pm\frac{1}{4}^{\circ}\text{C}$ Typical |

- 0.5°C Ensured Accuracy (at 25°C)
- Rated for Full –55°C to 150°C Range
- Suitable for Remote Applications
- Low-Cost Due to Wafer-Level Trimming
- Low-Impedance Output, 0.1 Ω for 1-mA load
- Less than 60-µA Current Drain
- Operates from 4 V to 30 V

WORKING:

LM35 output voltage is proportional to centigrade/Celsius temperature. LM35 Celsius/centigrade resolution is 10mV. 10mV represents one degree centigrade/Celsius. So if LM35 outputs 100mV the equivalent temperature in centigrade/Celsius will be $100/10 = 10$ centigrade/Celsius. LM35 can measure from -50 degree centigrade/Celsius up to 150 degree centigrade/Celsius.

Arduino analog pin is used to read the analog output signals from the sensor. The circuit diagram of the project is given below. To Pin#1 of LM35 apply 5V, make Pin#2 ground, and the third one the middle pin is the output pin. It gives a voltage signal that is actually the temperature of the particular place.

Note: LM35 is an absolute temperature sensor. It can only measure the temperature of the surroundings within the circle of between 100 to 500 feet. So if you are using the internet and you are matching your temperature reading from the one that is given for your city on a weather forecast site then your reading will not be the same as theirs. It will be near but not the same.

LM35 TEMPERATURE SENSOR VOLTAGE TO TEMPERATURE CONVERSION

Now one of the most difficult thing is how to convert the voltage generated/output by the LM35 at output in Celsius or Fahrenheit scales. Well this needs you to first go through the data sheet of the temperature sensor and know about the characteristics of the sensor.

LM35 Output temperature in Celsius form. It Increments the output by 1 on every 10 mV change in temperature.

- when the sensor outputs 500 mV voltage, the temperature in Celsius is 50 degree Centigrade.
- For 400 mV output temperature in Celsius is 40 degree centigrade.
- For 600 mV the temperature is 60 degree Celsius.

4.13 LCD DISPLAY

16×2 LCD is a basic 16 character by 2 line display Yellow/Green Backlight. Utilises the extremely most common HD44780 parallel interface chipset (datasheet). Even more, it has JHD162A Compatible Pinout Diagram, and Command Interface code is freely available. Finally, You will need 7 general I/O pins (If used in 4-bit Mode) to interface to this LCD screen. It also includes an LED back-light



Fig 4.3 LCD display.

Features of 16×2 Display LCD:

- Commonly Used in Student Project, College, copiers, fax machines, laser printers, industrial test equipment, networking equipment such as routers and storage devices
- LCD display module with Green/Yellow Backlight
- SIZE: 16×2 (2 Rows and 16 Characters per Row)
- Can display 2-lines X 16-characters
- Operate with 5V DC

- Wide viewing angle and high contrast
- Built-in industry standard HD44780 equivalent LCD controller

4.14 10K POTENTIOMETER

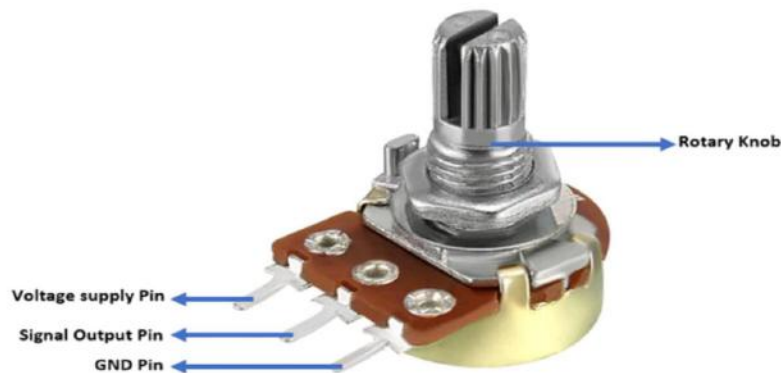


Fig 4.4 10K Potentiometer

These potentiometers are also commonly called a rotary potentiometer or just POT in short. These three-terminal devices can be used to vary the resistance between 0 to 10k ohms by simply rotating the knob.

4.15 BREADBOARD

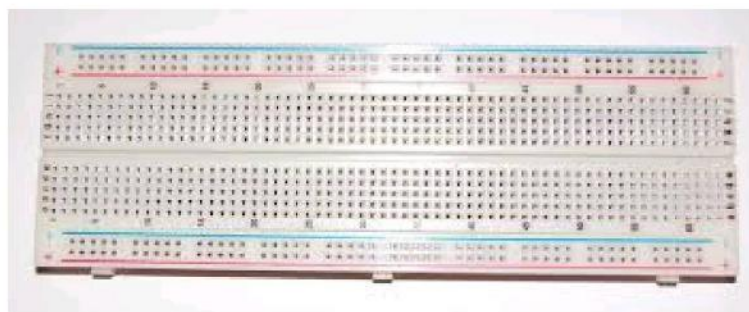


Fig 4.5 Breadboard

A Breadboard is a construction base for prototyping of electrons. The word referred to a literal breadboard , a polished piece of wood used for slicing bread. Later solderless breadboards became available which means it is reusable and this reason makes it popular among students for many projects. The bread board consists of clips which are called tie or contact points, the clips will be maintaining a gap of 2.54mm between each one of them. They are connected from one pin to another using metal strips.

4.2 Software specifications

The software needed to implement]digital thermometer using an Arduino and LM35 temperature sensor is Arduino IDE , or Integrated Development Environment ,version-1.8.14.0.The software is downloaded and installed on the PC or laptop. This is an open source software that makes it easy to write code to Arduino Uno.^[6] The programs written in this IDE are called sketches. The software can easily be downloaded from the official website ,www.arduino.cc. The software of the Arduino is well-suited with all kinds of in operation systems like Linux, Windows, and Macintosh, etc.Some of the basic functions of Arduino technology are,

- void setup()-It is technically a function that you create at the top of each program. Inside the curly brackets is the code that you want to run one time as soon as the program starts running.
- Void loop()-This is where the bulk of the Arduino sketch is executed
- digitalRead()- It reads the digital value of the given pin.
- digitalWrite()-It is used to write the digital value to the given pin.
- analogRead()-It reads the analog pin and returns the value.
- analogWrite()-It is used to write the analog value to the given pin.
- pinMode()- It is used to set the pin to I/O mode.

- Serial.begin(9600)- It is used to set the beginning of serial communication by setting the rate of bit.
- Serial.println()-It is used to print any message, any value of a variable or the values returned by the functions on the serial monitor, which is a screen that displays such information for the user.^[6,8]

Given below are the steps to upload a sketch to the arduino board:-

Step 1:Enter the code in the arduino IDE.

Step 2:Compile the program and correct the syntax errors.

Step 3:Connect the Arduino using the USB cable.

Step 4:Select the port.

Step 5: Choose the upload option to upload the sketch to the arduino UNO.



Fig 4.6:Arduino IDE software

CHAPTER 5

METHODOLOGY

5.1 CONSTRUCTION

Digital thermometer using an arduino uno board and LM35 temperature sensor is constructed in the following steps:

1. Interfacing of LM35 with arduino UNO

Output of the temperature sensor LM35 is given to the analog channel of the A1 of Arduino UNO for sensing real time temperature.

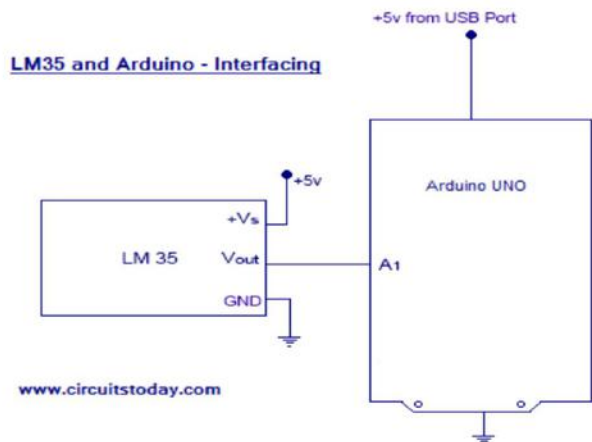


Fig 5.1 LM35 and Arduino interfacing

2. Interfacing arduino with LCD

Interfacing of Arduino with LCD is as shown in figure 5.2. Circuit diagram for Arduino based digital thermometer is shown in the figure. Here the 16x2 LCD unit is directly connected to Arduino in 4-bit mode. Data pins of LCD, namely RS, EN, D4, D5, D6, D7 are connected to Arduino digital pin number 7, 6, 5, 4, 3, 2. A temperature sensor LM35 is also connected to Analog pin A0 of Arduino, which generates 1 degree Celsius temperature on every 10mV output change at its output pin.^[7]

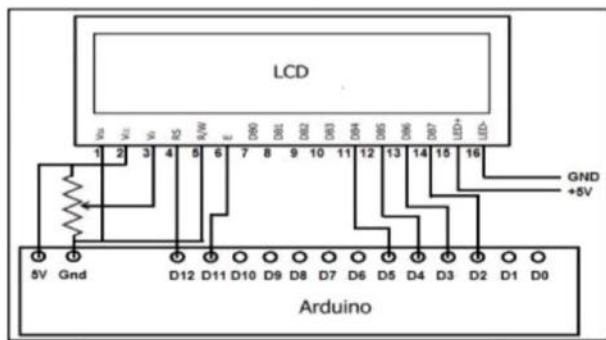


Fig 5.2 Arduino LCD circuit

5.2 DIGITAL THERMOMETER USING ARDUINO UNO , LM35 AND LCD CIRCUIT

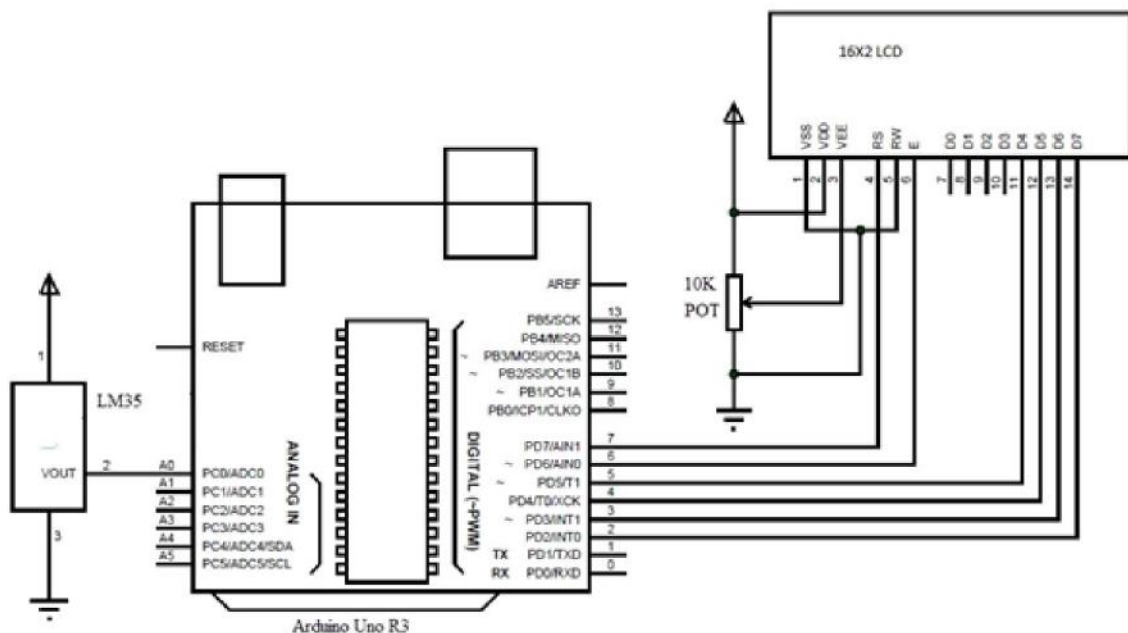


Fig 5.3 Circuit diagram for digital thermometer using Arduino UNO, LM35 and LCD

- Connect LCD PIN 1 to Ground and PIN 2 to Supply respectively.
 - Connect LCD PIN 3 to the 10K Potentiometer and connect the rest of the terminals to the ground.
 - Connect LCD PIN 15 to Ground and PIN 16 to Supply respectively.
 - Connect LCD PINS D4,D5,D6 and D7 to PINS 5 - 2 of the Arduino.
 - Connect LCD PIN 4(RS) to PIN 12 of the Arduino.

- Connect LCD PIN 5(RW) to Ground.
- Connect LCD PIN 6(E) to PIN 11 of the Arduino.
- Attach the LM35 to the Bread Board.
- Take the output of the LM35 i.e. PIN 2 of the LM35 and connect it to the Analog Input Ao of the Arduino.
- The Rest of the Connections made are to connect the Two Breadboards together.

5.3 LM35 VOLTAGE CONVERSION TO TEMPERATURE FORMULA / EQUATION DERIVATION FOR ARDUINO

LM35 Celsius/centigrade resolution is 10Mv

- Arduino analog pins can measure up-to +5 volts OR the voltage on which it is working normally +5 volts.
- The Arduino analog pin resolution is 1023 starting from 0. On +5 volts input it counts to 1023.
- LM35 max voltage output is 1500mV(At 150 degree centigrade). 1500mV is equal to $1500/1000 = 1.5$ volts. So LM35 at max outputs 1.5 volts.
- Arduino analog pin count for 1.5 volts equals to $(1.5 / 5)*1023 = 307.5$. At +5 volts it's 1023 and at 1.5 volts it's 307.5.
- New Arduino-LM35 Resolution = $307.5 / 150 = 2.048$. Now if the arduino analog pin counts 2.048 it is equal to 1 degree change in centigrade/Celsius temperature of LM35.

5.4 CODING

The code for Temperature Measurement using LM35 is simple. First we include a library for the LCD unit and then we define data and control pins for the LCD and temperature sensor. After getting analog value at an analog pin we read that value using the analog read function and store that value in a variable. And then convert the value into temperature by applying the below given formula.

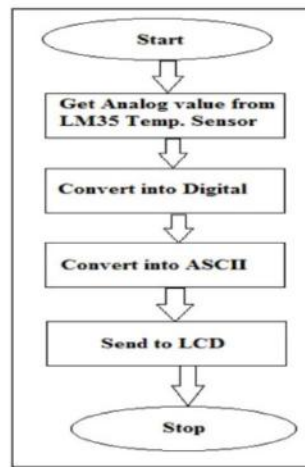


Fig 5.4 Software algorithm of arduino uno microcontroller

The temperature condition at any instant as sensed by the LM35 is displayed on a Liquid Crystal Display (LCD). To do this the Arduino UNO is programmed to copy the output of the ADC (which is inbuilt ADC) and convert the result to ASCII then transfer to the LCD to be displayed. The flow chart in the figure shows the software algorithm of the Arduino UNO microcontroller.

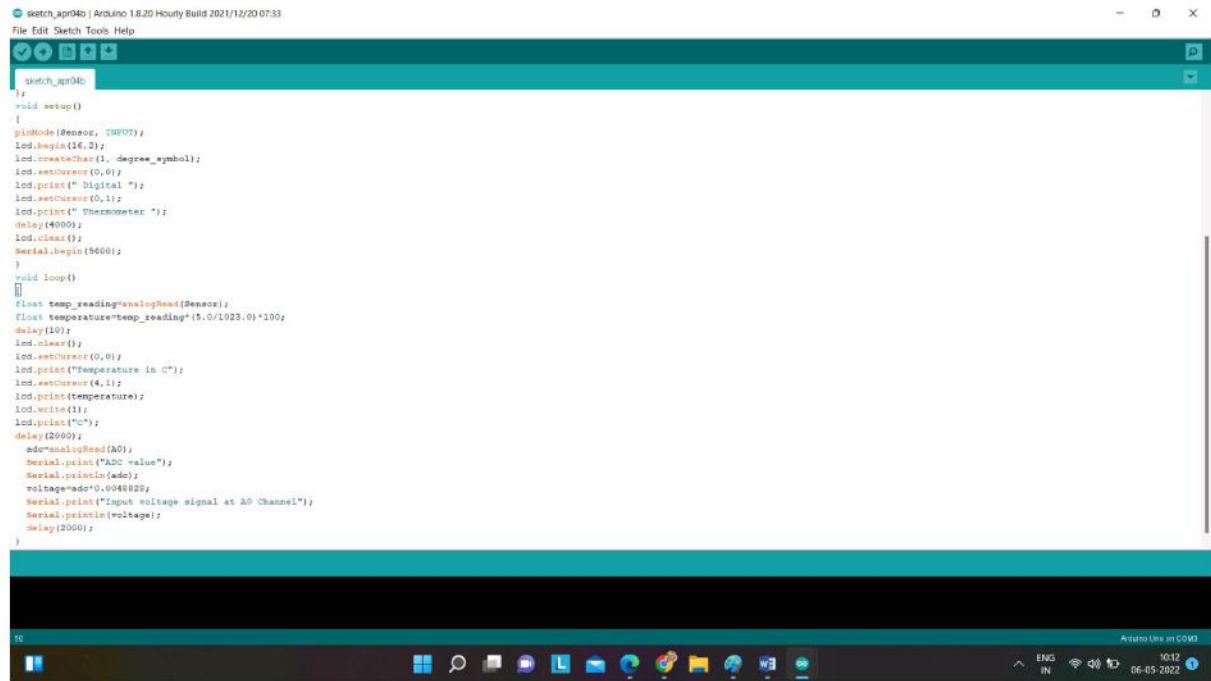
The code that we used is given below:

```

sketch_apr04b | Arduino 1.8.20 Hourly Build 2021/12/20 07:33
File Edit Sketch Tools Help
sketch_apr04b
#include<LiquidCrystal.h>
LiquidCrystal lcd(12,11,5,4,3,2);
const int Sensor = A0;
int adc=0;
float voltage=0;
byte degree_symbol[8] =
{
  0b00111,
  0b00100,
  0b00111,
  0b00000,
  0b00000,
  0b00000,
  0b00000,
  0b00000
};
void setup()
{
pinMode(Sensor, INPUT);
lcd.begin(14,2);
lcd.createChar(1, degree_symbol);
lcd.setCursor(0,0);
lcd.print(" Digital ");
lcd.setCursor(0,1);
lcd.print(" Thermometer ");
delay(4000);
lcd.clear();
Serial.begin(9600);
}
void loop()
{
float temp_reading=analogRead(Sensor);
float temperature=temp_reading*(5.0/1023.0)*100;
delay(10);
}

```

Fig 5.5 Programme code(a)



```
sketch_apr04b | Arduino 1.8.20 Hourly Build 2021/12/20 07:33
File Edit Sketch Tools Help
sketch_apr04b
/*
void setup()
{
pinMode(Sensor, INPUT);
lcd.begin(16,2);
lcd.createChar(1, degree_symbol);
lcd.setCursor(0,0);
lcd.print(" Digital ");
lcd.setCursor(0,1);
lcd.print(" Thermometer ");
delay(4000);
lcd.clear();
serial.begin(9600);
}
void loop()
{
float temp_reading=analogRead(Sensor);
float temperature=temp_reading*(5.0/1023.0)*100;
delay(10);
lcd.clear();
lcd.setCursor(0,0);
lcd.print("Temperature in C");
lcd.setCursor(4,1);
lcd.print(temperature);
lcd.write(1);
lcd.print("C");
delay(2000);
adcValue=analogRead(A0);
serial.print("A0c value");
serial.println(adcValue);
voltage=adc*0.0048828;
serial.print("Input voltage signal at A0 Channel");
serial.println(voltage);
delay(2000);
}

```

Fig 5.6 Programme code(b)

5.5 WORKING

A high precision digital thermometer is designed in this project. It is constructed with simple components like Arduino, LM35 temperature sensor and an LCD display. The working of the circuit is very simple and is explained below.

Once the connections are completed and the coding is done, the USB pin of the arduino UNO is connected to a computer. The temperature sensor i.e. LM35 continuously monitors the room temperature and gives an analogue equivalent voltage which is directly proportional to the temperature. This analogue data is given to Arduino through A0. As per the code written, the Arduino converts this analogue voltage value to digital temperature readings. This value is displayed on the LCD. Our Arduino Uno has an in-built 10 bit ADC (6 channel). We can make use of this inbuilt ADC of arduino to convert the analog output of LM35 (or other device/sensor) to digital output. As Arduino Uno has a 6 channel inbuilt ADC, there are 6 analog input pins numbered from A0 to A5. You can connect an analog output of LM35 to any of these analog input pins of an arduino but we are using A0 for now.

The rate of change of temperature capture can be programmed in the code. The output displayed on the LCD is an accurate reading of temperature in centigrade.^[8]

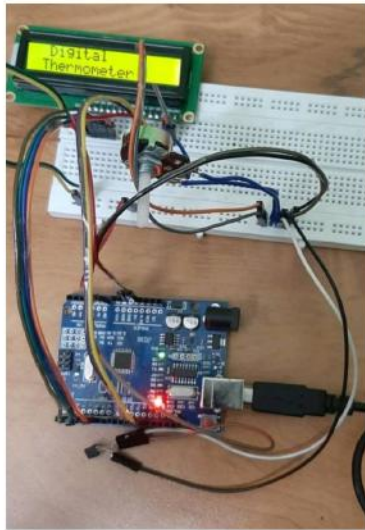


Fig 5.7 Constructed Circuit (a)

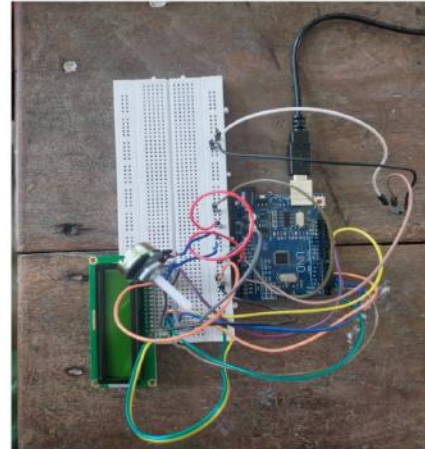


Fig 5.8 Constructed Circuit(b)

5.6 OBSERVATION

If we need to measure the temperature of a specific object, for example if we need to measure the temperature of the soldering iron, we have to place it on the tip of the LM35 temperature sensor, now we will be able to see the increase in temperature on the LCD screen. Similarly, if we remove the soldering iron from the tip of the LM35 temperature sensor, we will be able to observe the decrease in temperature on the LCD screen.

Actual Temperature	Temperature using the constructed Digital Thermometer	Difference	Percentage Error
36.9	36.1	0.8	2.17%
35.4	34.2	1.2	3.39%
37.7	36.6	1.1	2.92%
39.2	38.3	0.9	2.29%

37	35.2	1.8	4.86%
37.6	36.3	1.3	3.45%

Table 5.1 Observation

The experimental observation shows the difference between constructed digital thermometer and the actual temperature. Also the percentage error of corresponding temperatures also identified.

SUBSTITUTION:

Difference = Actual temperature - temperature measured using the constructed digital

$$\text{Thermometer} = 36.9 - 36.1 = 0.8$$

$$\begin{aligned}\text{Percentage Error} &= (\text{Difference} / \text{Actual Temperature}) * 100 \\ &= (0.8 / 36.9) * 100 = 2.17\end{aligned}$$

$$\begin{aligned}\text{Average Percentage Error} &= (2.17 + 3.39 + 2.92 + 2.29 + 4.86 + 3.45) / 6 \\ &= 3.18\%\end{aligned}$$

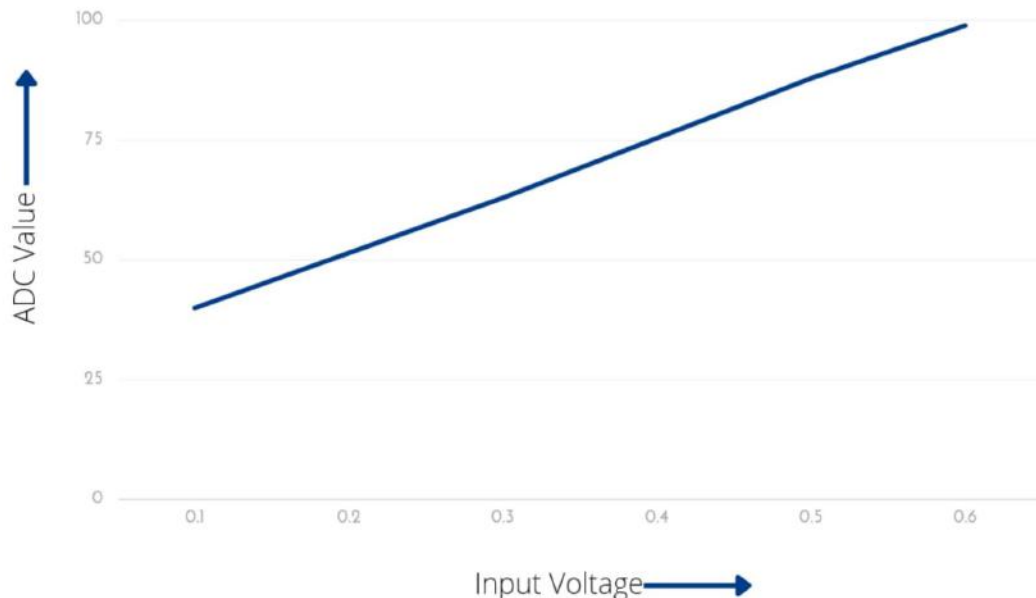
ADC Values

ADC value	Input Voltage
40	0.1955
63	0.3079
88	0.4301
99	0.4839
155	0.7576
177	0.8651

Table 5.2 ADC Value and Input Voltage

ADC vs VOLTAGE

The given graph plotted contains ADC value in X axis and input voltage in Y axis. An analogue to digital converter takes a snapshot of an analogue voltage at one instant in time and produces a digital output code which represents this analogue voltage.



5.7 EXPERIMENTAL RESULT

Practical test has been conducted to evaluate the real time performance of the constructed temperature sensor. The temperature using the constructed digital thermometer is noted. And the difference between actual temperature and using the constructed Digital thermometer is identified. The percentage error is calculated and the average percentage error is found out.

Average Percentage Error = 3.18%

5.8 FUTURE SCOPE OF THE PROPOSED SYSTEM

Thermometers are used in industries, weather studies, medicinal fields and scientific research. Measuring temperature is an important part of many applications. Maintaining precise temperatures in storage rooms, laboratories, incubators, etc. is of high priority.. Now a days, the use of digital thermometers is increasing as they are accurate and safe to use.Digital thermometers can furthermore be advanced into home automations, use in cold rooms, food temperature reserve and so on. Due to its accuracy, preciseness and low cost the proposed system can be used in many applications.

CONCLUSION

From the experimental results we can conclude that the proposed system is highly accurate and nullifies the effect of external parameters.Digital thermometer is a less hazardous instrument used for taking/recording temperature from a specific body. It works just like a liquid or glass thermometer but in a different way because of its accuracy in reading.LM35 sensor is a very handy component for making projects.The low price and accuracy reading make it popular in making projects.With the aid of advancing technology in the past few years, Digital thermometers will be advanced enough to end the error due to parallax reading in liquid in glass thermometers and also comfort the easy access and accurate reading of temperature.

REFERENCES

- [1] Oyebola, B. and Toluwan, O., 2017. LM35 Based digital room temperature meter: a simple demonstration. *Equatorial Journal of Computational and Theoretical Science*, 2(1).
- [2] Changela, B., Parmar, K., Daxini, B., Sanghani, K. and Shah, K., 2016. Digital thermometer: design & implementation using arduino UNO based microcontroller. *IJSRD-International Journal for Scientific Research & Development*, pp.1-2.
- [3] Bajaj, K.A. and Mote, T.S., 2013. Review on intelligent street lightening system. . *International Journal of Science and Research (IJSR)*.
- [4]<https://www.electronicshub.org/arduino-based-digital-thermometer/>
- [5]<https://www.electronicwings.com/sensors-modules/lm35-temperature-sensor>
- [6]<https://www.elprocus.com/digital-thermometers/>
- [7]<https://www.circuitschools.com/build-digital-thermometer-using-lm35-and-arduino/>
- [8]<https://how2electronics.com/digital-thermometer-arduino-lm35-temperature-sensor/>

Project Report

On

AN INTRODUCTION TO FRACTALS

Submitted

in partial fulfilment of the requirements for the degree of

BACHELOR OF SCIENCE

in

MATHEMATICS

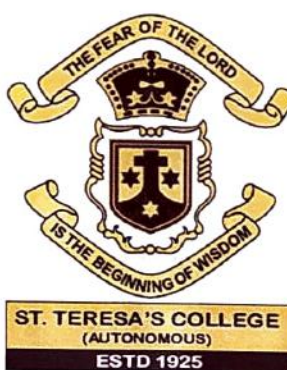
by

AISWARYA PS

(Register No.AB19AMAT036)

Under the Supervision of

SUSAN MATHEW

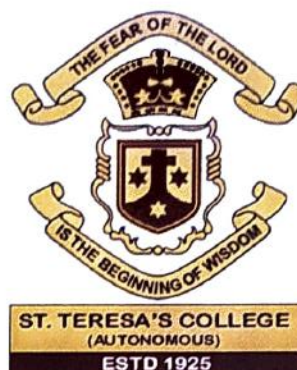


DEPARTMENT OF MATHEMATICS

ST. TERESA'S COLLEGE (AUTONOMOUS)

ERNAKULAM, KOCHI - 682011

APRIL 2022



CERTIFICATE

This is to certify that the dissertation entitled, **AN INTRODUCTION TO FRACTALS** is a bonafide record of the work done by Ms. **AISWARYA PS** under my guidance as partial fulfilment of the award of the degree of **Bachelor of Science in Mathematics** at St. Teresa's College (Autonomous), Ernakulam affiliated to Mahatma Gandhi University, Kottayam. No part of this work has been submitted for any other degree elsewhere.

Date:06/04/2022

Place: Ernakulam

Susan Mathew

Assistant Professor,
Department of Mathematics,
St. Teresa's College(Autonomous),
Ernakulam.



Ursala

Dr.Ursala Paul
Assistant Professor and Head ,
Department of Mathematics,
St. Teresa's College(Autonomous),
Ernakulam.

External Examiners

1:.....Tume....Jax....*J...m...*

2:

DECLARATION

I hereby declare that the work presented in this project is based on the original work done by me under the guidance of Susan Mathew, Assistant Professor, Department of Mathematics, St. Teresa's College(Autonomous), Ernakulam and has not been included in any other project submitted previously for the award of any degree.



Ernakulam.

AISWARYA PS

Date:06/04/2022

AB19AMAT036

ACKNOWLEDGEMENT

For any accomplishment or achievement, the prime requisite is the blessing of the Almighty and it's the same that made this world possible. We bow to the lord with a grateful heart and prayerful mind. It is with great pleasure that we express our sincere gratitude to our beloved teacher Ms. Susan Mathew , Department of Mathematics, St. Teresa's College, for her overwhelming support, motivation and encouragement.

We would like to acknowledge our deep sense of gratitude to Dr. Ursala Paul, Head of Department of Mathematics and all the faculty members of the department and our friends who helped us directly and indirectly through their valuable suggestions and self-criticisms, which came a long way in ensuring that this project becomes a success.

Ernakulam.

AISWARYA PS

Date:06/04/2022

AB19AMAT036

Contents

<i>CERTIFICATE</i>	ii
<i>DECLARATION</i>	iii
<i>ACKNOWLEDGEMENT</i>	iv
<i>CONTENT</i>	v
1 INTRODUCTION	1
1.1 PRELIMINARY ANALYSIS	2
2 A CHAOTIC OUTLINE	3
2.1 CHAOS THEORY	3
2.2 FAMOUS SETS IN CHAOS THEORY	4
3 FRACTALS	7
3.1 CHARACTERISTICS OF FRACTALS	7
3.2 SPECIFIC FUNCTION FRACTALS	9
3.2.1 SIERPINSKI TRIANGLE	9
3.2.2 VON KOCH CURVE	10
3.2.3 CANTOR SET	11
4 FRACTAL DIMENSION	13
4.1 SELF-SIMILARITY DIMENSION	13
4.2 BOX DIMENSION	14
5 APPLICATION OF FRACTALS	17
5.1 FRACTALS IN BIOLOGICAL SCIENCE	17
5.2 FRACTALS IN HUMAN BODY	17
5.2.1 THE LUNGS	17
5.2.2 THE BRAIN	18

5.2.3 MEMBRANES	19
5.3 FRACTAL ART	19
5.4 FRACTALS IN ECONOMY	19
5.5 FRACTALS IN NATURE	20
5.6 FLUID MECHANICS	21
6 CONCLUSION	22
REFERENCES	24

Chapter 1

INTRODUCTION

Many people are fascinated by the beautiful images termed Fractals. Extending beyond the typical perception of mathematics as a body of complicated, boring formulas, fractal geometry mixes art with mathematics to demonstrate that equations are more than just a collection of numbers. What makes fractals even more interesting is that they are best existing mathematical description of many natural forms, such as coast lines, mountains or parts of living organisms. . . . In mathematics, any of a class of complex geometric shapes commonly have fractional dimension, a concept of first introduced by the mathematician Felix Hausdorff in 1918. Although fractals are closely connected with computer techniques, some people had worked on fractals long before the invention of computer. Those people were British cartographers. Who encountered the problem in measuring the length of the Britain Coast? The coastline measured on a large-scale map was approximately half the length of the coastline measured on a detailed map. The closed they looked, the more detailed and longer the 2 coastline became. They did not realize that they had discovered one of the main properties of fractals.

1.1 PRELIMINARY ANALYSIS

COMPLEX NUMBERS

Complex numbers are the numbers that are expressed in the form of $a+ib$ where a,b are real numbers and "i" is an imaginary number.

CANTOR SET

cantor set is a closed set consisting entirely of boundary points. It is the set of all numbers 0 and 1 expressible without 1's in it's base expansion.

Chapter 2

A CHAOTIC OUTLINE

To understand the significant of fractals and their role in modern mathematics, it is to know something about the area of scientific and mathematics inquiry known as chaos theory. The importance of this new area, together with the excitement and frustrations experienced by scientists and the mathematicians as they made their initial discoveries, often without knowledge of other related work is wonderfully portrayed in James Gleick's *Chaos: Making a new science*. Gleick suggests that chaos is "a new science of the global nature of systems" Chaotic behavior exists in many natural systems such as weather and climate.

2.1 CHAOS THEORY

BUTTERFLY EFFECT:

1. This is the defining property of chaotic system.
2. In chaos theory, the butterfly effect is the sensitive dependence on initial condition in which a small change in one state of a deterministic nonlinear system can result in large differences in a later state.
3. The term is closely associated with the work of mathematician and meteorologist Edward Lorenz. He noted that butterfly effect is derived from the metaphorical example of the details of a tornado (the exact time of formation, the exact path taken) being influenced by minor perturbations such as a distant butterfly flapping its wings several weeks earlier.

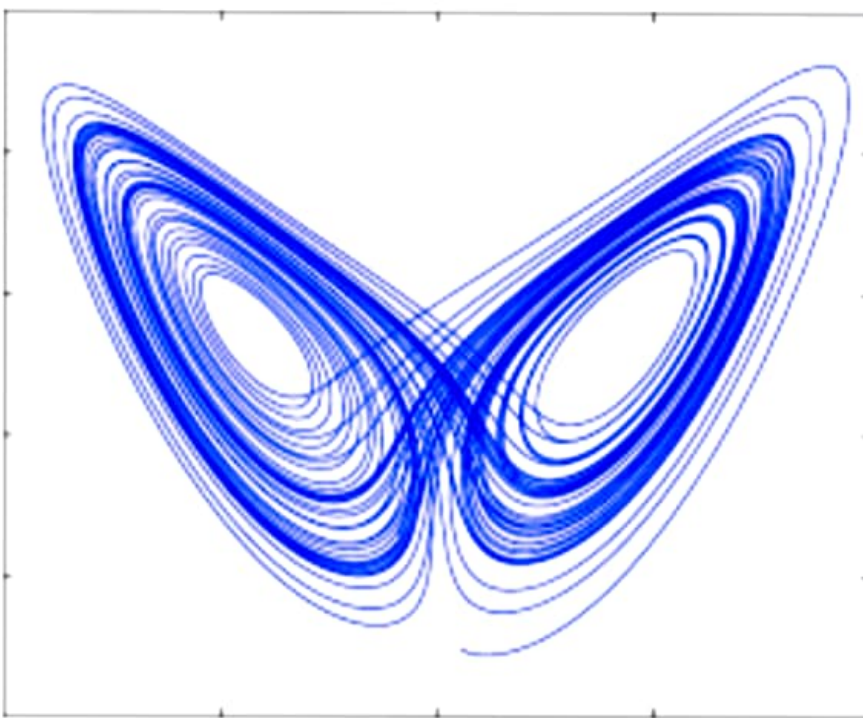


Figure 2.1: butterfly effect

2.2 FAMOUS SETS IN CHAOS THEORY

Chaos theory is a part of mathematics. It looks at certain systems that are very sensitive. A very small change may make the system behave completely differently. The collection of sets that play significant role in chaos theory, namely Julia sets and the even more well-known Mandelbrot set. Julia sets are named after the French mathematician Gaston Julia, invented and studied these sets in the early 20th century. The Mandelbrot set is named after the contemporary French mathematician Benoit Mandelbrot whose work from the 1950s through the 1970s at IBM in New York is generally recognized as the foundation of fractal geometry. With this connection, it is most appropriate that the Mandelbrot set has become a “logo” for fractal geometry and chaos theory.

MANDELBROT SET

1. Mandelbrot set is the set of complex numbers C for which the function $f(z) = z^2 + C$ does not diverge to infinity at $z=0$, that is, sequence

remain unchanged at absolute value. The points of the Mandelbrot set have been colored black. It is also possible to assign color to the point outside the Mandelbrot set. Theirs color depend on how many iterations have been required to determine that they are outside the Mandelbrot set.

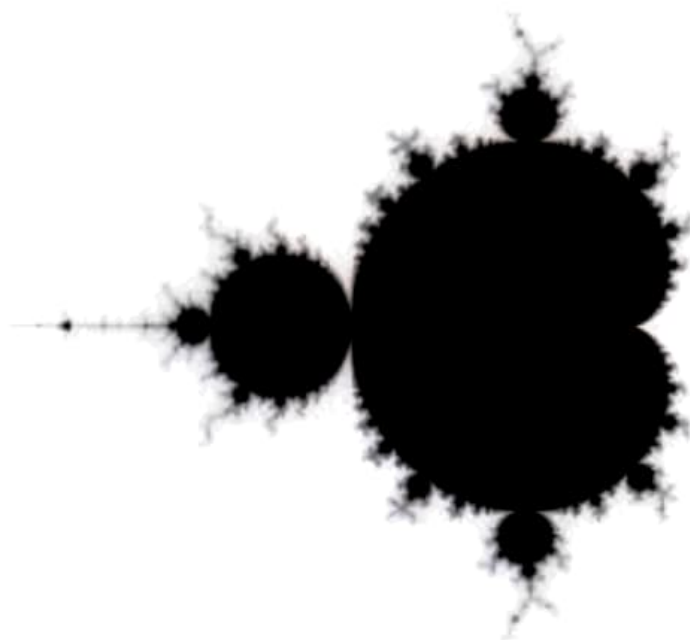


Figure 2.2: mandelbrot set

JULIA SET

1. Julia set consists of values such that an arbitrarily small perturbation can cause drastic changes in the sequence of iterated function values. Thus the behaviour of Julia set is chaotic. The boundary between points in the Co number plane that diverge to infinity and those that finite under repeated iteration of same mapping.

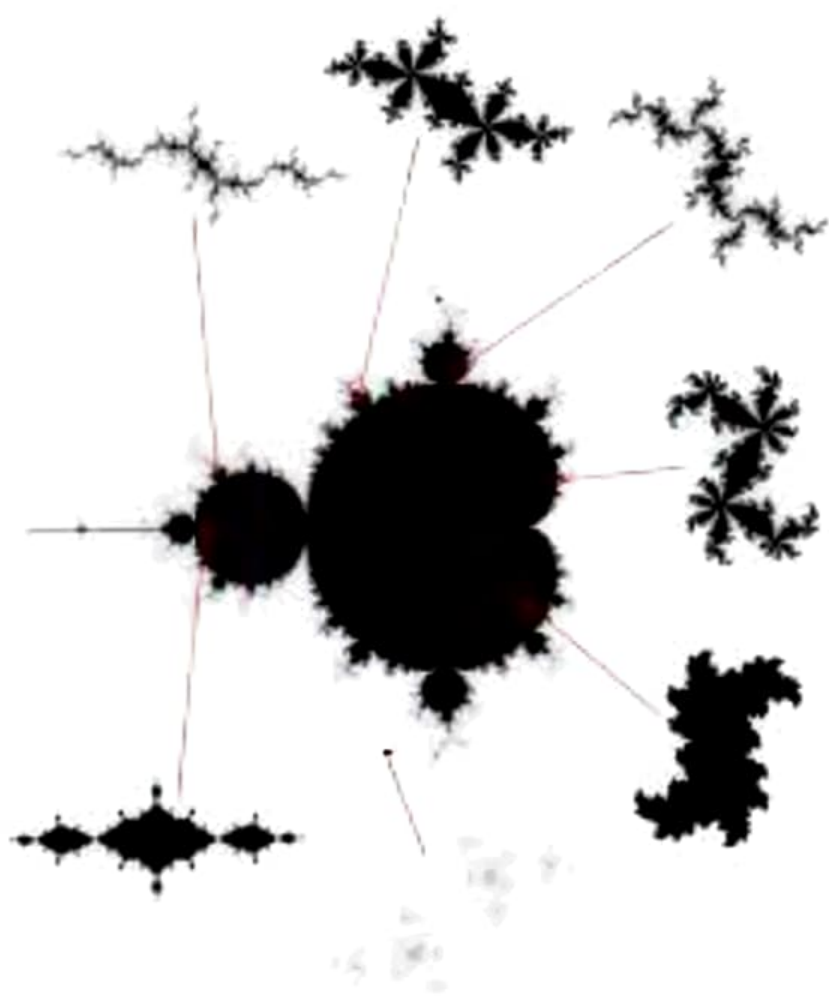


Figure 2.3: julia set

Chapter 3

FRACTALS

Fractal is a new branch of mathematics and art. Perhaps this is the reason why most people recognize fractals only as pretty pictures useful as background on the computer screen or original postcard patterns. The term "FRACTALS" is derived from the Latin word "fractus" which means fragmented or broken. A fractal is a never-ending pattern. Fractals are infinitely complex patterns that are self-similar across different scales. They are created by repeating a simple process over and over in an ongoing feedback loop. Fractal patterns are extremely familiar, since nature is full of fractals. For instance: trees, rivers, coastlines, mountains, clouds, seashells, hurricanes etc.

DEFINITION 1: A complex geometric Pattern exhibiting self-similarity in those small details of its structure viewed at any scale repeat elements of the overall pattern

DEFINITION 2: MANDELBROT DEFINITION A fractal is a non regular geometric shape that has the same degree of non-regularity on all scales.

3.1 CHARACTERISTICS OF FRACTALS

Exact self-similarity: Identical at all scales

1. Fern possess exact self similarity.
2. Each fond branch is similar to the whole fond, and so on. In addition, as we move towards the top of the fern we see a smaller and



Figure 3.1: fern

smaller copy of the whole fern.

Quasi self-similarity :

Approximates the same pattern at different scales may contain small copies of the entire fractal in distorted and degenerate forms.

1. This is a looser form of self similarity.
2. The fractal appears approximately (but not exactly)

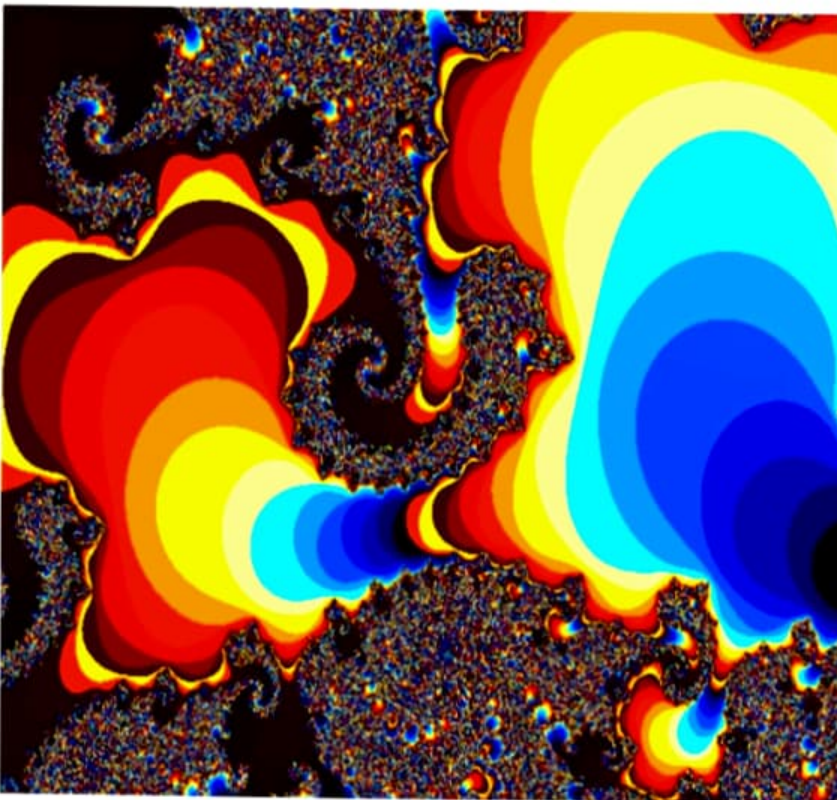


Figure 3.2: mandelbrot satellite

identical at different scales.

3. The Mandelbrot set is a quasi self-similar as the satellites are approximations of entire set but not exact copies.

3.2 SPECIFIC FUNCTION FRACTALS

ITERATED FUNCTION SYSTEM FRACTALS

1. In mathematics, iterated function systems (IFSs) are a method of constructing fractals; the resulting fractals are often selfsimilar. IFS fractals are more related to set theory than fractal geometry. They were introduced in 1981.

2. IFS fractals, can be of any number of dimensions, but are commonly computed and drawn in 2D. The fractal is made up of the union of several copies of itself, each copy being transformed by a function. The canonical example is the Sierpinski triangle. The functions are normally contractive, which means they bring points closer together and make shapes smaller.

3. Hence, the shape of an IFS fractal is made up of several possibly overlapping smaller copies of itself, each of which is also made up of copies of itself, ad infinitum. This is the source of its self-similar fractal nature.

3.2.1 SIERPINSKI TRIANGLE

The Sierpinski triangle (also called the Sierpinski gasket or the Sierpinski Sieve), is a fractal and attractive fixed set with the overall shape of an Equilateral triangle, subdivided recursively into smaller equilateral triangles. Originally constructed as a curve, this is one of the basic examples of self similar sets, i.e., it is a mathematically generated pattern that is reproducible at any magnification or reduction. It is named after the Polish Mathematician Wacław Sierpinski, but appeared as a decorative pattern many centuries before the work of Sierpinski. 1. Properties: For integer number of dimensions d , when doubling a side of an Object, 2^d Copies of it are created, i.e. 2 copies for 1- dimensional object, 4 Copies for 2- dimensional object and 8 copies for 3- dimensional object. For The Sierpinski triangle, doubling its side creates 3

copies of itself. Thus, the Sierpinski triangle has Hausdorff dimension $\log(3)/\log(2) = \log_2 3 \approx 1.585$, which follows from solving $2d = 3$ for d . The area of a Sierpinski triangle is zero. The area remaining after each iteration is clearly $\frac{1}{4}$ of the area from the previous iteration, and an infinite number of iterations results in an area approaching zero. The points of a Sierpinski triangle have a simple characterization in barycentric coordinates. If a point has coordinates $(0.u_1u_2u_3\dots 0.v_1v_2v_3\dots 0.w_1w_2w_3\dots)$ expressed as binary numerals, then the point is in Sierpinski's triangle if and only if $u_i + v_i + w_i = 1$ for all „ i “.

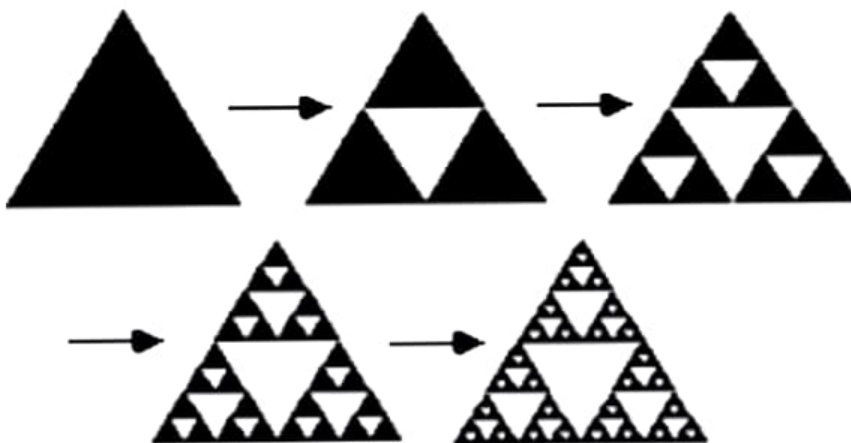


Figure 3.3: sierpinski triangle

3.2.2 VON KOCH CURVE

The genuine Von Koch curve, also called snowflake curve, is derived as the limit of a polygonal contour. At every step, the middle third of every side of the polygon is replaced with two linear segments at angles 60° and 120° . Starting from an equilateral triangle, the two first steps lead to the star-like curves plotted on the left. If one goes on long enough one finally gets the curve right below. Ideally, the process should go on indefinitely, but, in practice, the curve displayed on the screen no longer changes when the elementary side becomes less than the pitch, and then the iterations can be stopped. What is

thus obtained was long considered a mathematical monster, a curve plotted in a bounded domain, but with an infinite length (one easily sees that the length is multiplied by $4/3$ at every step), continuous but nowhere differentiable (i.e. nowhere a tangent can be defined). It is now regarded as an elementary example 14 of fractal –"elementary" because of the simplicity of the construction. The pattern motif can be seen everywhere along the curve, at every scale, from visible to infinitesimal. This feature is called self-similarity.

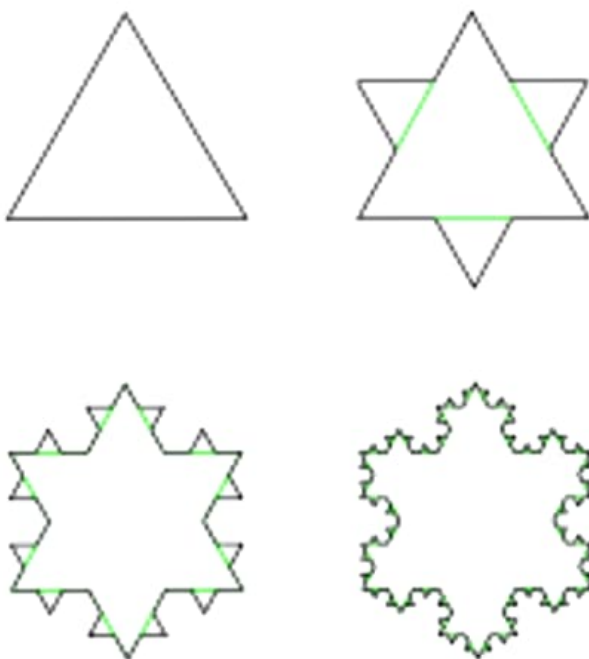


Figure 3.4: von koch curve

3.2.3 CANTOR SET

In mathematics, the Cantor set is a set of points lying on a single line segment that has a number of remarkable and deep properties. It was discovered in 1874 by Henry John Stephen Smith and introduced by German mathematician George Cantor in 1883. Through consideration of this set, Cantor and others helped lay the foundations of

modern point-set topology. Although Cantor himself defined the set in a general, abstract way, the most common modern construction is the Cantor ternary set, built by removing the middle thirds of a line segment. Cantor himself mentioned the ternary construction only in passing, as an example of a more general idea, that of a perfect set that is nowhere dense.

Chapter 4

FRACTAL DIMENSION

The fractal dimension of a set is a number that tells how densely the set occupies the metric space in which it lies. It is invariant under various stretching and squeezing's of the underlying space .Applying traditional method of size measurement to highly irregular fractals leads to a meaningless results. Instead, Mandelbrot and others discovered that to make any meaningful statement about the size of a fractal, they needed to resort to assigning it a dimension value; but in order to do so, concept of dimension had to be expanded. **SELF-SIMILARITY:** Fractals are self-similar at any level of magnification; many things around us look the same way no matter how you magnify them. When parts of some objects are similar to the entire object, we call it self-similar.

4.1 SELF-SIMILARITY DIMENSION

To assign fractals a self-similarity dimension, it is helpful to consider how segments, squares, and cubes can be tiled with a number of smaller tiles such that magnification of each tile by an integer scaling factor (using the same scaling factor for each tile) results in an object congruent to the original. To illustrate this, note that a segment can be tiled using two segment-shaped tiles (meeting at the midpoint of the original segment) so the magnification of each tile by each tile by the scaling factor 2 creates a segment congruent to the original. Similarly, a square can be tiled by four square shaped tiles so that magnification of each tile by four square shaped tiles so that magnification of each tile by the

scaling factor 2 (doubling each side) creates a square congruent to the original.

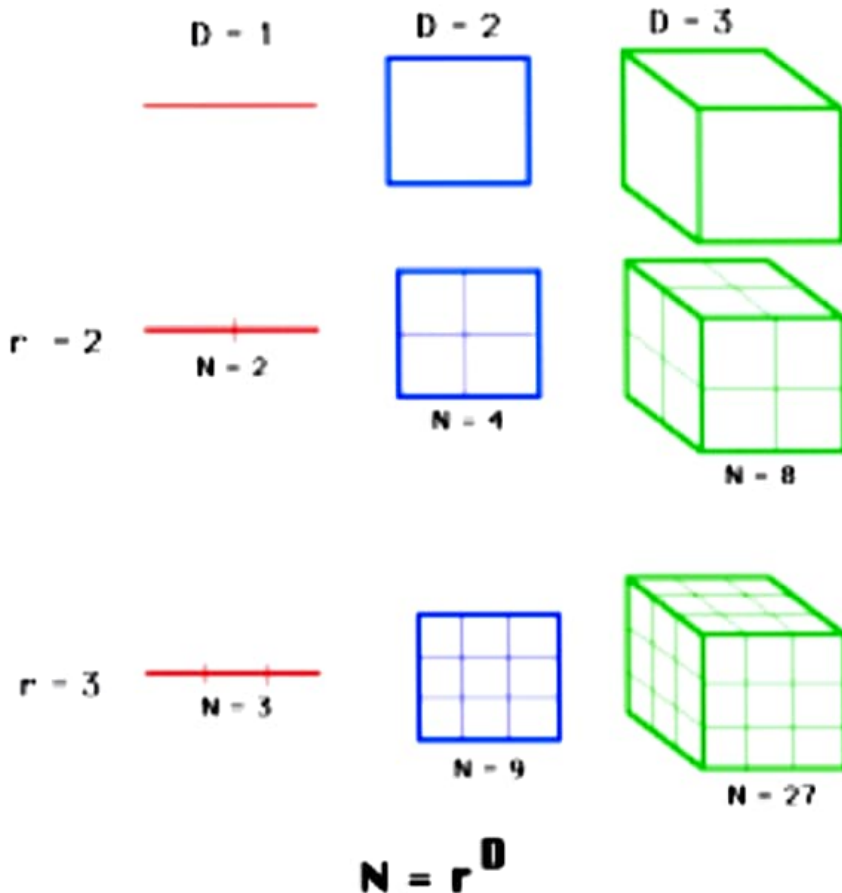


Figure 4.1: self-similarity dimension

4.2 BOX DIMENSION

Self-similarity dimension applies only to sets that are strictly self-similar; there are more generalized dimensions that can be applied to sets that are only "approximately" self-similar, including natural fractals like coastlines. One of these generalizations that move in the direction of the more esoteric Hausdorff-Besicovitch dimension is called box dimension. Here the term box refers to a segment, a square, or a cube, that is, a d-cube of the appropriate dimension d . To understand how box dimension generalizes self-similarity dimension, recall that the self-similarity dimension d of a set A given by the equation $N = s^d$, where s is the

scaling-factor and N is the number of tiles in an s -scale tiling of A . solving for d yields, Self-similarity dimension: $ds = \ln N / \ln s$ (1) when a set A is strictly self-similar and we have determined an appropriate scaling factor s , it is possible to tile the set with congruent s -tiles. Using the number of these tiles as N in Equation (1) above, we can immediately compute the fractal dimension of A . However, when A is not strictly self-similar , we cannot tile it with congruent " shrunken" copies of itself. So in good mathematical fashion, we appropriate such a covering. To do so, we do not attempt to use smaller version of the original set, but instead choose a box-shaped set with a side length l and place a grid of these boxes over the set A . The dimension d of the box chosen depends on the nature of the set A . For example, even though it may be seem that the appropriate box shape for any curve should be that of a segment, curves that are extremely "wiggly" are usually covered with square grid as shown below. With a grid in place, we count the number of boxes that contain at least some portion of the set A . Then we reduce the side-length l and repeat this procedure with the same box shape. Clearly, the number of boxes required varies as l changes since, as we reduce the side length of our boxes to achieve better fits, the number of "covering" boxes will generally increase. We use the notation $N(l)$ to represent the 18 number of covering boxes of side-length l . In theory this process is iterated over and over as l continues to shrink, thus explaining the need for the limit in the definition below.

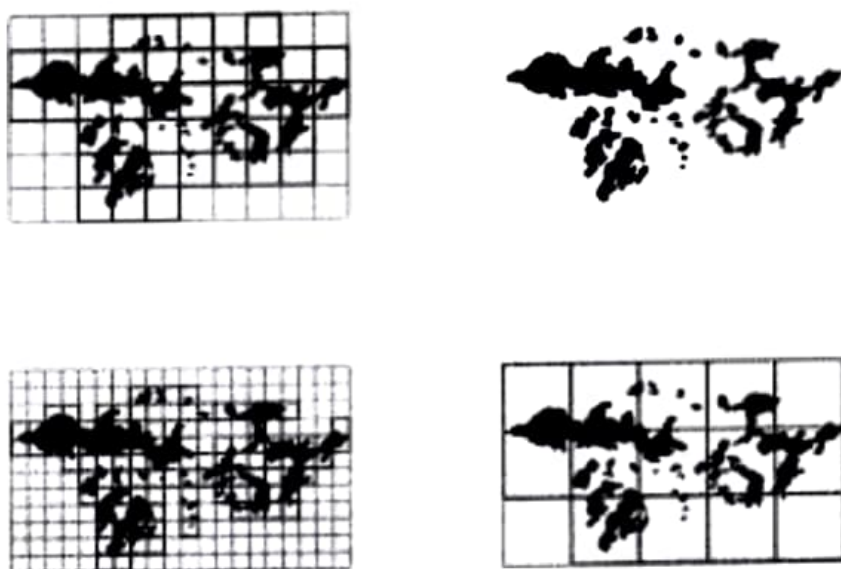


Figure 4.2: box dimension

Chapter 5

APPLICATION OF FRACTALS

5.1 FRACTALS IN BIOLOGICAL SCIENCE

Biologists have traditionally modeled nature using Euclidian representations of natural object or series. Scientists discovered that the basic architecture of a chromosome is treelike, every chromosome consist of many „mini - chromosomes“ and therefore can be treated as fractal. For example, a human chromosome has fractal dimension $d = 2, 3, 4$ (between the plane and the space dimension). Self similarity has been found also in DNA sequences. In the opinion of some biologists fractal properties of DNA can be used to resolve evolutionary relationships in animals.

5.2 FRACTALS IN HUMAN BODY

5.2.1 THE LUNGS

The pulmonary system is composed of tubes, through which the air passes into microscopic sacks called alveoli. The main tube of the system is trachea, which splits into smaller tubes that lead to different lungs. The bronchi are in turn split into smaller tubes which are even further split. This splitting continues further and further until the smallest tubes called the bronchioles which lead into the alveoli. This description is similar to that of a typical fractal canopy, which is formed by splitting lines: The end points of the pulmonary tubes, the

alveoli are extremely close to each other. The property of end points being interconnected is another property of fractal canopies.

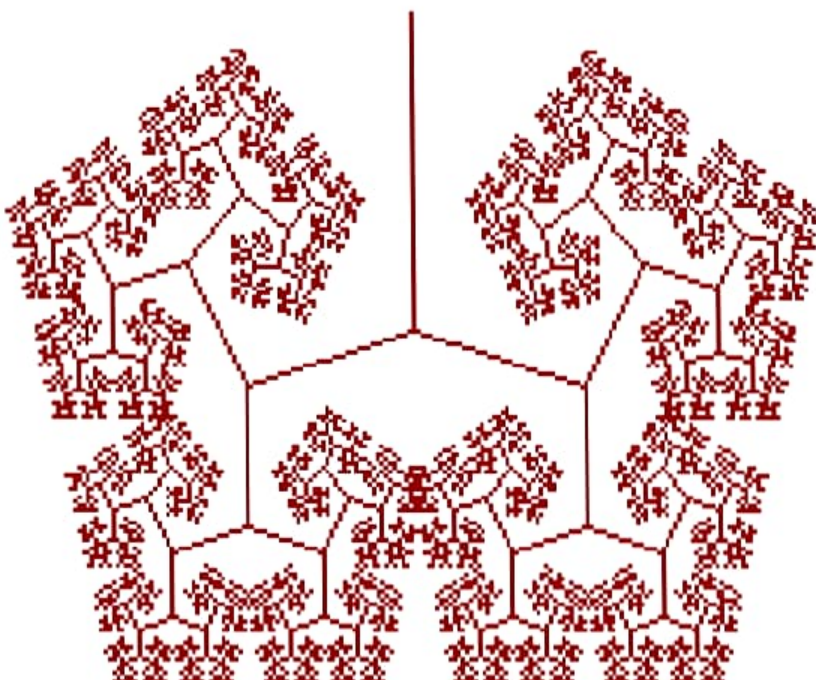


Figure 5.1: fractals in lungs

5.2.2 THE BRAIN

The surface of the brain, where the highest level of thinking takes place contains a large number of folds. Because of this, a human, who is the most intellectually advanced animal, has the most folded surface of the brain as well. Geometrically, the increase in folding means the increase in Intellectuality. Instead of 2, which is the dimension of a smooth surface, the surface of a brain has a dimension greater than 2. In humans, it is obviously the highest, being as large as between 2.73 - 2.79. Here's another topic for science fiction: super-intelligent beings with a fractal brain of dimension up to 3.

5.2.3 MEMBRANES

The surface folding similar to that of a brain was found in many other surfaces, such as the ones inside the cell 21 on mitochondria, which is used for obtaining energy and the endoplasmic reticulum, which is used for transporting materials. The same kind of folding was found in the nasal membrane, which allows sensing smells better by increasing the sensing surface. However, in humans this membrane is less fractal than in other animals, which makes them less sensitive to smells.

5.3 FRACTAL ART

Fractal art is a form of algorithm art created by calculating fractal objects and representing the calculation results as still images, animations, and media. Fractal art developed from the mid-1980s onwards. Fractal art (especially in the western world) is rarely drawn or painted by hand. It is usually created indirectly with the assistance of fractal software; generating, iterating through three phases: setting parameters of appropriate fractal software; executing the possibly lengthy calculation; and evaluating the product. In some cases, other graphic programs are used to further modify the images produced. This is called post-processing.

5.4 FRACTALS IN ECONOMY

In economy perhaps the most important thing is to be able to predict more or less accurately what happens to the market after some time. Until very recently, the dominant theory that was used for this was the so-called portfolio theory. According to it, the probability of various changes of the market can be shown using the standard bell curves:

STANDARD BELL CURVE

Assuming this theory is accurate; we can conclude that very small changes happen very often, while very big changes happen extremely rarely. However, this is not true in practice. Recently, in about 20 years after discovering fractals, Benoit Mandelbrot introduced a new fractal

Student Testing: Normal Distribution

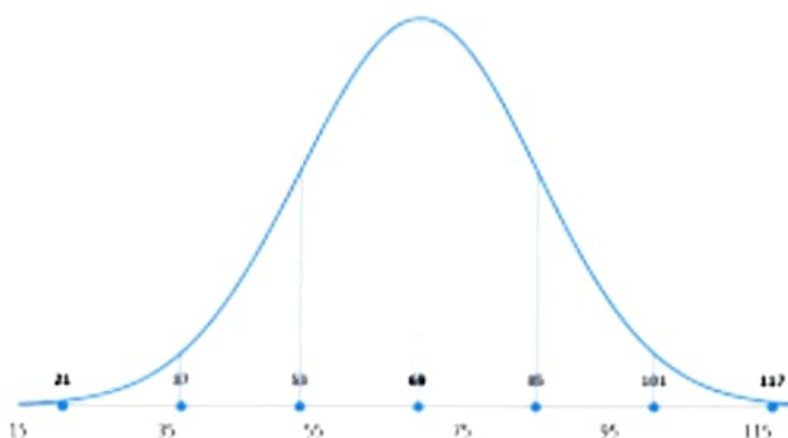


Figure 5.2: standard bell curve

theory that can be used much more efficiently than the portfolio theory to analyze the market. Considered taking a year of market activity and graphing the price for every month. You will still get a broken line with some rise and falls. Now if you take one of the months and graphs it in a detailed way with every week shown, you will get a very similar line with some rises and falls. If you make it more and more detailed, by showing every day, every hour, and even every minute or second you will still get the same, only smaller rises and falls. There is your Brownian self-similarity.

5.5 FRACTALS IN NATURE

Choose a bundle of leaves on a branch. To chaologists, all three of the objects described - the tree, the branch, and the leaves - are identical. To many, the word chaos suggests randomness, unpredictability and perhaps

even messiness. Chaos is actually very organized and follows certain patterns. One purpose of studying chaos through fractals is to predict patterns in dynamical systems that on the surface seem unpredictable. A system is a set of things, - an area of study -A set of equations is a

system, as well as more tangible things such as cloud formations, the changing weather, the movement of water currents, or animal migration patterns. Fractals are used to model soil erosion and to analyze seismic patterns as well.

5.6 FLUID MECHANICS

The study of turbulence in flows is very adapted to fractals. Turbulent flows are chaotic and very difficult to model correctly. A fractal representation of them helps engineers and physicists to better understand complex flows. Flames can also be simulated.

Chapter 6

CONCLUSION

The term “fractal” was invented by Mandelbrot to describe geometric shapes that in simplistic terms can be described as very fractured. Fractals have always been associated with the term chaos. One author elegantly describes fractals as “the pattern of chaos”. Fractals depict chaotic behaviors, yet if one looks closely enough; it is always possible to spot glimpses of self-similarity within a fractal. The main property in every fractal object is self similarity .If we zoom on a picture of a mountain again and again we still see a mountain. This is the self-similarity of fractal. In recent years, the science of fractal has grown into vast area of knowledge, with almost all branches of science and engineering gaining from the new insight it has provided. Chemists, biologists, physicists, geologists and economists have all used methods developed in fractal to explain a magnitude to diverse physical phenomena; from trees to turbulence, cities to cracks, music to moon, craters, measles epidemics and much more. Ecologists have found fractal geometry to be an extremely useful tool for describing ecological systems. Many population, community, ecosystem, and landscape ecologists use fractal geometry as a tool to help define and explain the systems in the world around us. As with any scientific field, there has been some dissension in ecology about the appropriate level of Study . Some future applications of fractal geometry to ecology include climate modeling, weather prediction, land management, and the creation of artificial habitats. Many scientists have found that fractal geometry is a powerful tool for

uncovering secrets from a wide variety of systems and solving important problems in applied science. The list of known physical fractal systems and their applications are long and growing rapidly.

REFERENCES

- [1] David p.Feldman,Chaos and Fractals; An Elementary Introduction ,OUP Oxford,2012
- [2] Miroslav M Novak and M M Novak, Thinking in patterns; Fractals and related Phenomenon In Nature .World Scientific, 2004 .
- [3] C. Wayne Patty, Foundations of topology, Jones Bartlett Learning, 2nd edition, 2009.
- [4] Kenneth Falconer, Fractal Geometry: Mathematical Foundations and Applications, Wiley, 1990.
- [5] C. Wayne Patty, Foundations of topology, Jones Bartlett Learning, 2nd edition, 2009.
- [6] www.fractal.org/Bewustzijns-Besturings-Model/Fractals-Useful-Beauty.htm
- [7] <https://en.m.wikipedia.org/wiki/Fractal>
- [8] <https://kluge.in-chemnitz.de/documents/fractal/node2.html>



Project Report
On

INTRODUCTION TO MATROID THEORY

Submitted
in partial fulfilment of the requirements for the degree of
BACHELOR OF SCIENCE
in
MATHEMATICS
by
DEVIKA SHERIN
(Register No. AB19AMAT047)

Under the Supervision of
SMT. BETTY JOSEPH



DEPARTMENT OF MATHEMATICS
ST. TERESA'S COLLEGE (AUTONOMOUS)
ERNAKULAM, KOCHI - 682011
APRIL 2022

ST. TERESA'S COLLEGE (AUTONOMOUS), ERNAKULAM



CERTIFICATE

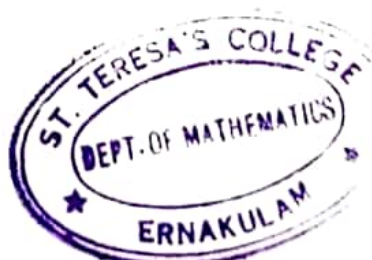
This is to certify that the dissertation entitled, **INTRODUCTION TO MATROID THEORY** is a bonafide record of the work done by Ms. **DEVIKA SHERIN** under my guidance as partial fulfillment of the award of the degree of Bachelor of Science in Mathematics at St. Teresa's College (Autonomous), Ernakulam affiliated to Mahatma Gandhi University, Kottayam. No part of this work has been submitted for any other degree elsewhere.

Date:08/03/2022

Place: Ernakulam

Betty Joseph

Associate Professor,
Department of Statistics,
St. Teresa's College(Autonomous),
Ernakulam.



Ursala Paul

Dr. Ursala Paul
Assistant Professor and Head ,
Department of Mathematics,
St. Teresa's College(Autonomous),
Ernakulam.

External Examiners

1: *Jenna Park June*

2:

DECLARATION

I hereby declare that the work presented in this project is based on the original work done by me under the guidance of Smt. Betty Joseph, Associate Professor, Department of Statistics, St. Teresa's College(Autonomous), Ernakulam and has not been included in any other project submitted previously for the award of any degree.

Ernakulam.

Date:08/03/2022


DEVIKÀ SHERIN

AB19AMAT047



Scanned with
CamScanner

Scanned with CamScanner

Scanned with CamScanner

ACKNOWLEDGEMENT

First and foremost I thank God almighty, for bestowing upon me abundance of grace, wisdom and power throughout the course of this study and making it a success.

I am extremely grateful to Dr. Ursala Paul, Head of the Department of Mathematics and to all members of the teaching faculty for their moral support and encouragement in accomplishing the work.

I take pleasure in acknowledging my immense gratitude to Smt. Betty Joseph, whose valuable help and guidance has made possible the completion of this thesis.

I take this opportunity to thank my parents and friends for their valuable support and cooperation all throughout this work.

Ernakulam.

Date:08/03/2022

DEVIKA SHERIN

AB19AMAT047

Contents

<i>CERTIFICATE</i>	ii
<i>DECLARATION</i>	iii
<i>ACKNOWLEDGEMENT</i>	iv
<i>CONTENT</i>	v
1 Introduction	1
1.1 Notations	3
1.2 Preliminary Analysis	4
2 Graph Theory and Vector Space	5
2.1 Graph Theory	5
2.2 Vector Space	9
3 Different Axiomatic Definitions of Matroids	13
3.1 Independent sets	13
3.2 Bases	15
3.3 Circuits	16
3.4 Rank	17
3.5 Closure	18
4 Fundamental Features of Matroids	20
4.1 Duality	20
4.1.1 Self-dual matroids	22
4.2 Minors	23
4.2.1 Deletion	23
4.2.2 Contraction	24
4.3 Connectivity	26

5 Conclusion	28
5.1 Applications of Matroid	28
<i>REFERENCES</i>	30

Chapter 1

Introduction

The study of matroids is an analysis of an abstract theory of dependence. Matroid theory was introduced by Hassler Whitney (1935) through his seminal paper 'On the abstract properties of linear dependence'. In his seminal paper, Whitney provided two axioms for independence, and defined any structure adhering to those axioms to be "matroids". He observed that these axioms provide an abstraction of "independence" that's common to both graphs and matrices. Because of this, many of the terms found in matroid theory resemble the terms for their analogous concepts in linear algebra or graph theory.

Whitney (1935) demonstrated the existence of equivalent axiomatic definitions, which is a characteristic feature of matroids, and established fundamental properties like representability, duality, and connectivity. The primary set of basic structural results on matroids appear in a series of papers by Tutte (1956, 1958a, b, 1959). Tutte provided characterizations for several important classes of matroids, like graphic matroids, matroids representable over the binary field, and over any field, and in doing so he expanded the theory by introducing notions such as higher connectivity and also the theory of bridges. The connection of matroids to optimization was established by Jack Edmonds by recognizing that matroids

can be defined algorithmically by the greedy algorithm, and showing a variety of important results on matroid partitioning and intersection, polymatroids, and submodular function.

A matroid is a mathematical structure that generalizes the properties of independence. Relevant applications are found in graph theory and linear algebra. There are several ways to define a matroid, each relate to the concept of independence. This project will concentrate on the various axiomatic definitions of a matroid in terms of bases, the rank function, independent sets and circuits. This paper is simply an introduction to the theory of matroids.

1.1 Notations

(E, \mathcal{I})	Independence system
N	Set of natural numbers
Z	Set of integers
Q	Set of rational numbers
R	Set of real numbers
$\langle X \rangle$	Span of a set of vectors X
\mathcal{B}	Family of bases
\mathcal{C}	Family of circuits
\mathcal{I}	Family of independent sets
$\dim(V)$	Dimension of vector space V
$A - B$	Difference of sets
$A \Delta B$	Symmetric difference of sets
$\text{cl}(X)$	Closure of a set X
M/X	Contraction of elements X from matroid M
$M.X$	Contraction to elements X in matroid M
$M \setminus X$	Deletion of elements X from matroid M
$M \mid X$	Deletion to elements X in matroid M
$M(E, \mathcal{I})$	Matroid M on E with independence family \mathcal{I}
M^*	Dual matroid of M
$M(G)$	Graphic matroid of G
$M_1 \cong M_2$	Matroid M_1 isomorphic with M_2
$r(G)$	Rank of a graph G

1.2 Preliminary Analysis

The set of natural numbers 1, 2, 3,... is denoted by N , the set of integers by Z , the set of non-negative integers by $Z+$, and the set of realnumbers by R .Here we'll just state some frequently used notations.All the sets considered within this project are finite, unless otherwise stated.

The number of elements in a set A is denoted by $| A |$. The power-set of a set A will be the set of all subsets of A , including the empty set and A , and we write 2^A .We denote with $A-B$ the deletion of B from A , that is, the set which contains the elements of A which are not contained in B . The symmetric difference of two sets A and B is defined as

$$A \Delta B = (A \cup B) - (A \cap B)$$

For a set A and some index set I , by $(a_i : i \in I)$ we denote the family of elements in A indexed by I , as defined by some mapping $\phi : I \rightarrow A$ where $\phi(i) = a_i$. For the family of subsets of some set A we can write $\mathcal{F} = (S_i : i \in I)$, where the corresponding mapping are $\phi : I \rightarrow 2^A$. We will refer to the tuple (A, \mathcal{F}) as a set system. Given a set system (A, \mathcal{F}) a subset $X \subseteq A$ is maximal with respect to \mathcal{F} , if $X \in \mathcal{F}$ and there doesn't exist $Y \in \mathcal{F}$ such that $X \subsetneq Y$. Moreover, $X \subseteq A$ is minimal with respect to \mathcal{F} , if $X \in \mathcal{F}$ and there doesn't exist $Y \in \mathcal{F}$ such that $Y \subset X$.

Chapter 2

Graph Theory and Vector Space

2.1 Graph Theory

In this section basic definitions and results from graph theory are presented.

A graph $G = (V(G), E(G))$ consists of two finite sets. $V(G)$, the vertex set of the graph, often denoted by just 'V', which is a nonempty set of elements called **vertices**, $E(G)$ be the edge set of the graph often denoted by just 'E', which is possibly empty set of elements called **edges**, such that each edge e in E is assigned an unordered pair of vertices (u, v) called the **end vertices of e** .

Vertices are also called points, nodes or just dots. If e is an edge with end vertices u and v then e is said to join u and v .

Note that the definition of a graph allows the possibility of the edge e having identical end vertices, that is , it's possible to have a vertex u joined to itself by an edge. Such an edge is called a **loop**.

Example 1 :

Let $G = (V, E)$ where $V=\{a, b, c, d, e\}$, $E=\{e_1, e_2, e_3, e_4, e_5, e_6, e_7, e_8\}$ and the ends of the edges are given by $e_1 \leftrightarrow (a, b)$, $e_2 \leftrightarrow (b, c)$, $e_3 \leftrightarrow (c, c)$,

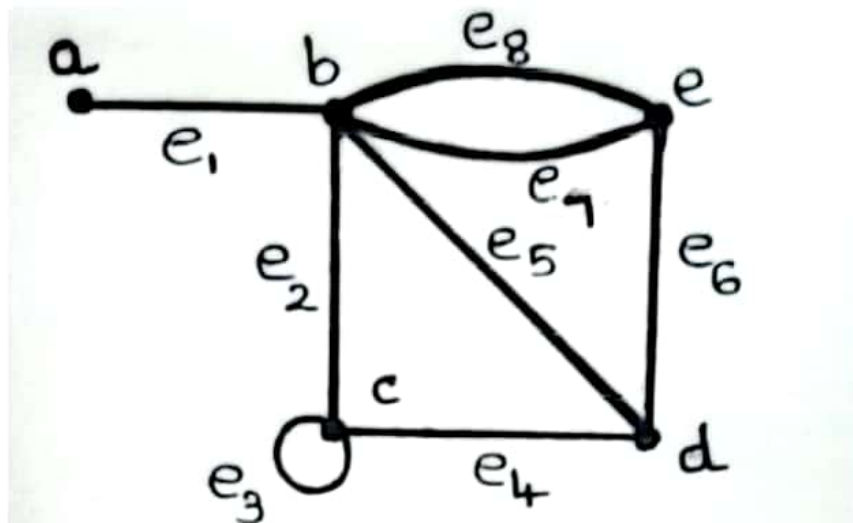


Figure 2.1:

$$e_4 \leftrightarrow (c, d), e_5 \leftrightarrow (b, d), e_6 \leftrightarrow (d, e), e_7 \leftrightarrow (b, e), e_8 \leftrightarrow (b, e)$$

We can then represent G diagrammatically in figure 2.1.

Let G be a graph. If two or more edges of G have the same end vertices then the edges are called **parallel edge**.

For example, the edges e_7 and e_8 of the graph of **figure:2.1** are parallel.

A graph with no loops and parallel edges is called **simple graph**.

A vertex of G which is not the end of any edges is called **isolated**. Two vertices which are joined by an edge are said to be **adjacent** or **neighbours**. The set of all neighbours of a fixed vertex v of G is called **neighbourhood set of v** and is denoted by $N(v)$.

Thus in the graph of **figure : 2.2** C_1 and C_4 are adjacent but C_2 and C_5 are not.

The neighborhood set $N(C_3)$ of C_3 is $\{ C_2, C_4, C_5 \}$ A graph $G_1=(V_1,E_1)$ is said to be isomorphic to the graph $G_2=(V_2,E_2)$ if there is a one-to-one correspondence between the vertex sets V_1 and V_2 and a one-to-one correspondence between the edge sets E_1 and E_2 in such a way that if e_1 is an edge with end vertices u_1 and v_1 in G_1 then the corresponding edge e_2 in G_2 has its end points the vertices u_2 and

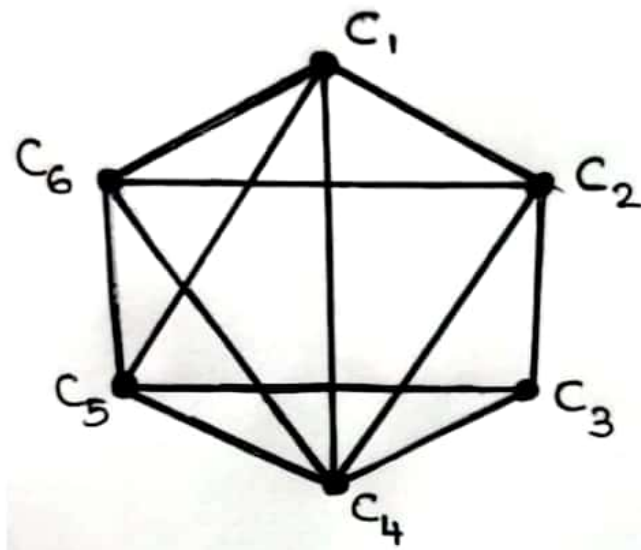


Figure 2.2:



Figure 2.3: Isomorphic pair of graph

v_2 in G_2 which correspond to u_1 and v_1 respectively , such a pair of correspondence is called a **graph isomorphism**.

A **complete graph** is a simple graph in which each pair of distinct vertices is joined by an edge. An **empty or trivial** graph is a graph with no edges.

Let G be graph. If the vertex set V of G can be partitioned into 2 nonempty subsets X and Y (that is $X \cup Y = V$ and $X \cap Y = \emptyset$) in such a way that each edge of G has one end in X and one end in Y then G is called **bipartite**.The partition $V = X \cup Y$ is called a **bipartition** of G .

A **complete bipartite** graph is a simple graph G , with bipartition $V = X \cup Y$

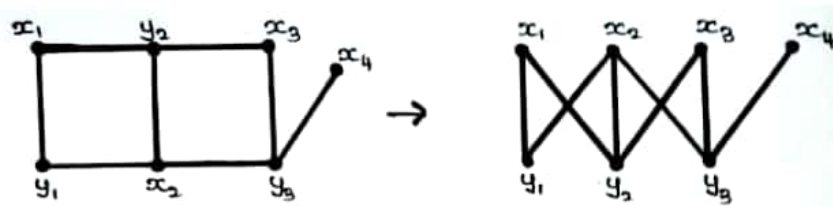


Figure 2.4: Bipartite graph

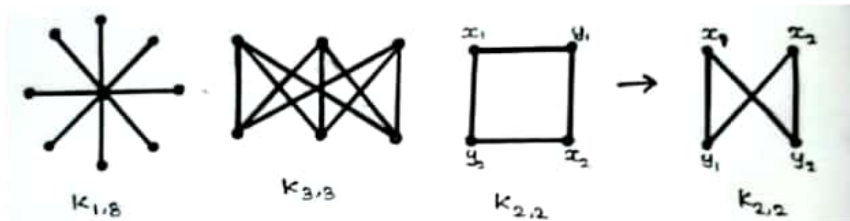


Figure 2.5: Complete bipartite graph

in which every vertex in X is joined to every vertex of Y . If X has m vertices and Y has n vertices such a graph is denoted by $K_{m,n}$.

If an edge e of a graph G is said to be incident with vertex u if v is an end vertex of e . In this case we also say that u is incident with e . Two edges e and f which are incident with a common vertex u are said to be adjacent.

Let v be a vertex of the graph G . The degree $d(v)$ (or $d_G(v)$) if we want to emphasize G of v is the number of edges of G incident with v , counting each loop twice, that is, it is the number of times v is an end vertex of an edge.

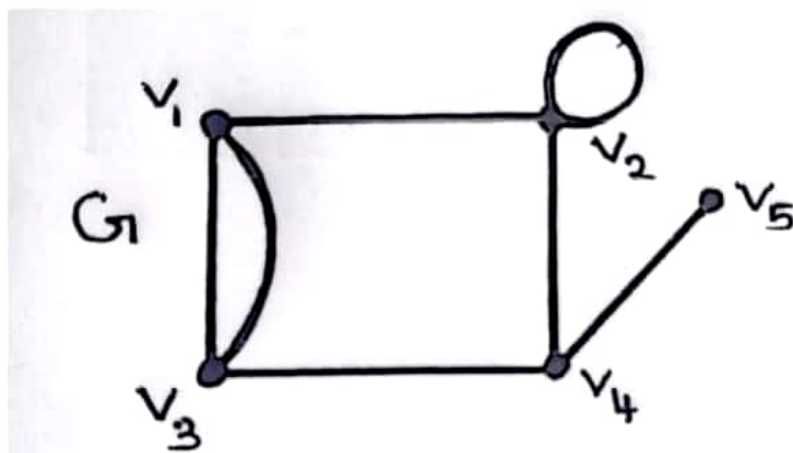
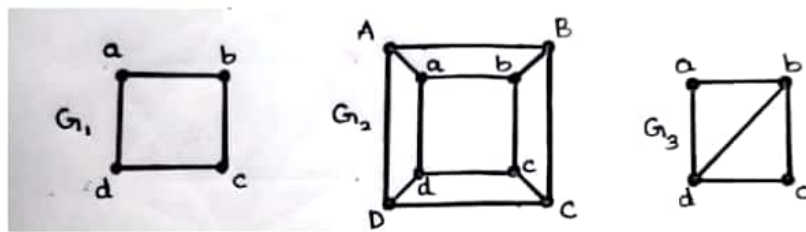


Figure 2.6:

Figure 2.7: $G_1 \subseteq G_2$, $G_1 \subseteq G_3$ but $G_3 \not\subseteq G_2$

In the graph **figure : 6** we have $d(v_1) = 3$, $d(v_2) = 4$, $d(v_3) = 3$,

$$d(v_4) = 3 ,$$

$$d(v_5) = 1$$

$$d(v_1)+d(v_2)+d(v_3)+d(v_4)+d(v_5) = 14 = (2 \times \text{number of edges in } G)$$

A vertex of graph is called **odd** or **even** depending on whether it's degree is odd or even.

If for some positive integer k , $d(v) = k$ for every vertex v the graph G , then G is called **K-regular**.

A regular graph is one that is k -regular for some k .

Subgraph : Let H be a graph with vertex set $V(H)$ and edge set $E(H)$ and similarly, let G be a graph with vertex set $V(G)$ and edge set $E(G)$. Then we say that H is a subgraph of G if $(V(H) \subseteq V(G))$ and $(E(H) \subseteq E(G))$. In such a case we also say that G is a super graph of H .

For example, in **figure:2.7** G_1 is a subgraph of both G_2 and G_3 but G_3 isn't a subgraph of G_2 .

2.2 Vector Space

In this section are going to present some basic definition of vector space and linear independence.

Definition:

A set of objects $V = \{\vec{u}, \vec{v}, \vec{w}, \dots\}$ and scalars $\{\alpha, \beta, \gamma, \dots\}$ along with a binary operation of vector addition \oplus on the object and a scalar multiplication \odot is a vector space if it possess following 10 properties,

Vector addition:

- Closure under addition : If \vec{u} and \vec{v} belongs to V then so does

$$\vec{u} \oplus \vec{v} \in V$$

- Commutative law for addition : $\vec{u} \oplus \vec{v} = \vec{v} \oplus \vec{u} \quad \forall \vec{u}, \vec{v}$.
- Associative law for addition : $(\vec{u} \oplus \vec{v}) \oplus \vec{w} = \vec{u} \oplus (\vec{v} \oplus \vec{w}), \forall \vec{u}, \vec{v}, \vec{w}$.
- There exist a zero vector in V denoted by $\vec{0}$, such that

$$\forall \vec{u} \in V,$$

$$\vec{u} \oplus \vec{0} = \vec{u}.$$

- For every vector \vec{u} in V , there exist a vector $-\vec{u}$ called the additive inverse of \vec{u} such that $\vec{u} \oplus -\vec{u} = \vec{0}$

Scalar multiplication:

- Closure under scalar multiplication : If \vec{u} belongs to V , then

$$\alpha \odot \vec{u} \in V \text{ for any scalar } \alpha.$$

- For any two scalars α and β and any vector \vec{u} in V ,

$$\alpha \odot (\beta \odot \vec{u}) = (\alpha \beta) \odot \vec{u}.$$

- For any \vec{u} in V , $1 \odot \vec{u} = \vec{u}$

- For any two scalars α and β and any vector \vec{u} in V ,

$$(\alpha \oplus \beta) \odot \vec{u} = \alpha \odot \vec{u} \oplus \beta \odot \vec{u}.$$

- For any scalar α and any two vectors \vec{u} and \vec{v} in V ,

$$\alpha \odot (\vec{u} \oplus \vec{v}) = \alpha \odot \vec{u} \oplus \alpha \odot \vec{v}.$$

Subspaces:

A subspace of a vector space V is a subset of V that is a vector space in its own right.

Theorem : Let S be a nonempty subset of a vector space V with operations \oplus and \odot . S is a subspace of V if and only if the following two closure conditions hold,

- Closure under addition : If $\vec{u} \in S$ and $\vec{v} \in S$, then

$$\vec{u} \oplus \vec{v} \in S$$

- Closure under scalar multiplication: If $\vec{u} \in S$ and α is any scalar then $\alpha \odot \vec{u} \in S$.

A vector \vec{u} is a linear combination of vectors $v_1, v_2, v_3, \dots, v_n$ if there exist scalars $d_1, d_2, d_3, \dots, d_n$ such that

$$\vec{u} = d_1 v_1 + d_2 v_2 + \dots + d_n v_n$$

A set of vectors $\{v_1, v_2, v_3, \dots, v_n\}$ in a vector space V is linearly dependent if there exist scalars $C_1, C_2, C_3, \dots, C_n$ not all zero, such that,

$$C_1 v_1 + C_2 v_2 + \dots + C_n v_n = 0$$

The vectors are linearly independent if the only set of scalars that satisfies the equation,

$$C_1 v_1 + C_2 v_2 + \dots + C_n v_n = 0 \text{ is the set}$$

$$C_1 = C_2 = \dots = C_n = 0$$

Spanning Set :

We define a set of vectors S in a vector space V as a spanning set for V if each

vector in V can be written as a linear combination of the vectors in S that is, $V = \text{span}(S)$.

Basis:

A basis for a vector space V is of vectors that is, linearly independent and also a $\text{span}(V)$.

Dimension:

The cardinality of basis in a vector space V will be called the dimension of V , and we write $\dim(V)$

Chapter 3

Different Axiomatic Definitions of Matroids

3.1 Independent sets

A matroid M is a pair of (E, I) , where E is a finite set (called the ground set) and I is a family of subsets of E (called independent sets) with the following properties:

- (I1) $\emptyset \neq I$
- (I2) If $X \in I$ and $Y \subseteq X$ then $Y \in I$.
- (I3) If $X, Y \in I$ and $|X| > |Y|$ then there exist $x \in X - Y$ such that $Y \cup \{x\} \in I$

Example:1

Consider for example the graph in **Fig. 3.1** and let the ground set be

$E = \{e_1, e_2, \dots, e_7\}$. If $I_1 = \{X \subseteq E : G[X] \text{ does not contain any cycle}\}$, then the set system (E, I_1) trivially satisfies axioms (I1) and (I2), while (I3) is

Proposition: Therefore, (E, I_1) is a matroid. Let now

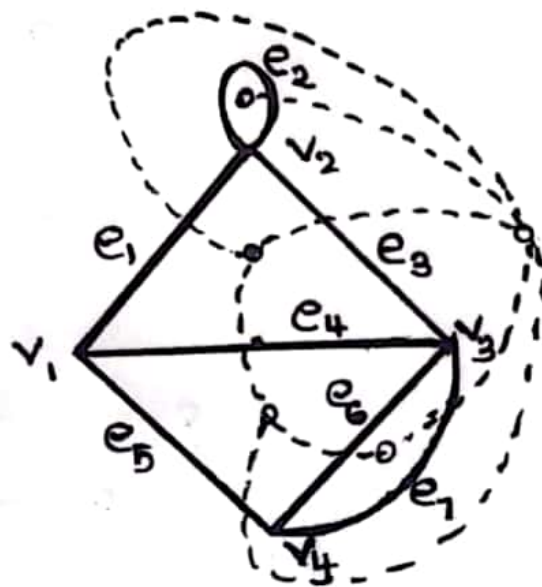


Figure 3.1:

$(I2) = \{X \subseteq E : X \text{ is a matching in } G\}$. One can check that $(E, I2)$ is an independence system since axioms (I1) and (I2) are satisfied. However axiom (I3) is not satisfied, since if we take

$X = \{e_1, e_6\}$ and $Y = \{e_4\}$ we have that both $Y \cup \{e_1\}$ and $Y \cup \{e_6\}$ are not in $I2$.

Theorem : Suppose that X, Y are independent sets in a matroid $M(E, I)$ and $|X| > |Y|$. Then there exists some

$Z \subseteq X - Y$ such that

$$|Y \cup Z| = |X| \text{ and } Y \cup Z \in I.$$

Proof:

Let $Z \subseteq X - Y$ be a maximal set such that $Y \cup Z \in I$ and assume that $|Y \cup Z| < |X|$. We know from (I3) that such a Z exists, at least for $|Z| = 1$. Since both X and $Y \cup Z$ are independent, there exists some $x \in X - (Y \cup Z)$ such that

$(Y \cup Z) \cup \{x\} \in I$. Since $x \in Z$ it implies that Z is not maximal, a contradiction.

Two matroids M_1 and M_2 are isomorphic and we write

$M_1 = M_2$, if there exists a bijection $\emptyset: E(M) \rightarrow E(M_2)$ such that $X \in I(M_1)$ if and only if $\emptyset(X) \in I(M_2)$ for all $X \subseteq E(M_1)$.

3.2 Bases

Given an independence system (E, I) , the maximal independent sets will be called bases. The family of bases will be denoted by B .

A collection B is the set of bases of a matroid $M(E, I)$ if and only if the following are satisfied:

(B1) $B \neq \emptyset$

(B2) If $B_1, B_2 \in B$ and $x \in B_1 - B_2$ then there exists

$$y \in B_2 - B_1 \text{ such that } (B_1 - \{x\}) \cup \{y\} \in B.$$

Theorem:

An independence system (E, I) is a matroid if and only if for any $X \subseteq E$ all bases of X have the same cardinality.

Proof:

Let (E, I) be a matroid and consider some $X \subset E$. Assume by contradiction that there exist $B_1, B_2 \in B(X)$ with $|B_1| > |B_2|$. Since $B_1, B_2 \in I$, we can find some $x \in B_1 - B_2$ such that

$B_2 \cup x \in I$. Thus, B_2 is not maximally independent, a contradiction.

Let now (E, I) be an independence system, $X, Y \in I$ with $|X| > |Y|$, and consider the set $X \cap Y$. By assumption all bases of $X \cup Y$ have the same size, which is

at least $|X|$ since $X \in I$. This implies that Y is not a base of $X \in Y$, so there exists some $x \in (X \cup Y) - Y = X - Y$ such that $Y \cup \{x\} \in I$, which is axiom (I3) of Definition 3.1.

3.3 Circuits

Given an independence system (E, I) the minimal dependent sets will be called circuits. The family of circuits will be denoted by C . The collection of circuits for some $X \subseteq E$ will be denoted by $C(X)$ and is defined as,

$$C(X) = \{Y \subseteq X : Y \notin I, Y - \{y\} \in I \text{ for all } y \in Y\}.$$

A collection $C \subseteq 2^E$ is the set of circuits of a matroid $M(E, I)$ if and only if the following are satisfied:

(C1) $\emptyset \notin C$.

(C2) If $C_1, C_2 \in C$ and $C_1 \subseteq C_2$ then $C_1 = C_2$.

(C3) If $C_1, C_2 \in C$, $C_1 = C_2$ and $e \in C_1 \cap C_2$ then there exists $C_3 \in C$ such that $C_3 \subseteq (C_1 \cup C_2) - \{e\}$.

Preposition(1):

If $B \in B(E)$ for a matroid $M(E, I)$ and $x \in E - B$, then there exists a unique circuit $C(x, B)$ contained in $B \cup \{x\}$ and it contains x . Any circuit in a matroid of the type defined in Proposition 1 will be called a fundamental circuit of a base.

Preposition(2):

If $B \in B(E)$ for a matroid $M(E, I)$, then for any $x \in E - B$ the set $(B - \{y\}) \cup \{x\}$ is a base of M if and only if $y \in C(x, B)$.

Proof:

Assume by contradiction that $(B - \{y\}) \cup \{x\}$ is a base of M for some $y \in B - C(x, B)$. Then $C(x, B)$ is contained in

$(B \{y\}) \cup \{x\}$, a contradiction. Consider now any $y \in C(x, B)$ and assume that $(B \{y\}) \cup \{x\} \notin I$. Then $B \cup \{x\}$ contains a circuit other than $C(x, B)$, which contradicts Proposition(1).

Lemma of proposition(2):

If M_1 and M_2 are two matroids on the same ground set, such that any circuit of M_1 contains a circuit of M_2 and vice versa, then $M_1 = M_2$.

Proof:

If $X \in C(M_1)$ there exists a circuit $Y \in C(M_2)$ such that

$X \subseteq Y$ and for Y there exists a circuit $Z \in C(M_1)$ such that $Z \subseteq Y$. We have $Z \subseteq Y \subseteq X$, and by axiom(C2) we must have $Z = X$, which implies that $X = Y$. Similarly, we show that any circuit of M_2 is a circuit of M_1 , thus both matroids have the same family of circuits and they are equal.

3.4 Rank

Given an independence system (E, I) , the rank function

$r : 2^E \rightarrow Z^+$ is defined as,

$$r(X) = \max\{ |Y| : Y \subseteq X, Y \in I \} \text{ for any } X \in E.$$

A function $r : 2^E \rightarrow Z$ is the rank function of a matroid $M(E, I)$ if and only if the following are satisfied for all

$X, Y \in E$:

$$(R1) 0 \leq r(X) \leq |X|.$$

$$(R2) \text{ If } Y \subseteq X \text{ then } r(Y) \leq r(X).$$

$$(R3) r(X) + r(Y) \geq r(X \cup Y) + r(X \cap Y) \text{ (Submodularity of } r\text{)}$$

Definition : Low Rank

Given an independence system (E, I) , the lowrank function $lr : 2^E \rightarrow Z$ is defined as,

$$lr(X) = \min\{|Y| : Y \subseteq X, Y \in I, Y \cup \{x\} \notin I$$

for all $x \in Y - X$ for any $X \subseteq E$.

So while rank is defined as the cardinality of the largest base of X , low rank is the cardinality of the smallest base.

Note that $r(X) = |X| \leftrightarrow lr(X) = |X|$, that is, rank and low rank are equivalent when X is an independent set.

3.5 Closure

Given an independence system (E, I) the closure operator is a set function $cl : 2^E \rightarrow 2^E$ defined as,

$$cl(X) = \{y \in E : r(X \cup \{y\}) = r(X)\} \text{ for any } X \subseteq E.$$

For some $X \subseteq E$, it follows from the definition that

$X \subseteq cl(X)$, since $r(X \cup \{x\}) = r(X)$ for all $x \in X$. Moreover, it follows from the definition that,

$$cl(X) = E \leftrightarrow r(X) = r(E).$$

A function $cl : 2^E \rightarrow 2^E$ is the closure operator of a matroid $M(E, I)$ if and only if the following are satisfied for all

$X, Y \subseteq E$ and $x, y \in E$:

- (CL1) If $X \subseteq E$ then $X \subseteq cl(X)$.
- (CL2) If $X \subseteq Y \subseteq E$ then $cl(X) \subseteq cl(Y)$.
- (CL3) If $X \subseteq E$ then $cl(cl(X)) = cl(X)$.
- (CL4) If $X \subseteq E$, $x \in E$, $y \in cl(X \cup \{x\}) - cl(X)$ then,
 $x \in cl(X \cup \{y\})$.

Example: If $M(E, I) = M[A]$ for some matrix $A \in F^{m,n}$, then for $X \subseteq E$

We have $cl(X) = \{x \in E : x = \sum_i a_i x_i, x_i \in X, \text{ for some}$

$a_i \in F\}$, or equivalently $cl(X) = \langle X \rangle \cap E$.

Consider now that we have the graphic matroid $M(G)$ of the graph G given in Fig. 3.1. In this case for $X = \{e1, e3\}$.

We have $cl(X) = X \cup \{e4, e2\}$, while for $X = \{e5, e6\}$ we have $cl(X) = X \cup \{e4, e7, e2\}$. Actually, since $r(e2) = 0$ the loop $e2$ is included in the closure of every subset of E . For the transversal matroid of the set system (E, F) in example 2.1, for $X = 1, 3, 5$ we have $cl(X) = X \cup \{4\}$ while for $X = \{1, 2\}$ we have $cl(X) = X$.

Chapter 4

Fundamental Features of Matroids

4.1 Duality

The notion of duality in matroids is similar to the one in optimization, and it generalizes the concepts of orthogonality in vector spaces, and planarity in graphs. For any matroid M we are able to define another matroid M^* on the same ground set called the dual of M , such that independent sets, bases, circuits, rank, and any other property of M have well-defined dual counterparts in M^* .

The dual matroid M^* to a matroid M is the matroid with bases that are complements of the bases of M

$$B(M^*) = \{E - B / B(M)\}$$

$$\text{ie; } B(M^*) = B^*(M)$$

Theorem:

Let M be a matroid and $B^*(M)$ be $\{E-B/B(M)\}$. Then $B^*(M)$ is the set of bases of matroid on $E(M)$

Proof

Proof is proved with the help of following lemma.

Lemma

The set B of bases of a matroid M has the subsequent property

If B_1 and B_2 are in B and $x \in B_2 - B_1$, then there's an element of $B_1 - B_2$ such that $(B_1 - y) \cup x \in B$

Proof of lemma

$B_1 \cup x$ contains a unique circuit, $C(x, B_1)$. As $C(x, B_1)$ is dependent and B_2 is independent, $C(x, B_1) - B_2$ is non-empty. Let y be an element of this set. Evidently $y \subseteq B_1 - B_2$. Moreover,

$(B_1 - y) \cup x$ is independent since it doesn't contain $C(x, B_1)$. As $|B_1 - y| = |B_1|$, it follows that $(B_1 - y) \cup x$ can be a basis.

Proof of theorem

As $B(M)$ is non empty so is $B^*(M)$. Suppose B_1^* and B_2^* are in $B^*(M)$ and $x \in B_1^* - B_2^*$. Writing E for $E(M)$. $B_i = E - B_i^*$ be for every i in $\{1, 2\}$. Then

$$B_i = E - B_i^*$$

$$B_1^* - B_2^* = B_1^* \cap B_2 = B_2 - B_1$$

By lemma 4.1.2 as $x \in B_2 - B_1$, there is an element y of $B_1 - B_2$ such that

$(B_1 - y) \cup x \in B(M)$. Clearly $y \in B_2^* - B_1^*$ and $E - ((B_1 - y) \cup x) \in B^*(M)$

But $E - (B_1 \cup x) = E - (B_1 \cup y) = (B_1^* - x) \cup y$. Thus $B^*(M)$ satisfies the theorem and

$B^*(M)$ is indeed the set of bases of a matroid on E

Theorem:

A set $B \subseteq E$ is a basis in a dual matroid M^D iff its complement $E \setminus B$ is a basis in the original matroid M .

This justifies the earlier claim that the bases in the dual matroid are exactly the complements of the bases in the original matroid. It also shows that duality is truly an involution. With this result, it's not hard to work out that a codependent set in a matroid M , i.e., a dependent set in the dual matroid M^D , is just a set which intersects every basis of M .

4.1.1 Self-dual matroids

An individual matroid is self-dual (generalizing e.g. the self-dual polyhedra for graphic matroids) if it is isomorphic to its own dual. The isomorphism may, but is not required to, leave the elements of the matroid fixed. Any algorithm that tests whether a given matroid is self-dual, given access to the matroid via an independence oracle, must perform an exponential number of oracle queries, and therefore cannot take polynomial time.

Many important matroid families are self-dual, meaning that a matroid belongs to the family if and only if its dual does. Many other matroid families are seen in dual pairs. Examples of this phenomenon include:

- The binary matroids (matroids representable over $\text{GF}(2)$), the matroids representable over any other field, and the regular matroids, are all self-dual families.
- The gammoids form a self-dual family. The strict gammoids are dual to the transversal matroids.

- The uniform matroids and partition matroids are self-dual. The dual to a uniform matroid U_n^r is the uniform matroid $U^n - r_n$
- The dual of a graphic matroid is itself graphic if and only if the underlying graph is planar; the matroid of the dual of a planar graph is the same as the dual of the matroid of the graph. Thus, the family of graphic matroids of planar graphs is self-dual.
- Among the graphic matroids, and more generally among the binary matroids, the bipartite matroids (matroids in which every circuit is even) are dual to the Eulerian matroids (matroids which can be partitioned into disjoint circuits).

4.2 Minors

4.2.1 Deletion

The matroid $M \setminus X$ is the deletion of X from M

For a matroid $M(E,C)$ and X , the deletion of X in M is the matroid $M \setminus X$ on $E-X$ is defined as

$$C(M \setminus X) = \{C \subseteq E - X : C \in C(M)\}$$

Theorem:

For a matroid $M(E,C)$ and X , the set $C(M \setminus X) = \{C \subseteq E - X : C \in C(M)\}$ is the family of circuits of matroid on $E-X$. We will call the matroid $M \setminus X$ the deletion of X from M . Alternatively, we could define the deletion to X in M as the matroid M/X on the ground set X and family of circuits

$$C(M/X) = C(M \setminus X) = \{C \subseteq X : C \in C(M)\}$$

4.2.2 Contraction

In this section, we introduce the operation of contraction as the dual of the operation of deletion.

For a matroid M and $X \subseteq E(M)$, the contraction of X in M is the matroid M/X on $E(M)-X$ is defined as

$$M/X = (M^* \setminus X)^*$$

As in the operation of deletion we can also define the contraction to X in M as the matroid $M.X$ on X defined as

$$M.X = M/(E - X)$$

Minor

Minors of matroids are defined using two basic operations which is mentioned above, a deletion and a contraction of elements and their sets. Let M be a matroid on a ground set E and let X be a subset of the ground set E . The matroid obtained by deleting the subset X is the matroid with the ground set $E \setminus X$ whose independent sets are those subsets of $E \setminus X$ that are independent in M . The matroid obtained by contracting of a set X is defined through deleting X in the dual matroid: the matroid M/X obtained by contracting X is the matroid $(M^* \setminus X)^*$.

Clearly, the ground set of M/X is $E \setminus X$.

If a matroid M_1 can be obtained by operating combination of restrictions and contractions on a matroid M , then M_1 is called a minor of M .

Examples: $U_{2,4}$ is excluded by binary; F_7 and F_7^* are excluded by ternary.

For a matroid M and disjoint $X, Y \subseteq E(M)$ the matroid $M \setminus X/Y$ is called a minor of M , while if X or Y is non empty, it is called proper.

Let us now give formulas for the rank function of a matroid obtained by deleting or contracting a set of elements.

Proposition

Let M be a matroid on a ground set E . For every subset T of E and every subset X of $E \setminus T$, the following holds:

$$r_{M \setminus T}(X) = r_M(X) \text{ and}$$

$$r_{M/T}(X) = r_M(X \cup T) - r_M(T)$$

Proof

The first equality directly follows from the definition of the deletion. To prove the second equality, we use the identity

$r^*(X) = |X| - r_M(M) + r_M(E \setminus X)$ for the corank function of a matroid (r^* will always denote the corank of M throughout this proof).

In particular, the following equalities hold:

$$\begin{aligned} r_{M \setminus T}(X) &= |X| + r_{M^* \setminus T}(X) \\ &= |X| + r^*(E \setminus (T \cup X)) - r^*(E \setminus T) \\ &= |X| + (|E \setminus (T \cup X)| + r_M(T \cup X) - r_M(E) - (|E \setminus T|) + r_M(T) - r_M(E)) \\ &= r_M(T \cup X) - r_M(T) \end{aligned}$$

Note that the last equality holds since $|X| + |E \setminus (T \cup X)| = |E \setminus T|$ as $X \subseteq E \setminus T$

Theorem:

For a matroid M and $X \subseteq E(M)$ we have

$$1) (M \setminus X)^* = M^*/X$$

$$2) (M/X)^* = M^* \setminus X$$

Proof

By the definition of contraction operation in 4.1 and the fact $(M^*)^* = M$ we can prove this theorem. For (2) take the dual of 4.1, and for (1) do the same for the dual expression of 4.1 which is $M^*/X = (M)^*$

4.3 Connectivity

Connectivity is a fundamental structural property of matroids, and can be thought of as a measure of correlation between the elements of the ground set with respect to the structure imposed by the family of independent sets, circuits, etc. The more connected a matroid is, the less probable is the existence of sets of elements that are not members of the family that defines the matroid.

For a matroid $M(E, C)$ a set $X \subseteq E$ is called a separator of M if any circuit $C_1 \in C$ is contained in either X or $E - X$.

It follows from the definition of separators that both E and \emptyset are trivial separators for any matroid. Minimal nonempty separators will be called elementary separators.

A matroid will be called connected if it has no separators other than the trivial E

and ϕ

Corollary

Given a matroid M , a set $X \subseteq E(M)$ is a separator of M if and only if

$$M \setminus X = M/X.$$

Theorem

Given a matroid M and $Y \subseteq C(M)$. let X be a union of circuits of $M \setminus Y$ where $M \setminus Y|X$ is connected. Then either $X \cup Y$ is a union of circuits of M such that $M|(X \cup Y)$ connected, or

$$M/Y|X = M|X.$$

Proof

Since any circuit of $M \setminus Y$ is a circuit of M by the definition of the deletion operation, then clearly $X \cup Y$ is a union of circuits of M . If $M|(X \cup Y)$ is connected then there is nothing left to prove. If $M|(X \cup Y)$ is not connected, then we can assume that it has two separators S_1 and S_2 . Given that $M \setminus Y|X$ is connected, we must have $S_1 = X$ and $S_2 = Y$.

For a matroid $M(E, C)$ and $Y \subseteq X \subseteq E$ we have

$$(i) (M|X)|Y = M|Y.$$

$$(ii) (M.X).Y = M.Y.$$

Using this theorem and above Corollary , since $X \subseteq E - Y$ we have

$$\begin{aligned} (M/Y)|X &= (M.(E - Y))|X \\ &= (M|(E - (E - Y - X))).x \\ &= (M|(Y \cup X)).X \\ &= (M|(Y \cup X))|X \\ &= M|X. \end{aligned}$$

Chapter 5

Conclusion

Matroids provide a combinatorial abstraction of linear dependence. They have a remarkable tendency to be seen in diverse settings across mathematics. The first main bridge to algebraic geometry came within the 80s with the appearance of matroid polytope, linking Matroids to toric varieties and also the Grassmannian.

In combinatorics , a branch of mathematics , a matroid can be a structure that abstracts and generalises the notion of linear independence in vector spaces. Matroid theory borrows extensively from the terminology of algebra and graph theory, largely because it's the abstraction of assorted notions of central importance in these fields . Matroids have found application in geometry , topology, combinatorial optimization, network theory and coding theory.

5.1 Applications of Matroid

Matroids are mathematical structures. Matroids unite concepts from linear algebra , projective geometry , transversal theory, graph theory, combinatorial optimization, lattice theory and even transcendence theory. One application of the unifying concept of a matroid is to seek out the analogs of an interesting idea in vector

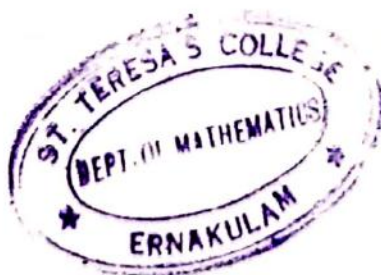
spaces to graphs and conversely. And matroids are useful in algorithm designs.

In mathematics matroids are widely used for specifying and representing geometric transformations and coordinate changes. In numerical analysis many computational problems are solved by reducing them to a matrix computation and this involves often to compute with matrices of great dimensions. In combinatorial optimization matroid theory was utilized in coding theory, secret coding, network coding. And it has an vital theory in studying the qualitative problems of electric networks. Networks derived from matroid have played a fundamental role in proving theoretical results about the bounds of network coding.

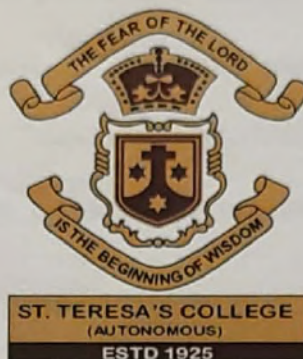
Matroid-theoretic methods are now starting to play a huge role in the understanding of decoding algorithms for error-correcting codes. Ideas from matroid theory are finding other novel applications within the broader realm of information theory. Specifically, they're being applied to explore the basic limits of secret sharing schemes and also to gain an understanding of information inequalities.

REFERENCES

- [1] Derek Allan Holton , John Clark : A first look at Graph Theory. World Scientific (1991).
- [2] Gabriel B Costa , Richard Benson : Linear Algebra : An Introduction. Second Edition, Academic Press (2007).
- [3] James Oxley : Matroid Theory, Second Edition. Oxford University Press (2011).
- [4] Leonidas S Pitsoulis : Topic In Matroid Theory. Springer Science-Business Media (2013).
- [5] <https://www.whitman.edu/documents/Academics/Mathematics/hillman.pdf>
- [6] https://www.math.lsu.edu/~oxley/matroid_intro_summ.pdf
- [7] <https://math.berkeley.edu/~charles/whatis/matroids.pdf>
- [8] <https://pdfs.semanticscholar.org/7fdf/7fbd4c616958eb0309844a19d6ff5b36b19d.pdf>
- [9] https://journalijcar.org/sites/default/files/issue-files/A10_0.pdf



ST. TERESA'S COLLEGE (AUTONOMOUS), ERNAKULAM



CERTIFICATE

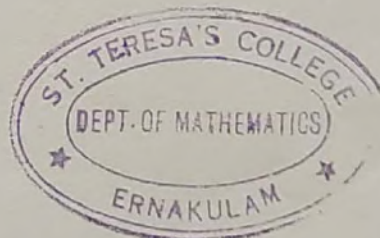
This is to certify that the dissertation entitled, **EFFECT OF COVID-19 MASK ON ECOSYSTEM** is a bonafide record of the work done by Ms. **ANJANA RAJESH** under my guidance as partial fulfillment of the award of the degree of Bachelor of Science in Mathematics at St. Teresa's College (Autonomous), Ernakulam affiliated to Mahatma Gandhi University, Kottayam. No part of this work has been submitted for any other degree elsewhere.

Date: 04-03-2022

Place: Ernakulam

Donna Pinherio

Assistant Professor,
Department of Mathematics,
St. Teresa's College(Autonomous),
Ernakulam.



Dr. Ursala Paul
Assistant Professor and Head ,
Department of Mathematics,
St. Teresa's College(Autonomous),
Ernakulam.

External Examiners

1:

2:

Project Report

On

MATHEMATICS IN FORENSIC SCIENCE

Submitted

in partial fulfilment of the requirements for the degree of

BACHELOR OF SCIENCE

in

MATHEMATICS

by

ROOPA SOMAN

(Register No. AB19AMAT025)

Under the Supervision of

DR. URSALA PAUL



DEPARTMENT OF MATHEMATICS

ST. TERESA'S COLLEGE (AUTONOMOUS)

ERNAKULAM, KOCHI - 682011

APRIL 2022

ST. TERESA'S COLLEGE (AUTONOMOUS), ERNAKULAM



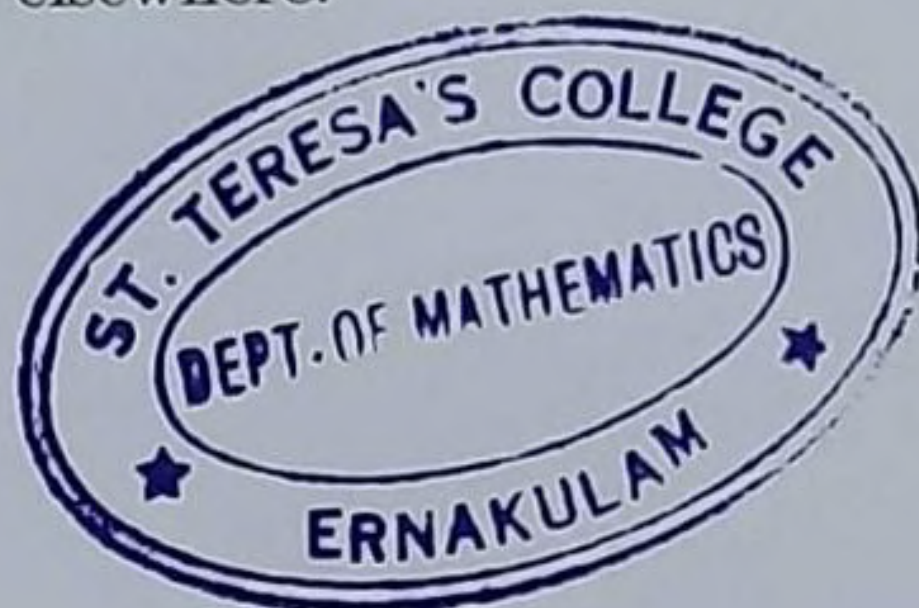
CERTIFICATE

This is to certify that the dissertation entitled, **MATHEMATICS IN FORENSIC SCIENCE** is a bonafide record of the work done by Ms. **ROOPA SOMAN** under my guidance as partial fulfillment of the award of the degree of **Bachelor of Science in Mathematics** at St. Teresa's College (Autonomous), Ernakulam affiliated to Mahatma Gandhi University, Kottayam. No part of this work has been submitted for any other degree elsewhere.

Date:

Place: Ernakulam

Dr.URSALA PAUL
Assistant Professor,
Department of Mathematics,
St. Teresa's College(Autonomous),
Ernakulam.



Dr. Ursala Paul
Assistant Professor and Head ,
Department of Mathematics,
St. Teresa's College(Autonomous),
Ernakulam.

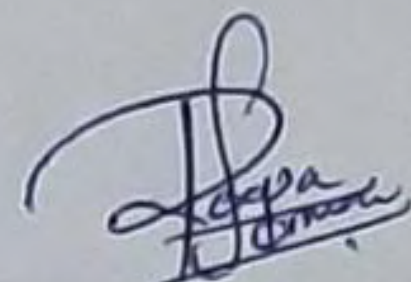
External Examiners

1:

2:

DECLARATION

I hereby declare that the work presented in this project is based on the original work done by me under the guidance of Dr.URSALA PAUL, Assistant Professor, Department of Mathematics, St. Teresa's College(Autonomous), Ernakulam and has not been included in any other project submitted previously for the award of any degree.



ROOPA SOMAN

AB19AMAT025

Ernakulam.

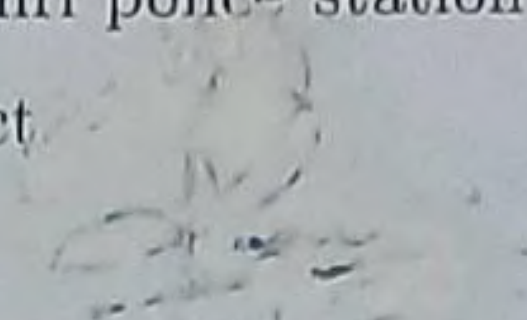
Date: 04/03/2022

ACKNOWLEDGEMENT

I would like to express my special thanks to our project guide and HOD Dr. Ursala Paul for her able guidance and support in completing my project. Also I would like to thank all my teachers for the constant support. Their continuous invaluable knowledgably guidance throughout the course of this study helped me to complete the work up to this stage

I am very grateful to all the police officers of Harbour janamithri police station who provided all the useful data for the case study of our project

Ernakulam.
Date: 04/03/2022


ROOPA SOMAN
AB19AMAT025

Contents

<i>CERTIFICATE</i>	ii
<i>DECLARATION</i>	iii
<i>ACKNOWLEDGEMENT</i>	iv
1 Forensic Mathematics	1
1.1 Introduction	1
1.2 Forensic Science	2
1.3 Forensic Mathematics	2
1.3.1 Measurements:	2
1.3.2 Proportion:	3
1.4 Applications of Mathematics in forensic Science	3
1.4.1 Trigonometry	4
1.4.2 Probability	4
2 Ballistics and Richochet analysis	6
2.1 Ricochet Analysis of the bullet	6
2.2 Aspects of ballistics	7
2.2.1 Worked out example	10
3 Determination of fall type	12
3.1 Introduction	12
3.2 Suicide,accident or murder?	12
3.3 Worked out example	14
3.4 Program to check the fall type	15
4 Case Study	18
4.1 Introduction	18

4.2 Case Details	19
5 Bloodstain shape analysis	21
5.1 Introduction	21
5.2 Bloodstain formation from a stationary source	21
5.3 Bloodstain formation from a moving source	22
5.3.1 Worked out example	23
5.4 Program to calculate walking speed of assailant	24
5.4.1 Output of the program	25
6 Probability in forensic science	26
6.1 Introduction	26
6.2 Calculating Probability	26
6.2.1 RULES OF COMBINING PROBABILITIES:	26
6.2.2 Worked out examples	28
6.3 Program	30
6.3.1 Output of the program	31
CONCLUSION	33
REFERENCES	34

Chapter 1

Forensic Mathematics

1.1 Introduction

Forensic science is a branch of science used to analyze crime scene evidence. All science uses mathematical concepts and equations, and forensic scientist are well educated in mathematical concepts they uses to analyze evidence from crime scenes.

Without mathematics it is impossible to analyze forensic evidence scientifically. One of the main things investigators do at the crime scene is to collect, measure and document evidence. This data help investigators to perform calculations and determine the facts of a crime. Mathematics shows proof of what ever happened during a crime in data and number.

The court ask the significance of evidence in the context of the crime and, as an expert witness the forensic scientist should be able to respond appropriately to such a challenge. Methods based on Bayesian statistic utilizing probability arguments may facilitate both the comparison of the evidence type and the weight that should be attach to each by the court.

The discussion and presentation of the data within the report submitted to the court by the expert witness must be prepared with rigour and clarity that can only come from a sound understanding of the essential mathematical and statistical method applied within forensic science.

1.2 Forensic Science

Forensic science is the application of science to criminal and civil, as governed by the legal standards of admissible evidence and criminal procedure. Forensic science is an ever growing field of science that can be further subdivided into toxicology, anthropology, serology and many others. Forensic scientist collect, preserve and analyze scientific evidence during the course of an investigation. While some forensic scientist travel to the scene of the crime to collect the evidence themselves and others occupy a laboratory role, performing analysis on object brought to them by other individuals.

1.3 Forensic Mathematics

One of the main thing crime scene investigators do is, collect, measure and document evidence. Their data help forensic scientists to perform calculation and determine the facts of a crime. Mathematics is the main key to analyze forensic evidence scientifically it is impossible to carry on without mathematics. For example, for pathologist calculus is need to estimate the time of death of victims. Overall, calculus has many application in the field forensic science. Mathematics make it possible to show the proof of what occurred during a crime in data and numbers.

1.3.1 Measurements:

One area of mathematics that is crucial for forensic science is take precise measurement at a crime scene. Knowing the exact length of shoe print from the crime scene help to rule out crime suspects whose shoe are the wrong size.

Forensic scientist need exact measurements of everything at a crime scene in order to perform scientific calculation properly. Investigators

spend a great deal of time measuring distance, weight, temperature, volume and other aspects of evidence to get the number correct.

1.3.2 Proportion:

Forensic scientist use not only measurements but proportions in their analysis. If a human leg bone is discovered in an unmarked grave forensic scientist use mathematical equations to determine what proportion or percentage of persons overall height of the leg bone would be. Once they know that they can determine how tall the person was and whether it was a child or an adult. Proportions are one way mathematics is involve in forensic science.

1.4 Applications of Mathematics in forensic Science

Forensic scientists analyze the evidence and search around crime scenes for clues pointing to possible suspects. Mathematics can be used to determine time of death, how crime are committed, when they were committed and who committed them. Some of the application of mathematics in various field of forensic science are given below :

- Psycho physical detection Monitoring pulse rate, blood pressure, and breathing patterns.
- Heights and distance Footprints in dirt and mud, length of objects.
- Bullet trajectories Geometry and trigonometry.
- Entomology Time of death.
- Trigonometry and industry physics can be used to reverse calculate height.
- To find an elevation consistent with two blood drops.
- Can be used to determine the height of the blood when it exceed to the body.

- Examining skid mark can help to reconstruct the accident. Marks are caused by the speed of the car, braking force, frictional force of the road and impacts with other vehicles.
- Newton's law of cooling describes the cooling of a warmer object to the cooler temperature of its environment.

1.4.1 Trigonometry

Trigonometry is very useful in forensic science. Knowledge about trigonometry is absolutely necessary for many crime scene reconstruction. Blood stain pattern analysis(BPA) is one of the several specialists in the field of forensic science. It involves the study and analysis of blood stain at a known or suspected violent crime scene. Blood stain evidence is most often assault, homicide abduction, suicide or even accidents associated with violent acts such Pythagoras theorem, trigonometry function, trigonometric rules are application of trigonometry in forensic science. Trigonometric function related to non right angled triangles and can be used to find an unknown angle or side.

1.4.2 Probability

In forensic science, empirical probabilities are particularly important and examples may be derived from data on height, fingerprint class, blood group, allele frequencies in DNA profiles or shoe size among the population. Some examples involving the use of empirical data like the matching of hair evidence and analysis of human teeth mark are discussed later

Forensic science uses several approaches for DNA statistics with computer programs such as match probability exclusion probability, likelihood ratios Bayesian approaches, and paternity and kinship testing. Random match probabilities (RMP) are used to estimate and express the rarity of a DNA profile. RMP can be defined as the probability that someone else in the population, chosen at random, would have the same genotype as the genotype of the contributor of the forensic evidence. RMP is calculated using the genotype frequencies at all the loci, or how

common or rare the alleles of a genotype are. The genotype frequencies are multiplied across all loci, using the product rule, to calculate the RMP. This statistic gives weight to the evidence either for or against a particular suspect being a contributor to the DNA mixture.

Chapter 2

Ballistics and Ricochet analysis

2.1 Ricochet Analysis of the bullet

Ricochet occurs when the incident angle is below the critical angle for the surface, a bullet after impact bounces off a solid surface at a glancing angle after impact and then continues its trajectory, otherwise the bullet will either fragment on the impact or penetrate the solid surface.

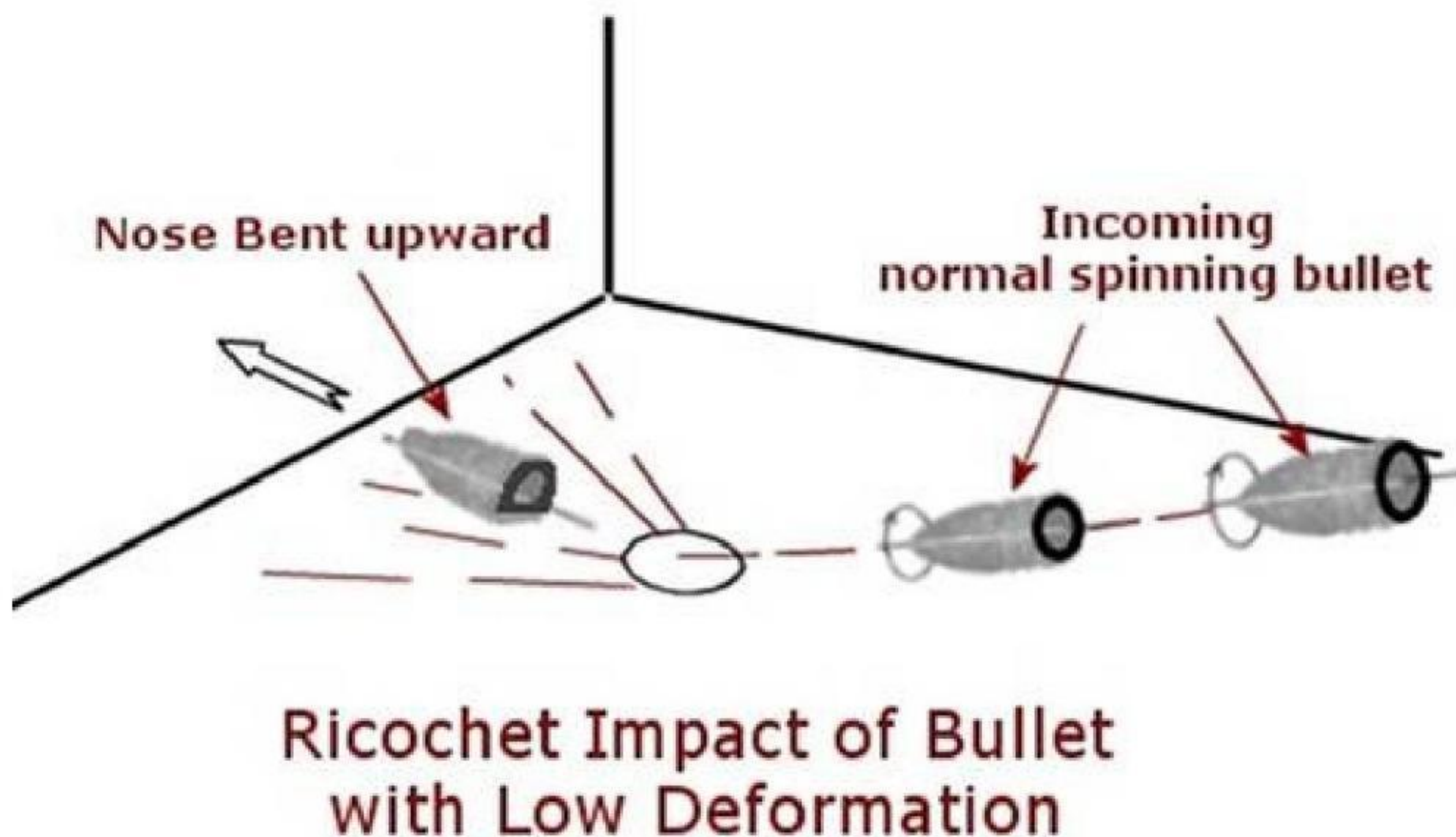


Figure 2.1:

For soil and water the critical angle is very low, at around $6-7^\circ$, whereas for hard surfaces this value will be much larger.

In almost all cases the ricochet angle θ_r at which the bullet leaves

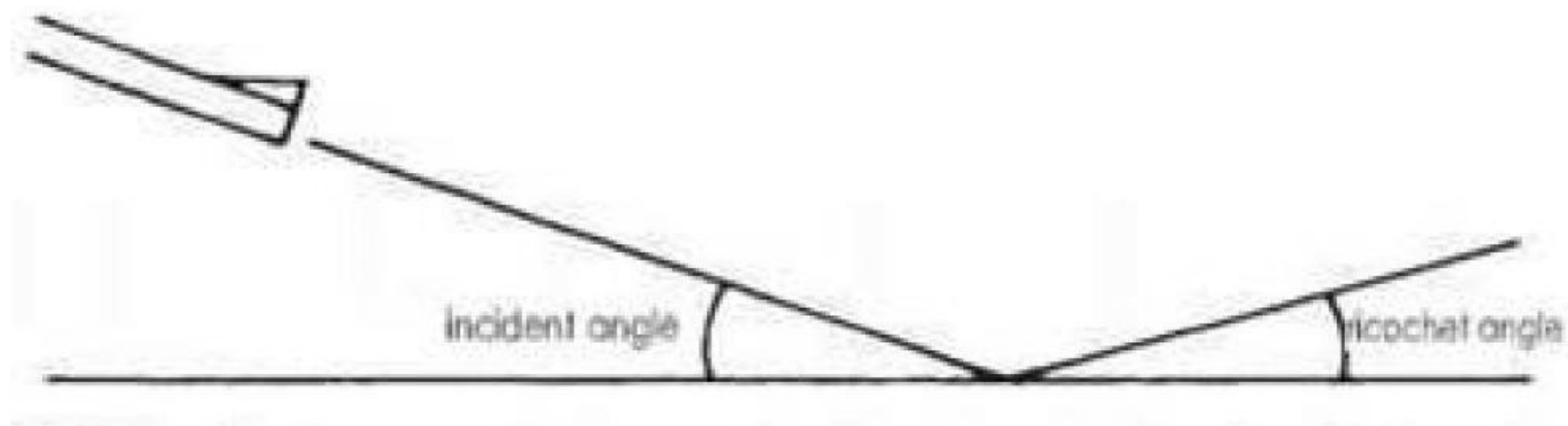


Figure 2.2: Incident and Ricochet angle

the surface is lower than the incident angle θ_i and these parameters are linked approximately by the equation

$$\tan \frac{\theta_r}{\theta_i} = C$$

where C is a constant dependent on the surface and the bullet involved.

θ_r : Ricochet angle

θ_i : Incident angle

C :constant

2.2 Aspects of ballistics

The effect of angle and the measurement of angle are important in understanding the trajectories followed by missiles such as bullets, arrows and cricket balls etc. All missiles start their motion with some initial speed and a specific launch angle from the initial force comes from the explosive charge in a rifle, the elastic energy in a tensioned string or human arm muscles strength. Once set on its trajectory, the only force acting on a missile is the vertically downward acting gravity. This is called the vacuum trajectory assumption. Horizontal component of the velocity remains unchanged. The result is that the missile follows a curved path, reaching a maximum height when the gravitational deceleration has reduced its upward velocity component to zero. It then descends with increasing downward vertical speed and constant horizontal speed until it impacts on the ground. (Fig 3)

If it is launched horizontally, for example from an elevated window, roof or cliff-top, it follows the downward part of this trajectory. (Fig 2.2)

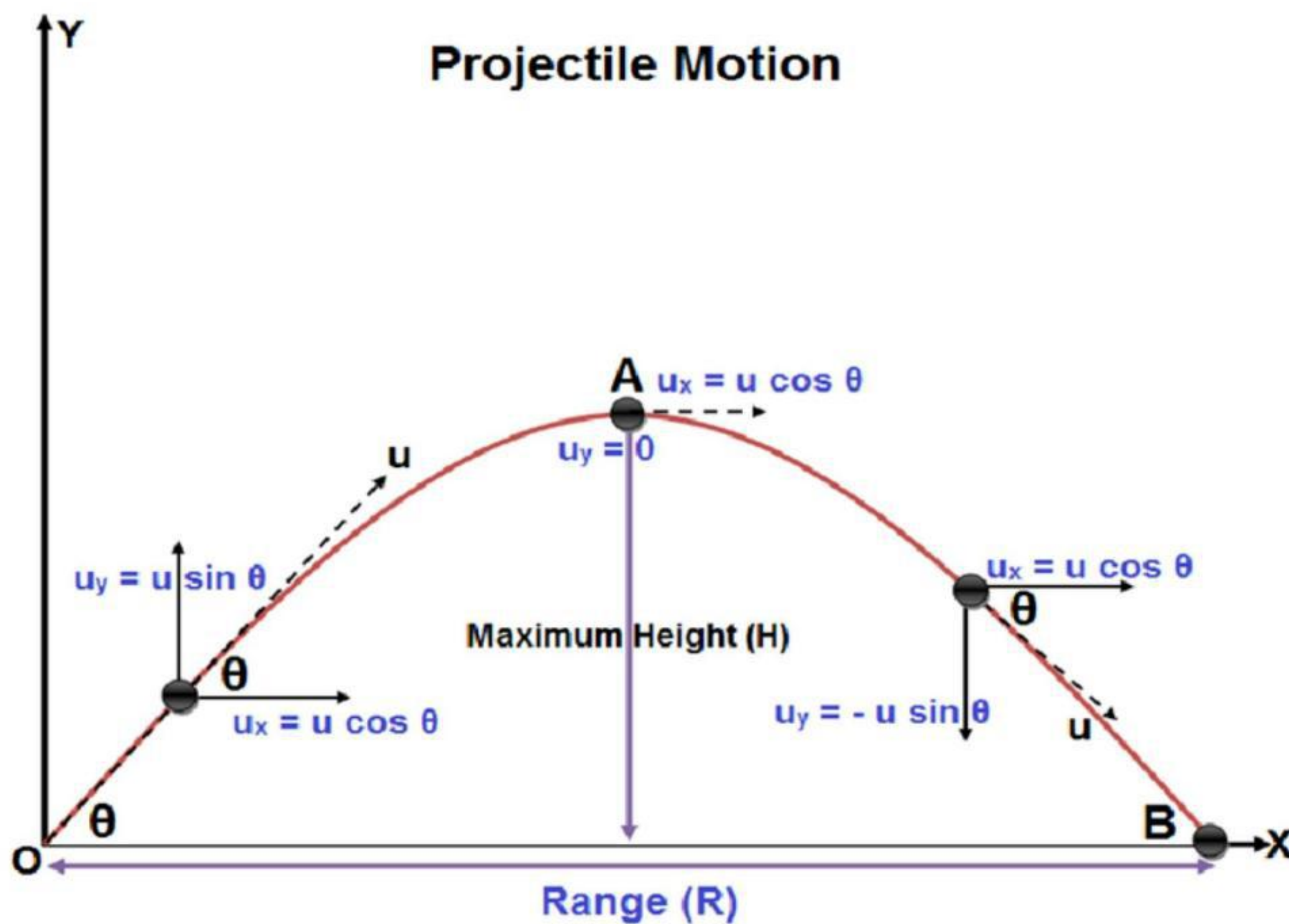


Figure 2.3:

The trajectory of a missile launched with speed u at an angle of θ to the horizontal is given by

$$y = \tan \theta x - \frac{g}{2u^2 \cos^2 \theta} x^2$$

where y is the height at any particular horizontal distance x and $g = 9.81 \text{ m/s}^2$ is the acceleration due to gravity.

In the equation ($y = (\tan \theta)x$) represents the straight line obtained in the absence of gravity by following the launch angle i.e. the line-of-sight path and the next term calculates how much the gravitational acceleration moves the projectile path downwards from this straight line. For specific initial conditions defined by u and θ , this equation is similar to the quadratic form:

$$y = Ax - Bx^2$$

This function represents a parabola with maximum altitude at $x = \frac{A}{2B}$

$$y_{max} = A\left(\frac{A}{2B}\right) - B\left(\frac{A}{2B}\right)^2 = \frac{A^2}{4B} = \frac{\tan^2 \theta}{4g} 2u^2 \cos^2 \theta = \frac{u^2 \sin^2 \theta}{2g}$$

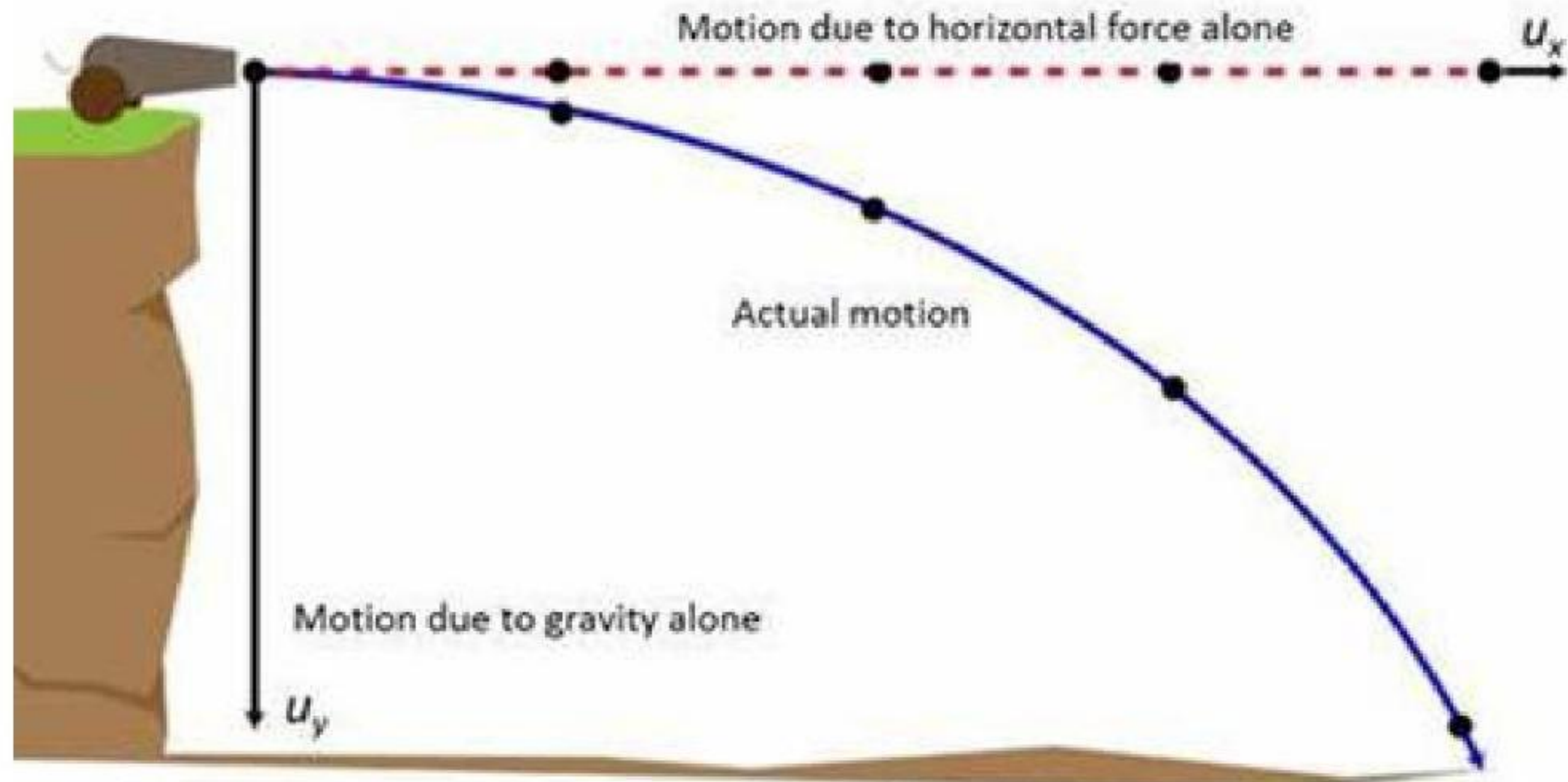


Figure 2.4:

The parabola is a symmetric shape, so if both initial and impact points are at the same height, the initial launch angle is the same as the angle at which the missile lands and also the speed with which it impacts on the same level surface is equal to the launch speed.e.g. a level surface. The horizontal range of the projectile occurs when horizontal distance

$$y = 0$$

$$(\tan \theta)x - \frac{g}{2u^2 \cos^2 \theta}x^2 = 0$$

$$x(\tan \theta - \frac{gx}{2u^2 \cos^2 \theta}) = 0$$

therefore either $x = 0$, which is the initial position, or :

$$\tan \theta - \frac{gx}{2u^2 \cos^2 \theta} = 0$$

$$x_{max} = \frac{2u^2 \cos^2 \theta \tan \theta}{g} = \frac{2u^2 \sin \theta \cos \theta}{g} = \frac{u^2 \sin 2\theta}{g}$$

Hence the maximum value of the sine function occurs when the angle is equal to 90° , the maximum range will occur here when $\theta = 45^\circ$.

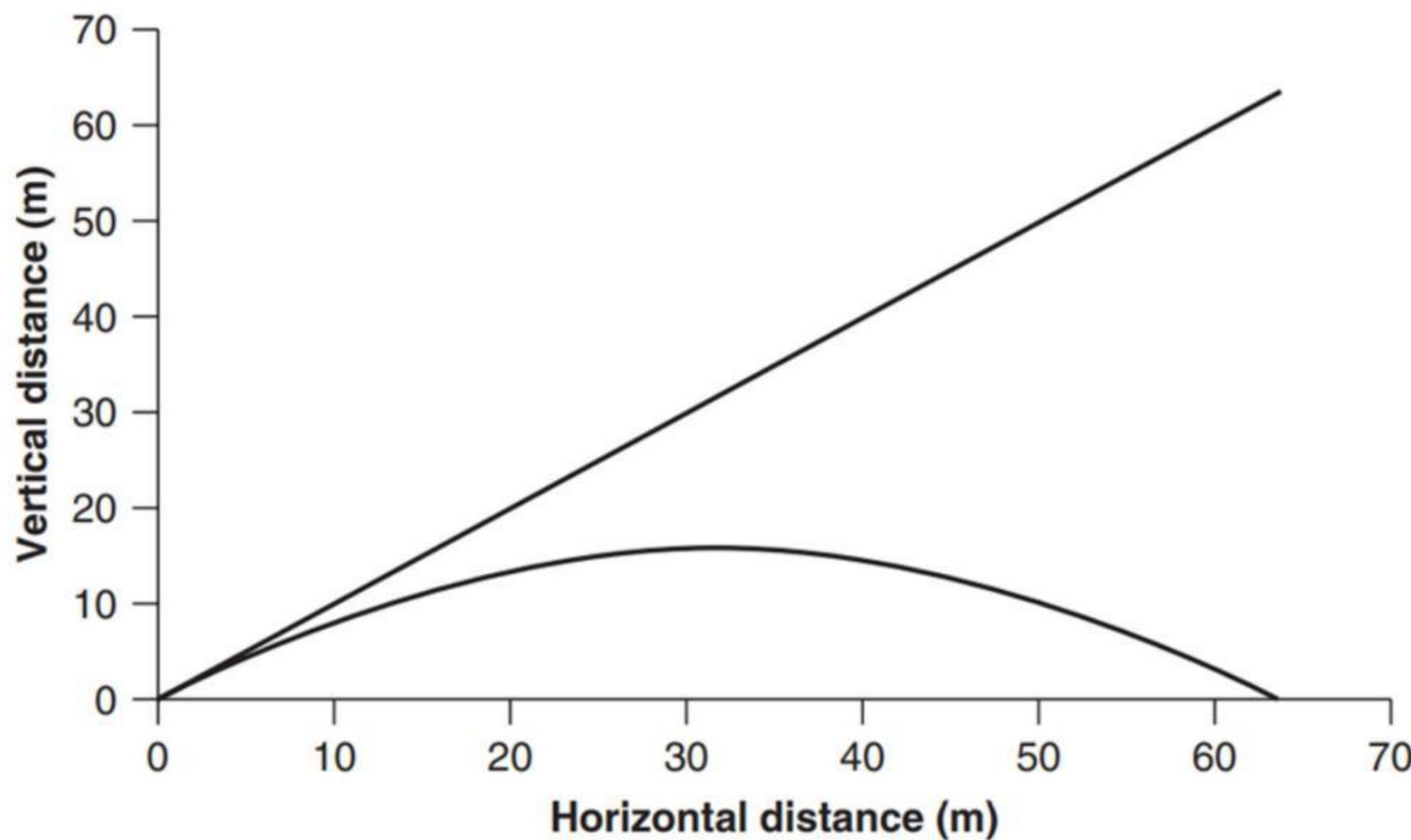


Figure 2.5:

2.2.1 Worked out example

Example :

An amateur archer who has the best launch speed of 25 m/s stands 20 m from a 5 m high wall and launches an arrow horizontally from a height of 1.6 m above the ground and at an angle of 20° horizontally, towards the wall from her standing position. Determine whether the arrow will clear the wall and if cleared by what distance? How much distance away from the other side should onlookers stand in order to be outside her range?

Solution :

Calculate the height attained over a horizontal distance of 20m under the given launch conditions using :

$$\begin{aligned}
 y &= (\tan \theta)x - \frac{g}{2u^2 \cos^2 \theta}x^2 = (\tan 20 \times 20) - \frac{9.81 \times 20^2}{2 \times 25^2 \cos^2 20} \\
 &= 7.28 - 3.55 = 3.73\text{m}
 \end{aligned}$$

Since the arrow was launched 1.6 m above the ground the net height will be 5.33m and hence the height of the wall 5m is given, hence the wall will be cleared by 0.33 m.

The horizontal range is given by the sum of two calculations. The distance travelled until it is again at launch height (1.6 m) above the ground is given by :

$$x_{max} = \frac{u^2 \sin 2\theta}{g} = \frac{25^2 \sin 40}{9.81} = 41.0m$$

The remaining distance taken from a height of 1.6m, travelling at the same speed but this time on a negative launch angle of 20/degree below the horizontal, down to ground level. This distance x is given as the solution of the equation :

$$\begin{aligned} -1.6 &= (\tan(-20))x - \frac{9.81}{2 \times 25^2 \cos^2(-20)} x^2 \\ 0.00889x^2 + 0.364x - 1.6 &= 0 \end{aligned}$$

Thus we evaluate the positive root of this quadratic equation.

$$x = \frac{-0.364 \pm \sqrt{0.364^2 + 4 \times 0.00889 \times 1.6}}{2 \times 0.00889} = \frac{-0.364 \pm 0.435}{0.0178} = 4.0m$$

Hence the total range of the arrow until it hits the ground is 45.0 m, which represents 25.0 m from the wall on the far side. The negative root is not taken, as it gives the distance below ground level which is against our assumption.

Chapter 3

Determination of fall type

3.1 Introduction

In a culture that values life, explaining the death in a public forum is crucial for many reasons. The examination of a death scene and collection of potential evidential material requires special and advanced skill, knowledge, aptitude and attitude. If a body is pronounced dead at the scene, many death investigation systems require a scene investigation. Others have many protocols as to which case types absolutely require a scene investigation (whether the body is present at the scene or not). Case types that should have a scene investigation include all confirmed or suspected homicides, suicides, accidents, traffic-related deaths, in-custody deaths, and workplace-related deaths. In this chapter we are going to see whether a death is suicide, accident, or murder using the relationship between the height above the ground (say y) and horizontal distance travelled (say x).

3.2 Suicide, accident or murder?

Studies have shown that the distance from the wall of a building at which a body is found can help us to establish how the fall from a height originated. This is because the initial conditions of launching differ according to whether the person simply loses his balance and falls or deliberately launches himself from the tall building by jumping or even running or jumping. In the former case i.e. accidental case,

the launch angle will be zero and the initial velocity will be minimal, whereas in the latter situation the jumping action will lead to a high launch angle and larger initial speed. It has been suggested that a launch speed of 2.7 m/s or greater can be used to indicate suicide and the jump angles likely to be between 21° and 38° . For the third possible scenario of murder by pushing the victim over the edge, the launch angle may be expected to be very low with the initial velocity higher than that achieved in case of accidental fall.

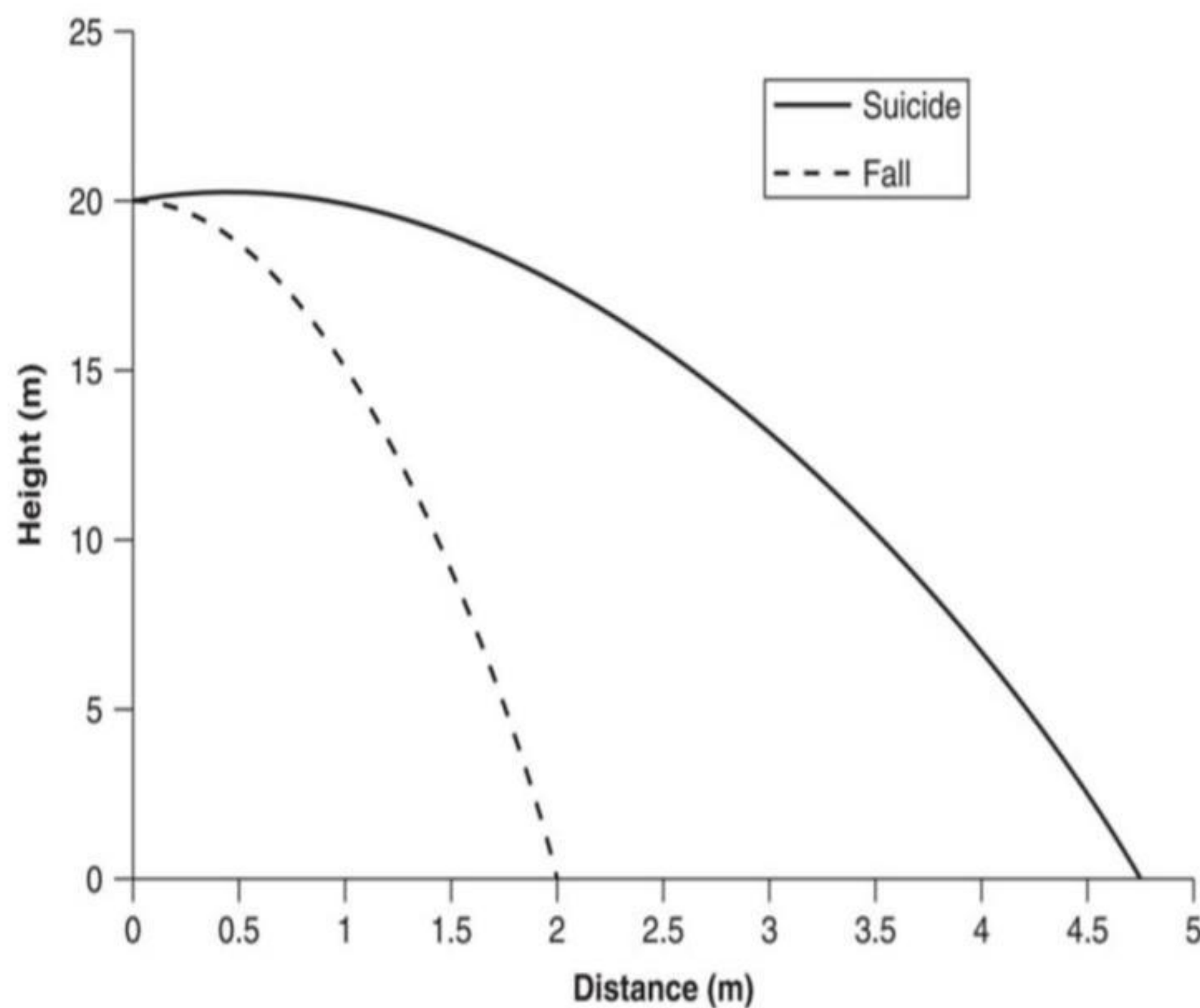


Figure 3.1:

The basic trajectory of the body is given by the same equation as before. If the ground level is set at $y = 0$ then we should simply add the fall height h , to give the relationship between y (the height above the ground) and x (horizontal distance travelled):

$$y = h + \tan \theta x - \frac{g}{2u^2 \cos^2 \theta} x^2$$

Typical trajectories, corresponding to accident or suicide, are given in the below graph. These have been calculated by assuming $\theta = 0^\circ$, $u = 1\text{m/s}$, in the former case and $\theta = 35^\circ$, $u = 3\text{m/s}$, in the latter case.

It can be seen that the impact distance for suicide is over twice that for accident. This result is supported by experimental data including an allowance for variation in the launching conditions.

3.3 Worked out example

Example : A woman jumps from the top of a vertical cliff-top 100m high

- a) At what distance from the base of the building will the body land assuming initial launch conditions of $\theta = 35^\circ$ and $u = 3m/s$?
- b) Compare this distance with the distance calculated on the basis of an accidental fall: $\theta = 0^\circ$ and $u = 1m/s$

Solution: a) This problem requires us to calculate x where all other parameters are known. This results in a quadratic equation:

$$0 = 100 + \tan 35x - \frac{9.8}{2*3^2*\cos^2 35} x^2$$

$$0.812x^2 - 0.70x - 100 = 0$$

This is solved using the standard equation for the solution of quadratic equations:

$$x = \frac{0.7 + \sqrt{0.49 + 324.5}}{1.62} = 11.6m$$

- b) The method is the same with these parameters; however, as the coefficient of the linear term in x is zero the solution is found more quickly:

$$0 = 100 + \tan 0x - \frac{9.8}{2*1^2*\cos^2 0} x^2$$

$$4.90x^2 - 100 = 0$$

$$x = \sqrt{\frac{100}{4.90}} = 4.5m$$

The former result is clearly different to the latter.

3.4 Program to check the fall type

```
#import required modules
import math
class Project:
    #Get user input through the constructor
    def __init__(self):
        self.height = float(input("Enter height of the building in meters: "))
        self.theta = float(input("Enter the angle: "))
        self.gravity = 9.81
        self.velocity = float(input("Enter the velocity in m/s: "))
        print("-----")
    # calculate the distance from the building for each type; of fall
    def calculateDistance(self, type):
        if type == "Maximum Accidental":
            self.theta = 0
            self.velocity = 1
        if type == "Minimum Suicide":
            self.theta = 38
            self.velocity = 2.7
        # make the quadratic equation ax2-bx-c=0
        x1 = 2 * (self.velocity ** 2) * (math.cos(math.radians(self.theta)) ** 2)
        a = self.gravity / x1
        b = math.tan(math.radians(self.theta))
        c = self.height
        # calculate the discriminant
        d = (b ** 2) + (4 * a * c)
```

```
# find the solutions
sol1 = (b - math.sqrt(d))/(2 * a)
sol2 = (b + math.sqrt(d))/(2 * a)
# print the distance calculated
if((sol1.real) > 0.0):
    print(type+' distance from the building is ', format(sol1.real))
    return(sol1.real)
else:
    print(type+' distance from the building is ', format(sol2.real))
    return(sol2.real)
# print the findings
def printFindings(self,Actual,Accidental,Suicide):
    if(Actual>=Suicide):
        print("The fall is SUICIDE!!")
    elif(Actual>Accidental):
        else:
            print("The fall is ACCIDENTAL!!")
            print("\n")
            print("-----")
#creating an object with the class
obj=Project()
#call methods
Actual=obj.calculateDistance("Actual")
Accidental=obj.calculateDistance("Maximum Accidental")
Suicide=obj.calculateDistance("Minimum Suicide")
obj.printFindings(Actual,Accidental,Suicide)
```

Output of the program

Enter height of the building in meters: 100

Enter the angle: 36

Enter the velocity in m/s: 5

Actual distance from the building is 19.516519331513965

Maximum Accidental distance from the building is 4.515236409857309

Minimum Suicide distance from the building is 9.974033289332445

The fall is SUICIDE!!

Chapter 4

Case Study

4.1 Introduction

Our group visited the Harbour Janamithri Police Station, Willington Island on 20 th December 2021 to collect data on a case based on Chapter 3(determination of fall type) of our project. There we checked some case files and found a case where an employer during the construction work of Dhruv complex were found dead due to the fall of a screw jack on his head. We got the measurements such as building height and measurements giving the exact position of the body. By examining the position of the body we came to a conclusion that the screw jack fell by accident.



4.2 Case Details

FIR No : 0948

Section : 174

Name : Benoy

Age : 41

Height :169cm

Date : 30.09.2021

Place:INS Venduruthy



A man named Benoy was found dead on the ground ($y=0$) near the constructing Dhruv complex after a screw jack fell on his head. The body was found 4.5m (say x) away from a tall building. The screw jack was said to be in the 6th floor of the building i.e. approximately 22.4m high. According to the witness statement the screw jack fell by accident and the police conclude the case with the same.

According to our study the impact angle and initial velocity should be minimal for an accidental fall. The body was lying at a short distance, 4.5m away from the building which would only be possible when the initial conditions i.e. initial velocity u and initial launge angle θ is minimal. Hence from our studies, we concluded that the fall was accidental.

$$\text{i.e. } y=0$$

$$h=22.4\text{m}$$

$$g=9.8$$

$$x=4.5$$

are the measurements obtained.

From the eqn

$$y = h + \tan \theta x - \frac{g}{2u^2 \cos^2 \theta} x^2$$

we usually calculate x which is used to determine the fall type provided u is minimal and $\theta = 0$ in the case of accidental fall. But here x=4.5m is already obtained without the calculation which is very small which implies u and θ are minimal. Hence the fall is accidental.



Chapter 5

Bloodstain shape analysis

5.1 Introduction

Correlating the basic shape of a bloodstain with the impact conditions of the droplet involves trigonometric functions. There are two types of bloodstain formation :

- 1.Bloodstain formation from a stationary source
- 2.Bloodstain formation from a moving source

5.2 Bloodstain formation from a stationary source

Blood droplets in free-fall through the air under gravity adopt a spherical shape, surface tension forces act on the blood droplet to minimize the surface energy leading to a surface with minimum area.

On perpendicular impact of blood on a surface, it will spread out equally in all directions, then circular stain is formed. If the impact is less than 90° , the blood spreads out at the same rate in all directions. On impact the spherical blood droplet will intersect the surface in an elongated fashion in the direction of travel of the victim, then the stain is in elliptical state. The long axis (L) lies in the direction of impact along the surface and the short axis (W) is in transverse direction.

By measuring the dimensions of the blood stain, the impact angle can be calculated using their ratio :

$$\sin \theta = \frac{W}{L}$$

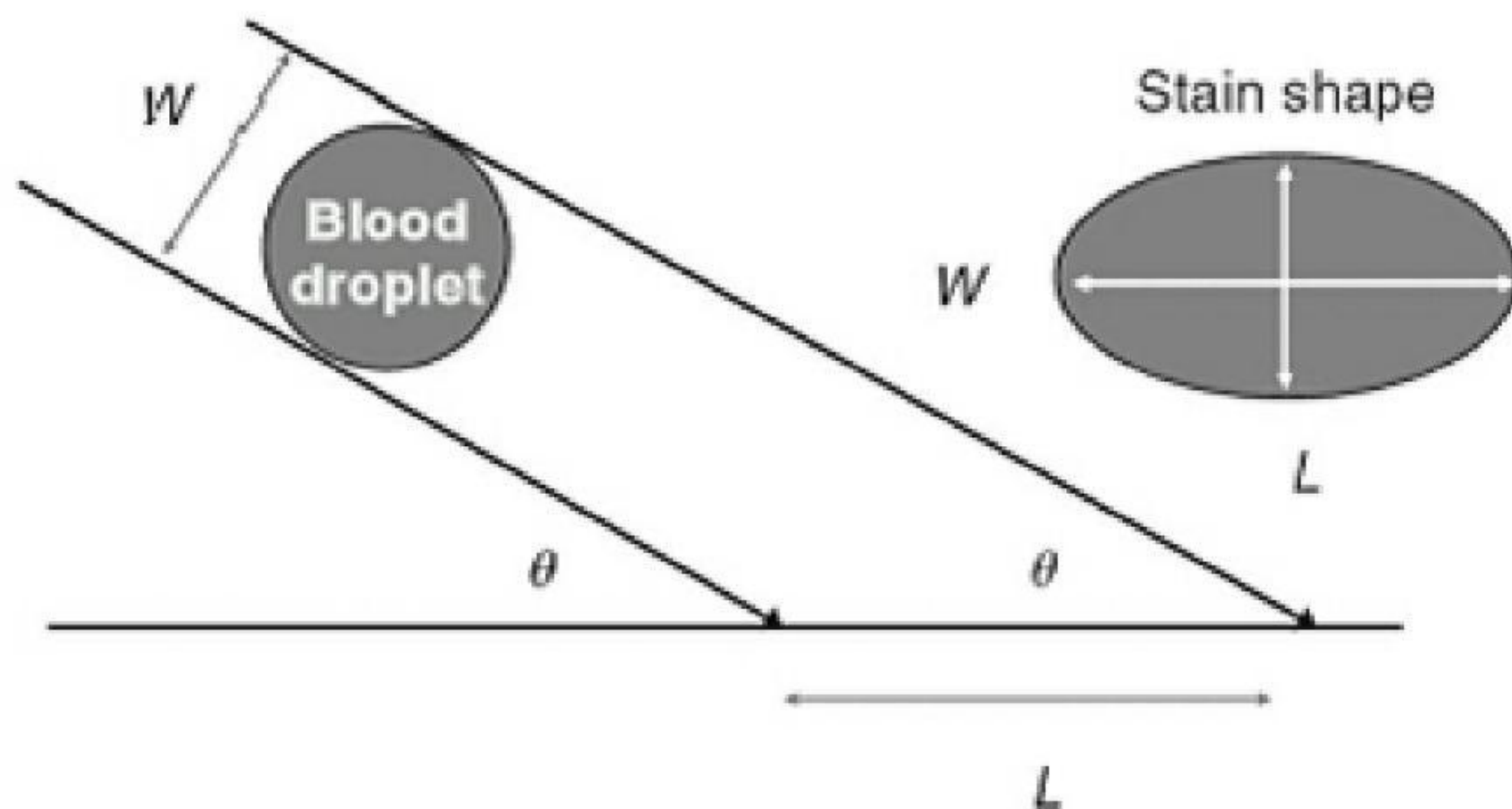
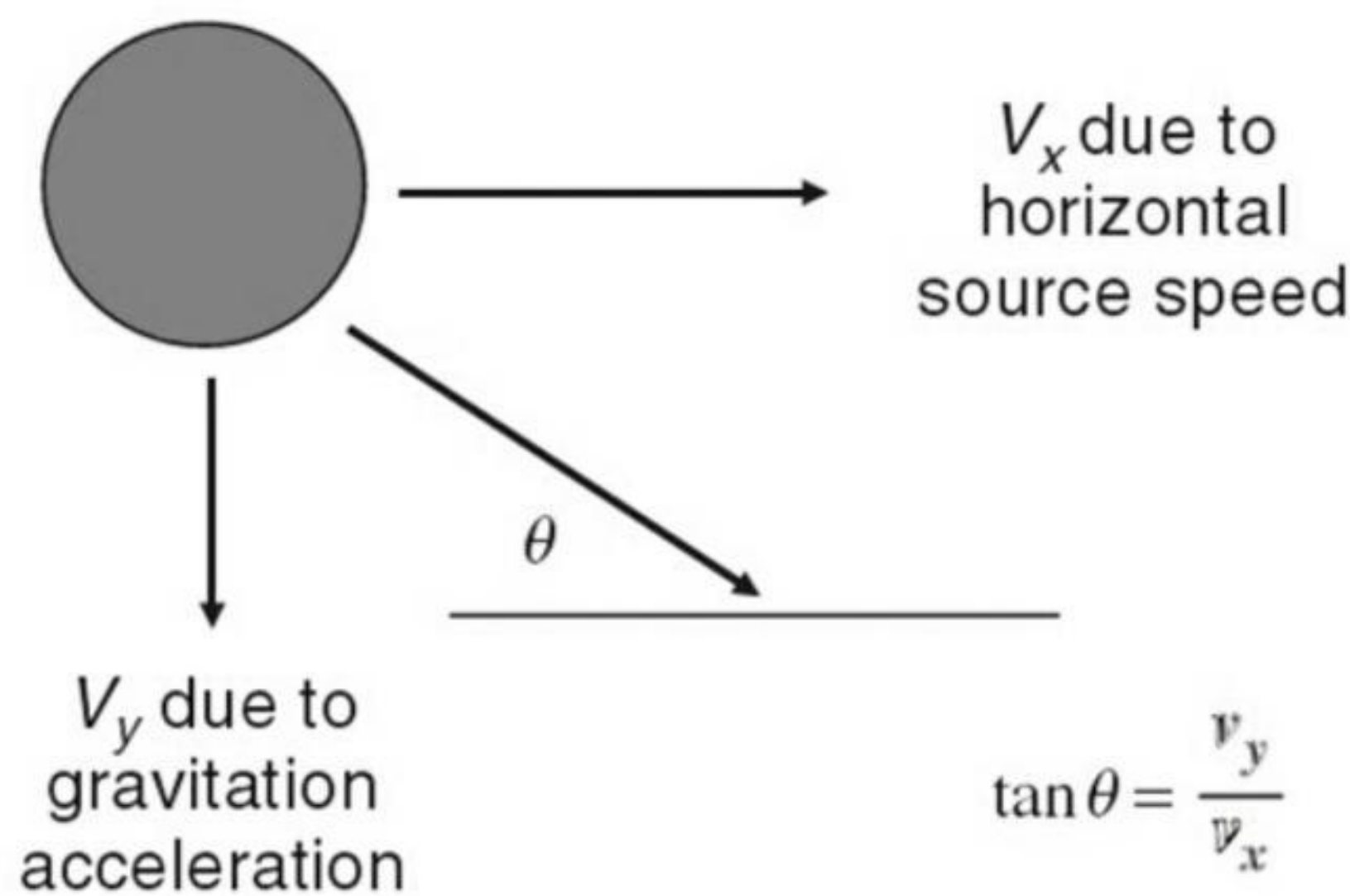


Figure 5.1: Angular impact of a blood droplet on a surface

5.3 Bloodstain formation from a moving source

Consider blood droplets falling from a moving source, the droplet under gravity starts falling vertically, it posses a horizontal component of velocity due to the moving source and when it impacts on the ground surface, its actual impact is not 90° and it depends on the relative values of these two components.



Impact on the ground of a blood droplet from a moving source

Figure 5.2:

The above diagram shows the relation between the velocity components as impact angle vectors. These components, from a right angled triangle, which are perpendicular to each other, includes the effective impact angle, θ . Inspection of this triangle gives:

$$\tan \theta = \frac{V_y}{V_x}$$

This equation enables us to calculate the walking speed of the victim V_x , from the measurement of the impact angle θ . The vertical velocity component V_y is calculated using the drop height h :

$$V_y = \sqrt{2gh}$$

In the above equation it is assumed that the air resistance has no significant effect, which will be true for large droplets of blood falling over relatively short distance.

5.3.1 Worked out example

Example: An assailant walks away from a crime scene, blood dripping from a wound to his hand. The elliptical bloodstain has a length of 7 mm and a width of 6 mm. Calculate his walking speed assuming that his hand is moving with the same velocity as his body.

Solution impact angle is calculated using the dimensions of the stain.

$$\sin \theta = \frac{6}{7}$$

$$\theta = \sin^{-1} \frac{6}{7} = 59^\circ$$

Estimation of drop distance of the blood droplet. Assuming a hand wound, this would be around 1 m; the vertical impact speed is given by:

$$V_y = \sqrt{2 \cdot 9.8 \cdot 1} = 4.43 \text{ m/s}$$

the horizontal speed is calculated using:

$$\tan 59^\circ = 4.43/v_x$$

$$v_x = 4.43/1.664 = 2.66 \text{ m/s}$$

5.4 Program to calculate walking speed of assailant

```
#import required modules
#import math
class Project:
    #get user input through the constructor
    def __init__(self):
        self.length=float(input("Enter the length of the bloodstain: "))
        self.width=float(input("Enter the width of the bloodstain: "))
        self.height=1.0
        self.gravity=9.81
        print("-----")
    #calculate the impact angle
    def calculateVelocity(self):
        x=self.width/self.length
        self.theta=math.asin(x)
        self.theta=math.degrees(self.theta)
        #calculate the velocity of the assailant from a crime scene
        a=2*self.gravity*self.height
        vy=math.sqrt(a)
        b=math.tan(math.radians(self.theta))
        vx=vy/b
        return vx,vy
    #print the findings
    def printFindings(self,vx,vy):
        print("The impact angle=",self.theta)
        print("The vertical impact speed=",vy)
        print("The walking speed of the assailant=",vx)
        print("\n")
        print("-----")
    #creating an object with the class
    obj=Project()
    vx,vy=obj.calculateVelocity()
```

obj.printFindings(vx,vy)

5.4.1 Output of the program

Enter the length of the bloodstain:7

Enter the width of the bloodstain: 6

The impact angle= 58.997280866126005

The vertical impact speed= 4.4294469180700204

The walking speed of the assailant= 2.6617663308412336

Chapter 6

Probability in forensic science

6.1 Introduction

The term probability is given to a proper measure of the certainty that a specific event or outcome will occur. In each cases of probability the result's based on unbaised outcomes where every possible result's equally likely.

In forensic science , empirical probabilities are particularly important and example could also be derived from data on height,fingerprint class,blood group,allele frequency in DNA.

6.2 Calculating Probability

The most common assumption in probability is that every event has the same random chance of happening. For instance, once we toss a coin,either the tail can come up or head can.Both these events can't be predicted.

$$Probability] = \frac{\text{Number of selected outcomes}}{\text{Total number of outcomes}}$$

6.2.1 RULES OF COMBINING PROBABILITIES:

We use some ground rules to combine probabilities of various situations. We can do that only when the events are independent of each other. When the outcome of one event doesn't depend upon the result of the other, the events are said to be independent.

RULE 1:

The probability of specified outcomes A and B occurring is given by:

$$P(A \text{ and } B) = P(A) \times P(B)$$

RULE 2:

The probability of specified outcomes A or B occurring, where both A and B cannot occur together (mutually exclusive), is given by:

$$P(A \text{ or } B) = P(A) + P(B)$$

In some applications it is possible that both A and B occur together (e.g. A and B aren't mutually exclusive). In such cases we should always exclude this possibility to obtain:

$$P(A \text{ or } B) = P(A) + P(B) - P(A \text{ and } B)$$

For example, some witnesses have claimed that a criminal has long, fair hair and data is out there that says that one cannot compute the probability of somebody having both these attributes ($P(A \text{ and } B)$) from this data alone as we do not know the probability of occurrence of one without the other $P(A \text{ or } B)$, e.g. long hair that is not fair and fair hair that is short. In other words, having long hair and having fair hair aren't mutually exclusive.

In cases where we've to seek out the probability of an event not occurring, for example, the probability that a coin wouldn't land on head when tossed. Such an event is denoted by ("A'") and therefore the following applies:

$$P(A') = 1 - P(A)$$

Note that this suggests certainty – a probability of unity – that either the event will occur or it'll not!

6.2.2 Worked out examples

Example 1: A violent incident leads to a multicolored vase being broken at a crime scene into very many small pieces. Half the ceramic pieces are white and the rest are coloured either red or blue in equal proportions. A CSI is tasked with retrieving pieces of this evidence randomly.

Calculate the probability of:

- (a) selecting a white piece
- (b) not selecting a red piece
- (c) selecting a white piece and a blue piece in either order
- (d) selecting one among each color in three attempts.
- (e) What assumption have you made in calculations (c) and (d)?

Solution: (a) Half the pieces are white so:

$$P(\text{white}) = \frac{1}{2} = 0.5$$

(b) A quarter of the pieces are red so:

$$P(\text{not red}) = 1 - \frac{1}{4} = 0.75$$

(c) The probability of choosing white then blue or blue then white is:

$$P(w \text{ and } b \text{ or } b \text{ and } w) = \frac{1}{2} \times \frac{1}{4} + \frac{1}{4} \times \frac{1}{2} = \frac{2}{8} = 0.25$$

(d) Similarly, we extend the calculation to three selections, in any order. Note that there are six different orders during which the three differently coloured pieces could also be selected, e.g. white, red, blue; white, blue, red etc. Each of these has the same probability.

$$P(\text{all three colours}) = \left(\frac{1}{2} \times \frac{1}{4} \times \frac{1}{4}\right) \times 6 = 0.1875$$

(e) In these calculations we've assumed that the removal of a couple of pieces does not change the total number significantly, i.e. it is very

large.

Example 2: The percentage distribution of shoe sizes for 2001 is given in Table

- (a) Calculate the probability that a man selected at random will have
 - (i) a shoe size of 10
 - (ii) a shoe size of 8 or less.
- (b) If two men are randomly selected from a really large population, what's the probability
 - (i) that both will have size 9 shoes
 - (ii) that both have identical shoe size.

Table: Distribution of men's shoe sizes

SIZE	5	5.5	6	6.5	7	7.5	8	8.5	9	9.5	10	10.5	11	11.5	>12
%	1	1	2	4	7	11	13	15	14	12	9	6	3	2	1

Solution : (a) .(i) Out of each hundred men, nine have this shoe size and then the proportion and thus the probability is given by:

$$P(10) = \frac{9}{100} = 0.09$$

(ii) Here we need the number of men who have shoe sizes of 8 or less.

Using the data from the table gives:

$$P(\leq 8) = \frac{1 + 1 + 2 + 4 + 7 + 11 + 13}{100} = \frac{39}{100} = 0.39$$

(b) .(i) This probability is given by combining the probability that the first man has size 9 shoes and that the second has size 9 as well:

$$P(\text{size 9 and size 9}) = \frac{14}{100} \times \frac{14}{100} = \frac{196}{10000} = 0.0196$$

(ii) If both men have identical size then we would like to sum up, over all sizes, the individual probabilities that both have a specific size:

$$P(\text{same size}) = \frac{1}{100} \times \frac{1}{100} + \frac{1}{100} \times \frac{1}{100} + \dots + \frac{2}{100} \times \frac{2}{100} + \frac{1}{100} \times \frac{1}{100}$$

$$\begin{aligned} P(\text{same size}) &= 0.0001 + 0.0001 + 0.0004 + 0.0016 + 0.0049 + 0.0121 \\ &+ 0.0169 + 0.0225 + 0.0196 + 0.0144 + 0.0081 + 0.0036 + 0.0009 + \\ &0.0004 + 0.0001 = 0.1057 \end{aligned}$$

The probability of two men having the same shoe size, based on this data, is therefore 0.1057

6.3 Program

```

shoes=5:1,5.5:1,6:2,6.5:4,7:7,7.5:11,8:13,8.5:15,9:14,9.5:12,10:9,10.5:6,11:3,11.5:2,12:1
option=0
while(option1==3):
    print("\n =====MENU====")
    print("1. Probability that a random man selected will have a given shoe
sizes ")
    print("2. Probability when two men are selected ")
    print("3. Exit")
    print("=====")
    option=int(input("Enter the option :"))
    if(option==1):
        sizes=list(map(float,input("Enter the shoe sizes :").strip().split()))
        p=0
        for size in sizes:
            p+=shoes[size]/100
            print("Probability is",round(p,4))
    elif(option==2):
        print("\n =====")
        print("1. Probability that they have a given size")
        print("2. Probability that they have same size")
        print("=====")
        option2=int(input("Enter the option :"))
        if(option2==1):
            size=float(input("Enter the size:"))
            p=(shoes[size]/100)**2
            print("Probability is",round(p,4))
        elif(option2==2):
            p=0

```

```
percent=shoes.values()
for value in percent:
    p+=(value/100)**2
print("Probability that they have same size is",round(p,4))
```

6.3.1 Output of the program

=====MENU=====

1. Probability that a random man selected will have a given shoe sizes
 2. Probability when two men are selected
 3. Exit
- =====

Enter the option :1

Enter the shoe sizes :9

Probability is 0.14

=====MENU=====

1. Probability that a random man selected will have a given shoe sizes
 2. Probability when two men are selected
 3. Exit
- =====

Enter the option :2

=====

1. Probability that the have a given size

2. Probability that they have same size

=====

Enter the option :1

Enter the size:9

Probability is 0.0196

=====MENU=====

1. Probability that a random man selected will have a given shoe sizes

2. Probability when two men are selected

3. Exit

Enter the option :2

1. Probability that they have same size

2. Probability that they have different size

Enter the option :2

Probability that they have same size is 0.1057

CONCLUSION

From the above it can be concluded that mathematics is a subject which can be incorporated in all types of sciences including the various branches of forensic science such as forensic biology, forensic chemistry, forensic physics, forensic ballistics, etc.

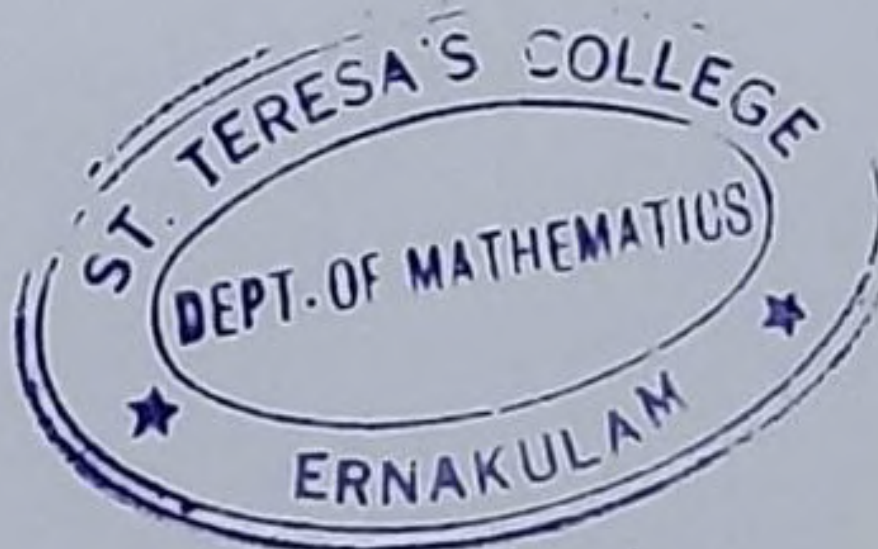
Mathematics has a wide scope in forensic science because it deals with the analysis of the evidence obtained from a crime scene followed by its interpretation and followed by mathematical calculations.

Moreover, only with the mathematics interpretation, it is possible to determine the findings such as height from which a blood drop has originated, or the angle at which a blood drop has struck a target surface resulting in the formation of bloodstains, or the probability that the blood types of any two randomly chosen individuals would match with each other and much more.

As it is clearly understood that mathematical calculations have a wide range of applications in forensic science. So, for a forensic expert, it is important to possess excellent knowledge of mathematics and statistics along with the principles and theory of different sciences to solve a crime efficiently and effectively.

REFERENCES

- [1] Craig Adam, Essential mathematics and statistic for Forensic Science, Wiley Balckwell(2010)
- [2] D.P.Lyle, Forensic for Dummies, Wiley(2004)
- [3] Eric Matthes, Python Crash Course, No Starch Press(2015)
- [4] Max M Houck, Fundamentals of Forensic Science, Academic Press(2006)
- [5] <https://forensicroader.com/need-of-forensic-mathematics/>
- [6] https://ngl.cengage.com/assets/downloads/forsci_pro0000000541/course_math_app_forens
- [7] <https://prezi.com/t2h82li7qjn/math-in-forensic-science/?frame=796a6632b4aa19719d60f7a00a68a62612beab6d>
- [8] <https://docs.python.org/3/reference/>
- [9] https://bugs.python.org/file47781/Tutorial_E_DIT.pdf
- [10] <https://static.realpython.com/python-basics-sample-chapters.pdf>



ST. TERESA'S COLLEGE (AUTONOMOUS), ERNAKULAM



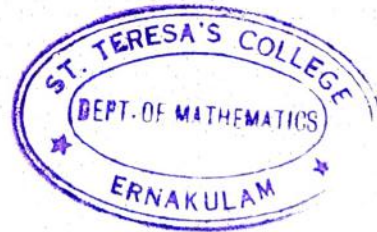
CERTIFICATE

This is to certify that the dissertation entitled, **QUEUING THEORY** is a bonafide record of the work done by Ms. **IVY TREESA** under my guidance as partial fulfillment of the award of the degree of **Bachelor of Science in Mathematics** at St. Teresa's College (Autonomous), Ernakulam affiliated to Mahatma Gandhi University, Kottayam. No part of this work has been submitted for any other degree elsewhere.

Date: 08-03-2022

Place: Ernakulam

Smt. Betty Joseph
Associate Professor,
Department of Mathematics and Statistics,
St. Teresa's College(Autonomous),
Ernakulam.



Dr. Ursala Paul
Assistant Professor and Head ,
Department of Mathematics and Statistics,
St. Teresa's College(Autonomous),
Ernakulam.

External Examiners

1: *[Signature]*

2: *[Signature]*

Project Report

On

QUEUEING THEORY

Submitted

in partial fulfilment of the requirements for the degree of

BACHELOR OF SCIENCE

in

MATHEMATICS

by

IVY TREESA

(Register No. AB19BMAT034)

Under the Supervision of

SMT. BETTY JOSEPH



DEPARTMENT OF MATHEMATICS

ST. TERESA'S COLLEGE (AUTONOMOUS)

ERNAKULAM, KOCHI - 682011

APRIL 2022

Project Report
On

QUEUEING THEORY
Submitted
in partial fulfilment of the requirements for the degree of
BACHELOR OF SCIENCE
in
MATHEMATICS
by
IVY TREESA
(Register No. AB19BMAT034)

Under the Supervision of
SMT. BETTY JOSEPH



DEPARTMENT OF MATHEMATICS
ST. TERESA'S COLLEGE (AUTONOMOUS)
ERNAKULAM, KOCHI - 682011
APRIL 2022

ST. TERESA'S COLLEGE (AUTONOMOUS), ERNAKULAM



CERTIFICATE

This is to certify that the dissertation entitled, **QUEUEING THEORY** is a bonafide record of the work done by Ms. **IVY TREESA** under my guidance as partial fulfillment of the award of the degree of **Bachelor of Science in Mathematics** at St. Teresa's College (Autonomous), Ernakulam affiliated to Mahatma Gandhi University, Kottayam. No part of this work has been submitted for any other degree elsewhere.

Date: 03-03-2022

Place: Ernakulam

Betty Joseph
Smt. Betty Joseph
Associate Professor,
Department of Mathematics and Statistics,
St. Teresa's College(Autonomous),
Ernakulam.



Ursula Paul
Dr. Ursula Paul
Assistant Professor and Head ,
Department of Mathematics and Statistics,
St. Teresa's College(Autonomous),
Ernakulam.

External Examiners

1: *[Signature]*

2:
[Signature]

DECLARATION

I hereby declare that the work presented in this project is based on the original work done by me under the guidance of Smt. Betty Joseph, Associate Professor, Department of Mathematics and Statistics, St. Teresa's College(Autonomous), Ernakulam and has not been included in any other project submitted previously for the award of any degree.



Ernakulam.

IVY TREESA

Date: **08.03.2022**

AB19BMAT034

ACKNOWLEDGEMENT

Firstly I thank God Almighty for giving me his grace to execute the project work successfully. I express my sincere gratitude to our guide Smt.Betty Joseph, Associate Professor of Department of Mathematics and Statistics, St.Teresa's College (Autonomous), Ernakulam, for her valuable guidance throughout the project. I would also like to mention Smt. Neem Susan Paul, Department of Mathematics and Statistics, St.Teresa's College (Autonomous), Ernakulam, for her help and support.

I do express my gratitude to Dr. Ursala Paul, HOD of Department of Mathematics and Statistics, St. Teresa's College (Autonomous) Ernakulam .

My gratitude to all the other teachers and all those for their valuable support throughout the work.

Ernakulam.

Date: **08.03.2022**

IVY TREESA

AB19BMAT034

Contents

<i>CERTIFICATE</i>	ii
<i>DECLARATION</i>	iii
<i>ACKNOWLEDGEMENT</i>	iv
<i>CONTENT</i>	v
<i>INTRODUCTION</i>	vii
1 BASICS OF QUEUING THEORY	1
1.1 Basic Definitions	1
1.1.1 Queue	1
1.1.2 Customer	1
1.1.3 Queue Length	1
1.1.4 Server	1
1.2 The Basic Components of a Queue	1
1.2.1 Arrival process	1
1.2.2 Service and Departure process	2
1.2.3 The number of servers	2
1.2.4 The queuing discipline	2
1.2.5 The queue capacity	2
1.2.6 The size of the client population	2
1.3 Types of Queues	3
1.3.1 Single server Single-phase	3
1.3.2 Single server Multi-phase	3
1.3.3 Multi server Single-phase	3
1.4 Queuing system	4
1.4.1 Queuing structure	4
1.4.2 Queuing system	5

1.4.3	Components of Queuing systems	5
1.5	Basic Terminologies	6
2	LAW AND NOTATION	8
2.1	Kendall's Notation	8
2.1.1	Poisson Distribution	9
2.1.2	Exponential Distribution	10
2.1.3	Markovian Distribution	10
2.2	Little's Law	11
3	QUEUEING MODELS	13
3.1	Model 1 - $(M/M/1) : (GD/\infty/\infty)$	13
3.2	Model 2 - $(M/M/C) : (GD/\infty/\infty)$	16
3.3	Model 3 - $(M/M/1) : (GD/N/\infty)$	19
4	APPLICATIONS	23
4.1	Daily Life Applications	23
	<i>CONCLUSION</i>	25
	<i>REFERENCES</i>	26

INTRODUCTION

Queuing theory is the mathematical study of formation, congestion and purpose of waiting lines .It is observed as a branch of Operations Research because the outcomes are often used for making business decisions about the measures needed to provide a service.

Queuing theory has its origin in 1909 when Professor A K Erlang Danish Mathematician and engineer published his fundamental paper in telephone traffic. He sought to determine how many circuits were needed to provide an acceptable level of telephone service for people not to be " on hold " for too long.



A queue is formed at a queuing system when either customers (human beings or physical entities) requiring service wait due to the number of customers exceeding the number of service facilities or service facilities do not work efficiently and take more time than prescribed to serve a customer.

Queuing theory can be applied to a variety of situations where it is not possible to predict accurately the arrival rate (or time) of customers and service rate (or time) of service facility or facilities. In particular,it can be used to determine the level of service (either the service

rate or the number of service facilities) that balances the following two conflicting costs.

- (i) cost of offering the service
- (ii) cost incurred due to delay in offering service

Chapter 1

BASICS OF QUEUING THEORY

1.1 Basic Definitions

1.1.1 Queue

A line or sequence of people or items awaiting their turn to be attended or for a service is called a queue.

1.1.2 Customer

A list of items or people that waits for a service is called customer.

1.1.3 Queue Length

Number of customers waiting in a system for service.

1.1.4 Server

Server provides service in the system.

1.2 The Basic Components of a Queue

1.2.1 Arrival process

Arrival defines the way customers enter the system , mostly the customers arrive randomly in between two adjacent arrivals.

1.2.2 Service and Departure process

It defines how long service will take, how many no. of servers are accessible, whether it is in series or parallel. Departure process is a Poisson process with rate that is statistically identical to the arrival process.

1.2.3 The number of servers

The number of servers available to serve the customers in the system. It may be single server or multi-server

1.2.4 The queuing discipline

It represents the order in which the customers are selected from the queue for service.

1.2.5 The queue capacity

The number of customers/items the queue can hold

1.2.6 The size of the client population

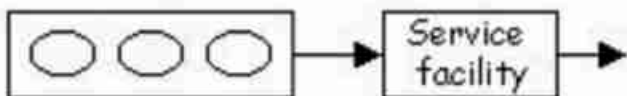
Also known as population size. The size of calling population can be finite or infinite. In case of large population, it is assumed as infinite



1.3 Types of Queues

1.3.1 Single server Single-phase

A waiting line in which single line of customers go through a single waiting line or phase and they are served by a single server. Queues in ATM is an example.



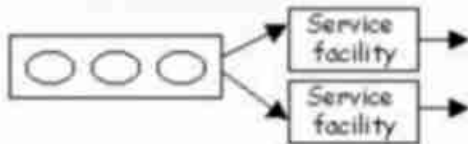
1.3.2 Single server Multi-phase

The system in Which there are multiple number of waiting lines or phase but only one server to serve. Queues in buffet restaurants is an example.



1.3.3 Multi server Single-phase

In this system there will be only one waiting line or phase and they are served by more than one servers. Queues in bank are commonly seen example.

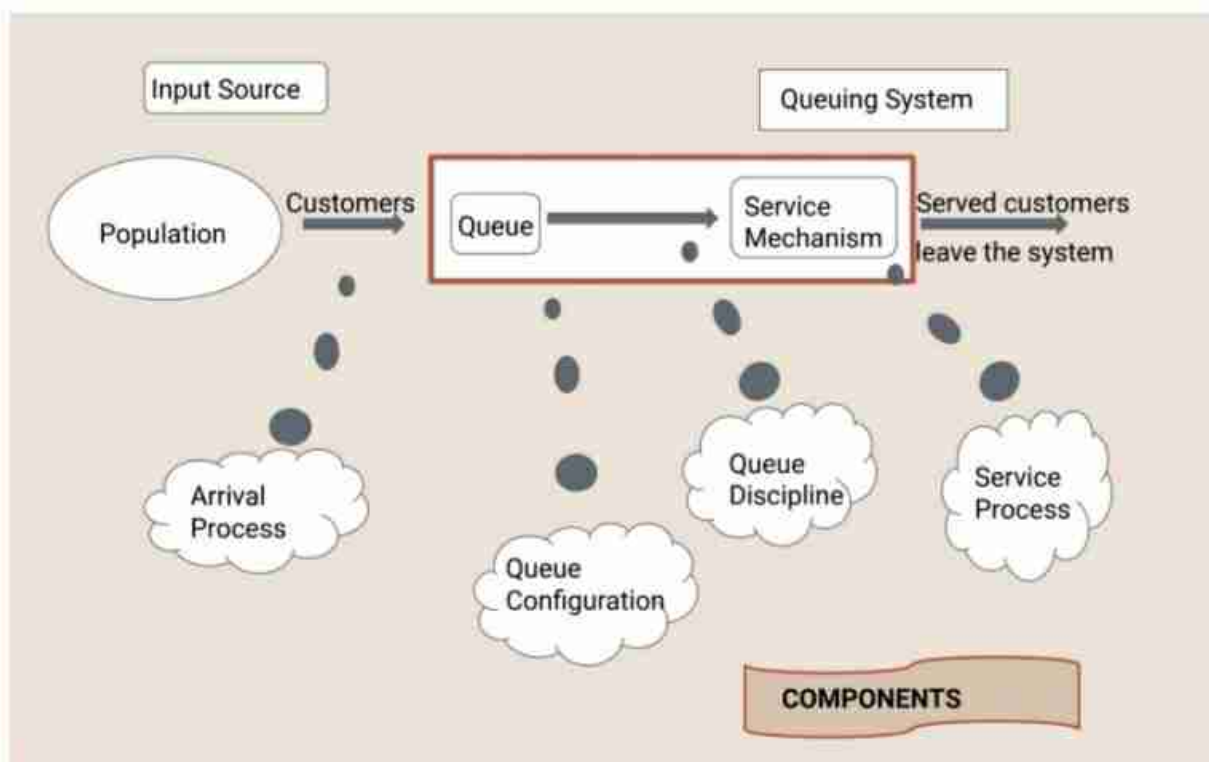


Multi server Multi-phase

Here we have two or more servers for serving multiple number of waiting lines. Supermarket queues are examples.



1.4 Queuing system



1.4.1 Queuing structure

It is the crucial element of queuing system, as it shows the queue discipline, which means the order in which the customers are picked from the queue for service.

1.4.2 Queuing system

Queuing systems are simplified mathematical models to explain congestion.

1.4.3 Components of Queuing systems

- **Input source** - The input source generates customers for the service mechanism. The most important characteristic of the input source is its size. It may be either finite or infinite.
- **Queue** - Queue represents a certain no. of customers waiting for a service.
- **Arrival process** - Arrival defines the way customers enter the system , mostly the arrivals are random intervals between two adjacent arrivals.
- **Queue configuration** - It refers to the queue in the system , their relationship to the servers. A queue may be a single queue or a multiple queue.
- **Queue discipline** - It indicate the order in which members of the queue are selected.

There are mainly three ways for queue discipline

(i) **FIFO(First In First Out)**

The first customer is served first or first item added will be the first one to be removed.

eg: Ticket supply in theaters

(ii)**LIFO(Last In First Out)**

The last customer is first or last item added will be the first one to be removed.

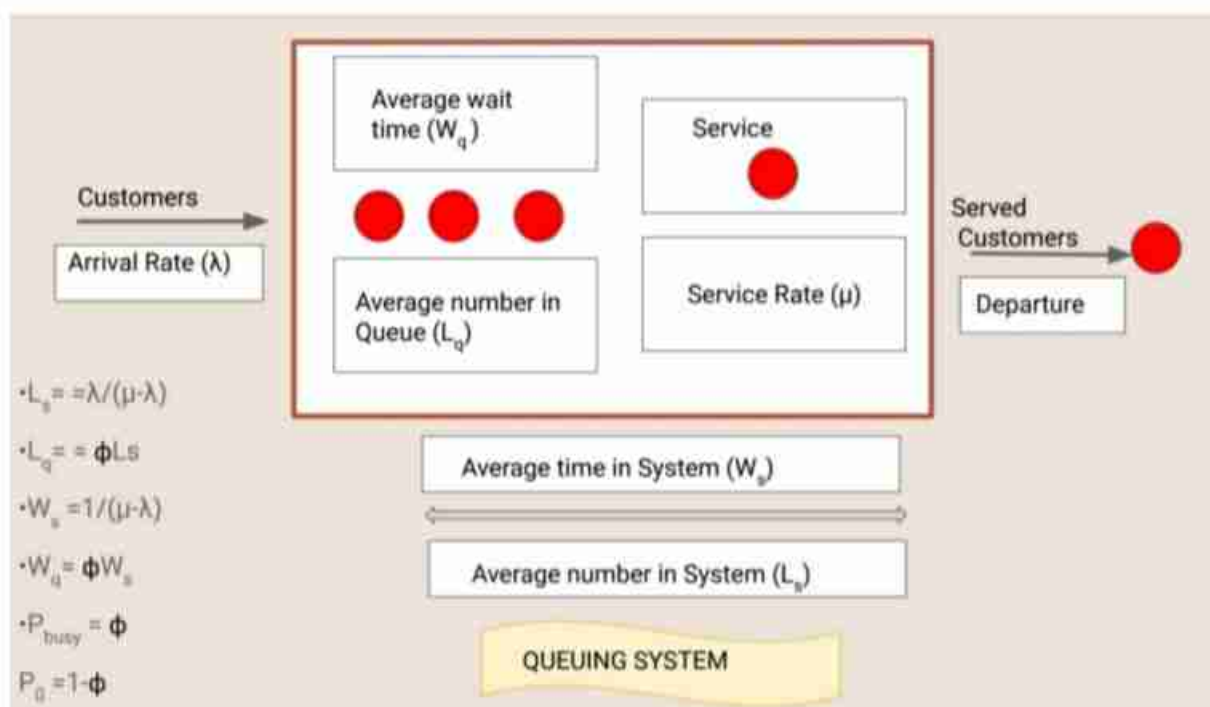
eg: A stack of plates that arrange in a pile

(iii)**SIRO(Serve In Random Order)**

In this system server selects one of the customers and service is provided randomly.

eg: Entering business

- Service process - It defines how long service will take, how many no. of servers available, whether the servers are in series or parallel.
- Service mechanism - Service represents some activity that takes time and that the customers are waiting for. it may be a real service carried on persons or machines. Typically a service takes random time.



1.5 Basic Terminologies

- **Arrival rate (λ):** Number of arrivals per unit time.
- **Service rate (μ):** Rate at which customers are served in the system.

- Utilisation factor (ϕ) : Average time the customers spends in the queue.

$$\phi = \frac{\lambda}{\mu}$$

- L_s = average no. of customers in the system

- P_0 = ideal probability = $1 - \phi$

- L_q = average no. of customers in the queue = ϕL_s

- W_s = average time in the system = $\frac{1}{\mu - \lambda}$

- W_q = average time in the queue = ϕW_s

- P_{busy} = standard busy probability = ϕ



Chapter 2

LAW AND NOTATION

2.1 Kendall's Notation

David George Kendall (15 January 1918 - 23 October 2007), well known English Statistician and Mathematician, known for his work on probability, statistical shape analysis, ley lines and queuing theory.



The standard system that describes and classifies a queuing node. D.G. Kendall proposed this in 1953. A general queuing system is denoted by

$$(P/Q/R) : (X/Y/Z)$$

The parameters of this notation are :

P - Arrival Rate distribution.

Arrival distribution can mainly be of Poisson distribution, Exponential distribution or Markov distribution.

Q - Service Rate distribution.

R - Number of servers.

X - Service discipline.

Y - Minimum number of customers permitted in the system.

Z - Size of the calling source of the customers.

2.1.1 Poisson Distribution

A discrete random variable X is said to follow a Poisson distribution with the parameter λ if its p.d.f is given by

$$f(x) = \frac{e^{-\lambda} \lambda^x}{x!}, \text{ when } x = 0, 1, 2, \dots (\lambda \text{ greater than 0})$$

$$f(x) = 0, \text{ elsewhere}$$

x-number of occurrences

$x = 0, 1, 2, \dots$

e-Euler's number ($e=2.71828\dots$)

Mean = λ

Variance = λ

Skewness = $\frac{1}{\sqrt{\lambda}}$

Kurtosis = λ^{-1}

MGF = $\exp[\lambda(e^t - 1)]$

$\lambda = E(X) = \text{Var}(X)$

2.1.2 Exponential Distribution

A continuous random variable X is said to follow exponential distribution with parameter λ (λ greater than 0) if it's p.d.f is given by

$$f(x) = \lambda e^{-\lambda x}, \text{ when } x \text{ greater than or equal to 0}$$

$$f(x) = 0, \text{ elsewhere}$$

x - No. of occurrences , $x= 0,1,2,\dots$

e - Euler's number , $e = 2.71828\dots$

Mean $= \lambda^{-1}$

Variance $= \lambda^{-2}$

Skewness $= 2$

Kurtosis $= 6$

MGF $= \left(1 - \frac{t}{\lambda}\right)$

2.1.3 Markovian Distribution

A mathematical model for the time between job arrivals to a system. Markov process is a stochastic process which is used to analyse decision problems in which the occurrence of a specific event depends on the occurrence of the event immediately prior to the current event. Basically Markov process help us to identify

- (i) A specific state of the system being studied, and
- (ii) The state - transition relationship.

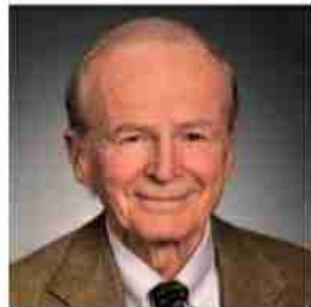
The occurrence of an event at a specified point in time (say, period n) put the system in a given state, say E_n . If, after the passage of one time unit, another event occurs (during time period $n+1$), the system has moved from state E_n to state E_{n+1} .

$$f(x) = \lambda e^{-\lambda x}, x \geq 0$$

2.2 Little's Law

Queuing Theory is a daily life applicable study that helps to work more easier in the queues. Waiting in line is a common process in daily life. Some theorems and laws were introduced to ensure the queues more effective. One of the theorem is Little Law.

John Little introduced Little Law in 1964. Initially, Little had not published the proof of the theorem. However in 1961, he published the proof.



Little law is a theorem that determines the average number of items in a stationary queuing system, based on the average waiting time of an item within a system and the average number of items arriving at the system per unit of time.

Little law states that the average number of customers in a queuing system is equal to their product of average arrival rate and average amount of time they spent in the system.

In other words, we can say that

Number of items in the queue = Arrival rate \times Average time spent in the queue

$$L = \lambda W$$

L - stands for the number of items inside the queuing system. It is

also known as WIP which means work in progress.

λ - Arrival rate and departure rate of items in and out of the system.

W - Average amount of time an item spends in the system.

Chapter 3

QUEUEING MODELS

3.1 Model 1 - $(M/M/1) : (GD/\infty/\infty)$

The parameters of the model :

- M - Arrival rate follows Poisson distribution.
- M - Service rate follows Poisson distribution.
- 1- Number of servers is one.
- GD - Service discipline is general.
- ∞ - Maximum number of customers permitted in the system is infinite.
- ∞ - Size of the calling source Infinite.

The steady-state formula to obtain the probability of having n customers in the system P_n are

$$P_n = (1 - \phi) \phi^n$$

$$L_s = \frac{\phi}{1-\phi}$$

$$L_q = L_s - \left(\frac{\lambda}{\mu} \right) = \frac{\phi^2}{(1-\phi)}$$

$$W_s = \frac{L_s}{\lambda} = \frac{\phi}{(1-\phi)\mu} = \frac{1}{\mu-\lambda}$$

$$W_q = \frac{L_q}{\lambda} = \frac{\phi}{\mu-\lambda}$$

Using the notation of the general model, we have

$$\lambda_0 = \lambda$$

$$\mu_0 = \mu$$

Also $\lambda_{eff} = \lambda$ and $\lambda_{lost} = 0$, because all arriving customers can join the system.

Letting $\rho = \frac{\lambda}{\mu}$, the expression for p_n in the generalised model reduces to

$$p_n = p^n p_0, n = 0, 1, 2, \dots$$

To determine the value of p_0 , we use the identity

$$p_0 (1 + \rho + \rho^2 + \dots) = 1$$

The sum of the geometric series is $\left(\frac{1}{1-\rho}\right)$, provided $\rho < 1$. Thus

$$\rho = 1 - \rho, \rho < 1$$

The general formula for p_n is thus given by the following geometric distribution

$$p_n = (1 - \rho) \rho^n, n = 1, 2, \dots (\rho < 1)$$

The mathematical derivation of p_n imposes the condition $\rho < 1$, or $\lambda < \mu$. If $\lambda \geq \mu$, the geometric series diverges, and the steady-state probabilities p_n do not exist. This result makes the intuitive sense, because unless the service rate is larger than the arrival rate, queue length will continually increase and no steady state can be reached.

The measure of performance L_q can be derived in the following manner :

$$\begin{aligned} L_s &= \sum_{n=0}^{\infty} np_n = \sum_{n=0}^{\infty} n(1-\rho)\rho^n \\ &= (1-\rho)\rho \frac{d}{d\rho} \sum_{n=0}^{\infty} \rho^n \\ &= (1-\rho)\rho \frac{d}{d\rho} \left(\frac{1}{1-\rho}\right) \\ &= \frac{\rho}{1-\rho} \end{aligned}$$

Because $\lambda_{eff} = \lambda$ for the present situation, the remaining measures of performances are computed using the relationships. Thus,

$$\begin{aligned} W_s &= \frac{L_s}{\lambda} = \frac{1}{\mu(1-\rho)} = \frac{1}{\mu-\lambda} \\ W_q &= W_s - \frac{1}{\mu} = \frac{\rho}{\mu(1-\rho)} \\ L_q &= \lambda W_q = \frac{\rho^2}{1-\rho} \\ \bar{c} &= L_s - L_q = \rho \end{aligned}$$

Example : The arrival rate of customers at a banking counter follows Poisson distribution with a mean of 45 per hour. The service rate of the counter clerk also follows Poisson distribution with a mean of 60 per hour.

1. What is the probability of having 0 customers in the system?
2. What is the probability of having 5 customers in the system?
3. What is the probability of having 10 customers in the system?
4. Find L_s, L_q, W_s, W_q ?

Solution : We have

Arrival rate, $\lambda = 45$ per hour

Service rate, $\mu = 50$ per hour

Utilisation factor, $\phi = \frac{\lambda}{\mu} = \frac{45}{50} = 0.75$

1. $P_0 = 1 - \phi = 1 - 0.75 = 0.25$
2. $P_5 = (1 - \phi) \phi^5 = (1 - 0.75)0.75^5 = 0.593$
3. $P_{10} = (1 - \phi) \phi^{10} = (1 - 0.75)0.75^{10} = 0.0141$
4. $L_s = \frac{\phi}{1-\phi} = \frac{0.75}{1-0.75} = 3 \text{ customers}$
 $L_q = \frac{\phi^2}{(1-\phi)} = \frac{0.75^2}{1-0.75} = 2.25 \text{ customers}$
 $W_s = \frac{1}{\mu-\lambda} = \frac{1}{60-45} = 0.067 \text{ hours}$
 $W_q = \frac{\phi}{\mu-\lambda} = \frac{0.75}{60-45} = 0.05 \text{ hours}$

3.2 Model 2 - $(M/M/C) : (GD/\infty/\infty)$

The parameters of this model are given below :

- M - Arrival rate follows Poisson distribution.
- M - Service rate follows Poisson distribution.
- C- Number of servers is C.
- GD - Service discipline is general discipline.
- ∞ - Maximum number of customers permitted in the system is infinite.
- ∞ - Size of the calling source is infinite.

The steady-state formula to obtain the probability of having n customers in the system P_n and the formula for P_0, L_s, L_q, W_q, W_s are presented below:

$$\begin{aligned} P_n &= \phi^n n! P_0, \text{ where } 0 \leq n \leq C \\ &= \phi^n \frac{1}{C^{n-c} C!} P_0, n > C \text{ where } \frac{\phi}{C} < 1 \text{ or } \frac{\lambda}{\mu C} < 1 \\ P_0 &= \sum_{n=1}^{C-1} \frac{\phi^n}{n!} + \frac{\phi^C}{C!} \left[1 - \left(\frac{\phi}{C} \right) \right]^{-1} \end{aligned}$$

$$P_0 = \left[\sum_{n=0}^{c-1} \frac{\phi^n}{n!} + \frac{\phi^c}{C! [1 - \frac{\phi}{c}]} \right]^{-1}$$

The expression for L_q can be determined as follows:

$$\begin{aligned} L_q &= \sum_{n=c}^{\infty} (n - c) P_n \\ &= \sum_{k=0}^{\infty} K P_{k+c} \\ &= \sum_{k=0}^{\infty} K \frac{\phi^{k+1}}{c^k k!} P_0 \\ &= \frac{\phi^{c+1}}{c! c} P_0 \sum_{k=0}^{\infty} K \left(\frac{\phi}{c}\right)^{k-1} \\ &= \frac{\phi^{c+1}}{c! c} P_0 \frac{d}{d\left(\frac{\phi}{c}\right)} \sum_{k=0}^{\infty} \left(\frac{\phi}{c}\right)^k \\ &= \frac{\phi^{c+1}}{(c-1)!(c-\phi)^2} P_0 \end{aligned}$$

$$L_s = L_q + \phi$$

$$\begin{aligned} W_q &= \frac{L_q}{\lambda} \\ &= \frac{L_q + \phi}{\lambda} \\ &= \frac{L_q}{\lambda} + \frac{\phi}{\lambda} \\ &= W_q + \frac{1}{\mu} \\ W_q &= \frac{L_q}{\lambda} \end{aligned}$$

Example: At a central ware-house, vehicles arrive at the rate of 18 per hour and the arrival rate follows Poisson distribution. The unloading time of the vehicles follows exponential distribution and the unloading rate is 6 vehicles per hour. There are 4 unloading crews. Find the following:

- a) P_0 and P_3
- b) L_q, L_s, W_q and W_s

Solution: we have,

Arrival rate, $\lambda = 18 \text{ per hour}$

Unloading rate, $\mu = 6 \text{ per hour}$

No. of unloading crews, $C = 4$

$$\phi = \frac{\lambda}{\mu}$$

$$= \frac{18}{6} = 3$$

a) Therefore P_0 is computed as :

$$\begin{aligned} P_0 &= \left[\sum_{n=0}^{c-1} \frac{\phi^n}{n!} + \frac{\phi^c}{C![1 - \frac{\phi}{c}]} \right]^{-1} \\ &= \left[\sum_{n=0}^3 \frac{3^n}{n!} + \frac{3^4}{4![1 - \frac{3}{4}]} \right]^{-1} \\ &= \left[\frac{3^0}{3!} + \frac{3^1}{1!} + \frac{3^2}{2!} + \frac{3^3}{3!} + \frac{3^4}{4!(1 - (\frac{3}{4}))} \right]^{-1} \\ &= 0.0377 \end{aligned}$$

Now we have to compute P_3 , we have

$$P_n = \frac{\phi^n}{n!} P_0, 0 \leq n \leq C$$

Therefore,

$$\begin{aligned} P_3 &= \frac{3^3}{3!} * 0.0377 \\ &= 0.1697 \end{aligned}$$

b) L_q, L_S, W_q and W_s are computed as under:

$$L_q = \frac{\phi^{c+1}}{(c-1)!(c-\phi)^2} P_0$$

$$= \frac{3^5}{31 * 1} * 0.0377 \\ = 1.53 = 2 \text{ vehicles}$$

$$L_s = L_q + \phi \\ = 1.53 + 3 \\ = 4.53 = 5 \text{ vehicles}$$

$$W_q = \frac{L_q}{\lambda} \\ = \frac{1.53}{18} \\ = 0.252 \text{ hour} = 5.1 \text{ minutes}$$

$$W_s = W_q + \frac{1}{\mu} \\ = 0.085 + \frac{1}{6} \\ = 0.252 \text{ hours} = 15.12 \text{ minutes}$$

3.3 Model 3 - $(M/M/1) : (GD/N/\infty)$

The parameters of this model are given below:

- M - Arrival rate follows Poisson's distribution.
- M - Service rate follows Poisson's distribution.
- 1 - Number of servers is one.
- GD - Service discipline is general discipline.
- N - Maximum number of customers permitted in the system is N.
- ∞ Size of calling source is infinite.

This model differ from $(M/M/1):(GD/\infty/\infty)$ in that there is a limit N on the number in the system (maximum queue length=N-1). Examples include manufacturing situations in which a machine may have a limited buffer space and a one-lane drive-in window in a fast-food restaurant. New arrivals are not allowed when the number of customers in the

system reaches N . Thus,

$$\lambda_n = \begin{cases} \lambda, n = 0, 1, \dots, N-1 \\ 0, n = N, N+1 \end{cases}$$

$$\mu_n = \mu, n = 0, 1, \dots$$

the value of P_0 is determined from the equation

$$\sum_{n=0}^{\infty} P_n = 1, \text{ which yields}$$

$$P_0(1 + p + p^2 + \dots + p^N) = 1$$

or

$$p_0 = \begin{cases} \frac{1-\phi}{1-\phi^{N+1}}, \phi \neq 1 \\ \frac{1-\phi}{N+1}, \phi = 1 \end{cases}$$

The steady-state formula to obtain the probability of having n customers in the system P_n and the formula for P_0, L_s, L_q, W_s and W_q are represented below.

$$\begin{aligned} P_N &= \frac{1-\phi}{1-\phi^{N+1}} \phi^N, \phi \neq 1 \text{ and } N = 0, 1, 2, \dots, n \\ &= \frac{1}{N+1}, \phi = 1 \end{aligned}$$

The expected number of customers in the system is computed as

$$\begin{aligned}
 L_s &= \sum_{n=1}^N nP_n \\
 &= \frac{1-\phi}{1-\phi^{N+1}} \sum_{n=0}^N n\phi^n \\
 &= \left(\frac{1-\phi}{1-\phi^{N+1}}\right)\phi \frac{d}{d\phi} \sum_{n=0}^N \phi^n \\
 &= \left(\frac{1-\phi}{1-\phi^{N+1}}\phi\right) \frac{d}{d\phi} \left(\frac{1-\phi^{N+1}}{1-\phi}\right) \\
 &= \frac{\phi[1-(N+1)\phi^N + N\phi^{N+1}]}{(1-\phi)(1-\phi^{N+1})}, \phi \neq 1 \\
 &= \frac{N}{2}, \phi \neq 1
 \end{aligned}$$

$$\lambda_{eff} = \lambda(1 - P_N)$$

$$\begin{aligned}
 L_q &= L_s - \frac{\lambda_{eff}}{\mu} \\
 &= L_s - \frac{\lambda(1 - P_N)}{\mu}
 \end{aligned}$$

$$\begin{aligned}
 W_q &= \frac{L_q}{\lambda_{eff}} \\
 &= \frac{L_q}{\lambda(1 - P_N)} \\
 W_s &= W_s + \frac{1}{\mu} \\
 &= \frac{L_q}{\lambda_{eff}} \\
 &= \frac{L_q}{\lambda(1 - P_N)}
 \end{aligned}$$

Example: Cars arrive at a drive-in restaurant with a mean arrival rate of 24 cars per hour and the service rate of the cars is 20 cars per hour. The arrival rate and the service rate follows Poisson distribution. The number of parking spaces for cars is only 4. Find the standard results of this system.

Solution:

Here ,Arrival rate, $\lambda = 24 \text{ cars per hour}$

Service rate, $\mu = 20 \text{ cars per hour}$

$N = 4$

$$\begin{aligned}\phi &= \frac{\lambda}{\mu} \\ &= \frac{24}{20} = 1.2\end{aligned}$$

Therefore we get,

$$L_s = \frac{\phi[1-(N+1)\phi^N + N\phi^{N+1}]}{(1-\phi)(1-\phi^{N+1})} = \frac{1.2[1-(4+1)1.2^4 + 4*1.2^5]}{(1-1.2)(1-1.2^5)} = 2.3 \text{ cars}$$

and

$$\begin{aligned}P_N &= \frac{1-\phi}{1-\phi^{N+1}} \phi^N \\ &= \left(\frac{1-1.2}{1-1.2^5}\right) * 1.2^4 = 0.2787 \text{ cars}\end{aligned}$$

the other results are:

$$\begin{aligned}\lambda_{eff} &= \lambda(1 - P_N) \\ &= 24(1 - 0.2787) \\ &= 17.3112 \text{ per hour}\end{aligned}$$

$$\begin{aligned}L_q &= L_s - \frac{\lambda_{eff}}{\mu} \\ &= 2.36 - \left(\frac{17.3112}{20}\right) \\ &= 1.494 \text{ cars} \\ \mathbf{W}_q &= \frac{L_q}{\lambda_{eff}} \\ &= \frac{1.494}{17.3112} \\ &= 0.0863 \text{ hours} \\ &= 5.2 \text{ min}\end{aligned}$$

$$\begin{aligned}W_s &= \frac{L_s}{\lambda_{eff}} \\ &= \frac{2.36}{17.3112} \\ &= 0.1363 \text{ hours} \\ &= 8.2 \text{ min}\end{aligned}$$

Chapter 4

APPLICATIONS

4.1 Daily Life Applications

SITUATION	CUSTOMERS	SERVICE
Clinic	Patients	Doctors
Job interviews	Applicants	Experts
Railway station	Travelers	Ticket window
Bank counter	Account holders	Counter clerk
Airport runways	Planes	Runway
Telephone booth	Customers	Telephone
Ration shop	Ration card holders	Shop clerk
ATM counters	Customers	ATM machine
Toll plaza	Vehicles	Toll collectors
Emigration department	Travelers	Emigration officers
Traffic system	Vehicles	Signal point
Supermarkets	Customers	Workers
Computer center	Programs	Computer
Library	Students	Counter clerk
Maintenance shop	Breakdown machines	Machines
Photostat shop	Papers	Photostat machine

- Queuing theory has a important role in casualties of hospital
- It is useful in evaluating the impact of breakdown down of disasters
- It is really helpful in making business decisions
- If we consider the rain in monsoon season in India then the waiting days for getting the rain is a queue, here days are the customers and the sky is the server.
- As Covid-19 cases increasing day by day, vaccination centres need to provide more number of servers to avoid congestion of people.

CONCLUSION

Queues are very common in our society. Every person has to stand in a queue atleast once. Queuing theory helps in enhancing business strategies. From this project, we can conclude that, when the Average Service Rate μ is greater than Average Arrival rate λ , the customers are served at a faster rate than they arrive and the service will be fast. This theory gives a basic information for successfully designing queuing systems that achieves a healthy balance between arrival rate and service rate.

REFERENCES

- <http://youtube.be/SqSUJ0UYWMQ>
- <http://youtube.be/BxYQWHOwQk>
- Basic Queuing Theory : Dr.Janos Sztrik, University of Debrecen.
Faculty of Information
- Queuing Theory Applied In Our Day To Day Life : S.Shanmughasundharam
and P Umarani
- Operations Research - R.Panneer selvam



Project Report

On

THE EFFECT OF COVID-19 ON ONLINE FOOD DELIVERY SERVICES.

Submitted

in partial fulfilment of the requirements for the degree of

BACHELOR OF SCIENCE

in

MATHEMATICS

by

ANAGHA JAYAPRAKASH

(Register No. AB19AMAT003)

Under the Supervision of

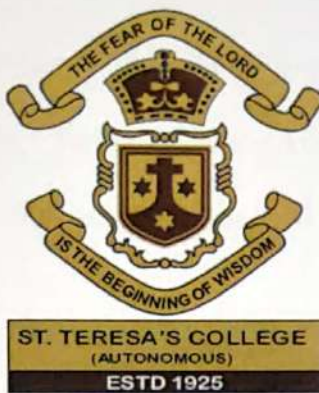
NEENU SUSAN PAUL



DEPARTMENT OF MATHEMATICS
ST. TERESA'S COLLEGE (AUTONOMOUS)

ERNAKULAM, KOCHI - 682011

APRIL 2022



CERTIFICATE

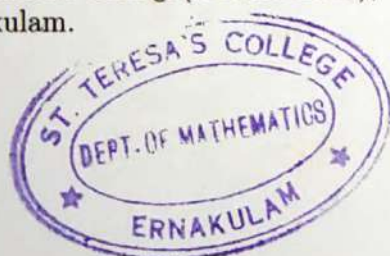
This is to certify that the dissertation entitled, **THE EFFECT OF COVID-19 ON ONLINE FOOD DELIVERY SERVICES.** is a bonafide record of the work done by Ms. **ANAGHA JAYAPRAKASH** under my guidance as partial fulfillment of the award of the degree of **Bachelor of Science in Mathematics** at St. Teresa's College (Autonomous), Ernakulam affiliated to Mahatma Gandhi University, Kottayam. No part of this work has been submitted for any other degree elsewhere.

Date: 4-3-2022

Place: Ernakulam

Neenu
Neenu Susan Paul

Assistant Professor,
Department of Mathematics,
St. Teresa's College(Autonomous),
Ernakulam.



Dr.Ursala Paul
Assistant Professor and Head ,
Department of Mathematics,
St. Teresa's College(Autonomous),
Ernakulam.

External Examiners

1:

2:

DECLARATION

I hereby declare that the work presented in this project is based on the original work done by me under the guidance of Neenu Susan Paul, Assistant Professor, Department of Mathematics, St. Teresa's College(Autonomous), Ernakulam and has not been included in any other project submitted previously for the award of any degree.

Ernakulam.



ANAGHA JAYAPRAKASH

Date: 4-03-2022

AB19AMAT003

ACKNOWLEDGEMENT

When we set goals for ourselves, there are always obstacles in the way that may deter us from accomplishing the goals. There are also people in our lives that are aware of those goals, and encourage us and also support us to continue regardless of the obstacles, it is now that I can formally thank those people for doing just that for me, before thanking anyone on this earth, I must first thank God for being at my side during this challenging time of my life. The spiritual support has helped to keep me focussed.Thanks to my Guide Neenu Susan Paul, St.Teresa's College for the support and encouragement through this process.

Ernakulam.

ANAGHA JAYAPRKASH

Date: 4-03-2022

AB19AMAT003

Contents

<i>CERTIFICATE</i>	ii
<i>DECLARATION</i>	iii
<i>ACKNOWLEDGEMENT</i>	iv
<i>CONTENT</i>	v
1 INTRODUCTION	1
1.1 Background of the Study	2
1.2 Literature Review.	3
1.3 E-Commerce	4
1.4 Objective	5
2 METHODOLOGY	6
2.1 Data Collection	6
2.2 Questionnaire	7
2.3 Chi-Square Test	7
3 DATA ANALYSIS	9
3.1 Survey Analysis	9
3.2 Data Analysis	20
4 RESULT AND CONCLUSION	27
4.1 Conclusion	27
4.2 Result	30
<i>REFERENCES</i>	32
<i>Annexure</i>	33

Chapter 1

Introduction

The COVID-19 pandemic has disrupted nearly every area of people's lives, including their capacity to buy products. Consumers have been confined at home as a result of government-imposed lockdowns, inhibiting regular purchasing habits, and many brick-and-mortar companies have closed. Pharmacies and supermarkets, for example, have stayed open albeit with shortened hours. Many eateries have shuttered or resorted to takeout in order to stay afloat. For many clients, home delivery has given a solution to some of COVID-19's issues. Employees that are required to work remotely, as well as a range of other groups, such as parents who must combine work and parental responsibilities, or individuals who are at risk of serious COVID-19 health concerns, may find e-commerce and home delivery to be a useful option. Despite the difficulties people have had in ordering food online as a result of the pandemic, such as a lack of food inventories, a lack of public transportation, and fewer hours to work at convenience stores and supermarkets, a large percentage of people have been able to obtain sufficient amounts of food stocks. All of this can be attributed to the rapid increase in the number of online food apps, which encourage people to order their meals online and have them delivered to their homes or picked up by themselves without having to enter the restaurant. Programs that encourage grocery shopping and food ordering online can also help to reduce the spread of the Covid-19 virus by reducing interaction between customers and sellers, thereby creating a safe environment in and

of itself. Considering all of the facts, the fact that customers are shifting to ordering food and shopping for groceries online as a result of the pandemic has implications for the retail market as well.

1.1 Background of the study

The early stages of the covid pandemic, as well as the strict lockdown, harmed India's online food delivery companies, which were dominated by Zomato and Swiggy. Consumers had resisted online food ordering due to safety concerns and a general preference for home cooked food. However, things improved later on, and recovery was quicker. According to analysts, the pandemic has assisted companies in improving unit economics and adding more customers, as the frequency of dining out has decreased.

As we stay at home to mitigate the impact of virus many of us have turned to delivery services for meals and groceries for the first time. Before the advent of the Covid nineteen, young people were increasingly buying food online. But now people of all ages are buying food online equally. In this way the spread of the covid is greatly reduced. In the past, large restaurants were mostly using online food delivery services but now it has changed and even smaller hotels started to use online food delivery platforms. The hospitality industry has adapted to make it easier for everyone to support a favourite local restaurant, avoid going out, and simply find a relaxing respite during these stressful times. Because of the nature of how Covid-19 spreads, close contact with others may pose the greatest risk of infection. Many restaurants now allow customers to pay ahead of time, either by phone or online, eliminating the need for physical cash transfers or credit card handling, both of which can potentially harbor the virus.

During the pandemic, diners became accustomed to ordering delivery, and the habit may persist long after dining rooms reopen. However, restaurants and delivery companies continue to be uneasy part-

ners, haggling over fees and struggling to make the service profitable for both parties. Companies such as Zomato and Uber Eats assisted many restaurants in remaining open during lockdowns by allowing diners to stay in and still order out. However, the convenience came at a cost delivery companies can charge commission fees of 30% or more per order, reducing restaurants already meager profits. Delivery was already increasing prior to the pandemic, but it sky rocketed during lockdowns around the world.

Prior to the outbreak of Covid-19, many young people preferred online food delivery. People belonging to other age categories mostly prefer home-cooked meals because they are safe and healthy. During the Covid-19 scenario, everyone was confined to their homes. There were no stores or hotels open, and all local businesses began delivering products through online platforms. And because it was convenient and time-saving, everyone began ordering food online. Online delivery was also safe and reduced the spread of the virus.

1.2 Literature Review

The impact of COVID-19 on restaurant meal ordering via apps 2020: This article was published on April 22, 2021 by Statista's Research Department. According to a Local Circles poll conducted in May 2020, approximately 65 percent of respondents stated that they would not order restaurant meals for delivery within 30 days of the corona virus lockdown being lifted. Approximately 3% of those polled said they would order more than four times during this time period.

According to Priyadharshini (2017), India has more people between the ages of 10 and 24, making it the world's largest young population. With more young people joining the workforce every day, economic growth, increased female labour power, and increased consumer mobility, the traditionally difficult Indian market has evolved and is in need of a more diverse menu.

Samsudin et al (2011) points out that alongside client feedback for an eatery, a plan and execution of wireless food ordering framework was completed. It empowers cafes proprietors to setup the framework in wireless environment and update menu presentations effectively. Advanced mobile has been coordinated within the adaptable wireless food ordering system requesting framework with continuous client criticism execution to encourage ongoing correspondence between eatery proprietors and clients.

Rathore et al (2018) states that 50.8% of consumers use a food delivery service because they don't want to cook because it allows them to have food delivered to their home or office in under 60 minutes.

According to Pathan et al(2017), an online food ordering system can be used to build up a restaurant and mess menu, and customers can quickly place orders. Also, with an online food menu, orders can be readily traced, the client database can be maintained, and the meal delivery business may grow. Restaurants and mess may quickly update their online restaurant menus and upload photographs. Potential consumers can quickly examine a restaurant menu on the internet and place orders at their leisure. As a result, an automated food ordering system with feedback and wireless communication is shown.

1.3 E-Commerce

According to Garret (1996), electronic commerce or e-commerce is the exchange of goods and services via the internet or other computer networks. Buyers and sellers conduct business via networked computers in e-commerce. Electronic commerce also includes the exchange of business information, the maintenance of business relationships, and the conduct of business transactions via communication networks. It contains the relationship between companies (business-to-business), customers (customer-to-customer), and companies and cus-

tomers (business-to-customer). Currently, the business to business sector dominates e-commerce, while the customer-oriented segment lags far behind, accounting for fewer than 10 even though they are all experiencing an exponential growth (Vladimir, 1998).

Buyers like the convenience that e-commerce provides. They can compare prices and make purchases without leaving the house by visiting the World Wide Web (www) sites of numerous suppliers 24 hours a day, seven days a week. For sellers, e-commerce offers a way to cut costs and expand their markets. They do not need to hire staff or maintain a store or distribute mail order catalogs. For retailers, e-commerce allows them to save money while also expanding their customer base. They don't have to hire people, keep a store running, or print and distribute catalogues. Sellers have the ability to market their products or services globally because they sell over the global internet and are not limited by the physical location of a store.

There are several drawbacks to e-commerce. Some customers are hesitant to make online purchases. Customers want to test the comfort of an expensive item, thus online furniture enterprises, for example, have failed for the most part. Many people consider shopping to be a social experience; for example, they may enjoy going to a shop or a shopping mall with family and friends, which they cannot get online. Customers Furthermore, must be guaranteed that credit card transactions are safe and secure. Their personal information is kept confidential. E-commerce not only expands the range of products available to customers, but it also makes it easier for them to find what they want, not only in terms of products and services, but also in terms of attracting new customers and retaining existing ones.

1.4 Objective

- To interpret and to find if there is any relation between place of residence and the mode of preference of food delivery services.

- To interpret and to find if there is any relation between age group and variation in the usage of online food delivery services.
- To interpret and to find if there is any relation between age group and amount of money spend on online food delivery services.
- To interpret and to find if there is any relation between age group and reasons for choosing on online food delivery services.

Chapter 2

METHODOLOGY

2.1 Data Collection

In order to meet the research objectives, it is critical that the data collected is accurate. All data sources can be divided into two categories: Primary data is gained by direct observation or data collected by the researcher. It refers to data that has been acquired for a specific purpose from a field of inquiry and is of a unique type. Primary data for the project was acquired primarily using the survey approach, utilising the tool questionnaire. Secondary data are ones that have already been acquired by others for a specific reason and are then used in a variety of situations. It is second hand information on an incident that the researchers have not personally witnessed.

Customers who order food online are considered the study's target group. The data was taken between November 23rd and January 1st, 2022. India's statewide lockdown began on March 25, 2020, in order to restrict population movement. The government, on the other hand, allowed e-commerce businesses to continue operating during this time. A well-structured online questionnaire was created using the Google forms and distributed to the responders. During the lockdown, an online-based survey is a viable option for data collection to safeguard the safety of respondents and researchers. Students, employed, and unemployed citizens were among those who responded. We distribute the survey via WhatsApp and social media sites. This study was carried out

with the permission of all participants, and no personal information was gathered. The samples were collected from Ernakulam district, Kerala. Numerous Indian state governments did not allow the operation of online food delivery during the statewide lockdown, although many well-established online food delivery businesses like Zomato and Swiggy were fully active in Ernakulam during the nationwide shutdown.

2.2 Questionnaire

The Questionnaire is used to collect data from responders, and it is created using Google Forms. It consists of a sequence of questions that the investigators are expected to ask and the respondents are supposed to choose an alternative for each individual enquiry. Questions are in the form of multiple choice questions. There is no personal information collected. Customers that order food online and live in the Ernakulam city area were chosen at random for primary data. Data was collected using a standardised questionnaire. The sample size was determined by taking 500 respondents from the total population of respondents in Ernakulam.

2.3 Chi-Square Test

A chi-square statistic is a measure of the difference between the observed and expected frequencies of the outcomes of a set of events or variables. Chi-Square depends on the size of the difference between actual and observed values, the degrees of freedom, and the samples size. Chi-Square can be used to test whether two variables are related or independent from one another. It can also be used to test the goodness-of-fit between an observed distribution and a theoretical distribution of frequencies.

When the chi-square test is used as a test of independence, it allows the researcher to test whether the two attributes being tested are associated or not. For this test, a null and alternative hypothesis is for-

mulated where the *null hypothesis* that the two attributes are not associated, and the *alternative hypothesis* is that the attributes are associated.

From the given data, the expected frequencies are then calculated i.e.,

$$\text{ExpectedFrequency} = \text{RowTotal} \times \text{ColumnTotal} \div \text{GrandTotal} \quad (2.1)$$

followed by the calculation of chi-square value. The null or alternative hypothesis is accepted based on the calculated chi-square value. If the calculated chi-square value is less than the value in the table at the given level of significance, the null hypothesis is accepted, indicating that no relationship exists between the two attributes. If the calculated chi-square value is greater than the value in the table, the alternative hypothesis is accepted, indicating that there is a relationship between the two attributes.

The *p-value* or the calculated probability is the best probability to provide the smallest level of significance at which the null hypothesis is not true. If the *p-value is small (less than 0.05)*, it indicates a piece of strong evidence against the null hypothesis. As a result, the null hypothesis is rejected and the alternative hypothesis is accepted. This means that the results of the research study are statistically significant. If the *p-value is large (greater than 0.05)*, it indicates weak evidence against the null hypothesis. As a result, the null hypothesis is not rejected and the alternative hypothesis is not accepted. This means that the results of the research study are not statistically significant.

In order to find the p-value from the chi-square test, at first, the chi-square test is to be performed to obtain the chi-square value. While performing the test, the *degree of freedom* is also calculated by the formula, $d.f = (c-1)(r-1)$ where c is the number of columns and r is the number of rows. Now the chi-square distribution table is entered, with the obtained degree of freedom, and the value of the chi-square is found in the table.

Chapter 3

DATA ANALYSIS

3.1 Survey Analysis

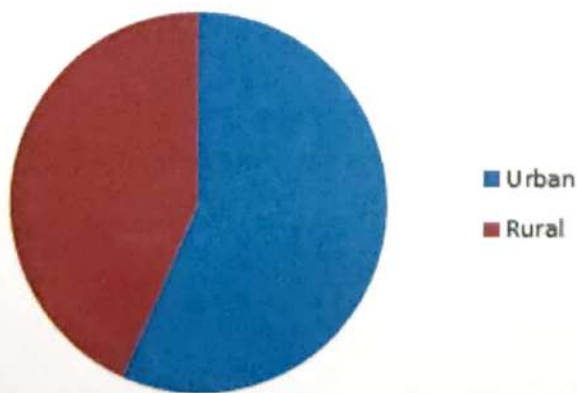
1.PLACE OF RESIDENCE

About 55.2% of responses were from urban area while 44.8% were from rural area.

Area	No Of Responses
Urban	276
Rural	224

Table 3.1: Frequency

Place of residence.



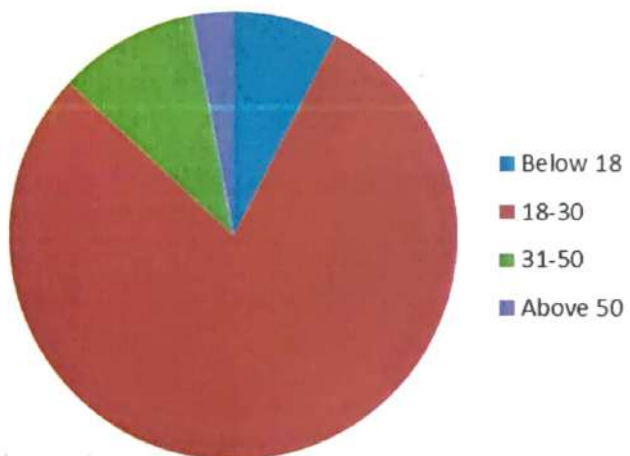
2) AGE CATEGORY

About 8.8% of the respondents belong to below 18 category, 74.2% belongs to 18- 30 category, 12.6% belongs to 30-50 category and 4.4% belongs to Above 50 category.

Area Group	No Of Responses
Below18	44
18-30	371
30-50	63
Above50	22

Table 3.2: Frequency

Age Category

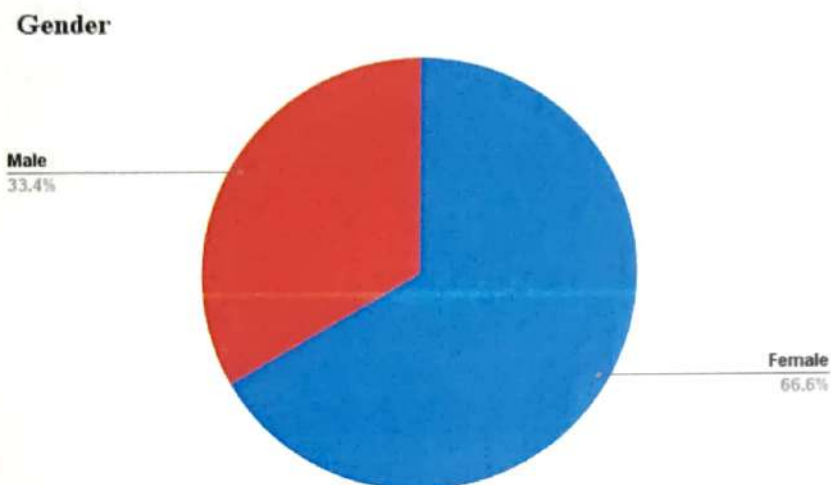


3) GENDER

About 66.6% responses were received from female category, about 33.4% responses were received from male category.

Gender	No Of Responses
Male	167
Female	333

Table 3.3: Frequency



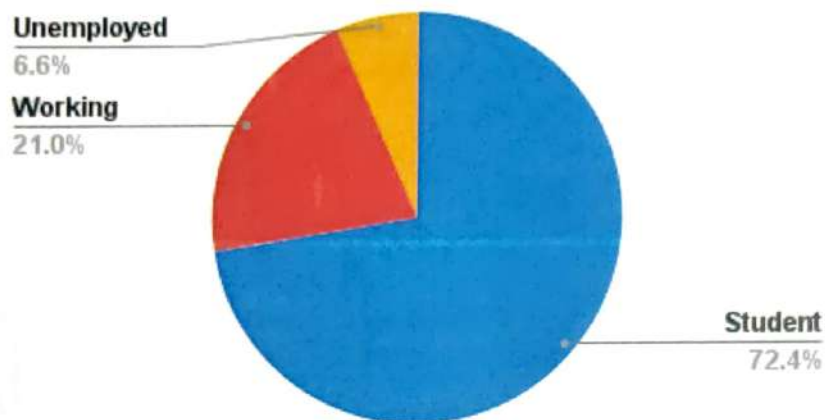
4) JOB PROFILE

About 72.4 % of respondents are students, 21 % of respondents are working and about 6.6 % of respondents are unemployed.

Job Profile	No Of Respondents
Students	362
Working	105
Unemployed	33

Table 3.4: Frequency

Job profile



5) PLACE OF RESIDENCE v/s FOOD SERVICE PREFERENCES.

Place	Going To Restaurants	Online Food Delivery
Urban	176	100
Rural	135	89

Table 3.5: Frequency

Place	Going to restaurant	Online food delivery
Urban	56.6%	52.91%
Rural	43.4%	47.09%

PLACE OF RESIDENCE v/s FOOD SERVICE PREFERENCES.



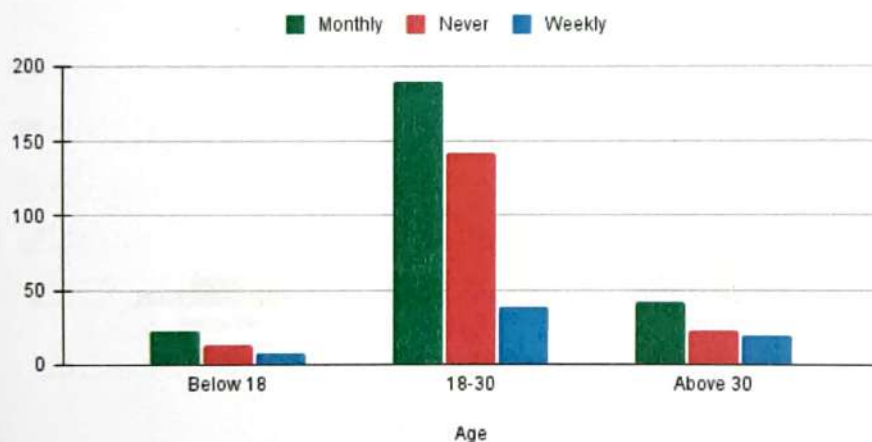
6. AGE CATEGORY V/S USAGE OF ONLINE FOOD DELIVERY SERVICES BEFORE COVID

Age	Weekly	Monthly	Never
Below 18	8	23	13
18-30	39	190	142
Above 30	20	42	23

Table 3.6: Frequency

Age	Weekly	Monthly	Never
Below 18	11.94%	9.01%	7.3%
18-30	58.21%	74.5%	79.78%
Above 30	29.85%	16.47%	12.92%

AGE CATEGORY V/S USAGE OF ONLINE FOOD DELIVERY SERVICES BEFORE COVID.



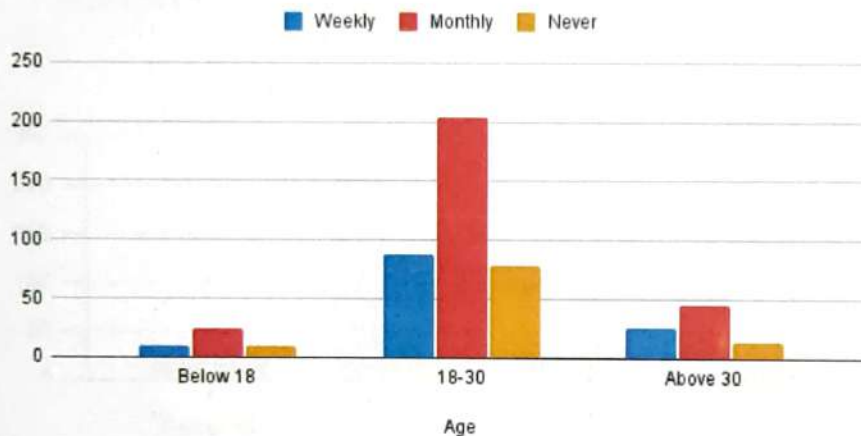
7. AGE CATEGORY V/S USAGE OF FOOD DELIVERY SERVICES DURING COVID

Age	Weekly	Monthly	Never
Below 18	10	24	10
18-30	88	204	79
Above 30	26	45	14

Table 3.7: Frequency

Age	Weekly	Monthly	Never
Below 18	8%	8.8%	9.7%
18-30	71%	75.72%	76.7%
Above 30	21%	16.48%	13.6%

AGE CATEGORY V/S USAGE OF ONLINE FOOD DELIVERY SERVICES DURING COVID.



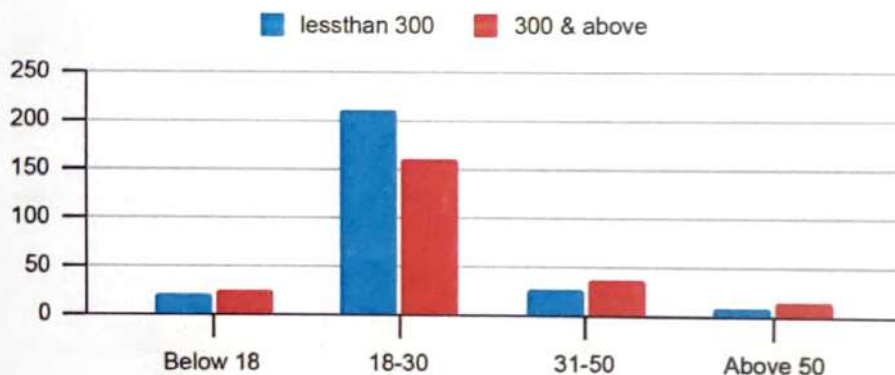
8. AGE CATEGORY V/S AMOUNT SPEND ON ONLINE FOOD DELIVERY BEFORE COVID

Age	Less than 300	300 and above
Below 18	20	24
18-30	211	160
31-50	27	35
Above 50	8	14

Table 3.8: Frequency

Age	Less than 300	300 and above
Below 18	7.51%	10.25%
18-30	79.32%	68.37%
31-50	10.15%	15.38%
Above 50	3%	6%

AGE CATEGORY VS AMOUNT SPEND ON ONLINE FOOD DELIEVRY BEFORE COVID



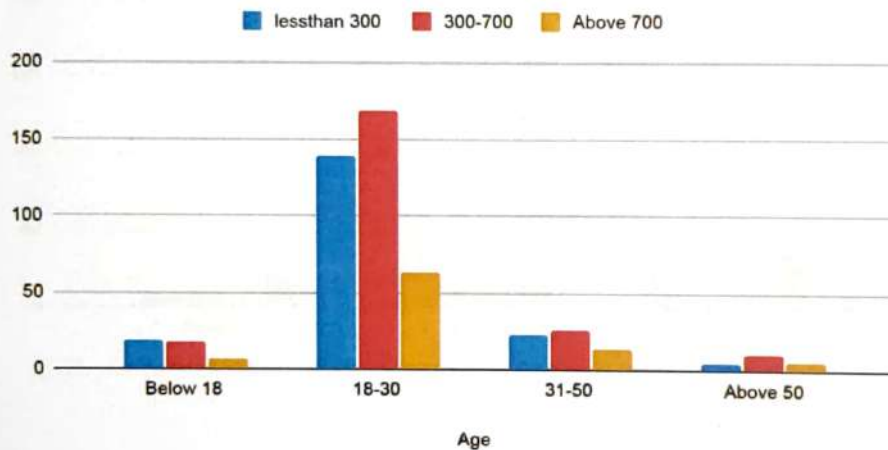
9. AGE CATEGORY V/S AMOUNT SPEND ON ONLINE FOOD DELIVERY DURING COVID

Age	Less than 300	300-700	Above 700
Below 18	19	18	7
18-30	139	169	63
31-50	23	26	14
Above 50	5	11	6

Table 3.9: Frequency

Age	Less than 300	300-700	Above 700
Below 18	10.21%	8.03%	7.78%
18-30	74.73%	75.44%	70%
31-50	12.36%	11.6%	15.55%
Above 50	2.68%	4.91%	6.67%

AGE CATEGORY V/S AMOUNT SPEND ON ONLINE FOOD DELIVERY DURING COVID



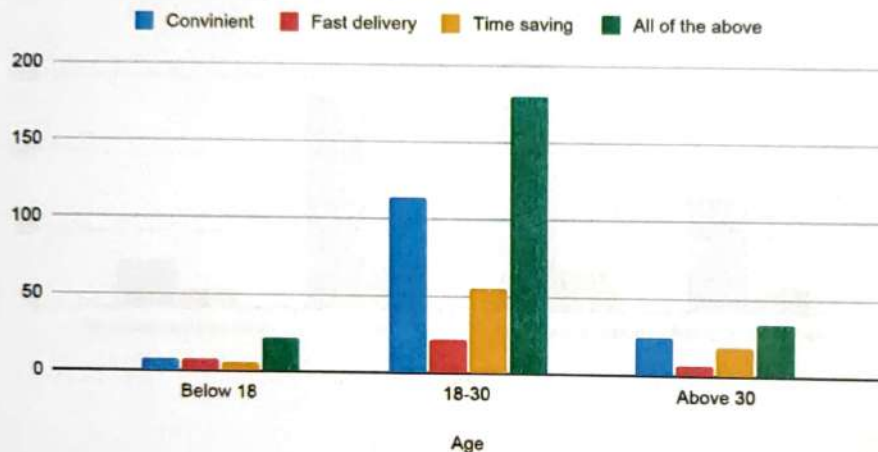
10. AGE CATEGORY v/s REASONS FOR CHOOSING ONLINE FOOD DELIVERY SERVICES BEFORE COVID.

Age	Convenient	Fast delivery	Time saving	All of the above
Below 18	8	8	6	22
18-30	114	22	55	180
Above 30	25	7	19	34

Table 3.10: Frequency

Age	Convenient	Fast delivery	Time saving	All of the above
Below 18	5.44%	21.62%	7.5%	9.32%
18-30	77.55%	59.45%	68.75%	76.27%
Above 30	17%	18.91%	23.75%	14.4%

AGE CATEGORY VS REASONS OR CHOOSING ONLINE FOOD DELIVERY BEFORE OVID



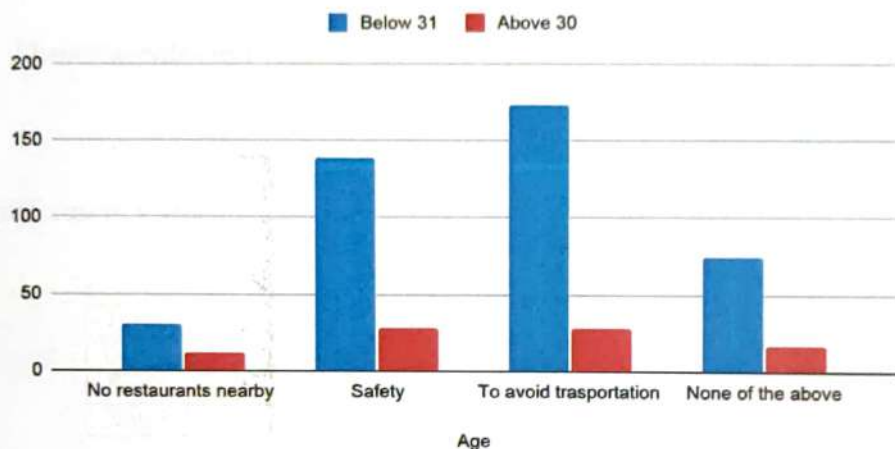
11. AGE CATEGORY v/s REASONS FOR CHOOSING ONLINE FOOD DELIVERY SERVICES AFTER COVID

Age	No restaurants nearby	Safety	To avoid transportation	None of the above
Below 31	30	138	173	74
Above 30	12	28	28	17

Table 3.11: Frequency

Age	No restaurants nearby	Safety	To avoid transportation	None of the above
Below 31	71.42%	83.13%	86.06%	81.31%
Above 30	28.57%	16.86%	13.93%	18.68%

AGE CATEGORY V/S REASONS FOR CHOOSING ONLINE FOOD DELIVERY DURING COVID



3.2 Data Analysis

1. MODE OF PREFERENCE V/S PLACE OF RESIDENCE

Place	Going to restaurant	Online food delivery	Total
Urban	176	100	276
Rural	135	89	224
Total	311	189	500

Table 3.12: Observed frequency

H_0 : There is no relation between place of residence and mode of preference.

H_1 : There is relation between place of residence and mode of preference.

Significance Value: 0.05

Place	Going to restaurant	Online food delivery	Total
Urban	171.672	104.328	276
Rural	139.328	84.672	224
Total	311	189	500

Table 3.13: Expected frequency

χ^2 value : $P = 0.422 > 0.05$

H_0 is accepted

Hence there is no relation.

2.USAGE OF FOOD DELIVERY BEFORE COVID V/S AGE CATEGORY

Age	Weekly	Monthly	Never	TOTAL
Below 18	8	23	13	44
18-30	39	190	142	371
Above 30	20	42	23	85
Total	67	255	178	500

Table 3.14: Observed frequency

H_0 There is no relation between age category and usage of food delivery services before covid

H_1 There is relation between age category and usage of food delivery services before covid

Significance Value: 0.05

Age	Weekly	Monthly	Never	Total
Below 18	5.896	22.44	15.664	44
18-30	49.714	189.21	132.076	371
Above 30	11.39	43.35	30.26	85
Total	67	225	178	500

Table 3.15: Expected frequency

χ^2 value : $P = 0.00714 < 0.05$

H_0 is rejected

Hence there is relation

3.USAGE OF FOOD DELIVERY DURING COVID V/S AGE CATEGORY

Age	Weekly	Monthly	Never	Total
Below 18	10	24	10	44
18-30	88	204	79	371
Above 30	26	45	14	85
Total	124	273	103	500

Table 3.16: Observed frequency

H_0 : There is no relation between age category and usage of food delivery services after covid

H_1 : There is relation between age category and usage of food delivery services after covid

Significance Value: 0.05

Age	Weekly	Monthly	Never	Total
Below 18	10.912	24.024	9.064	44
18-30	92.008	202.566	76.426	371
Above 30	21.08	46.41	17.51	85
Total	124	273	103	500

Table 3.17: Expected frequency

χ^2 value : $P = 0.24 > 0.05$

H_0 is accepted

Hence there is no relation

4. AMOUNT SPEND ON FOOD DELIVERY BEFORE COVID V/S AGE CATEGORY

Age	Less than 300	300 and Above	Total
Below 18	20	24	44
18-30	211	160	371
31-50	27	36	63
Above 50	8	14	22
Total	266	234	500

Table 3.18: Observed frequency

H_0 : There is no relation between age category and the amount spend on food delivery before covid.

H_1 : There is relation between age category and the amount spend on food delivery before covid

Significance Value: 0.05

Age	Less than 300	300 Above	Total
Below 18	23.408	20.592	44
18-30	197.372	173.628	371
31-50	33.516	29.484	63
Above 50	11.704	10.296	22
Total	266	234	500

Table 3.19: Expected frequency

χ^2 value : $P = 0.0405 < 0.05$

H_0 is rejected

Hence there is a relation.

5. AMOUNT SPEND ON FOOD DELIVERY DURING COVID V/S AGE CATEGORY

Age	Less than 300	300-700	Above 700	Total
Below 18	19	18	7	44
18-30	139	169	63	371
31-50	23	26	14	63
Above 50	5	11	6	22
Total	186	224	90	500

Table 3.20: Observed frequency

H_0 : There is no relation between age category and the amount spend on food delivery during covid

H_1 : There is relation between age category and the amount spend on food delivery during covid

Significance Value: 0.05

Age	Less than 300	300-700	Above 700	Total
Below 18	16.368	19.712	7.92	44
18-30	138.012	166.208	66.78	371
31-50	23.436	28.224	11.34	63
Above 50	8.184	9.856	3.96	22
Total	186	224	90	500

Table 3.21: Expected frequency

χ^2 value : $P = 0.652 > 0.05$

H_0 is accepted

Hence there is no relation

6. AGE CATEGORY V/S REASONS FOR CHOOSING ONLINE FOOD DELIVERY SERVICES BEFORE COVID

Age	Convenient	Fast delivery	Time saving	All of the above	TOTAL
Below 18	8	8	6	22	44
18-30	114	22	55	180	371
Above 30	25	7	19	34	85
TOTAL	147	37	80	236	500

Table 3.22: observed frequency

H_0 : There is no relation between age category and the reasons for choosing online food delivery before covid

H_1 : There is relation between age category and the reasons for choosing online food delivery before covid

Significance Value: 0.05

Age	Convenient	Fast delivery	Time saving	All of the above	TOTAL
Below 18	12.936	3.256	7.04	20.768	44
18-30	109.074	27.454	59.36	175.112	371
Above 30	24.99	6.29	13.6	40.12	85
TOTAL	147	37	80	236	500

Table 3.23: Expected frequency

χ^2 value : $P = 0.0302 < 0.05$

H_0 is rejected

Hence there is relation

7. AGE CATEGORY V/S REASONS FOR CHOOSING ONLINE FOOD DELIVERY SERVICES DURING COVID.

Age	No restaurants nearby	Safety	To avoid transportation	None of the above	TOTAL
Below 31	30	138	173	74	415
Above 30	12	28	28	17	85
TOTAL	42	166	201	91	500

Table 3.24: observed frequency

H_0 : There is no relation between age category and reason for choosing online food delivery during Covid.

H_1 : There is a relation between age category and reason for choosing online food delivery during Covid.

Significance level: 0.05

Age	No restaurants nearby	Safety	To avoid transportation	None of the above	TOTAL
Below 30	34.86	137.86	166.83	75.53	415
Above 30	7.14	28.22	34.17	15.47	85
TOTAL	42	166	201	91	500

Table 3.25: Expected Frequency

χ^2 value : $P = 0.137 > 0.05$

H_0 is accepted.

Hence there is no relation.

Chapter 4

RESULT AND CONCLUSION

4.1 Conclusion

1.PLACE OF RESIDENCE V/S FOOD SERVICE PREFERENCES.

In the case of online food delivery, people living in both rural and urban areas have equal accessibility and availability to online food services. Restaurants are growing at a fast rate in both rural and urban areas. People can directly go to the restaurants according to their needs. Hence there is no relation between place of residence and food service preferences.

2.USAGE OF FOOD DELIVERY SERVICES V/S AGE CATEGORY.

There is a relation between age categories and usage of food delivery services before covid. According to our survey, people belonging to the age category between 18-30 are most likely to order food online as most of them are working class and they do not have enough time to cook food. So it would be convenient for them to order food online. These are the ones who use smartphones more frequently and they are more familiar with food ordering applications. As we can see from the above conclusion, people belonging to the category above 50 are less likely to order food online because they are less aware of modern technologies. So they prefer to have healthy homemade foods. Hence here we can

conclude that age affect the usage of food delivery.

There is no relation between age categories and usage of food delivery services during covid. People have been held at home due to the govt imposed lockdowns, preventing regular shopping habits. Many restaurants have closed, thus forcing the consumers to buy food online irrespective of their preferences. Covid-19 hit everyone so badly that the working industry had to change to work from home. The people belonging to this sector didn't have enough time to cook, forcing them to order food online. All categories started showing a slight increase in the usage of online food delivery, because of the less accessibility of transportation services and safety concerns. All age groups faced equal difficulty during Quarantine period. Online food delivery platforms played a vital role in the lives of all people. Thus irrespective to their gender and age all people started using online food delivery services. Hence here we can conclude that age does not affect the usage of online food delivery services.

3. AMOUNT SPEND ON ONLINE FOOD DELIVERY SERVICES V/S AGE CATEGORY.

There is a relation between age categories and the amount spent on online food delivery services before covid-19. The people belonging to the age categories between 18-30 are usually the ones that spend more money on ordering food online. They love to live their lives to the fullest and also they love to try more new dishes. Before corona most of them were financially stable and it was affordable for them to order food. And also because they are hesitant to cook and they prefer to order food instead. On the other hand people of other age groups are very much self aware of their income and preferably would like to save money rather than spending more on eating junk food. Hence here we can conclude that age affects the amount spend on food delivery before covid.

There is no relation between age categories and the amount spent on online food delivery services during covid-19. Food is essential to human life since it supplies energy for all activities, growth, and development. People of all ages require food. During Covid-19, more individuals, particularly those in quarantine, had no choice but to purchase food online. People are willing to order food online even if it means spending more money for delivery because of food safety, quick delivery, and the availability of a wide variety of food items. As a result, when the pandemic began, people were not interested in purchasing food through online platforms. Because the population's fear and anxiety levels have increased, the perception of risk can also include the fear of contagion via food, packaging, and contact with the delivery person at the time of delivery. However, people's perspectives have gradually improved. All categories have begun to buy meals through these online platforms because they restrict customer contact with restaurant employees and let customers to enjoy their favourite restaurant food at home during a pandemic like COVID-19. Hence here we can say that age does not affect the amount spent on online food delivery services during covid.

4.REASONS FOR CHOOSING ONLINE FOOD DELIVERY SERVICES V/S AGE CATEGORY.

There is a relation between age categories and the reasons for choosing online food delivery services before covid. Because even before covid 19 pandemic people belonging to different age groups had different opinions. Nowadays people don't have enough time to go out and eat, so they started taking more advantage of the online food delivery platforms. Some might order food online as to reduce transportation, hesitation to cook (especially for those who find it difficult to cook well) or to save time. People are generally more satisfied with online delivery because it is done at their convenience and avoids the stress of waiting, standing in line, takeout, and so on. The waiting time is well spent by

doing something else at home or at work. The people belonging to the age category 18-30 are more likely to order food online and older adults are also making use of this online food delivery platforms. Therefore each of them have their own reasons. Hence here we can conclude that age affects the reasons for choosing online food delivery services.

There is no relation between age categories and the reasons for choosing online food delivery services during covid. Because majority of the respondents across all age groups started ordering food online as they practiced social distancing and safety as to minimise the spread of covid. Home delivery of food items helped people to avoid transportation. Hence, there was no any shortage or unavailability of food items occurred during the pandemic. Because of how covid-19 spreads, the greatest risk of infection could occur through intimate contact with others. Many restaurants now allow customers to pay in advance, either via phone or online, reducing the need for physical cash transfers or credit card processing, both of which might carry the virus. Hence here we can conclude that age does not affect the reasons for choosing online food delivery services.

4.2 Result

The sudden onset of the Covid-19 crisis has surprised consumers, companies and government agencies. This study focuses on the effect of Covid-19 pandemic on online food delivery services. Based on the data, we analysed online food delivery platform usage, how it has helped during the Covid-19 pandemic and whether current changes could be long lasting.

Overall, Covid-19 has had a net positive impact on frequency and spending on online food delivery. For those not cooking at home, online delivery service from restaurants is one way to limit the number of trips outside the home. From the survey, we can conclude that usage of food delivery services varies with age category before Covid-19. People belonging to age category 18-30 are likely to order food more often. And

also these people spend more money on food delivery. Despite the fact that a large section of the population in Ernakulam uses online food delivery apps, there are still people who do not use food apps owing to health and quality concerns.

In a nutshell, the majority of users are students and working people, indicating that the online food ordering system is gaining popularity among young people. The changing lifestyles of consumers, as well as the growth of online activity in India, have unquestionably changed the trends in online food ordering.

REFERENCES

- [1] Complementary Statistics : Author-Ramakrishna Pillai.
- [2] <https://www.statisticssolutions.com/free-resources/directory-of-statistical-analyses/chisquare/>
- [3] R., Priyadarshini. (2017). Consumer perception towards MNC fast food outlets in Coimbatore. International Journal of Applied Research,3(3).Retrieved from <http://www.allresearchjournal.com/archives/2017/vol3issue3/PartD/3-3-54-357.pdf>
- [4] Samsudin, N. A., Khalid, S. K., Kohar, M. F., Senin, Z., and Ihkasan, M. N.(2011). A customizable wireless food ordering system with real time customer feedback. 2011 IEEE Symposium on Wireless Technology and Applications (ISWTA). doi:10.1109/iswta.2011.6089405
- [5] Rathore, S. S., and Chaudhary, M. (2018). Consumer's Perception on Online Food Ordering. International Journal of Management and Business Studies,8(4). Retrieved from <http://www.ijmbs.com/Vol8/issue4/2-suryadev-singh-rathore.pdf>
- [6] R., A., Singh, A., Pathan, S., and Kanade, V. (2017). Online Food Ordering System. International Journal of Computer Applications,180(6), 22-24.doi:10.5120/ijca2017916046

Annexure

1. What age category do you belong to?

- Below 18
- 18-30
- 31-50
- Above 50

2. Gender

- Male
- Female
- Others

3. Place of residence

- Urban
- Rural

4. Job profile

- Working
- Unemployed
- Student

5. What do you prefer?

- Going to restaurants
- Online food delivery

6. How often do you order food online before covid-19?

- Daily
- Weekly
- Monthly

- Never

7. How often do you order food online during covid-19?

- Daily
- Weekly
- Monthly
- Never

8. How much do you spend on online food delivery before covid-19?

- Less than 300
- 300-700
- Above 700

9. How much do you spend on online food delivery during covid-19?

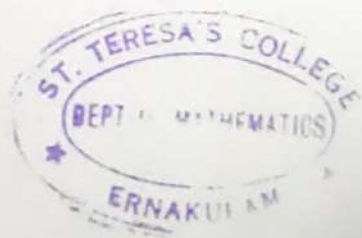
- Less than 300
- 300-700
- Above 700

10. Why do you prefer online food delivery before covid-19?

- Fast delivery
- Convenient
- Time saving
- All of the above

11. Why do you prefer online food delivery during covid-19?

- Safety
- To avoid transportation
- No restaurant nearby
- None of the above



ST. TERESA'S COLLEGE(AUTONOMOUS)

ERNAKULAM



B.Sc. PHYSICS

PROJECT REPORT

Name : CAROLINE LIZA ANIL

Register Number : AB19PHY005

Year of work : 2021 - 2022

This is to certify that this project work entitled '**VERIFICATION OF BEER'S LAW**' is an authentic work done by **CAROLINE LIZA ANIL.**

Staff member in-charge

Dr. SANTHI A

Head of the Department

Dr. PRIYA PARVATI AMEENA JOSE

Submitted for the University examination held at St. Teresa's College, Ernakulam.

DATE: 04-05-2022

EXAMINERS:

Ranjitha
Susan

ST. TERESA'S COLLEGE(AUTONOMOUS)
ERNAKULAM



CERTIFICATE

This is to certify that the project report entitled '**VERIFICATION OF BEER'S LAW**' is an authentic work done by CAROLINE LIZA ANIL, St. Teresa's College Ernakulam, under my supervision at Department of Physics, St. Teresa's College for the partial requirements for the award of Degree of Bachelor of Science in Physics during the academic year 2021-22. The work presented in this dissertation has not been submitted for any other degree in this or any other university.

Supervising guide

Dr. SANTHI A

Associate Professor

Priya
Head of the Department

Dr. PRIYA PARVATI AMEENA JOSE

Associate Professor



PLACE: Ernakulam

DATE: 04-05-2022

VERIFICATION OF BEER'S LAW

PROJECT REPORT

Submitted by

CAROLINE LIZA ANIL

Register Number: AB19PHY005

Under the guidance of

Dr. SANTHI A, Associate Professor

**Department of Physics, St. Teresa's College
(Autonomous),**

Ernakulam, Kochi-682011

Submitted to

Mahatma Gandhi University, Kottayam

In partial fulfilment of the requirements for the award of

BACHELOR DEGREE OF SCIENCE IN PHYSICS



ST. TERESA'S COLLEGE(AUTONOMOUS)

DECLARATION

I, CAROLINE LIZA ANIL (Register Number: AB19PHY005), final year B.Sc. Physics Students, Department of Physics, St. Teresa's College, Ernakulam do hereby declare that the project work entitled '**VERIFICATION OF BEER'S LAW**' has been originally carried out under the guidance and supervision of Dr. SANTHI A, Associate Professor, Department of Physics, St. Teresa's College (Autonomous), Ernakulam in partial fulfilment for the award of the degree of Bachelor of Physics. I further declare that this project is not partial or wholly Submitted for any other purpose and the data included in the project is collected from various sources and is true to the best of our knowledge.

ACKNOWLEDGEMENT

I express my sincere gratitude to all those who helped me to achieve this moment of satisfaction. Firstly, I thank the lord almighty for the immense grace at every stage of the project. I am highly indebted to my project guide Dr. Santhi A, Associate Professor, St. Teresa's College, Ernakulam for her valuable guidance and constant supervision as well as for providing necessary information regarding the project. I would like to express my gratitude to all the staff members of the Physics Department, St. Teresa's college, for their valuable guidance and suggestions for completing the project and for all those who have willingly helped me out of their abilities.

ABSTRACT

The report is presented in the aim of the **Verification of Beer's Law**. Beer's law also known as Beer- Lambert law relates to the absorption of light to the properties of the material through which the light is travelling. The law states that when light passes through a solution of a given thickness the fraction of incident light absorbed is dependent not only on the intensity of light but also on the concentration of the solution. It is done by an experiment where the absorption spectrum of a sample of solution of eosin yellow is measured and verified. The law is commonly applied to chemical analysis measurements and used in understanding absorption in physical optics, for photons, neutrons, or rarefied gases.

CONTENTS

Chapter No	Chapter Name	Page No
1	Mechanism of Absorption and Emission 1.1 Introduction 1.2 Absorption and Emission 1.3 Photoluminescence 1.4 Fluorescence and Phosphorescence 1.5 Classification of de-excitation	8 9 11 11 12
2	Absorption Spectrum 2.1 What is absorption spectrum? 2.2 Theory of Beer-Lambert Law 2.3 Factors that affect absorbance 2.4 Limitations of Beer-Lambert Law	14 15 18 19

3	Sample Preparation of BEER'S Law	20
4	Measurement of Absorption Spectrum	

	4.1 Spectrophotometer 4.2 Device Components 4.3 Principle 4.4 Working of Spectrophotometer 4.5 Applications	23 24 25 26 30
5	Result Conclusion Reference	32 34 35

CHAPTER 1

MECHANISM OF ABSORPTION AND EMISSION

1.1 INTRODUCTION

Atoms are the basic building blocks of all existing matter. They are responsible for the characteristic behavior of the basic different types of matter, that is, solid, liquid and gas. The term ‘Atom’ was derived from a Greek word ‘Atomos’ which means ‘non-divisible’. Many physicists did a lot of experiments to figure out if the speculations regarding the ‘un-cuttable’ nature of atoms was correct. The first atomic theory was given by John Dalton in 1808 and he thought of the atom as the ultimate particle of matter. Through his theory, he was able to explain the law of conservation of mass, law of constant composition and law of multiple proportion successfully but failed to explain the dissimilarities in the properties of some elements. Some of the other models were Thomson’s plum pudding model, Rutherford’s Nuclear Model of Atom, Bohr’s model, and so on. Many of these proposed models were able to explain the structure of atoms to a certain extent but could not account for several other important factors such as stability, existence of double spectral lines, etc. However, through the evolution of time and scientific techniques, scientists found that atoms are composed of smaller particles, such as electrons, protons and neutrons which are collectively known as ‘elementary particles’.

According to Bohr’s theory, electrons revolve around the nucleus in certain orbits of different energy levels. Energy levels show the distance of electrons from the nucleus of a particular element. Electrons are distributed to different shells of different levels corresponding to their energy. There are K, L, M...shells corresponding to the principal

quantum numbers $n = 1, 2, 3, \dots$. Each shell can only hold a fixed number of electrons and after filling a certain energy level, it jumps to higher energy levels, if provided with sufficient energy. The K shell lies closest to the nucleus and it can accommodate two electrons only. The L shell can hold a maximum of 8 electrons. The n^{th} shell can hold $2n^2$ numbers of electrons.

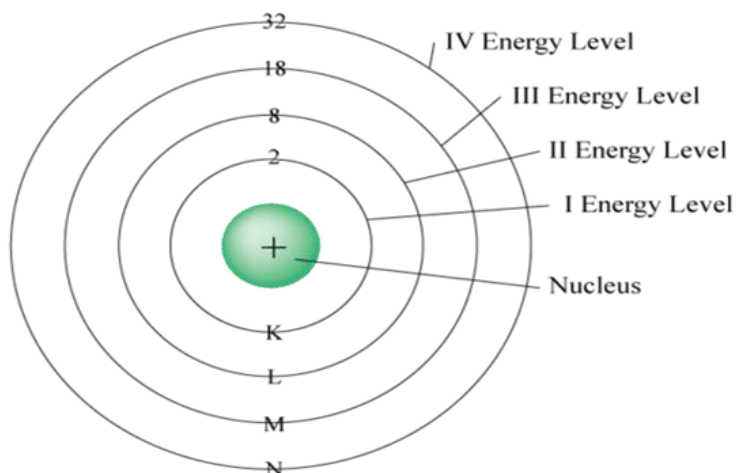


Figure 1(a) : Energy levels of an atom

1.2 ABSORPTION AND EMISSION

The binding energy of electrons to their parent nucleus is higher for the shells closest to it. As the energy level increases, the electrons are less tightly bound to the nucleus. The electrons at the outermost energy level are known as the valence electrons. They have more chances of becoming a free electron under the application of an external energy. When an incident photon having a frequency ν hits an atom, certain changes happen in its energy states. Its electrons absorb the quanta energy from the photon and excite to higher energy levels. This process is known as absorption of light. The excited electron stays at that

particular higher energy level for a very short time in the range of a few nanoseconds.

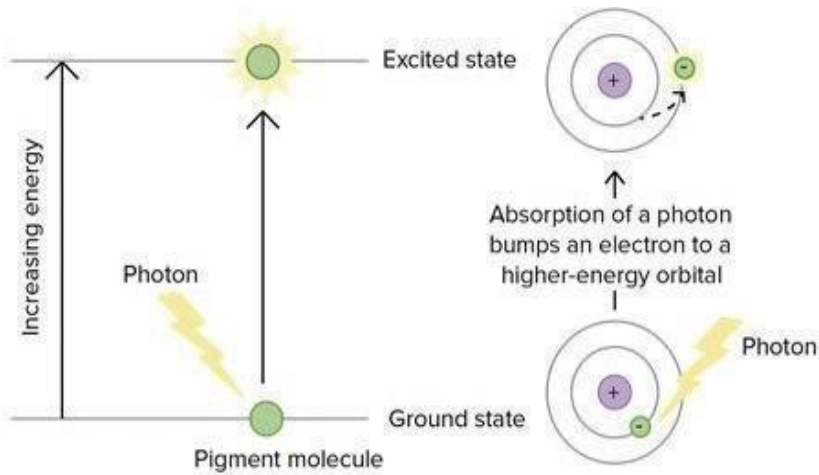


Figure 1(b): Absorption of a photon when it incidents on an atom

As the excited state is unstable, the electron de-excites back to its original state after some time. During de-excitation, electrons emit radiation in the form of photons and this process is known as Emission. That is, an atom can absorb or emit one photon when an electron makes a transition from one energy level to another. Conservation of energy determines the energy of the photon and thus the frequency of the emitted or absorbed light.

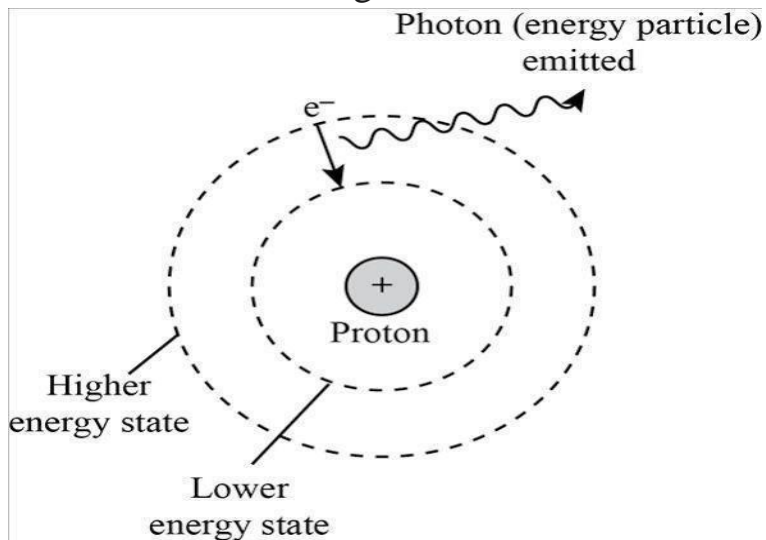


Figure 1(c) : De-excitation of an electron causing the emission of a photon

1.3 PHOTOLUMINESCENCE

When certain energy is absorbed by a molecule, it becomes excited and its electrons are raised to higher energy levels. The electrons do not remain there for a longer time and return to lower and more stable energy levels. This can occur by non-radiative process or through a radiative process. The radiative process involves the emission of electromagnetic radiations. This process of emitting radiation is collectively called luminescence. Photoluminescence is the emission of light which is caused by the irradiation of a substance with other light. The term embraces both fluorescence and Phosphorescence, which differ in the time after irradiation over which the luminescence occurs. The radiated light is often visible but can also be in the ultraviolet or infrared spectral region.

1.4 FLUORESCENCE AND PHOSPHORESCENCE

Fluorescence is the phenomenon in which a material absorbs light of a particular wavelength followed by a short-lived emission of light of a longer wavelength. This process involves a light source to excite the molecule, which is then transformed from a ground to an excited state. As the molecules return to the ground state, energy is released in the form of heat and light. The phenomenon of fluorescence is instantaneous and starts immediately after the absorption of light and stops as soon as the incident light is cut off. The fluorescent materials generally emit the radiation within 10^{-6} to 10^{-4} seconds of absorption. Thus, the lifetime of fluorescence is generally small. Also, no change in Spin state of the electron involved during the process of fluorescence.

Phosphorescence is the process in which the radiations are incident on certain substances, they absorb them and then emit light continuously for a long time even after the incident light is cut off. In this process the direction of the electron Spin may change when the electrons move to a lower energy state. In Phosphorescence the molecule does not return immediately to the ground state. Instead, it goes through a metastable state, a state where electrons stay for a longer period of time. This transition is known as intersystem crossing. The life-time of Phosphorescence is therefore much longer.

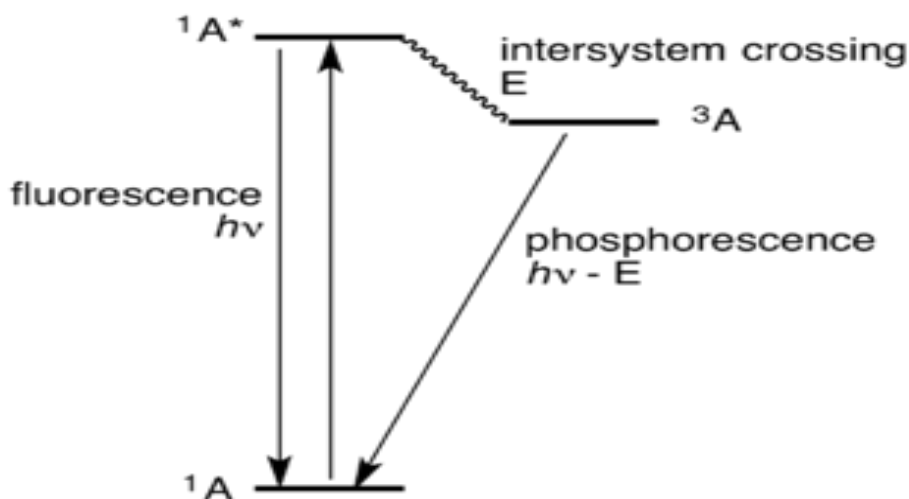


Figure 1(d) : Energy level diagram depicting fluorescence and phosphorescence

1.5 CLASSIFICATION OF DE-EXCITATION

Atomic de-excitation is the process by which an atom transfers from an excited electronic state back to the ground state electron configuration. It often occurs by emission of heat and light. Electronically excited states are unstable. Electrons drop back to their ground states. At the same time, the excitation energy is released again. One distinguishes between radiative and non-radiative decay processes. Most of the time,

the decay is non-radiative, for example through vibrational relaxation, quenching with surrounding molecules, or internal conversion.

Sometimes, a radiative decay can occur in the form of fluorescence and phosphorescence. The energy is emitted as electromagnetic radiation or photons. The emitted light has a longer wavelength and a lower energy than the absorbed light because a part of the energy has already been released in a non-radiative decay process. This is the reason that an emission in the visible spectrum can be achieved by excitation with non-visible UV-radiation.

CHAPTER 2

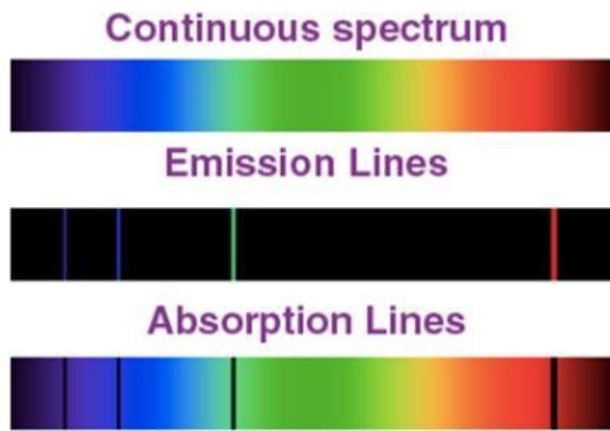
ABSORPTION SPECTRUM

In 1801 William Wollaston observed a rainbow in close detail and noticed tiny dark lines in the visible spectrum. In later years Fraunhofer took an even closer look at the Sun's spectrum (IR, UV and visible) by expanding the spectrum onto a large wall. As a result, he found thousands of slices that were missing. These are known as absorption lines or 'Fraunhofer lines'.

2.1 WHAT IS ABSORPTION SPECTRUM ?

Absorption spectra (singular spectrum) of chemical species (atoms, molecules, or ions) are generated when a beam of electromagnetic energy (i.e. light) is passed through a sample, and the chemical species absorbs a portion of the photons of electromagnetic energy passing through the sample. This spectrum is constituted by the frequencies of light transmitted with dark bands when the electrons absorb energy in the ground state to reach higher energy states. When light from any source is passed through the solution or vapour, a pattern comprising dark lines is obtained. This pattern is analysed using the spectroscope. Depending on the nature of the chemical or element, certain radiation is absorbed by the chemical or element when passed through it and dark line pattern is seen exactly in the same place where coloured lines are seen in the emission spectrum. The spectrum thus obtained is known as the absorption spectrum.

Emission spectra can emit all the colours in an electromagnetic spectrum, while the absorption spectrum can have a few colours missing due to the redirection of absorbed photons. The wavelengths of light absorbed help figure out the number of substances in the sample.



2.2 THEORY OF BEER-LAMBERT LAW

The Beer-Lambert law, known by various names such as the Lambert-Beer law, Beer-Lambert–Bouguer law or the Beer's law states that,

When light passes through a solution of a given thickness the fraction of incident light absorbed is dependent not only on the intensity of light but also on the concentration of the solution.

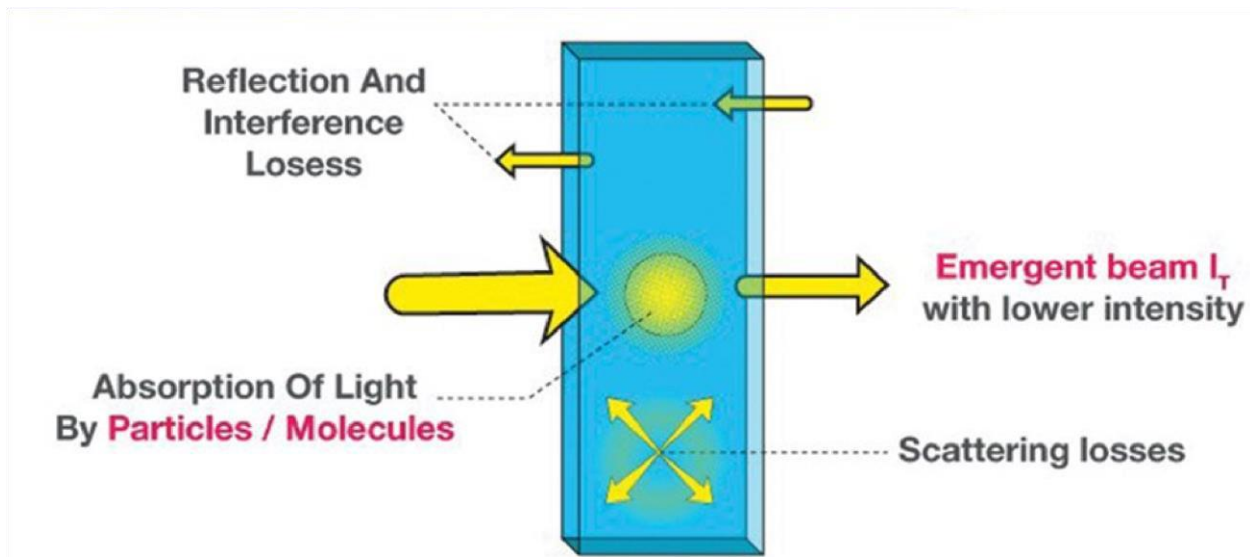
This law is taken from two other laws that laid the foundation to Beer-Lambert law. They are,

- Beer's law stated by August Beer : concentration and absorbance are directly proportional to each other
- Lambert law stated by Johann Heinrich Lambert : absorbance and path length are directly proportional

If material bodies are exposed to radiation, part of the incident radiation is absorbed, a part is scattered and a part is transmitted. As a result of absorption the intensity of light passing through material bodies, i.e. the intensity of transmitted light, decreases. The fraction

of incident light absorbed depends on the thickness of the absorbing medium.

When a monochromatic light of initial intensity I_0 passes through a solution in a transparent vessel, some of the light is absorbed so that the intensity of the transmitted light I is less than I_0 . There is some loss of light intensity from scattering by particles in the solution and reflection at the interfaces, but mainly from absorption by the solution. The relationship between I and I_0 depends on the path length of the absorbing medium, l , and the concentration of the absorbing solution, c . These factors are related in the laws of Lambert and Beer.



From the law we know that the decrease in intensity of light with thickness of the absorbing medium at any point is directly proportional to the intensity of light. If we express mathematically;

$$- dI / dx \propto I \quad (1)$$

Where dI is a small decrease in intensity of light upon passing through a small distance dx and I is the intensity of the monochromatic light just before entering the medium.

Equation (1) can be written as

$$-dI / dx = aI \quad (2)$$

Where $-dI / dx$ is the rate of decrease of intensity with thickness dx , **a** is called the absorption coefficient.

Integration of equation (2) after rearrangement gives,

$$-\ln I = ax + C \quad (3)$$

Where **C** is a constant of integration. At $x=0$, $I=I_0$. So, $C = -\ln I_0$.

Introducing this in equation (3) we get,

$$\ln I / I_0 = -ax \quad (4)$$

Equation (4) can also be written as,

$$I = I_0 e^{-ax} \quad (5)$$

Equation (5) can also be written

as, $\log I / I_0 = -a x / 2.303$

$$(6) \text{ or, } \log I / I_0 = -a' x$$

$$(7)$$

Where a' ($= a / 2.303$) is called extinction coefficient and $-\ln I / I_0$ is termed absorbance of the medium. Absorbance is represented by **A**.

Lambert's law was extended by Beer gives;

$$-dI / dx \propto c \quad (8)$$

The two laws may be combined to write

$$-dI / dx \propto I \times c$$

$$\text{Or, } -dI/dx = b \times I \times c \quad \dots \dots \dots \quad (9)$$

When the concentration, c , is expressed in mol /L, b is called the molar absorption coefficient.

As in the case of Lambert's law equation (9) may be

transformed into, $\log I/I_0 = -b/2.303 \times c \times x \dots \dots \dots$

$$(10) \log I/I_0 = -\epsilon \times c \times x \dots \dots \dots \quad (11)$$

Where $\epsilon (= b / 2.303)$ is called the molar extinction coefficient which is expressed in L/mol/cm.

The molar extinction coefficient ϵ is dependent on the nature of the absorbing solute as well as on the wavelength of the incident light used. The expression (equation 11) is commonly known as Beer-Lambert's law.

$A = -\epsilon \times c \times x$ where A is the

absorbance of the sample

The Beer-Lambert law allows you, the scientist, to measure the absorbance of a particular sample and to deduce the concentration of the solution from that measurement! In effect, you can measure the concentration of a particular chemical species in a solution as long as you know the species absorbs light of a particular wavelength.

2.3 FACTORS THAT AFFECT ABSORBANCE

These are the factors that affect absorbance:

- The concentration of a sample is one factor that affects its absorbance. As the concentration rises, more radiation should be

absorbed, increasing the absorbance. As a result, the concentration and absorbance are directly proportional.

- The length of the path is a second consideration. The longer the path length, the more molecules in the path of the radiation beam, and thus the absorbance increases. As a result, the length of the path is proportional to the concentration.
- The molar absorptivity is the third factor when the concentration is expressed in moles/litre and the route length is expressed in centimeters. This is more commonly referred to as the extinction coefficient in some sectors of study.

We may construct the Beer-Lambert law (commonly referred to as Beer's Law) to show this relationship because concentration, path length, and molar absorptivity are all directly proportional to absorbance.

The absorbance of a transition depends on two external assumptions:

- The absorbance is directly proportional to the concentration (c) of the solution of the sample used in the experiment
- The absorbance is directly proportional to the length of the light path (l), which is equal to the width of the cuvette.

2.4 LIMITATIONS OF BEER-LAMBERT LAW

This law can be used to study the absorptivity coefficient of the sample when the concentration is low ie; $<10\text{mM}$, but as the concentration becomes high ie; $>10\text{mM}$ there is a deviation as the electrostatic interactions become more.

CHAPTER 3

SAMPLE PREPARATION OF BEER'S LAW

The solute taken for the experiment is Eosin Yellow. It is a water-soluble dye and is a red crystalline powder. The purity of the dye content is 88%. The chemical formula of Eosin Yellow is $C_{20}H_6Br_4Na_2O_5$. Its molecular weight is 691.8515 g/mol. Stock solution is a solution which is prepared by weighing out an appropriate portion of a pure solid and placing it in a suitable flask, and diluting to a known volume. The steps to get the necessary sample and to obtain the absorption spectrum is as follows:

- To measure the mass of the solute:

Using butter paper tared on a balance, we carefully weigh the amount of Eosin Yellow required for the stock solution. We only need a very small scoop of material. Mass of Eosin Yellow content is measured using a digital weighing scale.

Weight of Eosin Yellow dye taken = 0.032g

- To make Stock solution :

0.032 g is dissolved in 10ml of distilled water in a beaker. This is taken as the Stock solution.

Number moles of solute, $n = (\text{Measured weight of solute}) / (\text{Molecular weight of solute})$

Volume of distilled water used to make the Stocks solution, V =
 $10 \text{ ml} = (0.032\text{g}) / (691.8515\text{g/mol}) = 4.62527 * 10^{-5}\text{mol}$

691.8515 g dissolved in 1L gives one molar (1 M)

i.e, 6.918515 g dissolved in 10 ml gives one molar

Therefore, there are $(0.032\text{g}) / (6.918515\text{g/mol})$ numbers of moles dissolved in 10 ml.

Molarity of the solution, M = Number of moles / Volume of the solvent

$$M = (0.032\text{g}) / (6.918515\text{g/mol}) * (10 \text{ ml}) = M = 0.4625 \text{ g/L} \quad (0.$$

$$032 / 6.9185) * (1000 / 10)$$

- Diluting the stock solution to make the standard solutions:

10 samples are to be prepared. 1 ml of the stock solution is taken in a clean test tube using a syringe. Different concentrations of its diluted solution gives us the required 10 samples. 1 ml of stock solution diluted in 15 ml is taken as the first sample and 1 ml of stock solution in 16 ml is taken as the second sample. Likewise, each of the ten samples are obtained by adding 1 ml into the previously diluted solution. Maximum concentration of the solute is found in the first sample and its concentration gradually decreases after each sample solution.

Concentration of first sample is obtained by

$$(0.032 / 0.69185) \text{ g in } (15 + 1) \text{ ml} = (2.89 \text{ g/L} \cdot 0.032 / 0.69185) * (1000 / 16)$$

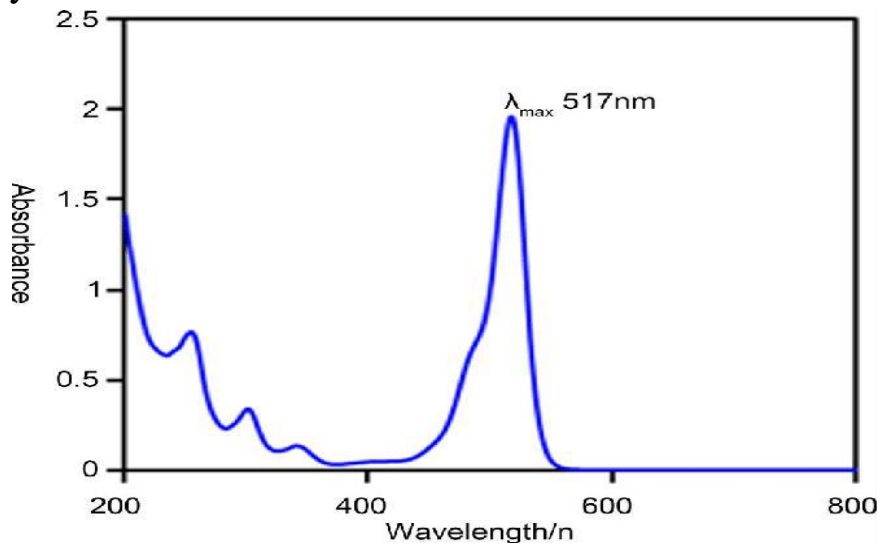
Similarly, concentrations of 10 samples can be calculated.

- Getting absorption spectrum from Spectrophotometer :



Each of the samples is taken in a cuvette and kept inside the device for obtaining required absorption spectrum. Absorption spectrum is obtained for 10 samples.

Eosin Y is a chemical compound with an absorbance peak at 517 nm. The actual absorption spectrum of a sample solution of eosin yellow is shown below :



CHAPTER 4

MEASUREMENT OF ABSORPTION SPECTRUM

4.1 SPECTROPHOTOMETER



Every chemical compound has the ability to absorb, transmit or reflect electromagnetic radiation over a certain wavelength.

Spectrophotometry is a method to determine how much a chemical substance absorbs light by measuring the intensity of light as a beam of light passes through a sample solution. Absorption spectroscopy is widely used in chemical analysis, for determining unknown samples from a given mixture, infrared gas analyser (which identifies pollutants in the air), remote sensing (for detecting the presence of hazardous elements in a mixture) and so on. A colored solution absorbs all the colours of white light and selectively transmits only one colour.

A spectrophotometer is an instrument that measures the amount of photons (the intensity of light) absorbed after it passes through sample solution. With the spectrophotometer, the amount of a known chemical substance (concentrations) can also be determined by measuring the intensity of light detected. Depending on the range of wavelength of light source, it can be classified into two different types:

- **UV-visible spectrophotometer:** It uses light over the ultraviolet range (185 - 400 nm) and visible range (400 - 700 nm) of electromagnetic radiation spectrum.
- **IR spectrophotometer:** uses light over the infrared range (700 - 15000 nm) of electromagnetic radiation spectrum

4.2 DEVICE COMPONENTS

Light Source

Unlike Deuterium or tungsten-halogen lamps, which provide a constant light source, a Xenon flash lamp emits light for an extremely short time, in flashes. Since it emits only for a short time and only during sample measurement, it has a longer life. The sample is only irradiated with light at the time of measurement. This short illumination time makes the Xenon flash lamp suitable for measuring samples that may be sensitive to photobleaching. Photobleaching can be observed on sensitive samples when exposed to a constant long exposure by a continuous light source. The Xenon flash lamp emits high intensity light from 190-1100nm, which means no secondary light source is required . The Xenon flash lamp may be used for many years before requiring replacement, which makes it a popular choice compared to

systems using D2 or tungsten halogen lamps. An extra benefit is that it does not require warm up time, unlike D2 or tungsten-halogen lamps.

Cuvettes

Monochromator source is used; before reaching the sample, light is divided in two parts of similar intensity with a half mirror splitter. One part travels via the cuvette having the solution of material to be examined in transparent solvent. Second beam or reference beam, travels via a similar cuvette having only solvent. Reference and sample beam containers have to be transparent towards the passing beam.

Photosensitive Detector

The detectors are devices that convert radiant energy into electrical signals. It should be sensitive, and has a fast response over a considerable range of wavelengths. The electrical signal produced by the detector must be directly proportional to the transmitted intensity.

4.3 PRINCIPLE

A light beam is passed through an object and wavelength of the light reaching the detector is measured. The measured wavelength provides important information about chemical structure and number of molecules (present in intensity of the measured signal). Thus, both quantitative and qualitative information can be gathered. Information may be obtained as transmittance, absorbance or reflectance of radiation in the 190 to 1100nm wavelength range. The absorption of incident energy promotes electrons to excited states. For this transfer to occur, photon energy must match the energy needed by the electron to be promoted to the next higher energy state.

This process forms the basic operating principle of absorption spectroscopy. When light having specific wavelength and energy is focused onto the sample, it absorbs some energy of the incident wave. A photodetector measures energy of transmitted light from a sample, and registers absorbance of the sample. The absorption or transmission spectrum of the light absorbed or transmitted by the sample against the wavelength is formed. Bouguer–Beer law or the Lambert–Beer rule is the basic principle of quantitative analysis, and it establishes that absorbance of a solution scales directly with analyte concentration.

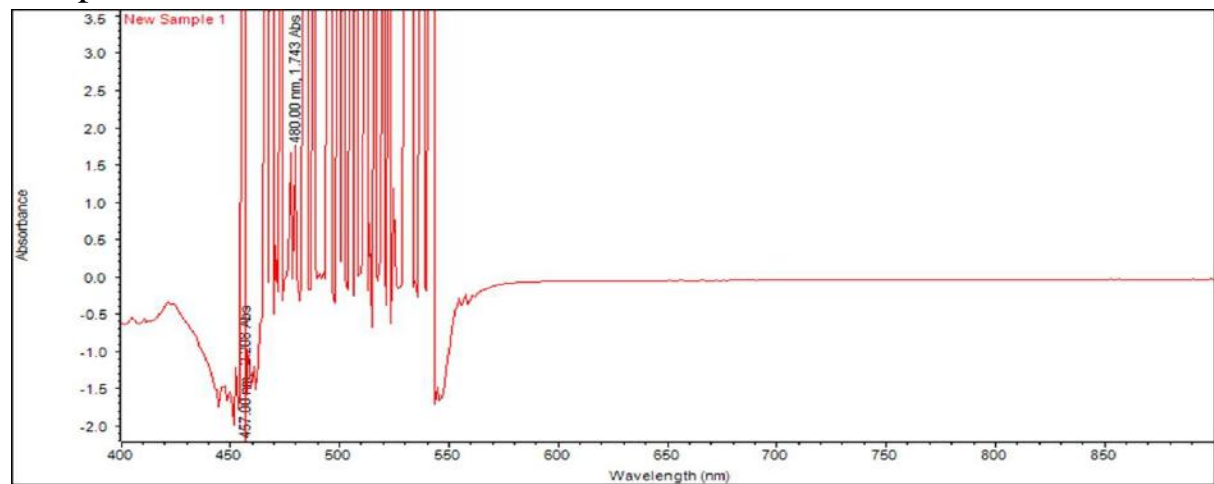
4.4 WORKING OF UV-VISIBLE SPECTROPHOTOMETER

Ultraviolet-visible spectrophotometer system focuses electromagnetic radiation from the light source to the sample. Depending on the configuration set in the system, light is transmitted through the sample or reflected off it. Then, the light is collected from the sample through reading.

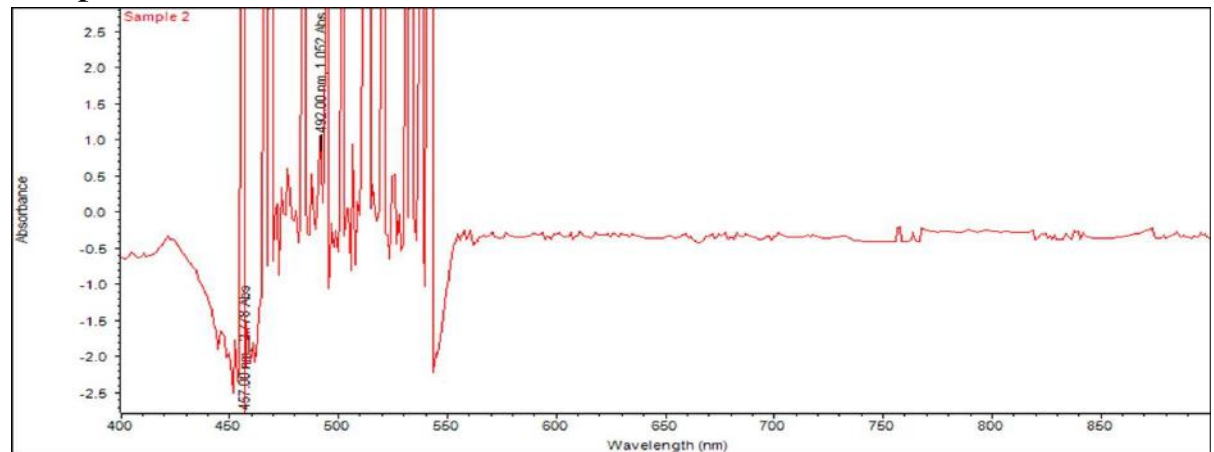
Initially, light is focused into the entrance slit of the monochromator from the source. Monochromator uses dispersing elements, namely optical grating to separate the light by wavelength. The light is passed into a charged coupled device (CCD), which is made up of individual tiny detectors, hence the intensity of light at each wavelength will be measured. CCD is read-off to a computer and the result obtained is a spectrum, which shows the intensity of each wavelength of light. Spectrophotometers are able to measure the electromagnetic radiation from ultraviolet to infrared. Spectrum will show the intensity of light versus the wavelength.

The absorption spectrum of 10 samples are as follows:

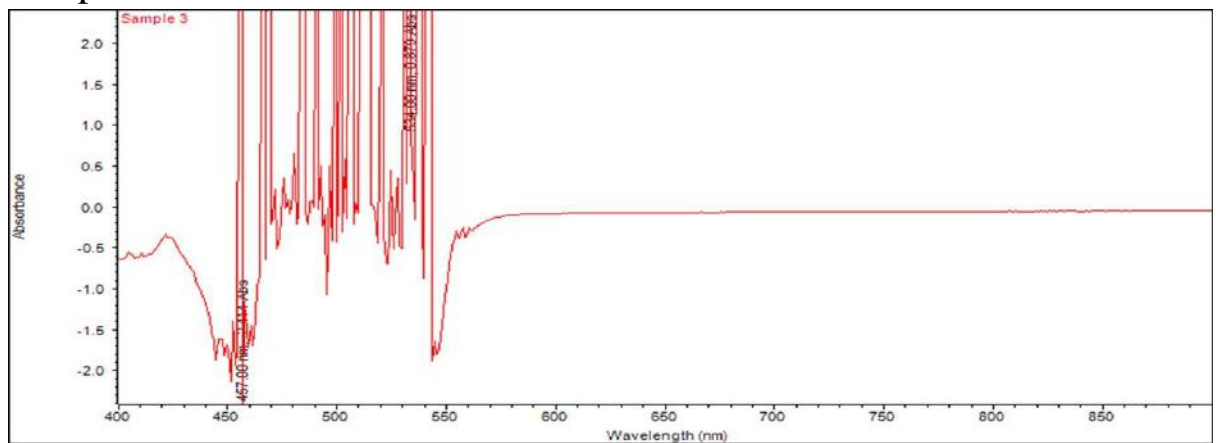
Sample 1:



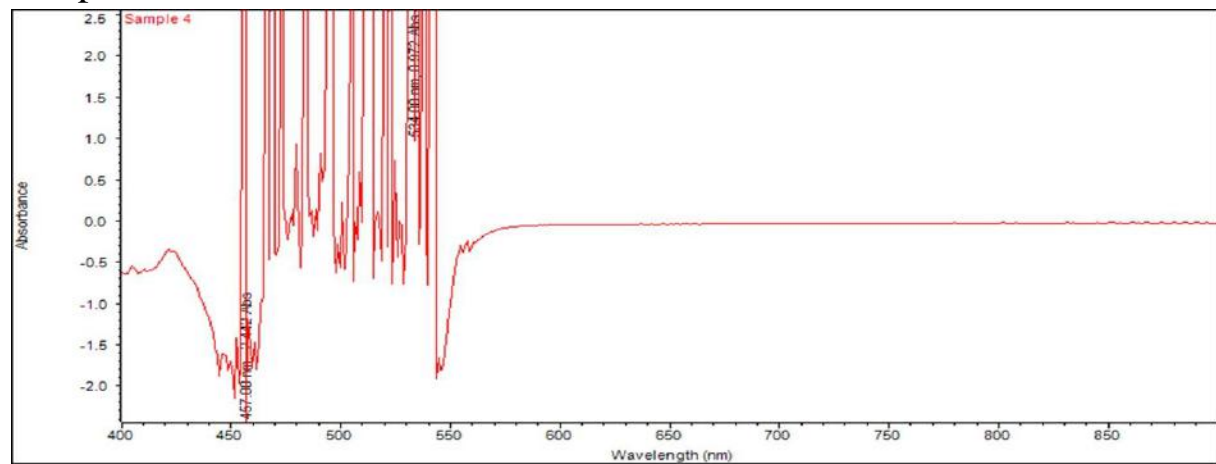
Sample 2:



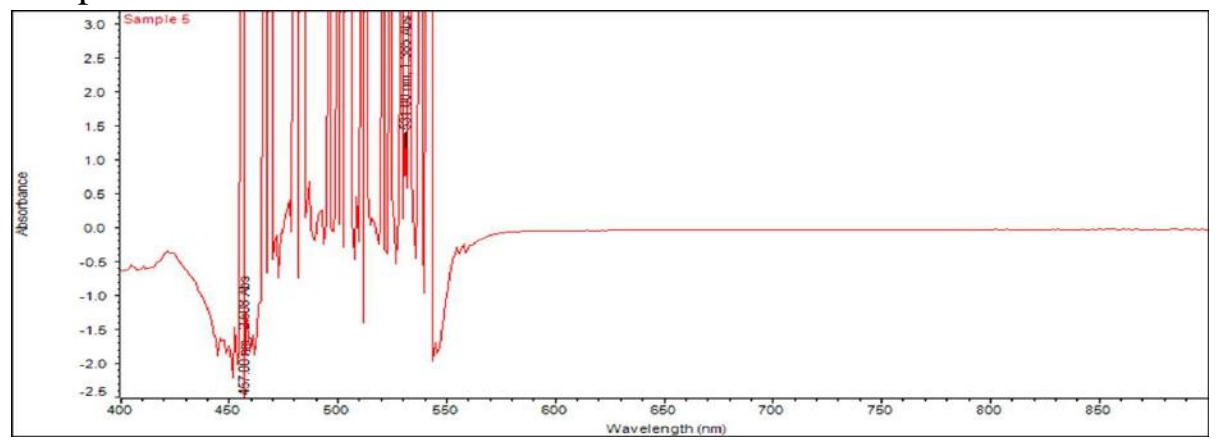
Sample 3:



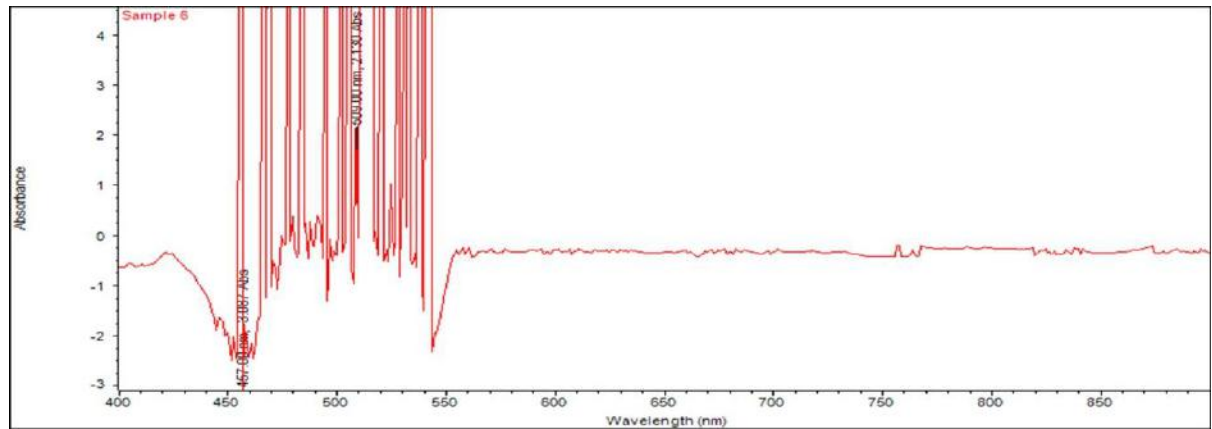
Sample 4:



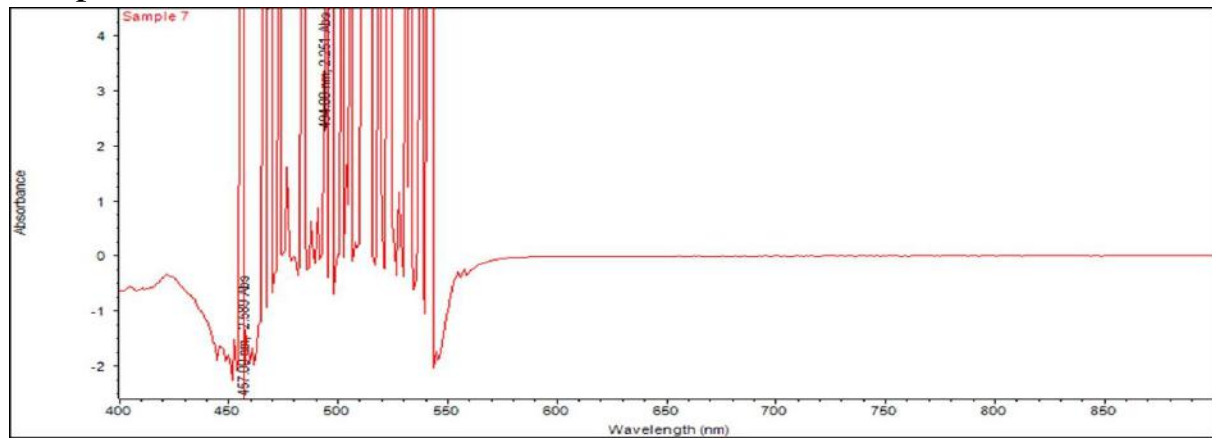
Sample 5:



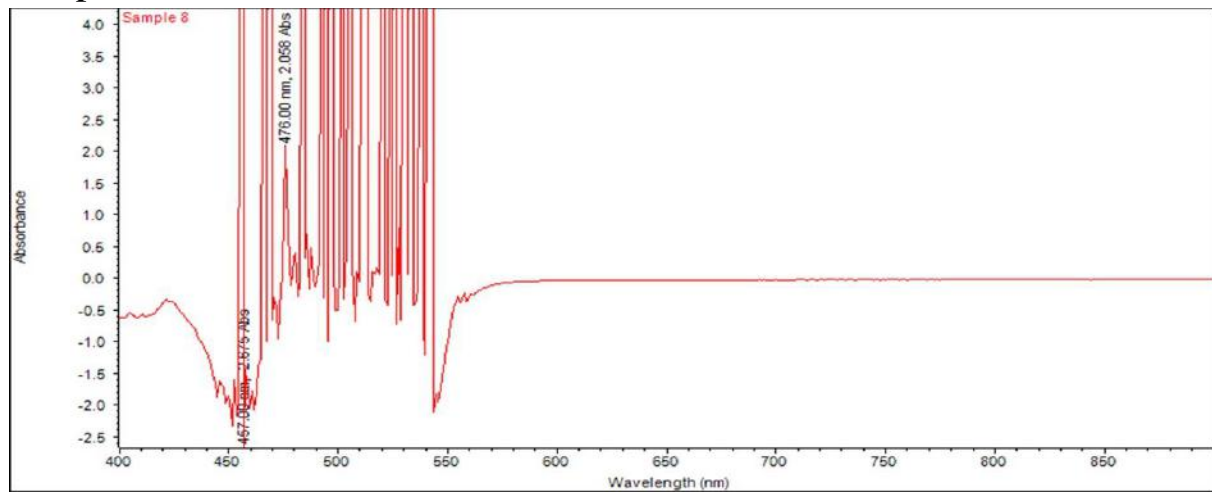
Sample 6:



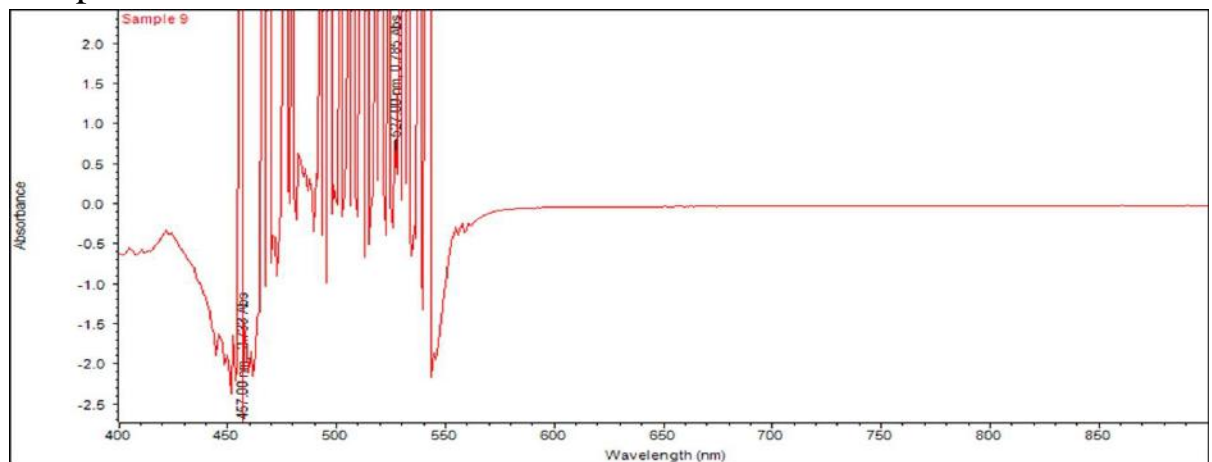
Sample 7:



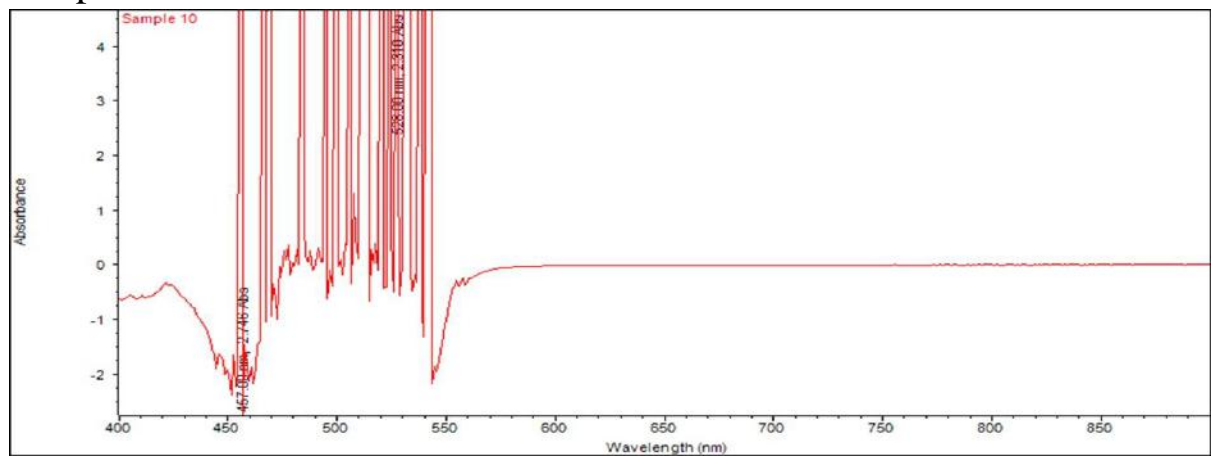
Sample 8:



Sample 9:



Sample 10:



4.5 APPLICATIONS

- The absorption of a reactant or product at constant wavelength provides a means of monitoring the progress of a chemical reaction. Clinical studies using indirect measurement of reactions characterised by enzymes can also be carried out.
- DNA or Deoxyribonucleic acids are involved in protein synthesis in living cells and preserve genetic information. Changes in pH or heating

can lead to denaturation with the resultant increase in absorption at 260 nm. Monitoring absorption at this wavelength is useful for denaturation monitoring.

- Appearance of additional peaks due to presence of impurities can help establish purity of standard materials.
- Absence or presence of functional groups results in absence of presence of their characteristic absorption bands.
- Identification and quantitative determination of polynuclear aromatic compounds
- Non – absorbing molecules can be estimated by combination with derivative forming molecules that produce new species with absorption characteristics in the UV – VIS region
- Quantitative estimation of ionic solutions of transition metals or complex forming ligands

CHAPTER 5

RESULTS AND CONCLUSION

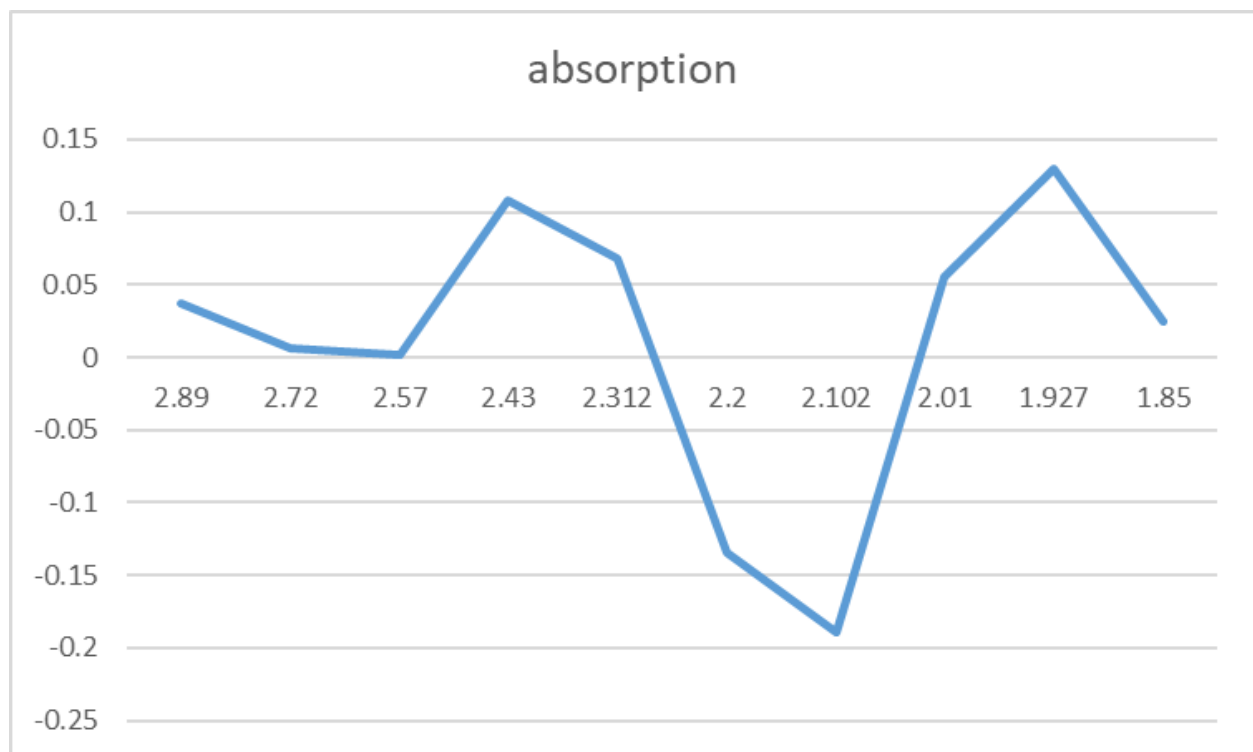
Absorption peak of the chemical compound Eosin yellow is at wavelength 517 nm. Absorbance (A) at this certain wavelength is noted from each of the samples and is plotted against their corresponding Concentrations (C).

They are given as follows:

Sample	Absorption (A)	Concentration (C)
1	0.03716	$(0.032/0.69185) \times (1000/16) = 2.89$
2	0.005833	$(0.032/0.69185) \times (1000/17) = 2.72$
3	0.00197	$(0.032/0.69185) \times (1000/18) = 2.57$
4	0.108443	$(0.032/0.69185) \times (1000/19) = 2.43$
5	0.068485	$(0.032/0.69185) \times (1000/20) = 2.312$
6	-0.134944	$(0.032/0.69185) \times (1000/21) = 2.20$
7	-0.18949	$(0.032/0.69185) \times (1000/22) = 2.102$
8	0.055654	$(0.032/0.69185) \times (1000/23) = 2.01$

9	0.129347	$(0.032/0.69185) \times (1000/24) = 1.927$
10	0.025064	$(0.032/0.69185) \times (1000/25) = 1.850$

The absorption versus concentration graph is given below:



CONCLUSION

In this project, an attempt has been made to verify Beer's law by taking the measure of absorption spectrum of the sample of eosin yellow solution. But the result was not completely in favour of the aim of the project since the absorption spectrum has noise. This has occurred due to few errors such improper baseline setting in the device, high concentration, impurities in the sample and scattering. This causes unclear absorption peaks. Therefore, the corresponding absorbance extracted from the data set has anomalies. This could be rectified by careful sample preparation of sample, optimization of concentration and proper initial settings in the spectrometer.

Beer's law plays a very significant part in industries as it is most commonly used for chemical analysis, to determine the properties, components and concentration of liquids. One of the major uses in forensic! By comparing the spectra of suspected toxins with those from the crime scene, the nature of the poison can be determined. Once the identity of the poison is determined, Beer's law can be used to determine the concentration of poison or even any liquid in concern. It is used to find out the concentration in terms of normality of an unknown solution. There are many more applications of this law in real life and also have the potential for more applications in many more fields.

REFERENCES

1. <https://byjus.com/physics/absorption-spectrum/>
2. <https://chem.libretexts.org/>
3. <https://www.sciencedirect.com/topics/agricultural-and-biological-sciences/spectrophotometers>
4. <https://www.ssi.shimadzu.com/products/uv-vis-spectrophotometers/faqs/instrument-design.html>
5. https://www.medchemexpress.com/eosin-y.html?src=google-product&gclid=CjoKCQjwl7qSBhD-ARIACvV1XoP-1pP4bHX1Ls-zBMzvfIVPEYOLykxPdLVvlN295mf6OWQfYZcUoAaAuluEALw_wcB
6. [https://chem.libretexts.org/Bookshelves/Analytical_Chemistry/Anal_ytical_Chemistry_2.1_\(Harvey\)/02%3A_Basic_Tools_of_Anal_ytical_Chemistry/2.05%3A_Preparing_Solutions](https://chem.libretexts.org/Bookshelves/Analytical_Chemistry/Anal_ytical_Chemistry_2.1_(Harvey)/02%3A_Basic_Tools_of_Anal_ytical_Chemistry/2.05%3A_Preparing_Solutions)
7. <https://byjus.com/physics/beer-lambert-law/>
8. <https://byjus.com/chemistry/absorbance-vs-concentration/>
9. [https://chem.libretexts.org/Bookshelves/Physical_and_Theoretical_Chemistry_Textbook_Maps/Supplemental_Modules_\(Physical_and_Theoretical_Chemistry\)/Spectroscopy/Electronic_Spectroscopy/Electronic_Spectroscopy_Basics/The_Beer-Lambert_Law#:~:text=The%20absorbance%20is%20directly%20proportional,the%20width%20of%20the%20cuvette.](https://chem.libretexts.org/Bookshelves/Physical_and_Theoretical_Chemistry_Textbook_Maps/Supplemental_Modules_(Physical_and_Theoretical_Chemistry)/Spectroscopy/Electronic_Spectroscopy/Electronic_Spectroscopy_Basics/The_Beer-Lambert_Law#:~:text=The%20absorbance%20is%20directly%20proportional,the%20width%20of%20the%20cuvette.)

10. [https://www.khanacademy.org/science/class-11-chemistry-india/xfbb6cb8fc2bdooc8:in-in-structure-of-atom/xfbb6cb8fc2bdooc8:in-i n-bohr-s-model-of-hydrogen-atom/a/absorptionemission-line1s](https://www.khanacademy.org/science/class-11-chemistry-india/xfbb6cb8fc2bdooc8:in-in-structure-of-atom/xfbb6cb8fc2bdooc8:in-i-n-bohr-s-model-of-hydrogen-atom/a/absorptionemission-line1s)
11. <https://medium.com/@ankur1857/principle-of-ultra-violet-uv-spectrophotometer-e6a1c435d258>
12. https://en.m.wikipedia.org/wiki/Agilent_Technologies
13. <https://lab-training.com/applications-of-uv-vis-spectroscopy/>

**MoS₂ NANO-SHEET LOADED TiO₂ NANOTUBE
ARRAY FOR VISIBLE LIGHT DRIVEN
PHOTO-CATALYSIS FOR WATER PURIFICATION
APPLICATIONS**

PROJECT REPORT

Submitted by

Jibila Mary Johnson

AM20PHY008

Under the guidance of

Dr. Kala M.S, Associate Professor

**Department of Physics, St. Teresa's College(Autonomous),
Ernakulam, Kochi-682011**

Submitted to the

Mahatma Gandhi University, Kottayam

In partial fulfillment of the requirements for the award of

MASTER'S DEGREE OF SCIENCE IN PHYSICS



**ST. TERESA'S COLLEGE (AUTONOMOUS),
ERNAKULAM, KOCHI-682011**

**ST. TERESA'S COLLEGE
(AUTONOMOUS)
ERNAKULAM**



**M.Sc PHYSICS
PROJECT REPORT**

Name : Jibila Mary Johnson

University Register No. : AM20PHY008

Year of Work : 2021-22

This is to certify that the project "**MoS₂ NANO-SHEET LOADED TiO₂ NANOTUBE ARRAY FOR VISIBLE LIGHT DRIVEN PHOTO-CATALYSIS FOR WATER PURIFICATION APPLICATIONS**" is done by Jibila Mary Johnson.

Staff Member in charge



Head of the Department

Submitted for the University examination held in St. Teresa's College (Autonomous), Ernakulam.

Examiners

- 1) Dr. Issac Paul, *[Signature]*
- 2) Dr. Gishamol Mathew *[Signature]*

Date: 14. 06. 2022

**ST. TERESA'S COLLEGE
(AUTONOMOUS)
ERNAKULAM**



CERTIFICATE

This is to certify that the project report titled "**MoS₂ NANO-SHEET LOADED TiO₂ NANOTUBE ARRAY FOR VISIBLE LIGHT DRIVEN PHOTO-CATALYSIS FOR WATER PURIFICATION APPLICATIONS**" submitted by **JIBILA MARY JOHNSON** towards partial fulfillment of the requirements for the award of the degree of Master's of Physics is a record of bonafide work carried out by her during the academic year 2021-22.

Supervising guide

Saleem

Dr. Kala M.S
Associate Professor
Department of Physics

Head of the Department

Priya

Dr. Priya Parvathi Ameena Jose
Assistant Professor
Department of Physics



PLACE: Ernakulam

DATE : 14-6-22

DECLARATION

I, JIBILA MARY JOHNSON, Register No. AM20PHY008 hereby declare that this project entitled "MoS₂ NANO-SHEET LOADED TiO₂ NANOTUBE ARRAY FOR VISIBLE LIGHT DRIVEN PHOTO-CATALYSIS FOR WATER PURIFICATION APPLICATIONS", is an original work done by me under guidance of Dr.KALA M.S, Associate Professor, Department of Physics and Centre for Research, St. Teresa's College (Autonomous), Ernakulam in partial fulfillment for the award of the Degree of Masters in Physics. I further declare that this project is not partly or wholly submitted for any other purpose and the data included in the project is collected from various sources and are true to the best of my knowledge.

PLACE: Ernakulam

DATE : 14-6-22

JIBILA MARY JOHNSON

ACKNOWLEDGEMENT

With immense pleasure, I express my deep sense of gratitude to the great God Almighty without whose divine blessings this work would have been never completed. I express my sincere gratitude towards Dr. Kala M.S, Associate Professor, Department of Physics and Centre for Research, and Dr. Anju K. Nair for their valuable guidance in the formation and successful completion of our study. I owe my sincere thanks to all other teachers and lab assistants for providing the facilities in completing this project and for their helping hands. Being a student of St. Teresa's College (Autonomous), Ernakulam, let me express my profound gratitude to the College. I owe my gratitude to the Department of Zoology, St. Teresa's College and Dr. Helvin Vincent for their helping hands during completion of our project. I express our heartfelt thanks to the MPhil scholar Merly Ann Peter for their guidance in completing our project. I'm grateful to the Sophisticated Test and Instrumentation Centre (STIC) for helping me during the characterization studies. I sincerely thank our parents for their guidance and support. Finally I thank our classmates for the valuable comments and suggestions they made during this project.

CONTENTS

SL. NO.	TITLE	PG NO.
	ABSTRACT	1
	CHAPTER 1 : INTRODUCTION	
1.1.	Nanoscience and nanotechnology	2
1.2	The origin of nanotechnology	3
1.3	The importance of nano scale	5
1.4	Different types of nano particles	5
	1.4.1. Carbon-based nano particles	6
	1.4.2. Ceramic nanoparticles	6
	1.4.3. Metal nanoparticles	6
	1.4.4. Semiconductor nanoparticles	6
	1.4.5. Polymeric nanoparticles	7
	1.4.6. Lipid-based nanoparticles	7
1.5	Approaches in nano fabrication	7-8
1.6	Advantages and disadvantages of nanotechnology	8-10
1.7	Water pollution	10
	1.7.1. Need of water purification	11
1.8	Role of nanotechnology in photocatalysis	11-12
	1.8.1. Mechanism for photocatalytic reaction	12
	1.8.2. Material selection for nanomaterials as photocatalyst	13
	1.8.3. Titanium dioxide (TiO ₂)	14-15
	1.8.4. Modification of TiO ₂ photo catalysts-	15
	1.8.4.a . Metal doping	15-16
	1.8.5. Molybdenum disulfide (MoS ₂)	16-17
	1.8.5.a . Applications	17
	References	18-20
	CHAPTER 2 : EXPERIMENTAL METHODS	
2.1.	Synthesis techniques	21
	2.1.1. Hydrothermal method	21
	2.1.1.a. Hydrothermal synthesis of TiO ₂ nano powder	21
	2.1.1.b. Synthesis of TiO ₂ nano tubes	22
	2.1.1.c. Hydrothermal synthesis of MoS ₂ nanosheet	22

	2.1.1.d. Surface sensitization of nano structured TiO ₂ by MoS ₂ nano sheet.	22-23
	2.1.1.e . Synthesis of TiO ₂ @ MoS ₂ heterostructure.	23-24
	2.1.2. Preparation of dye solution for photo catalysis	24
	2.1.2.a . Rhodamine B	24
	2.1.2.b. Methylene Blue	24-25
2.2	Characterization techniques	25-36
	2.2.1. X-ray diffraction	25
	2.2.1.a. Basic principle	26-27
	2.2.1.b. Lattice parameters	27-28
	2.2.1.c. XRD pattern	29
	2.2.1.d. Determination of the particle size from XRD pattern	30
	2.2.2. Transmission electron microscopy	30-32
	2.2.3. UV Visible spectroscopy	32-34
	2.2.3.a. UV- Visible absorption spectrum	34-36
	References	37-38
	CHAPTER 3 : RESULT AND DISCUSSION	
3.1	XRD analysis	39
	3.1.1. XRD spectrum of synthesized TiO ₂ nanopowder	39-40
	3.1.2. XRD spectra of synthesized MoS ₂ nanostructures obtained at different autoclaved time period.	40-41
3.2	TEM images of the synthesized TiO ₂ nanotubes	42-43
3.3	Photo catalytic studies	43-61
	3.3.1. Degradation of Methylene Blue dye(MB)	
	3.3.1.a. Degradation of MB with TiO ₂ nanotube	43-45
	3.3.1.b. Degradation of MB with MoS ₂ nano sheet	45-46
	3.3.1.c . Degradation of MB dye with MoS ₂ nanosheet doped TiO ₂ nanotube	46-48
	3.3.1.d . Degradation of MB with MoS ₂ nano sheet doped TiO ₂ nanotube prepared by mechano chemical method	48-49
	3.3.1.e . Comparison of the doped TiO ₂ nanotube (MT) with un doped TiO ₂ nanotube	50-52
	3.3.2. Degradation of Rhodamine B dye(Rh B)	
	3.3.2.a. Degradation of Rh B with TiO ₂ nanotube	52-53
	3.3.2.b. Degradation of Rh B with MoS ₂ nanosheet.	53-54
	3.3.2.c. Degradation of Rh B dye with MoS ₂ nanosheet doped TiO ₂ nanotube	55-56
	3.3.2.d. Degradation of Rh B with MoS ₂ nano sheet doped TiO ₂ nanotube prepared by mechano chemical method	56-58

	3.3.2.e . Comparison of doped TiO ₂ nanotube(MT) with un doped TiO ₂ nanotube	58-60
3.4	Re-usability studies	60
	References	61-63
	CHAPTER 4 : CONCLUSION AND FUTURE SCOPE	64-66
	References	67

ABSTRACT

The world is addressing global challenges- energy and water scarcity. Day by day water resources are getting more and more polluted. The sources available when compared to the need of the population are very limited. In such a situation it is necessary to find cost effective and efficient methods to purify the water resources. The water is mainly contaminated by dyes, heavy metals, plastic wastes, other organic and inorganic wastes from industries, households, hospitals etc. One of the methods that can be opted for the purification of water is photo catalytic degradation using nano catalyst. Two such photo catalyst are TiO_2 and MoS_2 which fall into the category of semiconductor photo catalysts.

In this work, we have doped TiO_2 nanotubes (NT) with MoS_2 so that we can increase the photo catalytic degradation of pollutants more effectively in the presence of visible light. For synthesis, we opted hydrothermal method. Structure and composition were determined using characterisation techniques X-ray diffraction, High resolution Transmission Electron Microscopy, Fourier transform infra-red spectroscopy. The photo catalytic degradation in two most commonly used dyes Rhodamine B and Methylene Blue was studied under visible light. The percentage of degradation was studied by using UV-visible spectroscopy. Our project is a small step for the betterment of society aiming the high scale water purification.

CHAPTER 1

INTRODUCTION

1.1. NANOSCIENCE AND NANOTECHNOLOGY

Nanoscience is the study of structures and molecules on the scales of nanometres ranging between 1 and 100 nm, and the technology that utilizes it is known as nanotechnology. Nanotechnology has become one of the most promising technologies of the 21st century. It has the ability to convert the ideas of nanoscience to useful applications by observing, manipulating, measuring, assembling, controlling and manufacturing the matter in the nanometre scale.

Nanoscale science and technology are based on the fact that materials at the nano scale have the properties (i.e., mechanical, optical, chemical, and electrical) quite different than the bulk materials. For example, macromolecules and particles are made up of limited number of molecules, i.e., in the size range of 1–50 nm, having distinct chemical (i.e., reactivity, catalytic potential, etc.) and physical properties (i.e., magnetic, optical). On comparing with bulk materials, it is seen that nanoparticles possess enhanced performance properties when they are used in similar applications. Size-dependent properties are one of the most important features of nanoscale objects.

Nanotechnology contributes to almost every field of science, which includes Physics, Chemistry, Biology, Computer Science and Engineering. In few decades, nanotechnology and nanoscience have become fundamental importance to industrial applications and medical devices such as diagnostic biosensors, drug delivery systems and imaging probes. Nanomaterials are useful in building solar cells, hydrogen fuel cells and novel hydrogen storage systems which are capable of delivering clean energy to countries still rely on traditional, non-renewable contaminating fuels. An important application of nanoparticles is recognized to be the production of a new class of catalysts known as nanocatalysts. The role of nanoparticles as catalysts results in improving chemical reaction performances. The most significant advances in nanotechnology are in the field of biomedicine and especially in cancer therapeutics. The innovative biomedical applications are currently exploited in a variety of clinical trials and in the near future, may support major development in the therapy of cancer. There are many expected advances in nanoscience and nanotechnology with applications in agriculture, electronics, energy, medicine etc., which are

rapidly increasing.

1.2. THE ORIGIN OF NANOTECHNOLOGY

The word ‘nano’ is originated from a Greek word means ‘dwarf’ or something very small and depicts one thousand millionth of a meter (10^{-9} m). The American physicist and Nobel Prize laureate Richard Feynman introduced the concept of nanotechnology in 1959. In the annual meeting of the American Physical Society, Feynman presented a lecture entitled “There’s Plenty of Room at the Bottom”. In this lecture, Feynman described a vision of using machines to construct smaller machines and down to the molecular level. Feynman is considered as the father of Modern Nanotechnology. It was Norio Taniguchi, a Japanese scientist who coined and defined the term “nanotechnology” in 1974.

In 1986, K. Eric Drexler published the first book on nanotechnology “Engines of Creation: The Coming Era of Nanotechnology”, which led to the theory of “molecular engineering”. Drexler proposed the idea of the build-up of complex machines from individual atoms, which independently manipulate molecules and atoms and thereby produces self-assembly nanostructures. Later on, in 1991, Drexler, Peterson and Pergamit published another book entitled “Unbounding the Future: the Nanotechnology Revolution” in which they use the terms “nanobots” or “assemblers” for nano processes in the medicine applications.

In 1981, a new type of microscope, the Scanning Tunnelling Microscope (STM), was invented by the physicists Gerd Binnig and Heinrich Rohrer at IBM Zurich Research Laboratory. In 1986, Binnig and Rohrer received the Nobel Prize in Physics for the design of the STM. This invention led to the development of the atomic force microscope (AFM) and scanning probe microscopes (SPM).

In 1985, Robert Curl, Harold Kroto and Richard Smalley discovered that carbon can also exist in the form of very stable spheres, the fullerenes or buckyballs. The carbon balls with the chemical formula C₆₀ or C₇₀ are formed when graphite is evaporated in an inert atmosphere. In 1991, Iijima et al. observed hollow graphitic tubes or carbon nanotubes by Transmission Electron Microscopy (TEM) which form another member of fullerene family. Carbon nanotubes are used as composite fibers in polymers and to improve the mechanical, thermal and electrical properties of the bulk product.

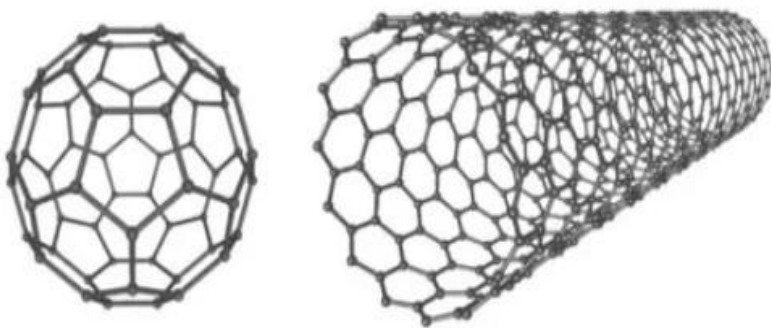


Illustration 1: Schematic diagram of a Carbon 60 buckyball(Fullerene) and carbon nanotube.

In 2004, a new class of carbon nanomaterials called carbon dots (C-dots) with size below 10 nm was discovered. C-dots have interesting properties due to their benign, abundant and inexpensive nature. Low toxicity and good biocompatibility makes C-dots suitable for applications in bioimaging, biosensor and drug delivery. By the discovery of “graphene” in 2004, carbon-based materials become the backbone of every field of science and engineering.

Recently, a number of studies prove that nanotechnology play an important role in biomedicine for the diagnosis and therapy of many human diseases. DNA nanotechnology has already become an interdisciplinary research area which made possible to use DNA and other biopolymers directly in array technologies for sensing and diagnostic applications. Nano-oncology is a very attractive application of nanoscience and allows for the improvement of tumour response rates in addition to a significant reduction of the systemic toxicity associated with current chemotherapy treatments.

Nanotechnology improves the environment and produces more efficient and cost-effective energy which generates less pollution during the manufacture of materials. Nano-informatics deals with the assembling, sharing, envisaging, modelling and evaluation of significant nano scale level data and information.

1.3. THE IMPORTANCE OF NANO SCALE

There are many specific reasons why nano scale has become so important;

- Quantum mechanical (wavelike) properties of electrons inside matter are influenced by variations on the nano scale. Quantum effects can begin to dominate the behaviour of matter at the nano scale – particularly at the lower end – affecting the optical, electrical and magnetic behaviour of materials.
- A key feature of biological entities is the systematic organization of matter on the nanoscale in nanoscience and nanotechnology has allowed us to place man-made nanoscale things inside living cells.
- Nanoscale components have very high surface-to-volume ratio, making them ideal for use in composite materials, reacting systems, drug delivery, and energy storage.
- Macroscopic systems consist of nanostructures with higher density than those made up of microstructures. They are better conductors of electricity which results in new electronic device concepts, smaller and faster circuits and greatly reduced power consumption by controlling nano structure interactions and complexity.

Nanostructured semiconductors are known to show various non-linear optical properties. Semiconductor Q-particles also show quantum confinement effects which has led to properties like luminescence in silicon powders and silicon germanium quantum dots as infrared optoelectronic devices.

Nanostructured metal-oxide finds application for rechargeable batteries for cars or consumer goods. Nanostructured metal-oxide thin films have a special impact in catalytic applications of gas sensors with enhanced sensitivity and selectivity.

1.4. DIFFERENT TYPES OF NANO PARTICLES

Nano particles can be classified into different types according to the size, morphology, physical and chemical properties. Some of them are carbon-based nano particles, ceramic nano particles, metal nano particles, semiconductor nano particles, polymeric nano particles and lipid-based nano particles.

1.4.1 CARBON-BASED NANO PARTICLES

Carbon-based nanoparticles contain two main materials: carbon nano tubes (CNTs) and fullerenes. CNTs are graphene sheets rolled into a tube. These materials are mainly used for the structural reinforcement as they are 100 times stronger than steel.

CNTs can be classified into single-walled carbon nanotubes (SWCNTs) and multi-walled carbon nanotubes (MWCNTs). CNTs are thermally conductive along the length and non-conductive across the tube.

1.4.2. CERAMIC NANOPARTICLES

Ceramic nanoparticles are inorganic solids made up of oxides, carbides, carbonates and phosphates. These nanoparticles have high heat resistance and chemical inertness. They have applications in photo catalysis, photo degradation of dyes, drug delivery and imaging.

By controlling the characteristics like size, surface area, porosity, surface to volume ratio, etc. they perform as good drug delivery agents. These nanoparticles can be used as drug delivery system for a number of diseases like bacterial infections, glaucoma, cancer etc.

1.4.3. METAL NANOPARTICLES

Metal nanoparticles are prepared from metal precursors. These nanoparticles can be synthesized by chemical, electrochemical or photochemical methods. They have the ability to adsorb small molecules and have high surface energy.

These nanoparticles have applications in research areas, detection and imaging of bio molecules and in environmental and bio-analytical applications.

1.4.4. SEMICONDUCTOR NANOPARTICLES

Semiconductor nanoparticles have intermediate properties between metals and non-metals. They are found in the periodic table in groups II-VI, III-V or IV-VI. Some examples of semiconductor nanoparticles are GaN, GaP, InP, InAs from group III-V, ZnO, ZnS, CdS, CdSe, CdTe from II-VI semiconductors and silicon and germanium from group IV.

They have a wide band gap, which on tuning shows different properties. They are used in photocatalysis, electronics devices, photo-optics and water splitting applications.

1.4.5. POLYMERIC NANOPARTICLES

Polymeric nanoparticles are organic based nanoparticles. Depending upon the method of preparation, they have structures shaped like nanocapsular or nanospheres. A nanosphere particle has a matrix-like structure whereas the nanocapsular particle has core-shell morphology.

They have applications in drug delivery and diagnostics. The drug deliveries with polymeric nanoparticles are highly biodegradable and bio-compatible.

1.4.6. LIPID-BASED NANOPARTICLES

Lipid nanoparticles are generally spherical in shape with a diameter ranging from 10 to 100nm. It consists of a solid core made of lipid and a matrix containing soluble lipophilic molecules.

The external core of these nanoparticles is stabilized by surfactants and emulsifiers. These nanoparticles have application in the biomedical field as a drug carrier and delivery and RNA release in cancer therapy.

1.5. APPROACHES IN NANO FABRICATION

Top-down and bottom-up methods are two types of approaches used in nano fabrication. The bottom-up approach is more advantageous than the top-down approach because the former has a better chance of producing nano structures with less defects, more homogeneous chemical composition and better short and long range ordering.

The top-down approach is the breaking down of bulk material to get nano-sized particles. Top-down methods begin with a pattern generated on a larger scale, which is reduced to nano-scale after a sequence of operations is performed over them. All the solid state routes fall into this category. Typical examples are etching through the mask, ball milling, cutting, grinding and application of severe plastic deformation, photo lithography, e-beam lithography etc.

Top-down approaches are based on grinding a material. The parts of mechanical devices used to shape objects are stiff and hard, so these methods are not suitable for soft samples. The major drawback of this method is that they require large installations and huge capital for building their setup and is quite expensive. Moreover the growth process is slow and is not suitable for large

scale production.

The bottom-up approach refers to the build-up of nano-structures from the bottom: atom-by-atom or molecule-by-molecule by physical and chemical methods which are in a nano range (1 nm to 100nm) using controlled manipulation of self-assembly of atoms and molecules. All the techniques that start with liquid and gas as the starting material fall into this category. Typical examples are quantum dot formation during epitaxial growth and formation of nanoparticles from colloidal dispersion, physical vapour deposition, chemical vapour deposition etc.

Bottom-up approach is based on the principle of molecular recognition (i.e., self assembly). The idea of self assembly is to gather precursors in random positions and orientations and supply energy to allow them to sample configuration space.

A bottom-up approach is capable of producing devices in parallel and is much cheaper than top-down methods but becomes difficult as the size and complexity of the desired assembly increases.

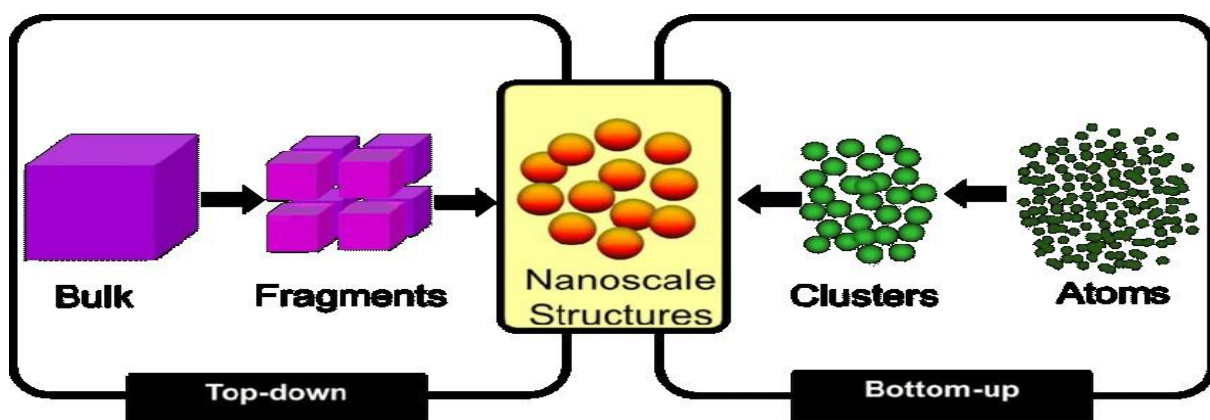


Illustration 2: Schematic diagram of Top-down and Bottom-up approaches

1.6. ADVANTAGES AND DISADVANTAGES OF NANOTECHNOLOGY

While nanotechnology is seen as the way of the future and as a technology that people think will bring a lot of benefit for all who will be using it, nothing is ever perfect and there will always be pros and cons to everything. The advantages and disadvantages of nanotechnology can be easily enumerated and here are some of them:

1.6.1. ADVANTAGES

- ❖ Nanotechnology can actually revolutionize a lot of electronic products, procedures and applications. The areas that benefit from the continued development of nanotechnology when it comes to electronic products include nano transistors, nano diodes, OLED, plasma displays, quantum computer sand many more.
- ❖ Nanotechnology can also benefit the energy sector. The development of more effective energy-producing, energy-absorbing and energy storage products in smaller and more efficient devices is possible with this technology. Such items like batteries, fuel cells and solar cells can be built smaller but can be made to be more effective with this technology.
- ❖ In the medical world, nanotechnology is also seen as a boon since these can help with creating what is called smart drugs. These help cure people faster and without the side effects that other traditional drugs have. The research of nanotechnology in medicine is now focusing on areas like tissue regeneration, bone repair, immunity and even cures for ailments like cancer, diabetes and other life threatening diseases.
- ❖ Nanotechnology pesticides for crops will directly attack the pathogens in agriculture fields without destroying or causing any harm to the crops. At the same time, it will help in increasing the efficiency of fertilizers.
- ❖ Nowadays manufacturing concerns require nano-products like nanotubes, nanoparticles, etc. which are durable, strong and lighter than the products which are not prepared with the help of nanotechnology. Therefore nanotechnology has changed the manufacturing scenario and made it much more advantageous to them.

1.6.2. DISADVANTAGES

- ❖ Possible loss of jobs in the traditional farming and manufacturing industry.
- ❖ Atomic weapons can now be made to be more powerful and more destructive. These can also become more accessible with nanotechnology.

- ❖ Since these particles are very small, problems can actually arise from the inhalation of these minute particles, much like the problems a person gets from inhaling minute asbestos particles.
- ❖ The development of nanotechnology can also bring about the crash of certain markets due to the lowering of the price of oil and diamonds due to the possibility of developing alternative sources of energy that are more efficient and won't require the use of fossil fuels.
- ❖ There are possibilities that nanotechnology will be a hazard for the environment in a sense that these nanoparticles have the tendency to accumulate in the atmosphere and even in the food chain.
- ❖ Nanotechnology is very expensive and developing it can cost a lot of money. It is also pretty difficult to manufacture, which is probably why products made with nanotechnology are very expensive.

1.7. WATER POLLUTION

Pollution has become a major environmental issue due to negligence and carelessness of man. Pollution is the introduction of harmful materials into the environment. All types of pollution are detrimental to human health and wildlife and contribute to climate change, which puts the entire planet in danger. The negative effects of pollution are serious and potentially fatal.

Water pollution is the release of substances into bodies of water which makes water unsafe for human use and disrupts aquatic ecosystems. Water bodies can be polluted by a wide variety of substances, including pathogenic microorganisms, organic waste, fertilizers and plant nutrients, toxic chemicals, sediments, heat, petroleum (oil) and radioactive substances.

Water pollution may cause diseases or they even act as poisons. Micro-organisms in poorly treated sewage may enter drinking water supplies and cause digestive problems such as cholera and diarrhoea. Hazardous chemicals, pesticides and herbicides from industries can cause acute toxicity and immediate death, or chronic toxicity that can lead to neurological problems or cancers. Hazardous chemicals in water bodies can also affect the animals and plants which live there. Sometimes these organisms will survive with the chemicals in their systems, only to be eaten by humans who may then become mildly ill or develop stronger toxic symptoms.

1.7.1. NEED OF WATER PURIFICATION

Our earth is covered with water two-third of its surface which is almost 330 million cubic mile of water. Only 3% of water on our planet is fresh and only 1% is surface water and rest of it is frozen or underground. One in six people on the planet do not have access to clean drinking water. According to WHO report in 2019 cause of second most death is Diarrhoea which is mainly caused by water pollution. Cholera also falls under this category and every year 95,000 death occur according to WHO.

Different types of toxic containments are present in water which have adverse effect on consumption and lead to various water-borne diseases. Pollutants can be present in the form of organic and inorganic chemicals or physical, biological, radiological or heavy metal substances. Industry waste is the major cause of water pollution because they discard about 20% of the annual dye consumption into the water bodies. There are different water purification methods like chemical transformation, distillation, biological treatments, reverse osmosis, coagulation and flocculation, micro filtration, ultraviolet treatment, ultra filtration etc. Each of these methods has specific limitations and is not sufficient to remove the containments from water and to supply 100% pure drinking water. These methods are also expensive and cannot afford by developing countries. This points to the necessity of water purification technology which is efficient at the same time less expensive. The use of nanomaterials as photo-catalyst has been reported to produce efficient and environmental friendly results.

1.8. ROLE OF NANOTECHNOLOGY IN PHOTOCATALYSIS

Accelerated photo-reaction in the presence of a catalyst is called photo-catalysis. In the reaction, light is absorbed by the substrate. Reaction rate of catalyst depends on the ability of catalyst in creating electron-hole pairs, which react with the substrate and produce the free radical. Secondary reactions take place and these radicals reacts with reactant to produce different useful products.

First Photo-catalysis was reported in 1911, by a German chemist Dr. Alexander Eibner who used the technique to bleach dark blue pigment by using Zinc Oxide in the presence of sun light. In 1938, there was a major breakthrough in the photo-catalysis.

One of the most promising photocatalyst TiO_2 was discovered. It was used as a photocatalyst for bleaching dyes. Another major breakthrough took place in 1972, when Akira Fujishima and Kenichi Honda reported the electrochemical photolysis of water using platinum and titanium dioxide electrodes.

Photo-catalysis is also very effective weapon against the water pollution. To increase the efficiency of photo catalytic reaction, instead of using bulk material as a catalyst we can use nanotechnology to improve the efficiency of photo catalytic reaction. The increased surface to volume ratio of nano materials increase catalyst efficiency as compared to bulk materials.

1.8.1. MECHANISM FOR PHOTOCATALYTIC REACTION

In photo-catalysis, reaction rate depends on crystal structure of catalyst and the energy of incoming photons of visible or UV light. Materials used as catalyst acts as a sensitizer for the irradiation of light-stimulated redox processes depending on their electronic structure which in turn, depends on filled valence and vacant conduction band.

If the band gap of the catalyst is equivalent or less than the energy of incident light, the electrons in valence band will absorb the photon and they will reach to the conduction band. Leaving holes in the valence band. Donor molecules are oxidized by these holes, also the hydroxyl is produced when H_2O react with these holes. Electron present in conduction band is absorbed by water to make superoxide ion, which is a reducing agent. This free electron is causes redox reactions to occur. These pairs of free electrons and holes can perform oxidation reduction reaction with any material which comes in contact with the catalyst and convert it into the desired products.

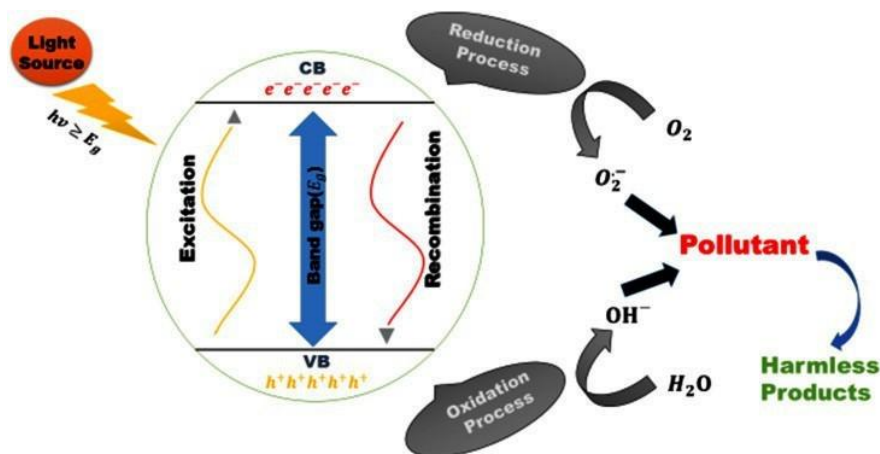


Illustration 3: General reaction mechanism for photocatalytic process

1.8.2 MATERIAL SELECTION FOR NANOMATERIALS AS PHOTOCATALYST

In photocatalytic reaction, oxidation and reduction reaction occur simultaneously. Therefore, the catalyst for photocatalytic reaction should support both oxidation and reduction reaction. Materials are divided into three categories on the basis of electronic properties -conductor, insulator and semiconductor.

In conductors, valence and conduction bands overlap. For photocatalytic reaction, the necessary condition is oxidation and reduction simultaneously, but in conductors only free electron are available and hence can perform only oxidation reaction at a time. Best conductors like alkali, alkaline earth metals and transition metals have no suitable band gap and hence are not suitable for photocatalytic reaction.

Insulators have high band gap, therefore high energy is required to perform oxidation and reduction reaction. Insulator is deficient of free electron so no oxidation takes place and is why insulators are not suitable for photolytic reaction.

Semiconductors have moderate band gap and have the capabilities of oxidation and reduction reactions to occur simultaneously. When light falls, free electron hole pairs are generated. Necessary condition for a semiconductor to be a photocatalyst is the low recombination rate.

Semiconductors whose absorption wavelength (350–700 nm) in visible region or band gap in (1.5–3.5 eV) are suitable for photo catalytic activity. Generally semiconductors have a wide range of band gap but for a photo catalyst of UV visible region, we require only 1.5–3.5 eV band gap. Metal oxides generally fall in this category and they have many other properties which make them suitable as photo catalysts.

They include stability of the structure, morphology, reuse-ability, high surface area etc. Oxides of chromium, zinc, vanadium, cerium and titanium are used as photo-catalysts.

1.8.3. TITANIUM DIOXIDE (TiO₂)

Improvements in the performance of photo catalytic materials have been largely correlated with advances in nanotechnology. Many of the materials have been studied for photocatalysis in which titanium dioxide (TiO₂; titania) has been extensively researched because it possesses many merits such as high photocatalytic activity, excellent physical and chemical stability, low cost, non-corrosive, nontoxicity and high availability. Titanium was first discovered in 1791 by William Gregor. It is white and a poorly soluble material. It consists of three crystalline phases; the anatase, rutile and brookite. The anatase phase is metastable and has a higher photocatalytic activity, while the rutile phase is more chemically stable but less active.

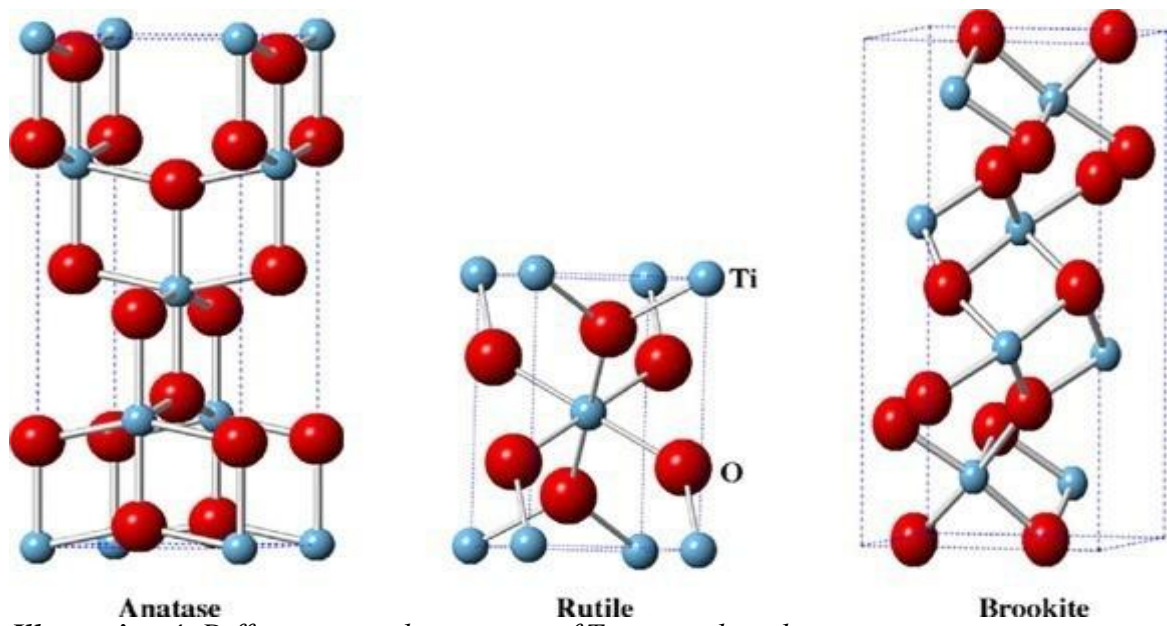


Illustration 4: Different crystal structures of Titanium dioxide

When titania is irradiated with light of sufficient energy, electrons from the valence band are promoted to the conduction band, leaving an electron deficiency or hole, h⁺, in the valence band and an excess of negative charge in the conduction band. The free electrons in the conduction band are good reducing agents while the resultant holes in the valence band are strong oxidizing agents and can participate in redox reactions.

Titania suffers from a number of drawbacks that limit its practical applications in photocatalysis. The photo generated electrons and holes coexist in titania and the probability of their recombination is high. The relatively large bandgap energy (~ 3.2 eV) requires ultraviolet light for photo activation, resulting in a very low efficiency in utilizing solar light. UV light accounts for only about 5% of the solar spectrum compared to visible light (45%). There is also the challenge to recover nano-sized titania particles from treated water. Several strategies have been used to overcome these drawbacks. These strategies aim at extending the wavelength of photoactivation of TiO_2 into the visible region of the spectrum thereby increasing the utilization of solar energy. preventing the electron/hole pair recombination and thus allowing more charge carriers to successfully diffuse to the surface.

1.8.4. MODIFICATION OF TiO_2 PHOTO CATALYSTS

The modifications have been done in many different ways which include metal and non-metal doping, dye sensitization, surface modification, fabrication of composites with other materials and immobilization and stabilization on support structures.

1.8.4.a METAL DOPING

Metal doping is used to modify TiO_2 photo catalysts to operate efficiently under visible light. Doping TiO_2 with metals results in an overlap of the Ti 3d orbitals with the d levels of the metals causing a shift in the absorption spectrum to longer wavelengths. This in turn favours the use of visible light to photo activate the material.

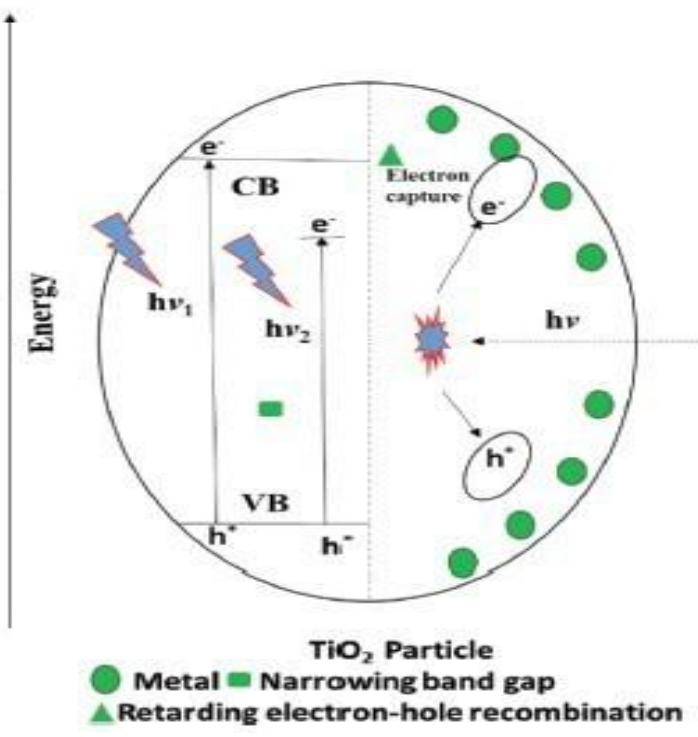


Illustration 5: Metal doped TiO₂

Doping of TiO₂ nanoparticles with Li, Na, Mg, Fe and Co by high energy ball milling with The metal nitrates was found to widen the TiO₂ visible light response range. Noble metal nanoparticles such as Ag, Pt, Pd, Rh and Au have also been used to modify TiO₂ for photocatalysis and have been reported.

During the past few decades, transition metal dichalcogenides have been proved to be useful in many fields such as water splitting, optoelectronics, supercapacitors, solar cells, photocatalysis, hydrogen generation, sensors and lithium-ion batteries due to their admirable chemical, electrical, optical and mechanical properties. Among these, MoS₂ has been established as a significant material in sensitizing a wide band gap TiO₂ due to its potential properties like having a two-dimensional layered structure, good charge carrier transport capacity, and high surface area. The surface sensitization of TiO₂ by MoS₂ can systematically control the electron–hole pair recombination by acting as trapping centers of the electron.

1.8.5 MOLYBDENUM DISULFIDE (MoS₂)

Molybdenum is a Block D, Period 5 element, and sulfur is a Block P, Period 3 element. MoS₂ has a S–Mo–S sandwich layered structure seized together via weak Van der Waals interaction.

It is analogous to graphene, in which Mo is surrounded by the S atoms through covalent bonding. Molybdenum does not occur naturally as a free metal on Earth. Molybdenum disulfide has very good chemical and thermal stability. They can form a highly efficient dry lubricating film. Molybdenum disulfide nanoparticles possess a low friction coefficient, good catalytic activity and excellent physical properties. They also have a large active surface area, high reactivity, and increased adsorption capacity compared to the bulk material. Molybdenum disulfide nanoparticles appear in a black solid form.

1.8.5.a APPLICATIONS

The key applications of molybdenum disulfide nanoparticles are as follows:

- ◆ In lubricant applications
- ◆ In difficult to maintain equipment, such as space vehicles, satellites and military fields
- ◆ In composite applications
- ◆ As a conductive filler
- ◆ As a catalyst for coal liquefaction
- ◆ Can be used to prepare special materials, catalytic materials and gas storage.

REFERENCES

1. Bayda, Samer, Muhammad Adeel, Tiziano Tuccinardi, Marco Cordani, and Flavio Rizzolio. "The history of nanoscience and nanotechnology: From chemical–physical applications to nanomedicine." *Molecules* 25, no. 1 (2019): 112.
2. Mansoori, G. Ali. "An introduction to nanoscience and nanotechnology." In *Nanoscience and Plant–Soil Systems*, pp. 3-20. Springer, Cham, 2017.
3. Kite, Sagar V., Abhijit Nanaso Kadam, Dattatraya J. Sathe, Satish Patil, Sawanta S. Mali, Chang Kook Hong, Sang– Wha Lee, and Kalyanrao M. Garadkar. "Nanostructured TiO₂ sensitized with MoS₂ nanoflowers for enhanced photodegradation efficiency toward methyl orange." *ACS omega* 6, no. 26 (2021): 17071-17085.
4. Navia-Mendoza, Jennifer María, Otoniel Anacleto Estrela Filho, Luis Angel Zambrano-Intriago, Naga Raju Maddela, Marta Maria Menezes Bezerra Duarte, Luis Santiago Quiroz-Fernández, Ricardo José Baquerizo-Crespo, and Joan Manuel Rodríguez-Díaz. "Advances in the application of nanocatalysts in photocatalytic processes for the treatment of food dyes: A review." *Sustainability* 13, no. 21 (2021): 11676.
5. Tahir, Muhammad B., Muhammad Sohaib, Muhammad Sagir, and Muhammad Rafique. "Role of nanotechnology in photocatalysis." *Reference Module in Materials Science and Materials Engineering* (2020).
6. Ram, Chhotu, Ravi Kant Pareek, and Varinder Singh. "Photocatalytic degradation of textile dye by using titanium dioxide nanocatalyst." *Int. J. Theor. Appl. Sci* 4, no. 2 (2012): 82-88.
7. Erdemoğlu, Sema, Songül Karaaslan Aksu, Funda Sayılıkan, Belgin Izgi, Meltem Asiltürk, Hikmet Sayılıkan, Fritz Frimmel, and Şeref Güçer. "Photocatalytic degradation of Congo Red by hydrothermally synthesized nanocrystalline TiO₂ and identification of degradation products by LC–MS." *Journal of hazardous materials* 155, no. 3 (2008): 469-476.
8. Lachheb, Hinda, Eric Puzenat, Ammar Houas, Mohamed Ksibi, Elimame Elaloui, Chantal Guillard, and Jean-Marie Herrmann. "Photocatalytic degradation of various types of dyes (Alizarin

S, Crocein Orange G, Methyl Red, Congo Red, Methylene Blue) in water by UV-irradiated titania." *Applied Catalysis B: Environmental* 39, no. 1 (2002): 75-90.

9. Moma, John, and Jeffrey Baloyi. "Modified titanium dioxide for photocatalytic applications." *Photocatalysts-Applications and Attributes* 18 (2019): 10-5772.

10. Ray, Unmesha. "What are the Different Types of Nanoparticles?". *AZoNano*. 25 May 2022. <https://www.azonano.com/article.aspx?ArticleID=4938>

11. <https://encryptedtbn0.gstatic.com/images?q=tbn:ANd9GcSsdIcLd0nvBfJJxPRoo2PYxaZLBJSRJPVFQ&usqp=CAU>.

12. https://www.pngkit.com/png/full/397-3973292_top-down-and-bottom-up-synthesis-of-nanofabrication.png

13. <https://www.molecularcloud.org/p/what-are-the-advantages-and-disadvantages-of-nanotechnology>

14. <https://www.basic-concept.com/c/what-is-nanotechnology-with-advantages-and-disadvantages>

15. <https://www.aplustopper.com/advantages-and-disadvantages-of-nanotechnology/>

16. <https://www.nrdc.org/stories/water-pollution-everything-you-need-know>

17. <https://www.nationalgeographic.org/encyclopedia/pollution/#:~:text=Encyclopedic%20Entry%20Vocabulary,Pollution%20is%20the%20introduction%20of%20harmful%20materials%20into%20the%20environment,air%2C%20water%2C%20and%20land.>

18. <https://www.omicsonline.org/conferences-list/pollution-and-environmental-issues>

19. <https://sciencing.com/negative-effects-pollution-5268664.html>

20. <https://www.britannica.com/science/waterpollution#:~:text=Water%20pollution%20is%20the>

%20release,%2C%20and%20disease%2Dcausing%20microorganisms.

21. <https://www.hsph.harvard.edu/ehep/82-2/#:~:text=Water%20pollution%20is%20the%20contamination,make%20their%20way%20to%20water>.

22. <https://www.beltecno-global.com/blog/10-reasons-why-purification-of-water-is-important-for-human-health>

23. <https://www.sciencedirect.com/topics/agricultural-and-biological-sciences/water-purification#:~:text=There%20are%20several%20methods%20used,the%20use%20of%20ultraviolet%20light>.

24. <https://ars.els-cdn.com/content/image/1-s2.0-S1385894719327974-gr1.jpg>

25. <https://wwwazonano.com/article.aspx?ArticleID=3351#:~:text=The%20key%20applictaions%20of%20molybdenum,In%20composite%20applicationshttps://wwwazonano.com/article.aspx?ArticleID=1872>

CHAPTER 2

EXPERIMENTAL METHODS

2.1. SYNTHESIS TECHNIQUES

2.1.1. HYDROTHERMAL METHOD

Hydrothermal synthesis is one of the solution reaction based approach that can be used for synthesizing the nano materials. In hydrothermal method it is possible to set the parameters according to our requirement and it will result in different nano structures with wide variety of properties. To control the morphology of the materials to be prepared we can use high/low temperature or pressure conditions. The time of the synthesis can be also varied. Many types of nano materials have been successfully synthesized by the use of this approach.

Opportunity to control the parameters is itself the significant advantage of the hydrothermal synthesis method over others. Hydrothermal synthesis can generate nano materials which are not stable at elevated temperatures. Nano materials with high vapour pressures can be produced by the hydrothermal method with minimum loss of materials. The compositions of nano materials to be synthesized can be well controlled in hydrothermal synthesis through liquid phase or multiphase chemical reactions.

2.1.1.a. HYDROTHERMAL SYNTHESIS OF TiO₂ NANO POWDER

7 ml of Titanium Isopropoxide(0.65 M) in 25 ml of isoproponol was prepared. After vigorous stirring for 5 minute at room temperature a clear solution was obtained to which 50 ml of distilled water was added under the magnetic stirring, turning the clear solution into a milky suspension which is done at 50 ⁰C for one hour and autoclaved at 50 ⁰C for one hour. Finally on, cooling, the sample is obtained in liquid form, which is washed with distilled water and centrifuged a number of times. The settled product is separated and dried at 80⁰C for 1.5 hours. The obtained sample is then crushed into fine powder using mortor and pestle.

2.1.1.b. SYNTHESIS OF TiO₂ NANO TUBES

0.6 g of TiO₂ nano powder was dispersed in 60 ml of 10M NaOH(24 g of NaOH) solution and is vigorously stirred at room temperature for 2 hours. The sample is autoclaved at 130 °C for 26 hours. It is re dispersed in 400 ml of 0.1 M HCl for 3 hours, centrifuged and washed with distilled water to stabilize PH to 7 and is dried at 400 °C for 2 hours.

Preparation of 0.1 M HCl

To prepare HCl solution, 3.6ml of 35% HCl is taken in a beaker. The beaker is filled with distilled water up to 400 ml and the mixture from Teflon vessel was added into the above beaker. This is stirred for 3 hours.

2.1.1.c. HYDROTHERMAL SYNTHESIS OF MoS₂ NANOSHEET

MoS₂ nano sheets were prepared by a hydrothermal route. In the typical synthesis process of MoS₂, 1.21 g sodium molybdate (0.005 mol) and 1.56 g thiourea (0.02 mol) were mixed into 30 mL double distilled water. The resulting mixture was stirred constantly for 30 min and poured into 50 ml Teflon-lined stainless autoclave. Then, the autoclave was placed in a hot air oven at 180 °C for different time (8 hours, 10 hours, 12 hours, 24 hours). Subsequently, the autoclave was allowed to cool and the obtained nano powder was centrifuged multiple times with double distilled water and ethanol. Finally, the resultant black powder was kept to dry under a vacuum oven at 80 °C.

2.1.1.d. SURFACE SENSITIZATION OF NANOSTRUCTURED TiO₂ BY MoS₂ NANOSHEET

The surface sensitization of nano structured TiO₂ was carried out by using hydrothermally synthesized MoS₂ via the mechano-chemical method. The typical synthesis process is as follows: an appropriate amount of TiO₂ nano powder is mixed with a certain amount of MoS₂ (2, 5 wt %) in a minute quantity of ethanol. The above mixture was ground constantly in a mortar and pestle for 2 h. At the completion of grinding, the obtained powder was rinsed with double distilled water and allowed to dry at 80 °C for 12 h. The sensitized material could be labelled as x wt % MoS₂–TiO₂.

Here, two different values were chosen for x; x=2 and 5 wt%.

For 2% wt MoS₂ in 0.25 g TiO₂ nanotube; the amount required can be calculated as:

$$x(2\%) = (100M_1)/(M_1+0.25)$$

$$50 M_1 = M_1+0.25$$

$$49 M_1 = 0.25$$

$$M_1 = \text{mass of MoS}_2 = 0.00510 \text{ g}$$

So, 0.00510 g of MoS₂ nano sheet is mixed with 0.25 g of TiO₂ nanotubes (NT). A small amount of ethanol is added and grounded for 30 minute in mortar and pestle. The mixture is then rinsed with distilled water and is kept in oven to dry at 80 degree Celsius for 5 hours. The obtained sample is kept in bottle as nanocomposite and termed as MT*2%.

For 5% wt MoS₂ in 0.25 g TiO₂ nanotube:

$$x(5\%) = (100M_1)/(M_1+0.25)$$

$$20 M_1 = M_1+0.25$$

$$19 M_1 = 0.25$$

$$M_1 = \text{mass of MoS}_2 = 0.01316 \text{ g}$$

So, 0.01316 g of MoS₂ nano sheet is mixed with 0.25 g of TiO₂ NT. A small amount of ethanol is added and grounded for 2 hrs. in mortor and pestle. The mixture is then rinsed with distilled water and is kept in oven to dry at 80 degree Celsius for 5 hours. The obtained sample is kept in bottle as nanocomposite and termed as MT*5%

The samples are named as follows:

2.1.1.e. SYNTHESIS OF TiO₂ @ MoS₂ HETEROSTRUCTURE

TiO₂ @ MoS₂ heterostructure with different phases were synthesized by using hydrothermal and mixing method. 1.6 g of ammonium molybdate and 0.5 g of thiourea were dissolved in 80 ml of distilled water in a beaker. 0.37 g of TiO₂ nanotube was added to it and stirred until it forms a suspension. Solution was transferred in to the autoclave of Teflon lined stainless steel and was

heated at 200°C for 24 hours in the oven. The obtained powder was washed using distilled water, centrifuged a number of times and dried at 80°C for 4 hours to obtain a grey coloured TiO₂@MoS₂ heterostructure.

SAMPLE	SYMBOL
2 wt% MoS ₂ -TiO ₂	MT*2%
5 wt% MoS ₂ -TiO ₂	MT*5%
MoS ₂ @TiO ₂	MT

Table1: Name of the sample and corresponding symbols used

2.1.2. PREPARATION OF DYE SOLUTION FOR PHOTO CATALYSIS

2.1.2.a RHODAMINE B

For photo catalytic study, 300 ml 0.00001 M Rhodamine B dye solution is prepared in distilled water. For this 300ml of distilled water and 0.00144 g of Rh B were added and stirred for 10 min in darkness.

From this 10 ml of the solution is taken and 2.5 mg of TiO₂ NT is added. And to another 10 ml solution 2.5mg of MoS₂@TiO₂ is added which is kept in the presence of sun light and absorption spectra is taken at different interval of time. The same procedure is repeated at dark also.

Similarly, the nanocomposite MT, MT*2%, MT*5% was added into 10ml of the dye solution. It was kept under dark and also sunlight and the UV-Vis spectra was taken at different time intervals.

2.1.2.b. METHYLENE BLUE

For photo catalytic study, 300 ml Methylene blue dye solution is prepared in distilled water. For this to 300ml of distilled water and 2.5mg of methylene blue was added and stirred for 10 min in darkness.

From this 10 ml of the solution is taken and 2 mg of TiO₂ nanotube is added. And to

another 10 ml solution 2mg of MoS₂@TiO₂ (MT) is added. And kept in presence of sun light and absorption spectra is took at different interval of time. The same procedure is repeated at dark also.

Similarly, the 2 mg nanocomposite prepared MT, MT*2%, MT*5% was added into 10 ml of the dye solution. It was kept in dark and also sunlight. The UV spectra was taken at different time intervals. And the data was studied.

2.2. CHARACTERIZATION TECHNIQUES

For exploring the features of the nano particles we can use two major domains. In one of the cases, we try to obtain the type of crystal group, determine lattice parameters and measure the average nano crystallite size. For such measurements, we generally perform X-ray diffraction experiments (XRD). The second domain is the microscopy/imaging in which we see the particles, lattice planes in the crystal and thus enabling direct measurement of the particle size, inter-planar distance and particle size distribution. We can use electron microscopy, atomic force microscopy; scanning tunnelling microscopy, field ion microscopy etc. for such informations.

The characterisation techniques employed in this study are discussed in detail in the following sections.

2.2.1. X-RAY DIFFRACTION

Most of the nano particles exhibit crystalline structure and therefore characterization techniques for these particles should be able to identify the crystallographic structure and lattice parameters. From X-ray diffraction pattern we can obtain these details.

X-ray powder diffraction is primarily used for the identification of the crystalline material and thus can provide information regarding the unit cell dimension. For preparing the sample for XRD, it must be finely grounded and spread to the substrate. Therefore, the result we obtain will be averaged over several crystallites.

From the XRD pattern we compare the theta values of X-ray diffraction peaks to the standard values provided by the already known elements and obtain the best match.

2.2.1.a. BASIC PRINCIPLE

When the propagating beam wavelength is of the order of inter-planar distances for a particular crystal, the rays get reflected from different planes and these monochromatic reflected rays will constructively interfere resulting in the diffraction pattern.

Typically X-rays used for diffraction are electromagnetic waves with wavelength in the range 0.05 to 0.25 nm. X-ray beam should be monochromatic. So, it is filtered by graphite, and the collimated, focused and directed towards the sample. The interaction of the incident rays with the sample produces constructive interference and it will depend upon the angle of incidence.

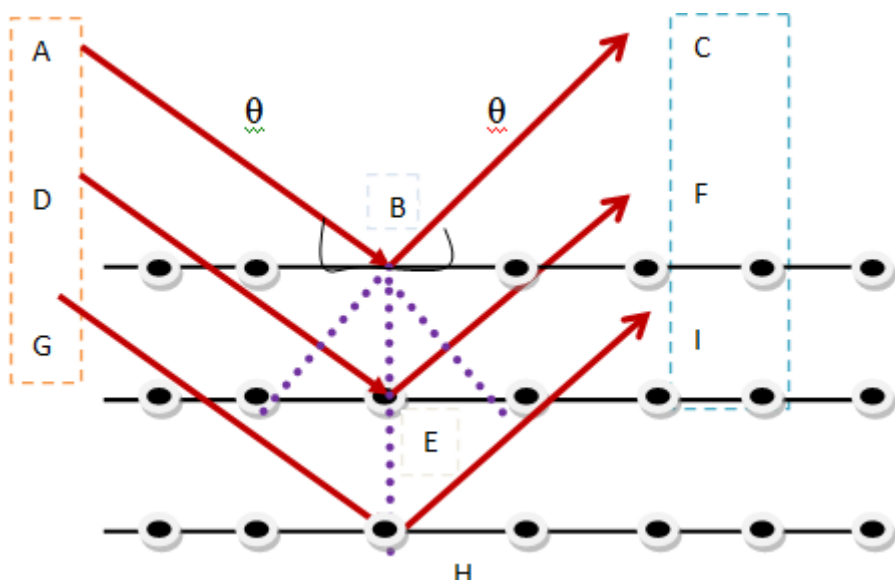


Illustration 6:X ray diffraction from parallel planes in a crystal.

Consider the illustration 6, in which different parallel planes with same (h,k,l) values are given. The distance between the adjacent planes is the inter-planar distance is taken as d .

AB, DE, GH are the incident radiation incident on the plane at an angle theta that get reflected along BC, EF, HI. The ray DEF travels an extra distance of $2d \sin\theta$ which is the path difference. For constructive interference of the reflected rays to occur path difference must be integral multiple of the wavelength of the X-ray ($n\lambda$)

The relation between the wavelengths of the electromagnetic radiation to the diffraction angle and the lattice spacing in a crystalline sample given as

$$n\lambda = 2d \sin\theta \dots \dots \dots \text{(eq. 1)}$$

This relation is what we call Bragg's law.

The inter-planar distance d in the Bragg's equation is decided by the lattice parameters a, b and c

$$1/d^2 = (h/a)^2 + (k/b)^2 + (l/c)^2 \dots \dots \dots \text{ (eq 2)}$$

If we find the value of d from the detected Bragg's angle, we can figure out the value of the lattice parameters which in turn provide vital information regarding the crystal.

2.2.1.b. LATTICE PARAMETERS

The lattice parameters are the quantities specifying a unit cell (smallest repeating unit of the crystal). Lattice parameters are represented by a , b , c as lengths of the unit cell in three dimensions, and " α , β , γ ," their mutual angles. The equations connecting lattice parameters (a , b , c) and the interplanar distance (d) different crystal structures are given below.

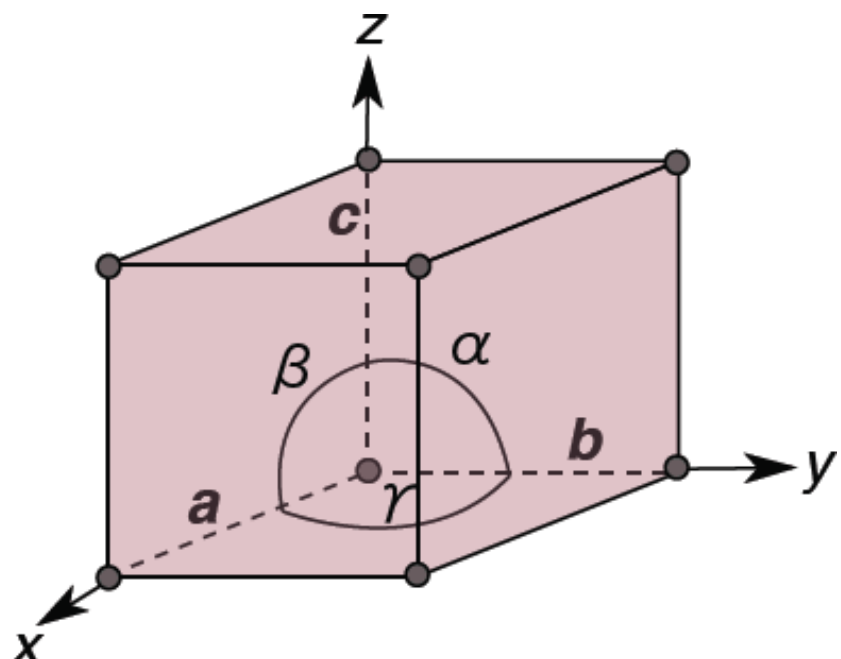


Illustration 7: Crystal axis, lattice paramters a,b,c and angle between them

Cubic:

$$\frac{1}{d^2} = \frac{h^2 + k^2 + l^2}{a^2}$$

Tetragonal:

$$\frac{1}{d^2} = \frac{h^2 + k^2}{a^2} + \frac{l^2}{c^2}$$

Hexagonal:

$$\frac{1}{d^2} = \frac{4}{3} \left(\frac{h^2 + hk + k^2}{a^2} \right) + \frac{l^2}{c^2}$$

Rhombohedral:

$$\frac{1}{d^2} = \frac{(h^2 + k^2 + l^2)\sin^2\alpha + 2(hk + kl + hl)\cos^2\alpha - \cos\alpha}{a^2(1 - 3\cos^2\alpha + 2\cos^3\alpha)}$$

Orthorhombic:

$$\frac{1}{d^2} = \frac{h^2}{a^2} + \frac{k^2}{b^2} + \frac{l^2}{c^2}$$

Monoclinic:

$$\frac{1}{d^2} = \frac{1}{\sin^2\beta} \left(\frac{h^2}{a^2} + \frac{k^2 \sin^2\beta}{b^2} + \frac{l^2}{c^2} - \frac{2hl \cos\beta}{ac} \right)$$

Triclinic:

$$\frac{1}{d^2} = \frac{1}{V^2} (S_{11}h^2 + S_{22}k^2 + S_{33}l^2 + 2S_{12}hk + 2S_{23}kl + 2S_{13}hl)$$

In the equation for triclinic crystals,

V = volume of unit cell (see below),

$$S_{11} = b^2 c^2 \sin^2\alpha,$$

$$S_{22} = a^2 c^2 \sin^2\beta,$$

$$S_{33} = a^2 b^2 \sin^2\gamma,$$

$$S_{12} = abc^2(\cos\alpha\cos\beta - \cos\gamma),$$

$$S_{23} = a^2 bc(\cos\beta\cos\gamma - \cos\alpha),$$

$$S_{13} = ab^2 c(\cos\gamma\cos\alpha - \cos\beta).$$

Where S represents constants relating lattice parameters.

2.2.1.c. XRD PATTERN

X ray pattern is a simple graph between intensity of diffracted X-rays and the angle of diffraction. To record this pattern, sample is needed to be scanned through a range of angles (2θ). Since the sample is in the form of powder, it presents all the diffraction direction of the beam. A single peak in the diffraction pattern will indicate a series of planes facing the X-ray beam at the correct angle to satisfy the Bragg's condition. So the peak can tag inter-planar distance (d) and will help in the identification of the material element involved having a set of unique d- spacing. This can be typically obtained by comparing these values with the standard reference pattern.

All planes in the crystal may not produce reflected signal or satisfy Bragg's equations. For example, in body centred mono atomic lattice, only those plane with $h+k+l = n$ will produce Bragg reflection only if n is an even integer. For face centred cubic lattice, constructive interference takes place when h, k and l are either all even or all odd which arises because of the effect of structure factor. From simple cubic structure, reflections from all the planes are possible.

The pattern will consist of sharp peaks for crystallite nano particle. And for the nano sheets like structures it is seen that the peak extends and become broader. Given below is an example of XRD pattern.

Intensity

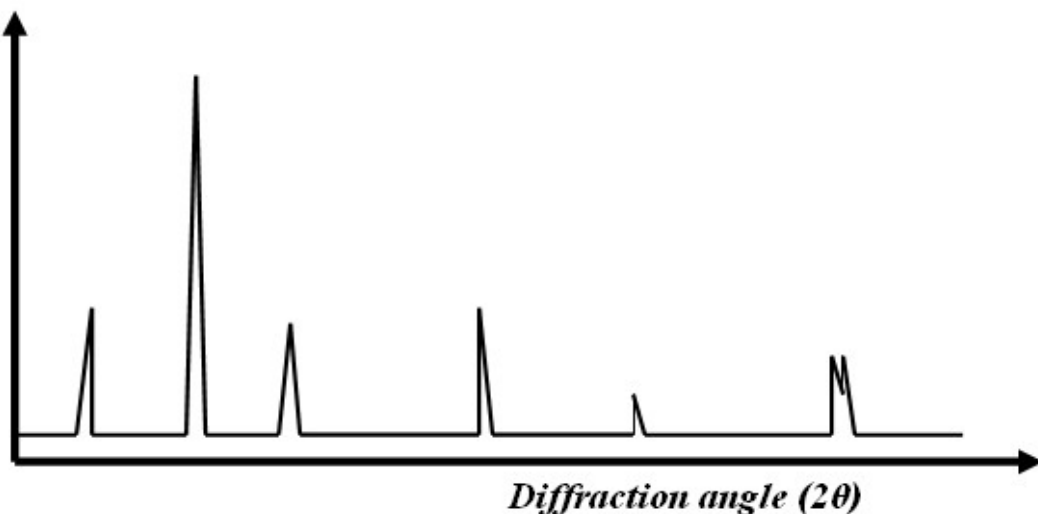


Illustration 8: XRD pattern with 2theta on x axis and intensity along y axis

2.2.1.d. DETERMINATION OF THE PARTICLE SIZE FROM XRD PATTERN

XRD gives account of the nano crystalline size from the width of the prominent diffraction pattern. It provides an easy and fast method for determining the size of nanocrystals using Debye-Scherrer's equation.

The coherence length of the particle/the particle size (L) is given by

$$L = \frac{0.94\lambda}{B \cos \theta} \dots \dots \dots \text{(eq 3)}$$

Where λ is the wavelength of the X-ray, B is the full width half maximum, ie the width of the peak(radian) at the half of the maximum intensity, θ is the angle of diffraction for that particular peak.

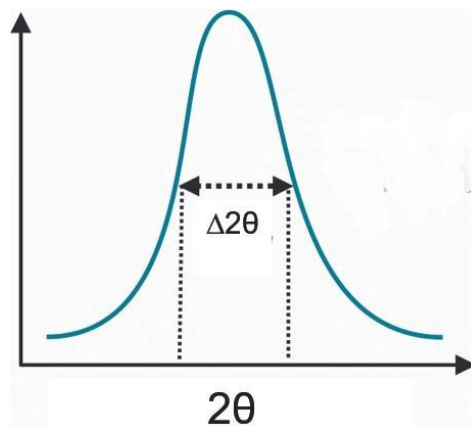


Illustration 9: XRD peak indicating the full width half maximum.

For spherical nanocrystals the coherence length (L) and the diameter (d) of the core of the nanocrystals/crystallite are related through the equations

$$d = (4L/3) \dots \dots \dots \text{eq 4}.$$

And no contribution to the XRD pattern from an amorphous segment in the sample.

2.2.2. TRANSMISSION ELECTRON MICROSCOPY

Electron microscopy is a powerful tool that can be used to measure the size and shape of the nanostructures. The image of the material can be obtained just like optical microscopy. The

resolution provided by electron microscope is in the order of nanometre and hence is very high. Electron microscope uses few thousand electron volt energized electron. The energy of such electron is very high and about 1000 times greater than that of the visible photon energy. So, a resolution of 0.01nm can be obtained.

TEM or Transmission electron microscopy is a tool that can be utilized to analyse the structure of very thin specimen through which electron can transmit through. TEM is much identical to the optical electron microscopy in the transmission mode with only difference that here instead of light, electron is transmitted through the specimen. Hence, the specimen must be thin enough so the electron can penetrate through. This transmitted beam then can be recorded and processed to get an image of the specimen.

The components of the transmission electron microscope are similar to that of the optical microscope which are as follows:

1. Source of energized electron – electron gun
2. A monochromatic source.
3. To focus electron beam to particular spot in the specimen – electromagnetic condenser lens. The lens will have current carrying coil surrounded by iron.
4. To eliminate the high angle electron and to restrict the size of the beam – condenser aperture.
5. To hold the sample – A sample holder.
6. To focus the transmitted beam another lens can be used.
7. To block the high angle diffraction and thus to enhance the diffraction image – optical objective and selection area metal aperture.
8. To enlarge the image and allowing optical image recording projector lens is used.

The sample will be kept in extreme vacuum condition. It should be thin enough so that high energetic electron will penetrate. The electron get scattered at the points on the specimen and degrees of scattering which can be elastic/ inelastic depend on the constituent atom of the specimen . Heavier the atoms, more will be the scattering. If scattering is more, then the transmitted intensity will be less. For lighter atom, scattering will be less, transmitted intensity will be high. So the intensity of the electron reaching the detector will be determined by the no. of the transmitted

beams, which in turn depends on the nature of the specimen atoms. Heavy atoms produce dark spot and lighter atom produce brighter spot. The transmitted beam is allowed to fall on the phosphor screen or is digitally processed with the help of a computer. From the TEM image we can obtain the information regarding the shape and size of the nano particle.

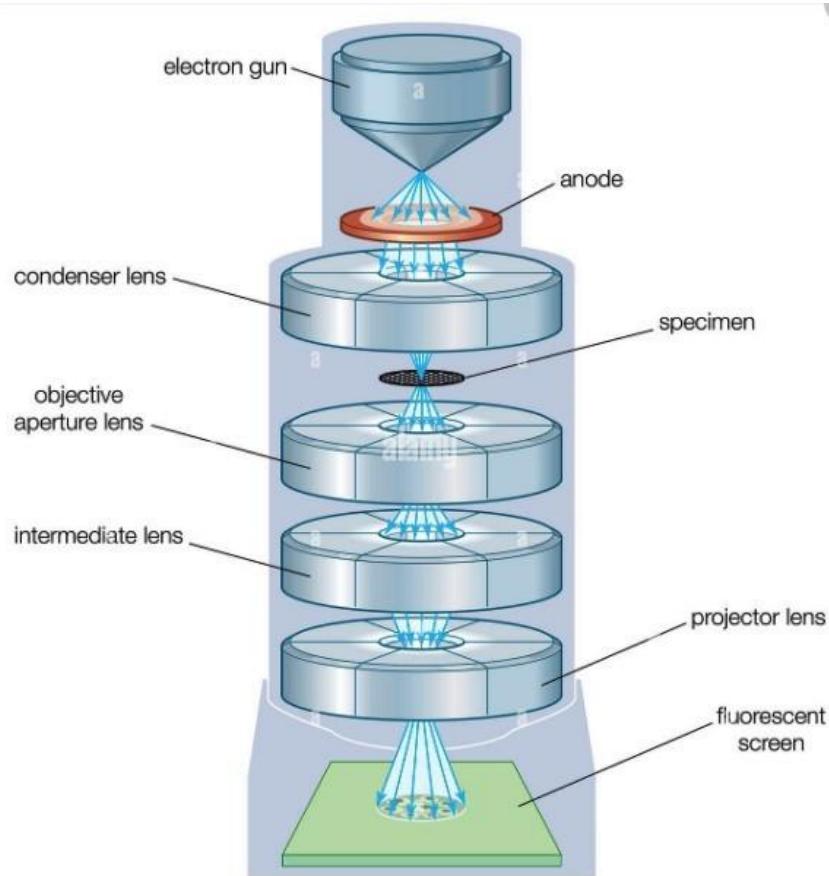


Illustration 10: Components of TEM

For obtaining atomic level image, one may use high resolution TEM (HRTEM) which is an improved version of TEM. It uses interference in image plane of electron wave itself instead of scattering by sample for image formation. Each imaging electron will interact with the sample and electron wave passes through the microscope system which will undergo a phase change and interferes with image wave in imaging plane. From such an image obtained even the inter planar distance d can be directly measured.

2.2.3. UV VISIBLE SPECTROSCOPY

UV-Vis spectroscopy is basically an analytical technique that is used to measures the amount

of discrete wavelengths of UV or visible light that are absorbed by or transmitted through a sample in comparison to a reference or blank sample.

This absorption/transmission of light is influenced by the sample composition, thus potentially able to provide information regarding the sample and concentration.

The energy of light/photon is inversely proportional to the wavelength of the light. Shorter wavelengths of light carry more energy and longer wavelengths carry less energy. Threshold energy is required to promote electrons in a substance to a higher energy state which we can detect as absorption. Electrons in different bonding environments in a substance require a different specific amount of energy to promote the electrons to a higher energy state. Thus, absorption of light for different substance occurs for different wavelengths. Humans can see the wavelength from approximately from 380 nm to 780 nm. UV light has wavelengths with shorter wavelength than visible light range. Thus light can be useful in UV-Vis spectroscopy to analyse or identify different substances by locating the specific wavelengths corresponding to maximum.

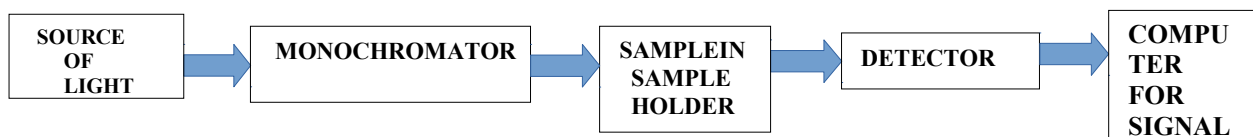


Illustration 11: Components of UV-Visible spectrophotometer

Tungsten lamp/xenon lamp are usually used as the source of light. The light will be poly chromatic and hence they must be made monochromatic by allowing it to pass through the monochromator. For beam splitting one may use prism/diffraction grating. This monochromatic light is then allowed to fall on the sample which will be kept in the sample holder. We can use cuvette made up of glass for visible light range and quartz for UV light range as sample holders. For all analysis, measuring a reference sample, often referred to as the "blank sample", such as a cuvette filled with a similar solvent used to prepare the sample, is imperative. If an aqueous buffered solution containing the sample is used for measurements, then the aqueous buffered solution without the substance of interest is used as the reference. The reference sample signal is later used automatically by the instrument to help obtain the true absorbance values of the analytes. The light incident on the sample, some of its part is absorbed by the sample and the rest is transmitted. This

light is then detected by the detector. The electric signal is fed in to the computer to get the output.

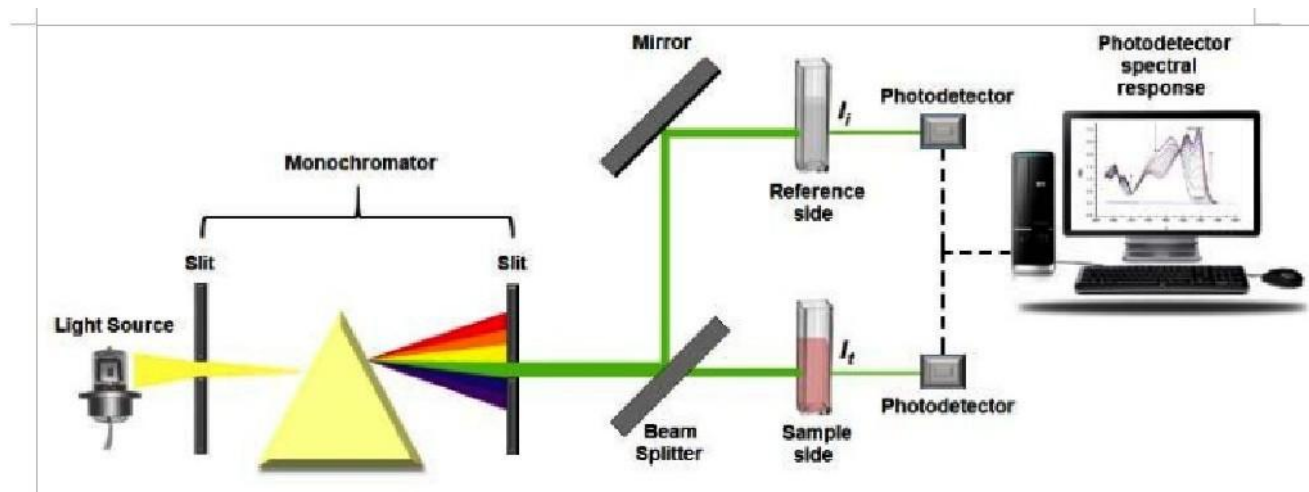


Illustration 12: Schematic diagram of dual beam UV-VIS Spectrometer.

2.2.3.a. UV- VISIBLE ABSORPTION SPECTRUM

UV-Vis spectroscopy information may be presented as a graph of absorbance/optical density/transmittance as a function of wavelength. However, the information is more often presented as a graph of absorbance on the vertical y axis and wavelength on the horizontal x axis.

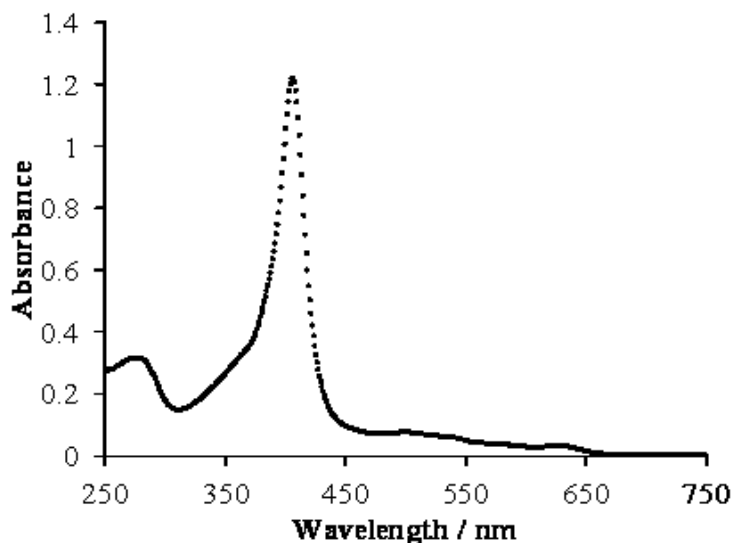


Illustration 13: Absorption spectra

The absorbance (A) is equal to the logarithm of a fraction involving the intensity of light before passing through the sample (I_0) divided by the intensity of light after passing through the sample (I). The fraction I divided by I_0 is also called transmittance (T), which expresses how much light has passed through a sample. Absorbance is the logarithm of the ratio of incident to transmitted radiant power through a sample. However, Beer–Lambert's law is often applied to obtain the concentration of the sample (c) after measuring the absorbance (A) when the molar absorptivity (ε) and the path length (L) are known. Typically, ε is expressed with units of $\text{L mol}^{-1} \text{cm}^{-1}$, L has units of cm , and c is expressed with units of mol L^{-1} . As a consequence, A has no units.

Beer–Lambert's law is especially useful for obtaining the concentration of a substance if a linear relationship exists using a measured set of standard solutions containing the same substance. Equation 6, shows the mathematical relationships between absorbance, Beer–Lambert's law, the light intensities measured in the instrument, and transmittance.

$$A = \varepsilon L c = \log_{10} \left(\frac{I_0}{I} \right) = \log_{10} \left(\frac{1}{T} \right) = -\log_{10}(T)$$

---(eq 5)

ADVANTAGES

- The technique is **inexpensive and non destructive**, allowing the sample to be reused or proceed to further processing or analysis.
- Measurements can be made **quickly**, allowing easy integration into experimental protocols and it's easy to use.
- Data analysis generally requires **minimal processing**; again meaning little user training is required.

DISADVANTAGES

- Possibility of presence of stray light since in practical instrumentation, wavelength selector may not be perfect.

- Light scattering caused by suspended solids in liquid samples, which may cause serious measurement errors. The presence of bubbles in the cuvette or sample will scatter light, resulting in irreproducible results.
- **Interference from multiple absorbing species** – if sample has multiple types of the species overlapping of the spectra may occur. For a proper quantitative analysis, each chemical species should be separated from the sample and examined individually.
- **Geometrical considerations** - Misaligned positioning of any one of the instrument's components, especially the cuvette holding the sample, may yield irreproducible and inaccurate results. Therefore, it is important that every component in the instrument is aligned in the same orientation and is placed in the same position for every measurement. Some basic user training is therefore generally recommended to avoid misuse.

REFERENCES

1. Infra-red Spectroscopy-Norman B. Colthup, in Encyclopedia of Physical Science and Technology (Third Edition), 2003
2. Sharpe, M. R. "Stray light in UV-VIS spectrophotometers." *Analytical Chemistry* 56.2 (1984): 339A-356A.<https://doi.org/10.1021/ac00266a003>
3. Gan, Y. X., A. H. Jayatissa, and Z. Yu. "Hydrothermal synthesis of nanomaterials. J Nanomater 2020." (2020).
4. Kite, Sagar V., Abhijit Nanaso Kadam, Dattatraya J. Sathe, Satish Patil, Sawanta S. Mali, Chang Kook Hong, Sang– Wha Lee, and Kalyanrao M. Garadkar. "Nanostructured TiO₂ sensitized with MoS₂ nanoflowers for enhanced photodegradation efficiency toward methyl orange." *ACS omega* 6, no. 26 (2021): 17071-17085.
5. Bumbrah, Gurvinder Singh, and Rakesh Mohan Sharma. "Raman spectroscopy–Basic principle, instrumentation and selected applications for the characterization of drugs of abuse." *Egyptian Journal of Forensic Sciences* 6.3 (2016): 209-215.
6. Handbook of instrumental techniques for analytical chemistry -Prentice, Inc., New Jersey (1997)- F.A. Settle.
7. Nano structure and nano materials synthesis, properties and applications- Guozhong Cao, Ying Yang
8. <https://khwarizmi.org/wp-content/uploads/2010/10/csd1.pdf>
9. https://encryptedtbn0.gstatic.com/images?q=tbn:ANd9GcSU2iCjZakuWEygjCnlTucBkRMCu3.WRAmlCkVzZt1G4Tm2Qd_Sqv8V0Dc2ydA5nlgfgEPp4&usqp=CAU
10. <https://www.alamy.com/stock-photo-the-components-of-a-transmission-electron-microscope-tem-24898253.html>

11..<https://www.alamy.com/stock-photo-the-components-of-a-transmission-electron-microscope-tem-24898253.html>

12.<https://www.technologynetworks.com/analysis/articles/uv-vis-spectroscopy-principle-strengths-and-limitations-and-applications-349865>

13. <https://cdn.technologynetworks.com/tn/images/body/uv-visfig2final1625048265694.png>

14.https://www.researchgate.net/profile/Mauro-SergioBraga/publication/336637497/_figure/fig2/AS_816063046512640@1571576000137/Schematic-representation-of-the-dual-beam-UV-VIS%20spectrometer.jpg

15. <https://wiki.anton-paar.com/en/basics-of-raman-spectroscopy>

16.<https://www.renishaw.com/en/raman-spectra-explained--25807>

17. <https://www.sciencedirect.com/science/article/pii/B0122274105003409>

CHAPTER 3

RESULT AND DISCUSSION

3.1. XRD ANALYSIS

3.1.1. XRD SPECTRUM OF SYNTHESIZED TiO₂ NANOPOWDER

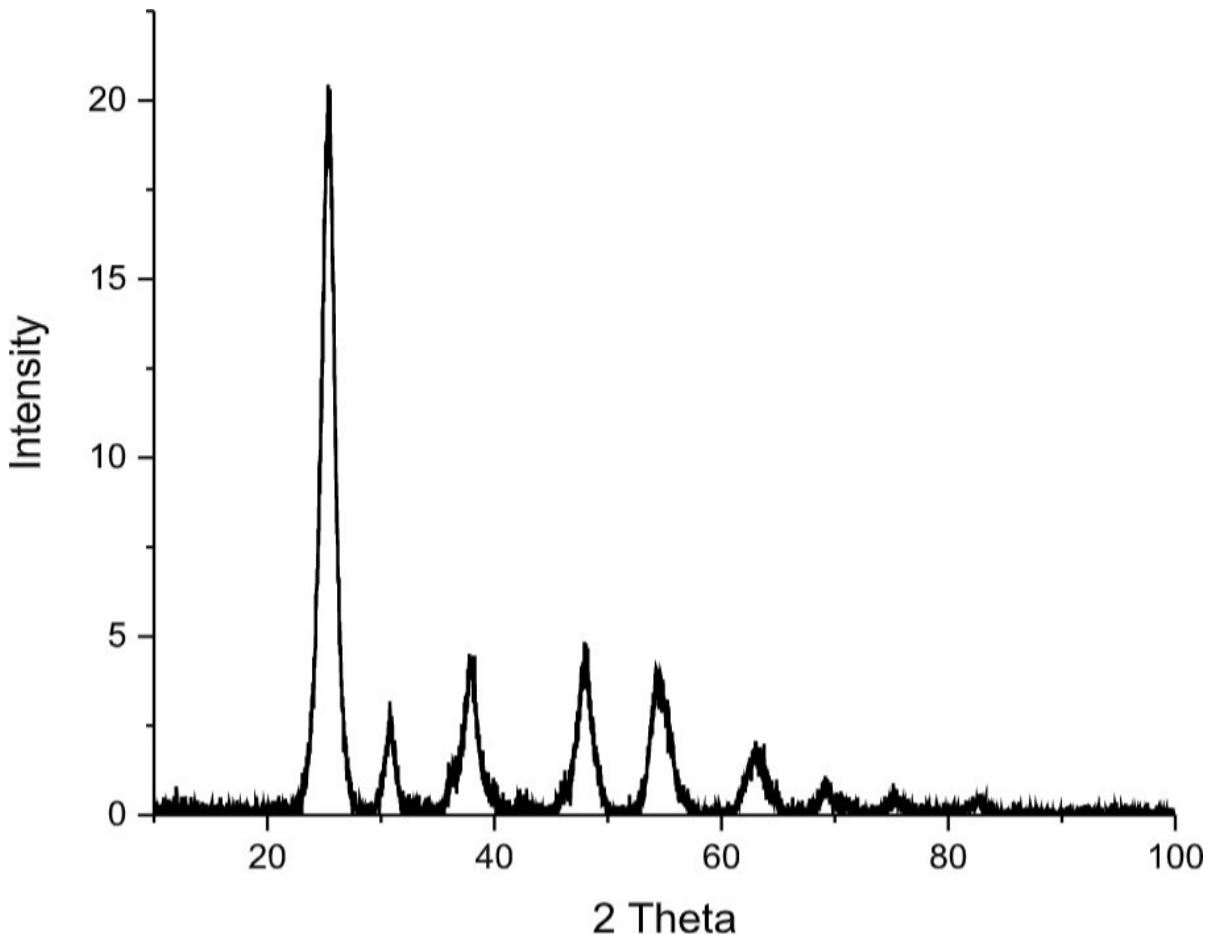


Illustration 14: XRD pattern of the TiO₂ nanopowder

The X Ray diffraction spectrum of synthesized TiO₂ nano powder is shown in illustration 15. The peaks in the spectrum match with the standard peaks of TiO₂ anatase phase. There is a major peak centered at 25.39°, which is of (101) plane of anatase TiO₂. Also, the peaks around 37.96°, 47.93°, 54.34°, 62.66° are compatible with the standard peaks of anatase TiO₂. The corresponding crystal planes are (004), (200), (105) and (204) respectively. Other than these peaks, an additional peak of TiO₂ Brookite phase is present around 30.77°.

Particle size is calculated using the formula,

$$\text{Particle size } L = \frac{0.94\lambda}{B \cos \theta} \dots \dots \dots \text{ (eq. 6)}$$

Where λ is the wavelength of x ray, B is the full width at half maximum of the xrd peak obtained and theta is the diffraction angle.

The particle sizes of the synthesized TiO₂ are tabulated below:

2Θ (DEGREE)	Θ (DEGREE)	Θ (RADIAN)	FWHM (DEGREE)	FWHM (RADIAN)	PARTICLE SIZE(NM)
25.33819	12.6691	0.221005	1.31089	0.022868	6.21445
37.87463	18.93732	0.330351	1.54064	0.026876	5.454008
47.96137	23.98069	0.41833	1.45075	0.025308	5.99579
54.62099	27.3105	0.476416	1.67964	0.0293	5.325142
63.1131	31.55655	0.550486	1.74207	0.030389	5.35343

Table 2. Particle size determination

Average Particle size = **5.66856453nm**.

3.1.2. XRD SPECTRA OF SYNTHESIZED MoS₂ NANO STRUCTURES OBTAINED AT DIFFERENT AUTOCLAVED TIME PERIODS

The X ray diffraction spectrum of synthesized MoS₂ nano structures at various autoclaved time periods are shown below. It is seen that, as the time duration increased the ex foliation of MoS₂ nano structures have taken place and finally after 24 hours we have got nanosheets of MoS₂. Also, the obtained peaks in the spectra are in agreement with the standard peaks of MoS₂. The detected peaks around 13.58°, 32.2°, 39.69°, 43.8° and 57.77° respectively correspond to (002), (100), (103), (006) and (110) planes of Hexagonal MoS₂.

It is seen that as time duration increases, the peaks decrease in intensity except the prominent ones. The peaks become less and less sharper as the time period increase from 8 to 24 hours. At 8 and 10 hours the peaks are sufficiently sharp but as the time increased to 24 hours it becomes more broadened which indicate the finite small size of the nanosheet developed.

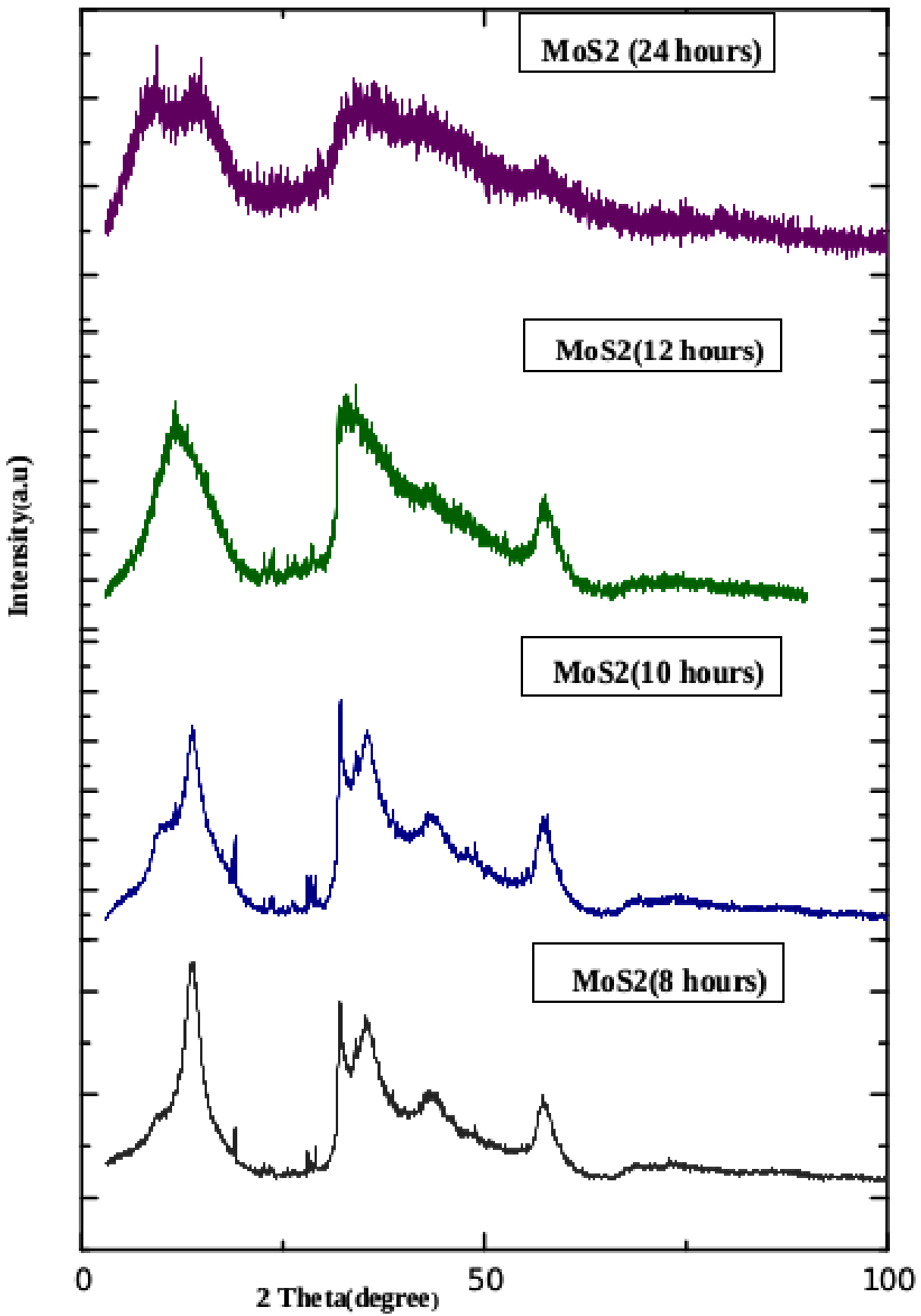
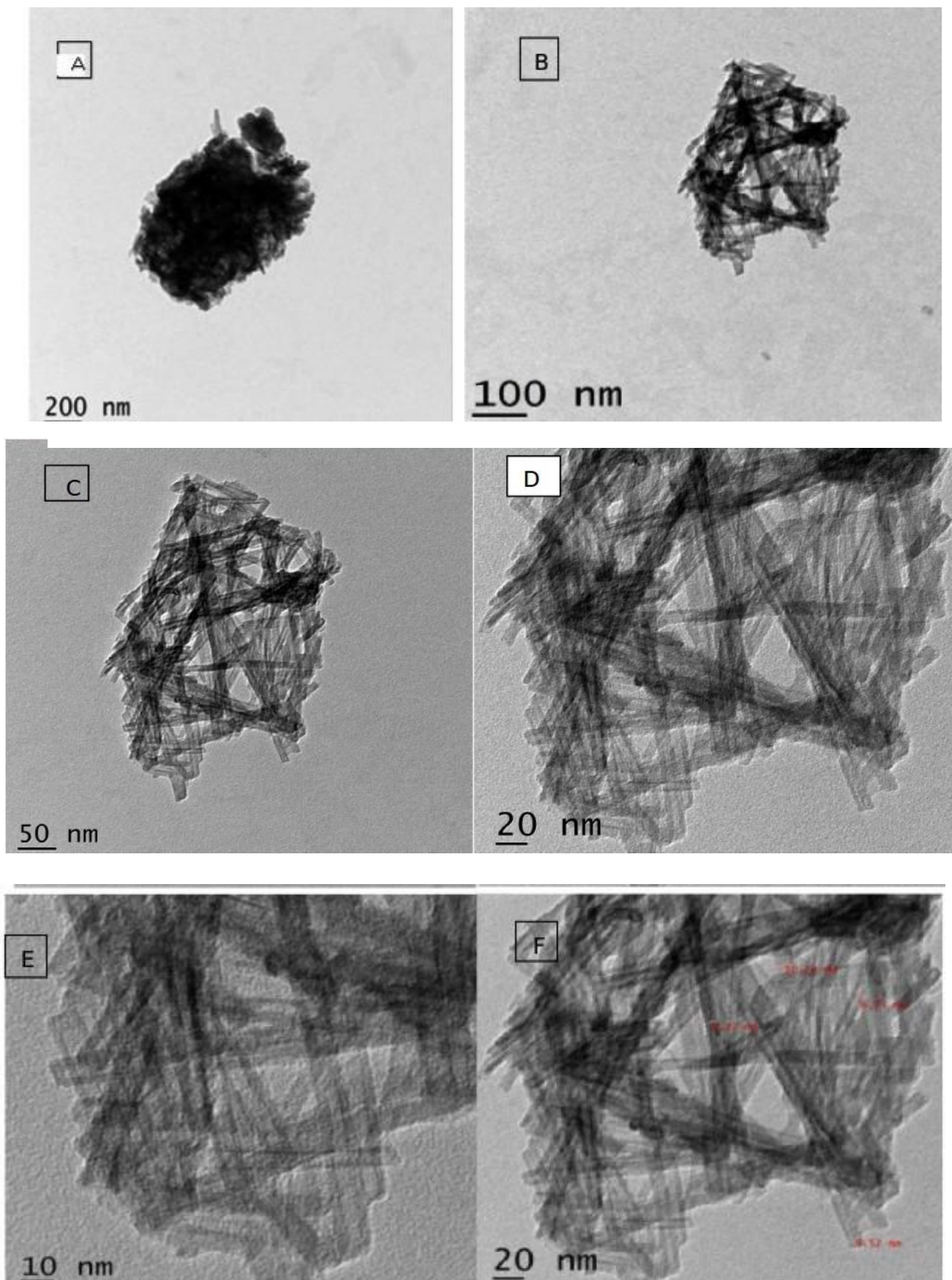


Illustration 15: Stack of the XRD pattern of the MoS₂ synthesised by varying time

3.2. TEM IMAGES OF THE SYNTHESIZED TiO₂ NANOTUBES



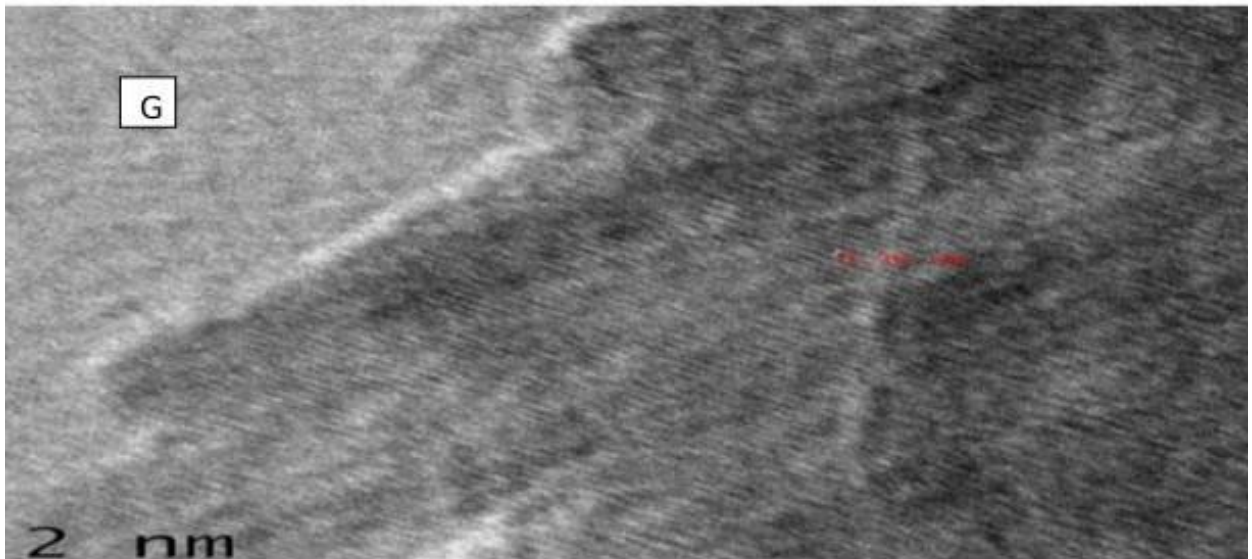


Illustration 16:A,B,C,D,E,F,G : HRTEM image of TiO_2 nanotube at different resolutions

Illustrations marked from A to G are the obtained TEM images of the synthesized nano tubes. Figure B reveals that the nanotubes are almost clustered in nature and randomly oriented. But, nanoparticles are not seen which indicates that the nanopowder has totally transformed into nanotubes. Illustration 21.F shows that the nano tubes are of thickness less than 10nm. We could synthesize nanotubes of average thickness 9.19 nm (marked in the image). From the HR TEM image of illustration 21 G, it can be understood that the inter planar spacing (d) is 0.30nm which is perfectly agreeing with the (101) plane of TiO_2 .

3.3. PHOTO CATALYTIC STUDIES

3.3.1 DEGRADATION OF METHYLENE BLUE DYE(MB)

3.3.1.a DEGRADATION OF MB WITH TiO_2 NANOTUBE

Methylene blue is a salt that is used as a dye and as medication. It is a thiazine dye. It is often used to treat condition called methemoglobinemia which is condition that occur when blood cannot deliver oxygen where it is needed in the body. It is a safe drug when used in therapeutic doses(<2 mg/kg). But it can cause toxicity at high level. Overdose symptoms include vomiting, stomach pain, feeling like you might pass out, confusion, numbness, blue coloured skin or lips etc.

Degradation of MB dye was studied by varying the amount of the TiO₂ nanotube added to the solution at 40 min.

The percentage of degradation of the dye can be calculated by the equation

$$\% \text{ of degradation} = \frac{A_0 - A_t}{A_0} \times 100 \dots \dots \dots \text{(eq. 7)}$$

where ,

A₀ – Absorbance of initial methylene blue

A_t – Absorbance after illumination at time t

MB dye shows absorbance peak at 609 nm and 668 nm and the corresponding absorbance were 1.088552 and 1.761653 respectively.

The table below shows the % of degradation of MB dye as amount of TiO₂ NT added to solution increase from 1 mg to 5 mg.

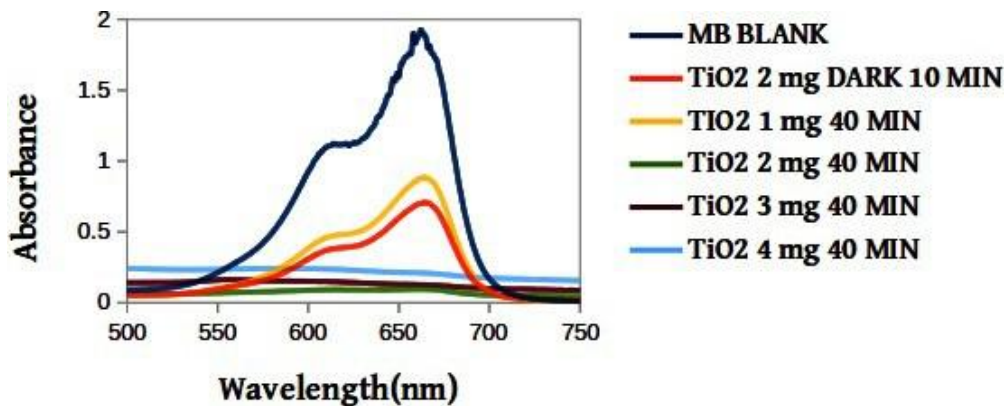


Illustration 17: Absorption spectra of MB dye with TiO₂ nanotube added.

TiO ₂ NT				
PEAK CORRESPONDING TO WAVELENGTH	TIME	A _t	A ₀	% OF DEGRADATION
668 nm	Dark 10 min- 2 mg	0.689198	1.761653	60.88
	40 min - 1 mg	0.857952		51.30
	40 min- 2 mg	0.095542		94.5
	40 min-3 mg	0.123523		92.99
	40 min-4 mg	0.20724		88.24
609 nm	Dark 10 min- 2 mg	0.365905	1.088552	66.39
	40 min - 1 mg	0.456166		58.09
	40 min- 2 mg	0.091345		91.61
	40 min-3 mg	0.149912		86.23
	40 min-4 mg	0.237715		78.16

Table 3. Percentage of degradation for various amount of TiO₂ nanotube added.

Comparing the percentage of degradation one can conclude that the degradation is maximum when 2 mg of TiO₂ NT added to the solution. At this amount the degradation reaches 94.58 and 91.61 percentage respectively at 40 min exposure to visible light. On adding further amount of TiO₂ NT the degradation efficiency is seen to decrease. This happened because photo catalysis happens only for optimum amount of photo catalyst. If the amount of photo catalyst is excessive, it reduces the capture of photons (a screening effect). In order to speed up the photo degradation TiO₂ NT is doped with MoS₂.

3.3.1.b. DEGRADATION OF MB WITH MoS₂ NANOSHEET

2 mg of MoS₂ nano sheet was added to 10 ml of the MB dye solution. The photo degradation of MB dye was studied at different times. The comparison of the absorption spectra

of MB when MoS_2 nano sheet is added at different time period is given below.

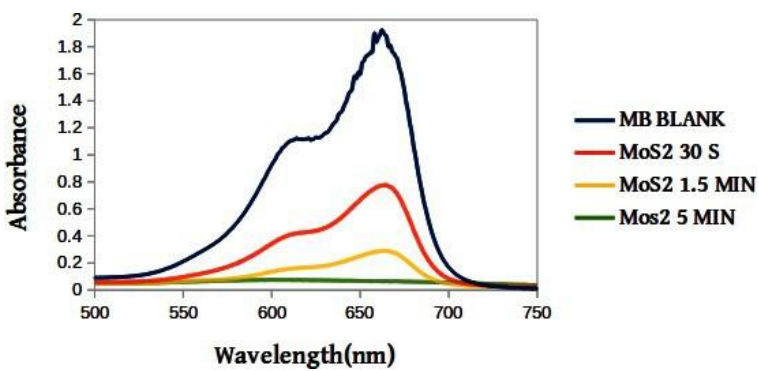


Illustration 18: Absorption spectra of MB dye with MoS_2 nanosheet

MoS ₂ NANO SHEET				
PEAK CORRESPONDING TO WAVELENGTH	TIME	A _t	A ₀	% OF DEGRADATION
668 nm	30 s	0.757522	1.761653	56.999
	1.5 min	0.281769		84.005
	5 min	0.063579		96.391
609 nm	30 S	0.402923	1.088552	62.985
	1.5 min	0.155858		86.682
	5 min	0.075074		93.103

Table 4. Percentage of degradation of MB with 2 mg of MoS_2 nano sheet.

From the data, we may conclude that MoS_2 nano sheet prepared can cause dye degradation up to 96.391 and 93.103 respectively within 5 min.

3.3.1.c. DEGRADATION OF MB DYE WITH MoS_2 NANOSHEET DOPED TiO_2 NANOTUBE (MT)

2 mg of the nanocomposite (MT) was added to the dye solution and photo degradation

was studied at different time. The absorption spectra was taken and the comparison plot is given below.

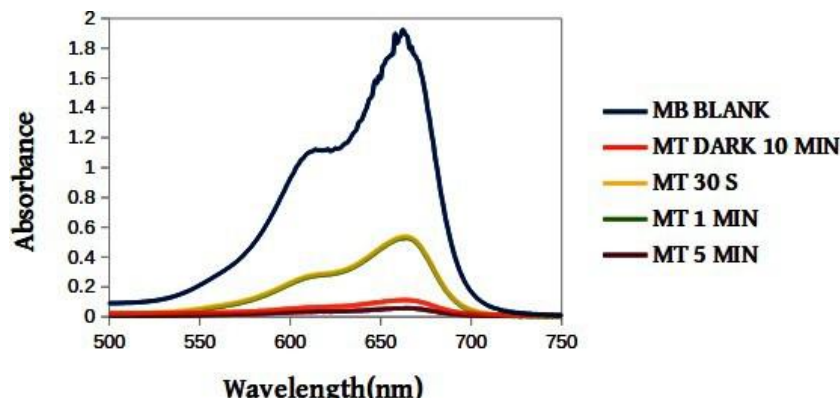


Illustration 19: Absorption spectra of MB dye with $\text{MoS}_2@\text{TiO}_2$

NANOCOMPOSITE(MT)				
PEAK CORRESPONDING TO WAVELENGTH	TIME	A_t	A_0	% OF DEGRADATION
668 nm	Dark 10 min	0.107152	1.761653	93.92
	30 s	0.523016		70.311
	1 min	0.51326		70.865
	5 min	0.056759		96.778
609 nm	Dark 10 min	0.062385	1.088552	94.269
	30 s	0.72019		75.011
	1 min	0.261978		75.933
	5 min	0.03354		96.919

Table 5. Percentage of photo catalytic degradation of MB dye with $\text{MoS}_2@\text{TiO}_2$

From the data we may conclude that the synthesized nanocomposite has high efficiency and the percentage of photo degradation increase as the time increased from approximately 70 to

97 percentage as the time increase from 30s to 5 min.

Also it is seen that the synthesized nanocomposite shows good degradation of the MB dye in darkness. In a time duration 10 min, the dye was degraded to approximately 94%.

3.3.1.d. DEGRADATION OF MB WITH MoS₂ NANOSHEET DOPED TiO₂ NANOTUBE PREPARED BY MECHANO CHEMICAL METHOD

Doping of TiO₂ NT with MoS₂ nanosheet was also done by physical method. They were respectively labelled as MT*2wt% (2 wt% MoS₂ in TiO₂) and MT*5wt%(5 wt% MoS₂ in TiO₂). The photo degradation of MB dye was studied for these composites at different times. The obtained absorption spectra and the tabulated percentage of the degradation of the dye are given below.

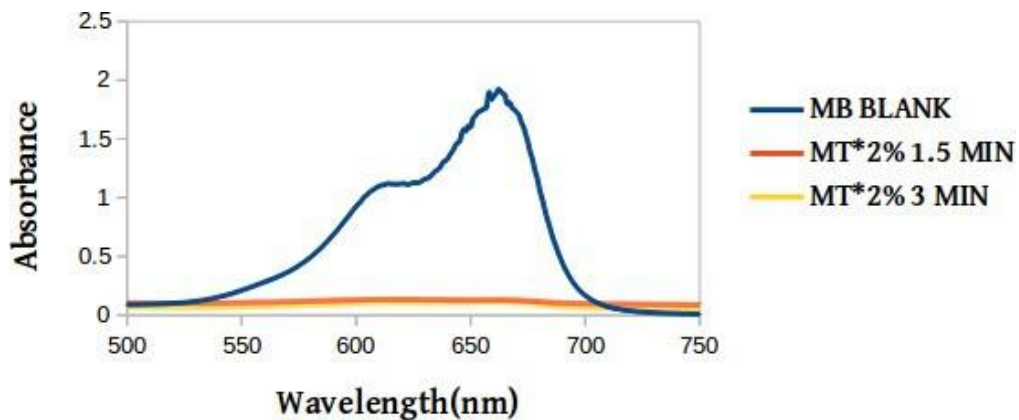


Illustration 20: Absorption spectra of MB with 2 wt% MoS₂@ TiO₂

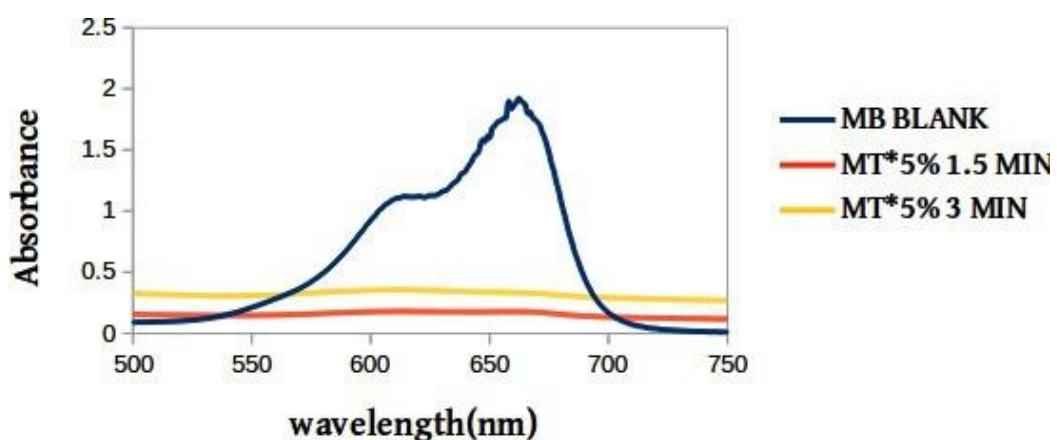


Illustration 21 Absorption spectra of MB with 5 wt% MoS₂@ TiO₂

MT*2%				
PEAK CORRESPONDING TO WAVELENGTH	TIME	A _t	A ₀	% OF DEGRADATION
668 nm	2 mg – 1.5 min	0.127689	1.761653	92.752
	2 mg-3 min	0.111401		93.676
609 nm	2 mg – 1.5 min	0.106708	1.088552	85.577
	2 mg-3 min	0.214923		90.197

Table 6. Percentage of photo catalytic degradation of MB dye with 2 wt% MoS₂@TiO₂

MT*5%				
PEAK CORRESPONDING TO WAVELENGTH	TIME	A _t	A ₀	% OF DEGRADATION
668 nm	2 mg – 1.5 min	0.17527	1.761653	90.051
	2 mg-3 min	0.328939		81.328
	2 mg – 5 min	0.208773		88.149
609 nm	2 mg – 1.5 min	0.179249	1.088552	83.533
	2 mg-3 min	0.355191		67.370
	2 mg – 5 min	0.206867		80.996

Table 7. Percentage of photo catalytic degradation of MB dye with MoS₂@TiO₂

MT*2wt% degraded the dye up to 93.676 % within 3 min while the MT*5% could degrade only 81.328 %. Further more MT*5% is showing a decrease in the percentage of the degradation when time increased from 1.5 to 3 min and an increase in the interval 3 to 5 min. From the degradation data, we confirm 2 wt% of MoS₂ in TiO₂ is more efficient when compared to the 5 wt% MoS₂ in TiO₂.

3.3.1.e COMPARISON OF THE DOPED TiO₂ NANOTUBE (MT) WITH UNDOPED TiO₂ NANOTUBE

A comparison of the photo-catalytic degradation of the MB dye was done by comparing the absorption spectra of the MoS₂ doped TiO₂ nanotube and undoped TiO₂ nanotube.

From the absorption spectra we may interpret that the photo-catalytic activity of the TiO₂ is improved when doped with MoS₂ nano sheet. TiO₂ undoped sample could degrade MB dye to 94.58% . but, it took almost 40 min. while the doped forms MT, MT*2%, MT*5% could degrade the dye up to 97 % , 93 %, 90% within 5, 1.5,1.5 minutes respectively. MT*2% is more efficient as a photo catalyst in the photo degradation of MB dye.

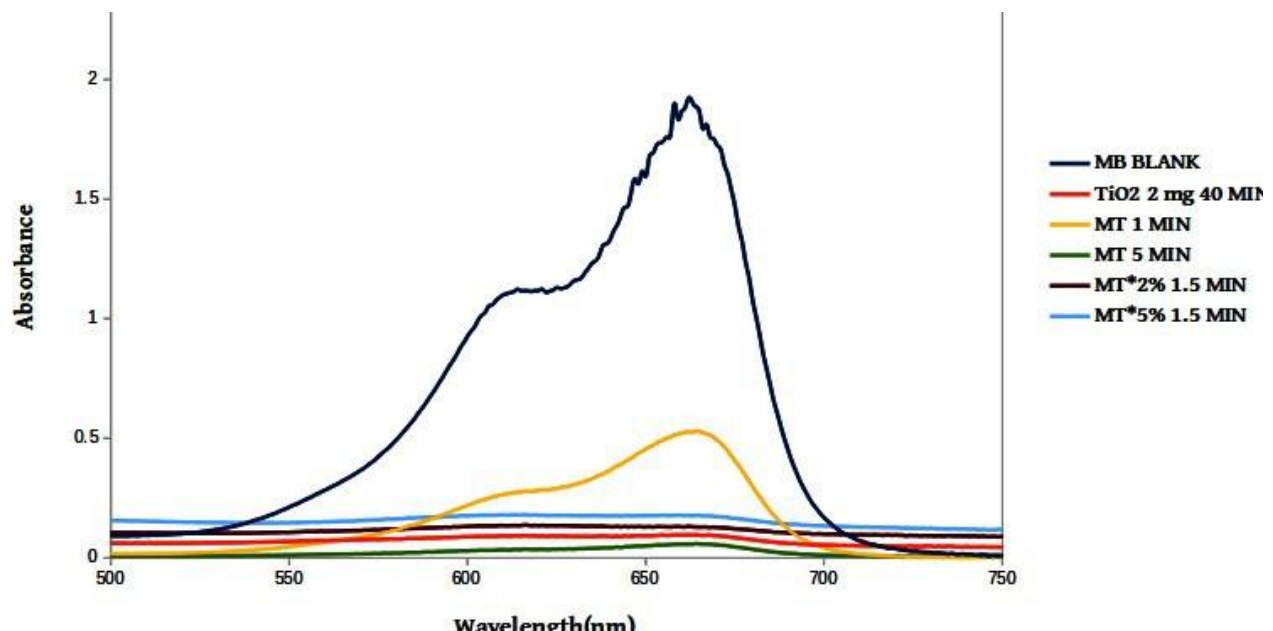


Illustration 22: Absorption spectra of undoped TiO₂ nanotube (NT) and doped composites MoS₂@TiO₂ NT, 2 wt% MoS₂@TiO₂ NT, 5wt% MoS₂ @ TiO₂ NT

TiO₂ and MoS₂ are semiconductors and hence falls into the category of heterogeneous photo catalyst. They posses forbidden energy gap which needs photon to excite an electron from valence band to conduction band thus producing electron hole pair. The generated holes react with redundant producing oxidised product and excited electron react with oxidant to produce reduced product. These oxidation-reduction reaction take place on the surface of photo catalyst. The positive holes, will react with the moisture on the surface to produce hydroxyl radicals. Hence adsorption of the dye on the surface of the photocatalyst is the first step towards photo

catalysis.

It is observed that, the dye was degraded upto 61% on stirring with 2 mg of TiO₂ nanotube for 10min in darkness. This is due to the adsorption of the molecule on the surface of the photo catalyst(TiO₂ NT). Thus, an amount of dye is removed along with the nanotube once we centrifuge it out. All other solutions with MB and TiO₂ nanotube(added in different quantity say 1 mg, 2 mg,3 mg,4 mg) were first stirred in darkness for 10 minute, so that the methylene blue dye get adsorbed on the surface of the nanotube and then exposed to light. When exposed to light, free radicals produced on the surface of the nanotube, will continuously react with the dye reducing it until it became harmless. From the comparative study, it is seen that the degradation reach the highest percentage (94. 58%) for 2 mg of TiO₂ nanotube added. For small amount of catalyst added, the degradation will increase as the amount of photo-catalyst added and reaches a maximum at the optimum quantity of photo catalyst. As the quantity of TiO₂ nanotube added to dye solution increase from 1 mg to 2 mg the the degradation has increased from 51.3% to 94.58 %. But, when we added 3 mg and 4 mg of TiO₂ nanotube, the percentage of degradation decreased from 94.58% to 93% and 88.24% respectively. This happens because, as the amount of photo catalyst increases, the photon density that can be absorbed by the photo catalyst will decrease. Thus production of reactive oxygen species will decrease. But, this high percentage of degradation was reached after 40 min.

Similarly, the comparison study of the photo degradation of the MB dye with MoS₂ nanosheet was done. Nano sheet being one of the quantum structure having high surface area, highly reactive and has high adsorbing capability. It was seen that the MB dye get reduced instantly, on adding 2 mg of MoS₂ nanosheet agreeing with the high adsorption efficiency of MoS₂ nanosheet. The adsorbed dye get further reduced on exposure to light. In this case, it is seen that dye get degraded 57%, 84%, 96.4% on exposure to visible light for 30s, 1.5 min and 5 min respectively.

The nanocomposite also shows better result in MB, as compared to un doped TiO₂ nanotube. On doping TiO₂ nanotube with MoS₂ nanosheet, the surface area increases thus providing more surface area for the dye to get adsorbed. More over, surface sensitization of TiO₂ nanotube with MoS₂ nanosheet can control the electron hole pair recombination by acting as trapping centres for electron, thus increasing the visible light driven photo-catalytic activity of

TiO_2 . This is clear from the observation. On doping with MoS_2 nano sheet, the percentage of degradation has enhanced from 94.58 % in 40 min to 97% (MT), 93% (MT*2%), 90%(MT*2%) within 5, 1.5, 1.5 minutes respectively. These result indicate that the nano composite developed are much better photocatalyst than un doped TiO_2 NT in degradation of MB dye.

It is observed that as MoS_2 nano sheet doped with TiO_2 nanotube, MoS_2 will trap the photo excited electron of TiO_2 . From the study of photo degradation of MB it was observed that 2 wt% MoS_2 - TiO_2 nanocomposite is more efficient than 5wt% MoS_2 - TiO_2 . The appropriate amount of MoS_2 would permit maximum photoelectrons trapping. Excessive amount of MoS_2 can hinder the efficient absorption of light by TiO_2 and screen the TiO_2 surface from catalytic reaction.

3.3.2. ANALYSIS OF DEGRADATION OF RHODAMINE B DYE(Rh B)

Rhodamine B is an organic chloride salt. It is a chemical compound and a dye which is most often used as tracer dye to determine the direction and rate of the water flow. Rh B dye is also used for dyeing purposes. It finds application in many other field like fluorescence microscopy, Fluorescence correlation spectroscopy and flow cytometry. But, the high doses of Rh B can cause several health issues, more over it is suspected to be carcinogenic.

3.3.2.a DEGRADATION OF Rh B WITH TiO_2 NANOTUBE

Degradation of Rhodamine B dye was studied by adding 2.5 mg of TiO_2 nanotube at different time Rh B dye shows absorbance peak at 554 nm and the corresponding absorbance is 1.5894. The table below shows the % of degradation of Rh B dye 2.5 mg TiO_2 NT added to solution at different times.

TiO_2 NT				
PEAK CORRESPONDING TO WAVELENGTH	TIME	A_t	A_0	% OF DEGRADATION
554 nm	2.5 mg Dark 10 min	1.4732	1.5894	7.3090
	2.5 mg – 15 min	1.5772		0.7671

	2.5 mg – 30 min	1.6055		-1.0123
	2.5 mg – 45 min	1.6600		-4.4438

Table 8. Percentage of degradation of Rh B dye with un doped TiO_2

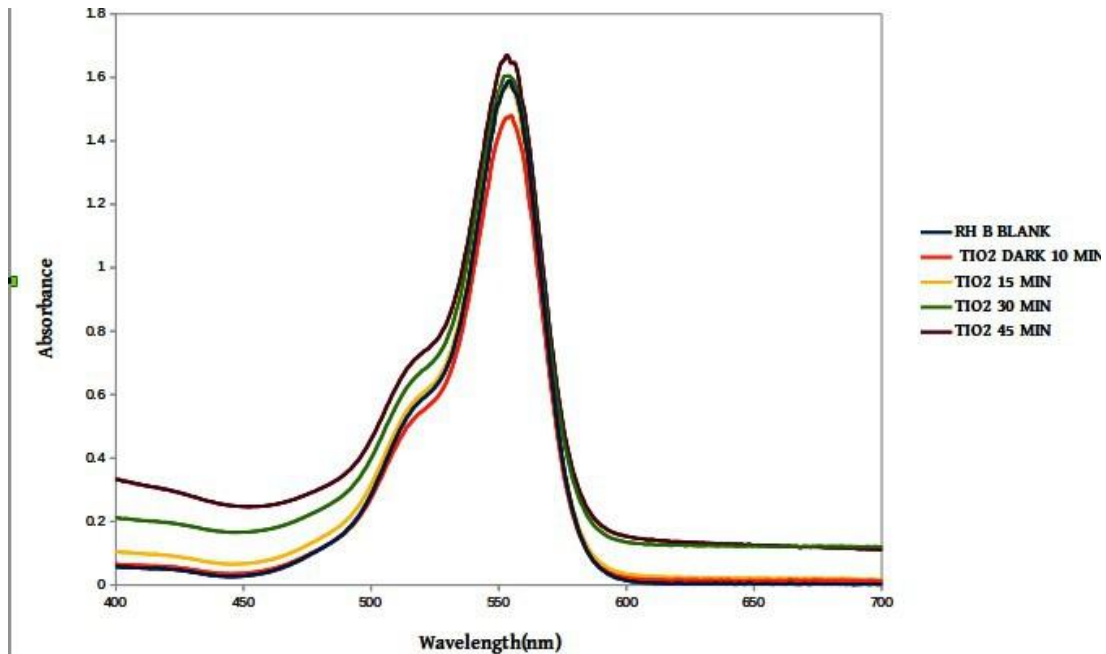


Illustration 23: Absorption spectra of Rh B dye with un doped TiO_2 nanotube

Comparing the percentage of degradation one can conclude that the degradation is maximum when 2.5 mg of TiO_2 NT added to the solution in dark. In the presence of light, TiO_2 does not have much effect on Rh B dye.

3.3.2.b . DEGRADATION OF Rh B WITH MoS_2 NANOSHEET

2.5 mg of MoS_2 nanosheet was added to 10 ml of Rh B dye solution. The photo degradation of Rh B dye was studied at different time intervals. The comparison of the absorption spectra of Rh B dye when MoS_2 nanosheet is given below.

MoS ₂ NANO SHEET				
PEAK CORRESPONDING GTO WAVELENGTH	TIME	A _t	A ₀	% OF DEGRADATION
554 nm	30 s	0.5089	1.5894	67.9980
	1.5 min	0.3913		75.3795
	5 min	0.4558		71.3207

Table 9. Percentage of degradation of Rh B dye with un MoS₂ nanosheet

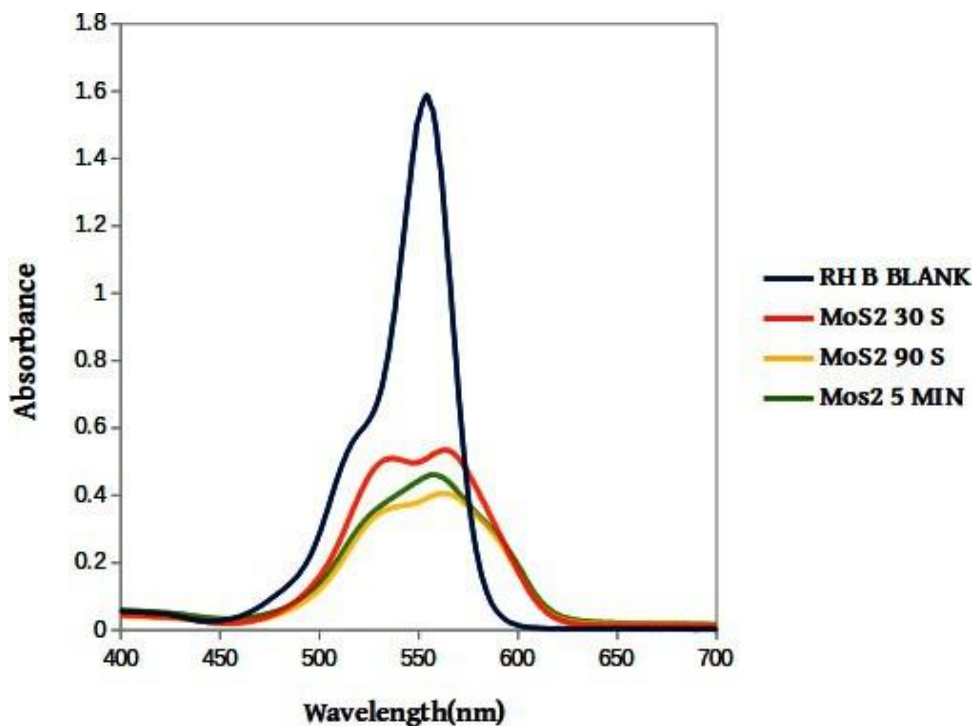


Illustration 24: Absorption spectra of Rh B dye with 2.5mg MoS₂ nanosheet

From the data, we may conclude that MoS₂ nanosheet prepared can cause dye degradation up to 75.3795% within 1.5 min.

3.3.2.c. DEGRADATION OF Rh B DYE WITH MoS₂ NANOSHEET DOPED TiO₂ NANOTUBE (MT)

2.5 mg of the nanocomposite(MT) was added to the dye solution and photo degradation was studied at different different time. The absorption spectra was taken and the comparison plot is given below.

The percentage of dye degradation are tabulated in the table given below.

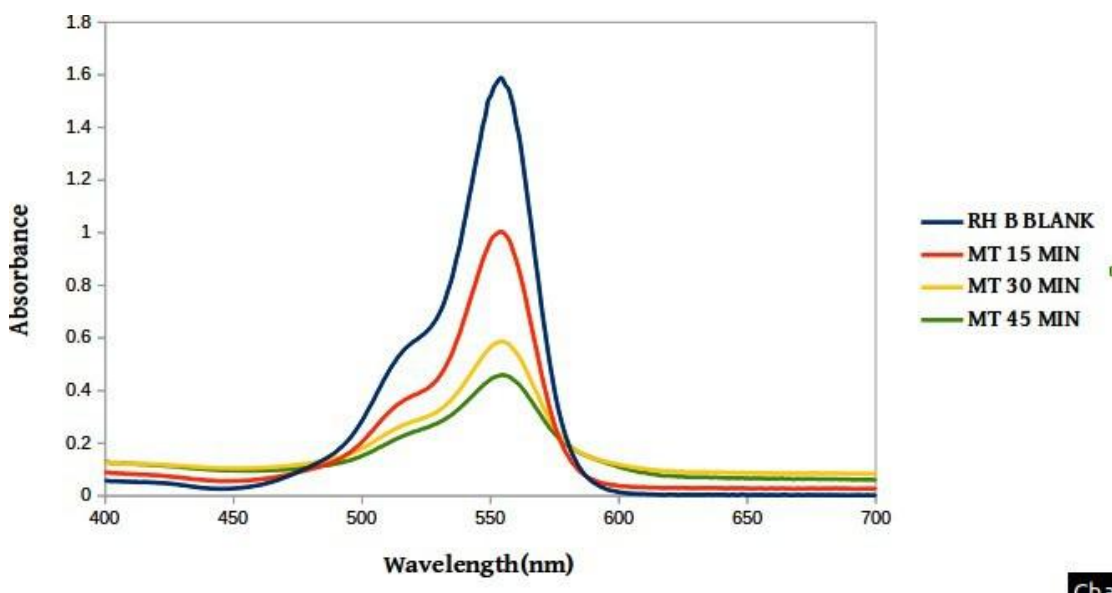


Illustration 25: Absorption spectra of Rh B with 2.5 mg of MoS₂ @TiO₂

NANOCOMPOSITE(MT)				
PEAK CORRESPONDING TO WAVELENGTH	TIME	A _t	A ₀	% OF DEGRADATION
554 nm	15 min	1.0031	1.5894	36.8855
	30 min	0.5861		63.1243
	45 min	0.4585		71.1497

Table 10. Percentage of degradation of RH B dye with un doped MoS₂ @TiO₂

From the data we may conclude that the synthesized 2.5 mg nanocomposite can cause degradation of Rh B dye up to 71.145% within 45 minutes. Its seen that the photo degradation percentage increase from 36.885 % to 71.1497 % on increasing the time of exposure to light from 15 to 45 minutes.

3.3.2.d. DEGRADATION OF Rh B DYE WITH MoS₂ NANOSHEET DOPED TiO₂ NANOTUBE PREPARED BY MECHANO CHEMICAL METHOD

The photo degradation of Rh B dye was studied for nanocomposites(MT*2%,MT*5%) at different time. The obtained absorption spectra and the tabulated percentage of the degradation of the dye are given below.

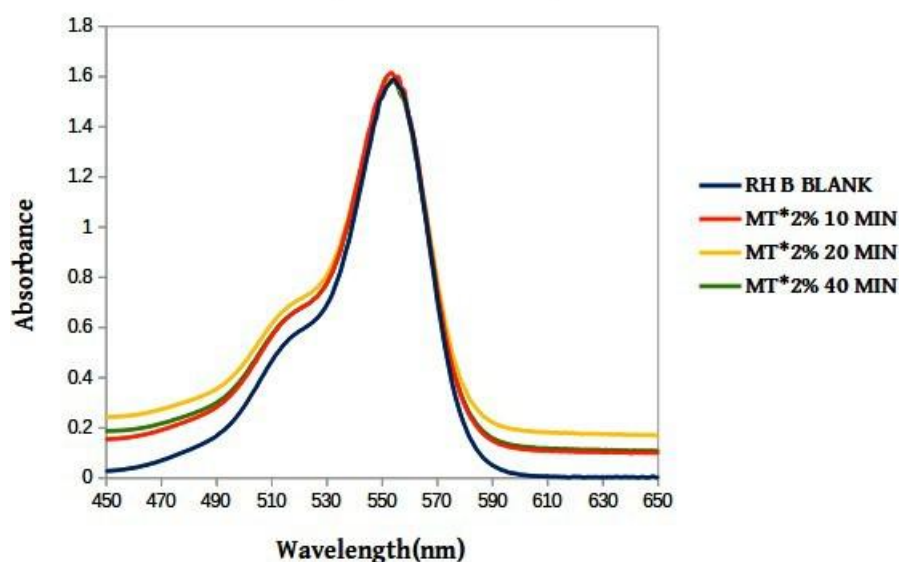


Illustration 26: Absorption spectra of Rh B with 2.5 mg of 2wt% MoS₂ @TiO₂

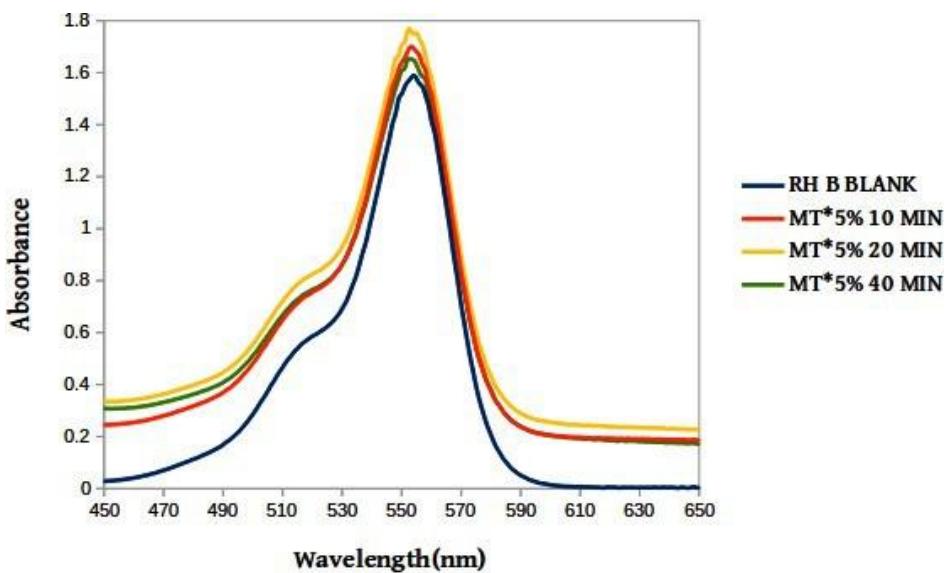


Illustration 27: Absorption spectra of Rh B with 2.5 mg of 5wt% MoS_2 @ TiO_2

MT*2%				
PEAK CORRESPONDING TO WAVELENGTH	TIME	A_t	A_0	% OF DEGRADATION
554 nm	2.5 mg – 10 min	1.6087	1.5894	-1.2146
	2.5 mg – 20 min	1.5783		0.6942
	2.5 mg – 40 min	1.5782		0.7024

Table 11. Percentage of degradation of Rh B dye with 2 wt% MoS_2 @ TiO_2

MT*5%				
PEAK CORRESPONDING TO WAVELENGTH	TIME	A_t	A_0	% OF DEGRADATION
554 nm	2.5 mg – 10 min	1.6946	1.5894	-6.6185
	2.5 mg – 20 min	1.7475		-9.9490
	2.5 mg – 40 min	1.6500		-3.8148

Table 12. Percentage of degradation of Rh B dye with 5 wt% MoS_2 @ TiO_2

From the spectra we can see that, the nanocomposite does not work in Rh B dye.

3.3.2.e. COMPARISON OF DOPED TiO₂ NT(MT) WITH UN DOPED TiO₂ NANOTUBE

A comparison of the photo-catalytic degradation of the Rh B dye may be done by comparing the absorption spectra of the MoS₂ doped TiO₂ NT and un doped TiO₂ NT. Since MT is more efficient in causing degradation of Rh B dye than MT*2% and MT*5% we may compare the absorption spectra of MT and un doped TiO₂ NT.

It is seen that as for TiO₂ NT alone, degradation was very less(below 1%). But, for the nanocomposite MT, the degradation was seen to increase with time and reached up to 71%.

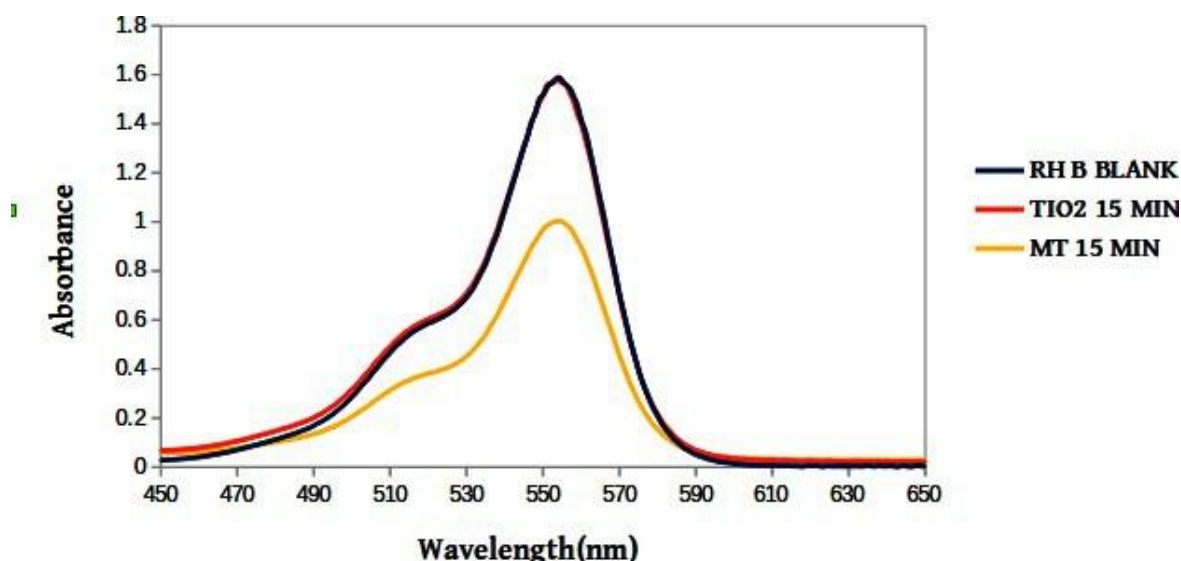


Illustration 28: Absorption spectra of Rh B with undoped TiO₂nanotube and MoS₂@TiO₂ nanotube composite at 15 min.

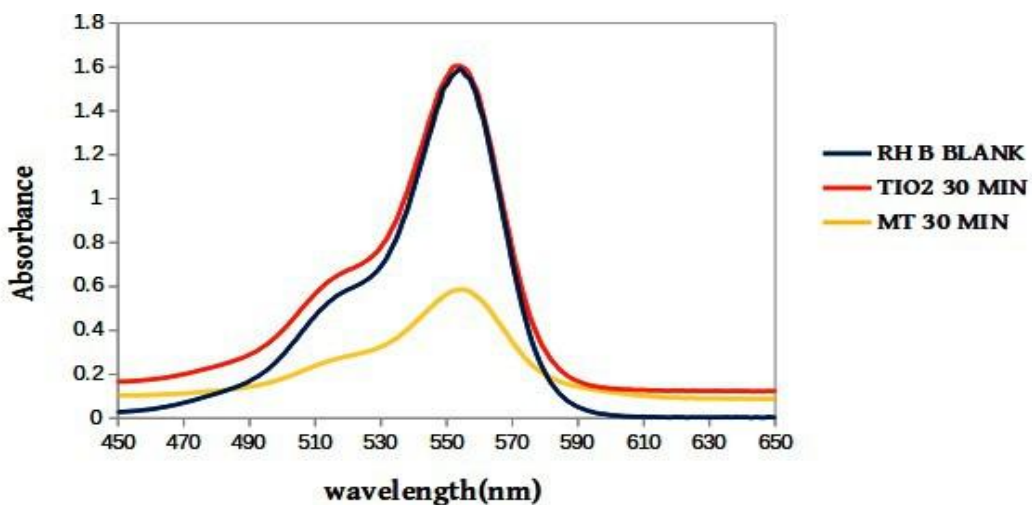


Illustration 29: Absorption spectra of Rh B with undoped TiO_2 nanotube and $MoS_2@TiO_2$ nanotube composite at 30 min.

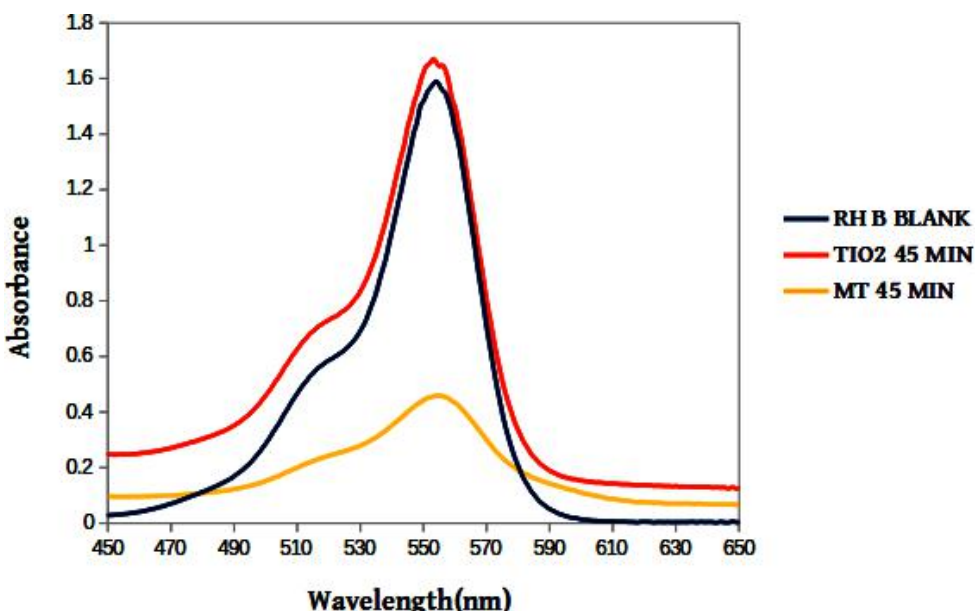


Illustration 30: Absorption spectra of Rh B with undoped TiO_2 nanotube and $MoS_2@TiO_2$ nanotube composite at 45 min.

From the absorption spectra, we may interpret that the photocatalytic activity of the TiO₂ nanotube is improved when doped with MoS₂ nano sheet. TiO₂ NT alone could degrade Rh B dye to less than 1% even kept under light up to 45 minute. MT*2% and MT*5% in which 2 wt% and 5wt % of MoS₂ nanosheet was doped to TiO₂ nanotube,no effect was observed. In this context Rh B adsorption on TiO₂ NT is less than that of Methylene blue dye. While the doped form MT could degrade the dye up to 71 % within the same time span. It is observed that, as the amount of MoS₂ increases photo catalytic degradation of Rh B increase. In comparison with TiO₂ NT, MT is more efficient as a photo catalyst in the photo degradation of Rh B dye.

When comparing the degradation, the nanocomposite MT*2% work in Methylene blue and nanocomposite MT work in Rhodamine B. This happens because Rh B is having stable structure. Hence, it is very difficult to degrade Rh B than MB. More over, MB adsorb more to TiO₂ nanotube owing to its cationic nature than Rh B which is anionic . MoS₂ shows affinity to anionic dyes. So, as the percentage of MoS₂ increases in nanocomposite, adsorption of Rh B increases. This is the reason why the less MoS₂ doping more efficient in the case of MB, while the nanocomposite with highest doping efficient in Rh B.

3.4 . RE-USABILITY STUDIES

The nanocomposite of TiO₂ nanotube and MoS₂ nano sheet synthesised by hydrothermal mixing does not dissolve in water. Because of this reason, it is possible to separate the nanocomposite from the solution by centrifuging a number of times and drying. Hence, it is a good photo catalyst for degradation of dyes since it increases the rate of degradation without getting dissolved itself.

REFERENCES

1. Kite, Sagar V., Abhijit Nanaso Kadam, Dattatraya J. Sathe, Satish Patil, Sawanta S. Mali, Chang Kook Hong, Sang– Wha Lee, and Kalyanrao M. Garadkar. "Nanostructured TiO₂ sensitized with MoS₂ nanoflowers for enhanced photodegradation efficiency toward methyl orange." *ACS omega* 6, no. 26 (2021): 17071-17085.
2. Zhao, Fenfen, Yuefei Rong, Junmin Wan, Zhiwen Hu, Zhiqin Peng, and Bing Wang. "MoS₂ quantum dots@ TiO₂ nanotube composites with enhanced photoexcited charge separation and high-efficiency visible-light driven photocatalysis." *Nanotechnology* 29, no. 10 (2018): 105403.
3. Cai, Liang, Jingfu He, Qinghua Liu, Tao Yao, Lin Chen, Wensheng Yan, Fengchun Hu et al. "Vacancy-induced ferromagnetism of MoS₂ nanosheets." *Journal of the American Chemical Society* 137, no. 7 (2015): 2622-2627.
4. Abdullah, M., and Siti Kartom Kamarudin. "Titanium dioxide nanotubes (TNT) in energy and environmental applications: An overview." *Renewable and Sustainable Energy Reviews* 76 (2017): 212-225.
5. Sun, Jie, Lixuan Duan, Qiang Wu, and Weifeng Yao. "Synthesis of MoS₂ quantum dots cocatalysts and their efficient photocatalytic performance for hydrogen evolution." *Chemical Engineering Journal* 332 (2018): 449-455.
6. Qinghua, C h u n n i X i a o , B i n g b i n g C h e n , L i n M a , a n d L i m e i X u . l . "Hydrothermal synthesis of MoS₂ nanoflowers and their capacitive property." *Micro & Nano Letters* 14.5 (2019): 493-495.
7. Zavala, Miguel Ángel López, Samuel Alejandro Lozano Morales, and Manuel Ávila-Santos. "Synthesis of stable TiO₂ nanotubes: effect of hydrothermal treatment, acid washing and annealing temperature." *Heliyon* 3, no. 11 (2017): e00456..
8. Lin, H., N. Wang, L. Zhang, C. Lin, and J. Li. "preparation and heat-treatment effects of tio~₂ nanotubes used in dye-sensitized solar cells." *Advances in technology of materials and materials processing journal* 9, no. 1 (2007):
9. Yang, Jin, Jun Du, Xiuyun Li, Yilin Liu, Chang Jiang, Wenqian Qi, Kai Zhang et al. "Highly hydrophilic TiO₂ nanotubes network by alkaline hydrothermal method for photocatalysis degradation of methyl orange." *Nanomaterials* 9, no. 4 (2019): 526.
10. Guin, Debanjan, Sunkara V. Manorama, J. Naveen Lavanya Latha, and Shashi Singh. "Photoreduction of silver on bare and colloidal TiO₂ nanoparticles/nanotubes: synthesis,

characterization, and tested for antibacterial outcome." *The Journal of Physical Chemistry C* 111, no. 36 (2007): 13393-13397.

11. Chacko, Levna, and P. M. Aneesh. "Effect of growth techniques on the structural and optical properties of TiO₂ nanostructures." *Materials Research Express* 5, no. 1 (2018): 015031.
12. Veeramalai, Chandrasekar Perumal, Fushan Li, Yang Liu, Zhongwei Xu, Tailiang Guo, and Tae Whan Kim. "Enhanced field emission properties of molybdenum disulphide few layer nanosheets synthesized by hydrothermal method." *Applied Surface Science* 389 (2016): 1017-1022.
13. Li, Minglin, Yaling Wan, Liping Tu, Yingchao Yang, and Jun Lou. "The effect of VMoS₃ point defect on the elastic properties of monolayer MoS₂ with REBO potentials." *Nanoscale research letters* 11, no. 1 (2016): 1-7.
14. Tontini, Gustavo, Guilherme Dalla Lana Semione, Cristian Bernardi, Roberto Binder, José Daniel Biasoli de Mello, and Valderes Drago. "Synthesis of nanostructured flower-like MoS₂ and its friction properties as additive in lubricating oils." *Industrial Lubrication and Tribology* (2016)..
15. Rendón-Rivera, A., J. A. Toledo-Antonio, M. A. Cortés-Jácome, and C. Angeles Chávez . "Generation of highly reactive OH groups at the surface of TiO₂ nanotubes." *Catalysis Today* 166, no. 1 (2011): 18-24.
16. Luo, Lijun, Miao Shi, Shimin Zhao, Wei Tan, Xi Lin, Hongbin Wang, and Fengzhi Jiang. "Hydrothermal synthesis of MoS₂ with controllable morphologies and its adsorption properties for bisphenol A." *Journal of Saudi Chemical Society* 23, no. 6 (2019): 762-773..
17. Guo, Yifei, Xiuli Fu, and Zhijian Peng. "Growth and mechanism of MoS₂ nanoflowers with ultrathin nanosheets." *Journal of Nanomaterials* 2017 (2017).
18. Thang, Nguyen Tat, Nguyen Hoang Thoan, Chu Manh Hung, Nguyen Van Duy, Nguyen Van Hieu, and Nguyen Duc Hoa. "Controlled synthesis of ultrathin MoS₂ nanoflowers for highly enhanced NO₂ sensing at room temperature." *Rsc Advances* 10, no. 22 (2020): 12759-12771
19. Liu, Chong, Desheng Kong, Po-Chun Hsu, Hongtao Yuan, Hyun-Wook Lee, Yayuan Liu, Haotian Wang . "Rapid water disinfection using vertically aligned MoS₂ nanofilms and visible light." *Nature nanotechnology* 11, no. 12 (2016): 1098-1104.
20. . Zhou, Fang, Zhiguang Zhang, Zhihua Wang, Yajing Wang, Liping Xu, Qiang Wang, and

Wenjun Liu. "One-step hydrothermal synthesis of P25@ few layered MoS₂ nanosheets toward enhanced bi-catalytic activities: photocatalysis and electrocatalysis." *Nanomaterials* 9, no. 11 (2019): 1636.

21. Kite, Sagar V., Abhijit Nanaso Kadam, Dattatraya J. Sathe, Satish Patil, Sawanta S. Mali, Chang Kook Hong, Sang- Wha Lee, and Kalyanrao M. Garadkar. "Nanostructured TiO₂ sensitized with MoS₂ nanoflowers for enhanced photodegradation efficiency toward methyl orange." *ACSomega* 6, no. 26 (2021): 17071-17085.
22. Muralikrishna, S., K. Manjunath, D. Samrat, Viswanath Reddy, T. Ramakrishnappa, and Doddahalli H. Nagaraju. "Hydrothermal synthesis of 2D MoS₂ nanosheets for electrocatalytic hydrogen evolution reaction." *RSC advances* 5, no. 109 (2015): 89389-89396.
23. Kite, Sagar V., Abhijit Nanaso Kadam, Dattatraya J. Sathe, Satish Patil, Sawanta S. Mali, Chang Kook Hong, Sang- Wha Lee, and Kalyanrao M. Garadkar. "Nanostructured TiO₂ sensitized with MoS₂ nanoflowers for enhanced photodegradation efficiency toward methyl orange." *ACSomega* 6, no. 26 (2021): 17071-17085r
24. Yan, Huiling, Lizhi Liu, Rong Wang, Wenxin Zhu, Xinyi Ren, Linpin Luo, Xu Zhang, Shijia Luo, Xuelian Ai, and Jianlong Wang. "Binary composite MoS₂/TiO₂ nanotube arrays as a recyclable and efficient photocatalyst for solar water disinfection." *Chemical Engineering Journal* 401 (2020): 126052.
25. Chen, Linjer, Chiu-Wen Chen, and Cheng-Di Dong. "Hydrothermal synthesis of Se-doped MoS₂ quantum dots heterojunction for highly efficient photocatalytic degradation." *Materials Letters* 291 (2021): 129537.
26. Zhao, Fenfen, Yuefei Rong, Junmin Wan, Zhiwen Hu, Zhiqin Peng, and Bing Wang. "MoS₂ quantum dots@ TiO₂ nanotube composites with enhanced photoexcited charge separation and high-efficiency visible-light driven photocatalysis." *Nanotechnology* 29, no. 10 (2018): 105403.

CHAPTER 4

CONCLUSION AND FUTURE SCOPE

Water pollution has become a global challenge to both nature and human beings. Our water resources are getting polluted because of the improper discharge of waste from industries and households. The organic contaminants like synthetic dyes, heavy metals, pesticides, phenols etc. Present in waste water are toxic/carcinogenic. Effluents from the textile industries are important sources of water pollution, because dyes in waste water undergo chemical as well as biological changes, consume dissolved oxygen, destroy aquatic life and endanger human health.

Synthetic dyes are employed extensively in a variety of industries, including textiles, leather, cosmetics, and paint industries. They are difficult to degrade due to its complex structure. For instance, methylene blue (MB, a thiazine cationic dye) has adverse health effects, which include breathing difficulties, vomiting, eye burns, diarrhoea, and nausea when MB is accumulated in waste water. Due to its non biodegradability, it is highly persistent in the environment. Another pollutant that is extensively used for dyeing purpose is Rhodamine B (Rh B). It is a water-soluble fluorescent xanthene dye used to dye various substances. It is highly toxic to various organisms and may cause long-term undesirable effects when improperly disposed of. The traditional physical methods like filtration, adsorption, filtration, ozonation, coagulation etc. are nondestructive, but instead of eradicating pollutants, they only transfer pollutants to other media, generating secondary pollution. Therefore, there are intensive demands for advanced technologies for the complete degradation of dye from the aquatic environment.

Photocatalysis has been recognised as an effective and economic method for dye degradation. This method is used for the removal of refractory pollutants from waste water and for the complete mineralization of organic dyes. It has the ability to convert pollutants into harmless end products like CO_2 , H_2O and mineral acids. TiO_2 is one of the most promising catalysts for the removal of toxic organic pollutants, because of its chemically inertness, cost-effectiveness, excellent durability, non-toxicity and environment-friendly characteristics. On the other hand, TiO_2 can only be absorbing UV light, because of its 3.2 eV bandgap, resulting in the faster electron–hole pair recombination, which restricts its activity for the photocatalysis process. Surface sensitization of TiO_2 is an effective approach to enhance photocatalytic performance;

additionally, surface sensitization contributes to shrinking the crystallite size and band gap of TiO_2 .

Among transition metal dichalcogenides, MoS_2 has been established as a significant interest in sensitizing a wide band gap TiO_2 due to its potential properties like having a two-dimensional layered structure, good charge carrier transport capacity, and high surface area. The present work focused on the surface sensitization of nanostructured TiO_2 surface by MoS_2 .

Transmission electron microscopy (TEM), X-ray diffraction (XRD) and Fourier transform infra red (FTIR) were used for structural analysis. The photocatalytic performance of surface-sensitized TiO_2 was tested for rhodamine B (Rh B) and methylene blue (MB) under UV-vis light, and its degradation mechanism are discussed.

The thesis has been divided into four chapters including summary. First chapter contains the introduction regarding the research and the second chapter elaborates details of experimental set up, materials used and the methods adopted. The third chapter contains the result and discussion followed by the summary in the fourth chapter.

TiO_2 nanotubes and MoS_2 nanosheet were synthesized by a facile hydrothermal technique. The surface sensitization of nano structured TiO_2 by MoS_2 was carried out via mechano - chemical method. $\text{MoS}_2\text{-TiO}_2$ nanocomposite of different x wt% ($x = 2.0, 5.0$ wt%) are obtained. The peaks in the X-ray diffraction spectrum of synthesized TiO_2 match with the standard peaks of TiO_2 anatase phase. The average particle size of the synthesized TiO_2 was found to be 5.668 nm. The X-ray diffraction spectrums of synthesized MoS_2 nano structures autoclaved for different time periods are obtained. The detected peaks corresponds to hexagonal MoS_2 . As the time duration increases the ex foliation of MoS_2 nano structures have taken place and we have got MoS_2 nano sheets.

The morphological investigations of TiO_2 nanotube were performed via TEM and HR-TEM analysis. Nano particles are not observed in the TEM image which implies that the nano powder has completely transformed into nanotubes. The obtained TEM images of the synthesized TiO_2 nano tubes reveals that the nano tubes are randomly oriented and are almost clustered in nature. The HR-TEM image shows that it has got an inter planar spacing (d) of 0.30nm, which is in perfect agreement with the (101) plane of TiO_2 .

The photodegradation efficiencies of MB and Rh B using TiO₂ NT, MoS₂ and MoS₂–TiO₂ nanocomposites were determined under UV-vis light irradiation. The absorption spectra shows that the photo-catalytic activity of the TiO₂ is improved when doped with MoS₂ nano sheet/nano flower TiO₂. Undoped TiO₂ could degrade MB dye to 94.58% which took almost 40 min, while the doped forms MT, MT*2%(2 wt% MoS₂ in TiO₂), MT*5%(5 wt% MoS₂ in TiO₂) could degrade the dye up to 97 %, 93 %, 90% within 5, 1.5, 1.5 minutes respectively. MT*2% is more efficient as a photo catalyst in the photo degradation of MB dye. MT is more efficient in causing degradation of Rh B dye than MT*2% and MT*5%. TiO₂ NT alone could degrade Rh B dye to less than 1% even kept under light up to 45 minute, while the doped forms of MT could degrade the dye up to 71 % within the same time span. This concludes that the photocatalytic activity of the synthesized nanocomposite is admirable toward Rh B and MB degradation.

FUTURE SCOPE

For efficient photocatalytic performance, the nanoparticles should have good adsorption capacity. There are various strategies to improve the photocatalytic efficiency of MoS₂–TiO₂ nanocomposite. The photocatalytic performance can be increased, by increasing the intensity of light source. The usage of xenon lamp having high intensity is efficient to increase the percentage of degradation.

By optimising the factors like effect of time, effect of temperature, nature of pollutant and nature of light source the photocatalyst can be commercialized. For practical applications, the uv light source must be replaced with sunlight in order to save energy and money. The increase in band gap hinders the widespread use of photocatalyst using sunlight. Surface modification of the photocatalyst can enhance the utilization of solar energy. The band gap of MoS₂–TiO₂ samples can be reduced by introducing co-catalysts.

REFERENCES

1. Liu, Peitao, Yonggang Liu, Weichun Ye, Ji Ma, and Daqiang Gao. "Flower-like N-doped MoS₂ for photocatalytic degradation of Rh B by visible light irradiation." *Nanotechnology* 27, no. 22 (2016): 225403.
2. Shathy, Romana Akter, Shahriar Atik Fahim, Mithun Sarker, Md Saiful Quddus, Mohammad Moniruzzaman, Shah Md Masum, and Md Ashraful Islam Molla. "Natural Sunlight Driven Photocatalytic Removal of Toxic Textile Dyes in Water Using B-Doped ZnO/TiO₂ Nanocomposites." *Catalysts* 12, no. 3 (2022): 308.
3. Wang, Ding, Ying Xu, Feng Sun, Quanhua Zhang, Ping Wang, and Xianying Wang. "Enhanced photocatalytic activity of TiO₂ under sunlight by MoS₂ nanodots modification." *Applied Surface Science* 377 (2016): 221-227.
4. Vieira, Yasmin, Jandira Leichtweis, Edson Luiz Foletto, and Siara Silvestri. "Reactive oxygen species-induced heterogeneous photocatalytic degradation of organic pollutant Rhodamine B by copper and zinc aluminate spinels." *Journal of Chemical Technology & Biotechnology* 95, no. 3 (2020): 791-797.
5. Kite, Sagar V., Abhijit Nanaso Kadam, Dattatraya J. Sathe, Satish Patil, Sawanta S. Mali, Chang Kook Hong, Sang- Wha Lee, and Kalyanrao M. Garadkar. "Nanostructured TiO₂ sensitized with MoS₂ nanoflowers for enhanced photodegradation efficiency toward methyl orange." *ACS omega* 6, no. 26 (2021): 17071-17085.
6. Ghaedi, Mehrorang, ed. *Photocatalysis: Fundamental Processes and Applications*. Academic Press, 2021.